Supplementary Material

Asteroid pairs: a complex picture

Photometric observations of paired asteroids

We carried out photometric observations using our standard asteroid lightcurve photometry techniques. The data were corrected for light-travel time and standard calibration with bias, dark and flatfield frames was applied to all images. We analysed the observations using our methods described in Pravec et al. (2006).

The individual observing sessions in the Supplementary Information are identified with the date given to the nearest 10th of a day to the midtime of the session's observational interval. All dates and times in Suppl. Figs. 5 to 200 are asterocentric JD (UTC), i.e., they were light-time corrected. In Suppl. Table 1, there are listed the participating observatories, instruments and observers. We give references and descriptions of observational procedures on the individual observatories in following. The original digital data are available at `http://www.asu.cas.cz/~ppravec/astpairs_201812_lc_data.zip`, at `http://alcdef.org/`, or their are prepared for publication in papers mentioned in the text.

Abastumani – The observations at the Abastumani Astrophysical Observatory were carried out with the 0.7-m meniscus Maksutov telescope with FLI IMG6303E CCD camera in the primary focus (f/3). Observational method and reduction procedures at Abastumani were the same as we used at Simeiz (see below). The observations were made without filter.

Blauvac – The observations at the Blauvac Observatory were carried out with the 0.40-m Newton telescope with focal reducer (f/3.7) equipped with the Atik 460EX CCD camera. The 60s-exposure images were acquired and bias-dark-flat corrected using the Prism software by C. Cavadore. Photometric reduction was done using Photo, a pipeline used at Geneva Observatory for asteroids and variable stars.

BOAO – The observations were made at The Bohyunsan Optical Astronomy Observatory with a 1.8-m Cassegrain telescope operating at f/8 with Back illuminated E2V 231-84 sensor, 2×2 binning (2048×2048 pixels) with 0.429 arcsec/pixel scale and 14.6×14.6 arcmin^2 field of view. All raw image frames were reduced using bias, dark and flat field frames with IRAF. Aperture photometry is carried out using the Asteroid Spin Analysis Package (Kim, 2014) that applies aperture photometry utilizing the IRAF/APPHOT package.

Calar Alto – The observations were obtained with the 1.2-m Ritchey-Chrétien f/8 telescope of the Centro Astronomico Hispano Aleman located at Calar Alto (Almería, Spain). The camera employed is the DLR-MKIII camera, which is a fast-readout, low noise, cryogenically cooled scientific camera. It is equipped with an e2v CCD231-84-NIMO-BI-DD CCD sensor with 4k×4k pixels and 15μm pitch. The sensor has 4 output amplifiers that can be used individually or in parallel for faster readout. It has a plate scale of 0.314 arcsec/pixel. The corresponding field of view is 21.4×21.4 arcmin^2. The setup and the observations were the same as those described in Fernández-Valenzuela et al. (2016).

Carbuncle Hill – Observational and reduction procedure at Carbuncle Hill Observatory is described in Warner and Pray (2009).

Dark Sky Observatory (DSO) – Observations were made with the 0.35-m C-14 telescope outfitted with an Alta U47+ camera by Apogee. The field of view is 10×10 arcmin^2. All raw image frames were processed (master dark, master flat, bad pixel correction) using the software package MIRA. Aperture photometry was then performed on the asteroid and three comparison stars. A master median image frame was created to identify any faint stars in the path of the asteroid. Data from images with background contamination stars in the asteroid's path were then eliminated.

IAC80 – Information on the telescope is available at `http://vivaldi.ll.iac.es/OOCC/iac-managed-telescopes/iac80/`.

Kharkiv – CCD photometry was done with the 0.7-m reflector at Chuguev Observatory of Kharkiv National University using the CCD camera IMG 47-10 (1056×1027 pixels, 13×13 μm pixel) installed in Newtonian focus (f/4) equipped with a 3-lens focal corrector (0.951 arcsec/pixel, FOV 16.7×16.3 arcmin^2). The method of observations and data reduction were described in Krugly et al. (2002).

La Hita – Observations were carried out with the 0.77-m f/3 telescope at La Hita observatory in Toledo, Spain. The detector used was a 4k×4k CCD camera which provided a field of view of 48.1×48.1 arcmin^2 with a 0.705 arcsec/pixel scale. The setup was the same as described in Santos-Sanz et al. (2015). We used the same or analogous reduction procedures as those that we used for observations from Ondřejov (see below) and for observations of Apophis (Pravec et al., 2014).

La Silla – For observations with the Danish 1.54-m telescope, we used the same or analogous procedures as those we used for observations from Ondřejov (see below) and for observations of Apophis (Pravec et al., 2014).

Leura/Blue Mountains Observatory – Observations were made with a 0.61-m Corrected Dall-Kirkham reflecting telescope operating at f/6.5 with Apogee U42 Back illuminated E2V-4240 sensor with NABG, 2048×2048 pixels CCD resulting in 0.70 arcsec/pixel scale at 24×24 arcmin^2 field of view. Most images were taken unguided with clear IR-blocking filter or Cousins R filter. Another telescope used to support the work on asteroid pairs was a 0.35-m

Schmidt Cassegrain Telescope operating at f/5.9 working with SBIG ST8XME 1530 × 1020 pixels CCD resulting in 0.88 arcsec/pixel scale. All images were taken unfiltered. Calibration was done using library of respective camera's median combined bias, dark and flat frames. Photometric reduction were done by differential photometry using MPO Canopus which incorporates the Fourier analysis algorithm (FALC) developed by Harris et al. (1989). The different sessions were calibrated by using a technique that used comparison field stars with approximated Cousins R magnitudes converted from 2MASS J-K colors providing ±0.05-mag accuracy.

Lowell – Observations were performed with the Large Monolithic Imager (LMI) at Lowell Observatory's 4.3-m Discovery Channel Telescope (DCT). LMI is a 6k×6k e2V CCD with a 12.3 arcmin field of view sampled at 0.12 arcsec/pixel. Images were binned 3×3 and taken in the SDSS g'r'i'z' filter set. Bias and flat field reductions followed standard procedures. Extraction of the color photometry employed the Photometry Pipeline (Mommert, 2017). This pipeline is fully automated and registers images using Source Extractor (Bertin and Arnouts, 1996) and the Gaia DR1 astrometric catalog, calibrates photometry by matching field stars to the PanSTARRS catalog (Flewelling et al., 2016), and identifies the asteroid in the field by querying the JPL Horizons system. The resulting photometric precision was generally quite good with errors less than 0.1 magnitude across all bands (Suppl. Table 2).
The observations of (43008) in 2017 were performed with the NASA42 instrument on Lowell Observatory's 42-inch Hall telescope. NASA42 employs a SITe 2k CCD that images a 19.4 arcmin square field of view sampled at 0.57 arcsec/pixel. Bias and flat field reductions followed standard procedures and the lightcurve photometry was measured with the procedures that we employed for the observations at La Silla (above).
The observations of (4905) in December 2013 were performed with the LONEOS Schmidt (0.55-m f/1.9, unfiltered, image scale 2.5 arcsec/pixel, 45-second exposures). They were reduced to Sloan r' for the comparison stars.

Maidanak – The Maidanak Astronomical Observatory is described in Ehgamberdiev (2018). The 1.5-m telescope AZT-22 (Cassegrain f/7.7) was equipped with back-illuminated Fairchild 486 CCD camera (4096 × 4096 CCD, 15 × 15 μm pixel, 0.27 arcsec/pixel, FOV 18.4 × 18.4 arcmin^2). The observations were carried out unfiltered to get higher S/N and they were reduced in the standard way with master-bias subtracting and median flat-field dividing. The aperture photometry of the asteroid and comparison stars in the images was done with the ASTPHOT package developed at DLR (Mottola et al. 1995). The effective radius of aperture was equal to $1-1.5\times$ the seeing that included more than 90% of the flux of a star or the asteroid. The relative photometry of the asteroid was done with typical errors in a range of 0.02–0.03 mag using an ensemble of comparision stars. The 0.6-m Zeiss-600 telescope was equipped with the 1k×1k FLI IMG1001E CCD camera with the resolution of 0.67 arcsec/pixel. All observations on this telescope were taken with the Bessel R filter. The FOV of the camera is 10.7 × 10.7 arcmin^2. The temperature of the camera was set at -30°C. Image acquisition was done with MaxIm DL.

Modra – Observational system, data analysis and reduction process are described in Galád et al. (2007) and later they made use of tools provided by Astrometry.net (Lang et al. 2010).

Ondřejov – Observational system, data analysis and reduction process are described in Pravec et al. (2006).

Pic du Midi – Details about the telescope are available at http://astrosurf.com/t60. Reduction was performed using the Prism V7 software.

PROMPT – The University of North Carolina at Chapel Hill's PROMPT observatory (Panchromatic Robotic Optical Monitoring and Polarimetry Telescopes) is on Cerro Tololo. PROMPT consists of six 0.41-m outfitted with Alta U47+ cameras by Apogee, which make use of E2V CCDs. The field of view is $10' \times 10'$ with 0.59 arcsec/pixel. All raw image frames were processed (master dark, master flat, bad pixel correction) using the software package MIRA. Aperture photometry was then performed on the asteroid and three comparison stars. A master image frame was created to identify any faint stars in the path of the asteroid. Data from images with background contamination stars in the asteroid's path were then eliminated. Data for (3749) from 2007 were reduced using the technique described in Marchis et al. (2013).

Réunion – Observations were made with the 60-cm André Peyrot telescope (f/8 reflector) using camera SBIG STL-11000 mounted at Les Makes observatory on Réunion Island, operated as a partnership among Les Makes Observatory and the IMCCE, Paris Observatory. The CCD covers a field of view unbinned of 25.8×16.9 arcmin^2 with 4008×2655 pixels (9μm per pixel) R filter were used. The observations were reduced with the Audela software (`http://www.audela.org/`).

Sierra Nevada – Observations were made with the 1.5-m Ritchey-Chrétien f/8 telescope of the Sierra Nevada Observatory in Granada, Spain, using a cryogenically cooled Roper Scientific 2048×2048 CCD camera. The CCD covers a field of view of 7.8×7.8 arcmin^2 with a scale of 0.23 arcsec/pixel. However, the images were obtained with 2x2 binning. The filter used was a Cousins R filter. The setup was the same as described in Fernández-Valenzuela et al. (2016). We used the same or analogous reduction procedures as those that we used for observations from Ondřejov (see below) and for observations of Apophis (Pravec et al., 2014).

Simeiz – The observations were carried with a 1-m Ritchey-Chrétien telescope at Simeiz Department of the Crimean Astrophysical Observatory using camera FLI PL09000. The observations were made in the Johnson-Cousins photometric system. Standard procedure of image reduction included dark removal and flatfield correction. The aperture photometry was done with the AstPhot package described in Mottola et al. (1995). The differential lightcurves were calculated with respect to an ensemble of comparison stars by the method described in Erikson et al. (2000) and Krugly (2004).

Skalnaté Pleso – The photometric observations at the Skalnaté Pleso Obser-

vatory were carried out with the 0.61-m f/4.3 reflector through the Cousins R filter and SBIG ST-10XME with 2×2 binning with resolution of 1.07 arcsec/px. CCD frames were reduced in standard way using bias, dark and flat field frames with IRAF tools. The images were photometrically reduced using the procedure described in Husárik and Kušnirák (2008).

Sozzago – The observations at Stazione Astronomica di Sozzago were carried out with the 0.40-m Cassegrain telescope (f/6.8) equiped with an unfiltered CCD camera based on a KAF1603ME with scale 0.68 arcsec/pixel. Exposure time was 60s. Photometry was extracted using Iris, a freeware by Ch. Buil.

SRO – The Sonoita Research Observatory (SRO) observations were collected with a 0.5-m folded Newtonian operating at f/4 and an SBIG STL-6303E with an image scale of 0.92 arcsec/pixel. The system was mounted on a Software Bisque Paramount ME. Image acquisition and observatory control are automated via DC-3 Dreams ACP. Integration times were 300 sec and images were unfiltered. The images were dark subtracted and flat fielded, then reduced using MIRA. The differential photometry was performed against an ensemble of comparison stars. The images were examined for interfering stars and those images were discarded.

Sugarloaf Mountain – Observations at Sugarloaf Mountain Observatory were made using a 0.5-m, f/4.0 reflector on a Paramount ME mount. The imaging CCD was a SBIG ST-10XME cooled to $-15°$C, where images were taken through a clear filter. The image scale was 1.38 arcsec/pixel, and the fov was 25.0×16.8 arcmin^2. Derived magnitudes were estimated using a method inherent in the analysis software, *MPO Canopus*. The method is based on referencing a hybrid star catalog consisting mostly of 2MASS stars in the V band. Images were calibrated using master bias, dark and flat field images.

Whitin - The observations at the Whitin Observatory were made using the Sawyer 0.61-m Cassegrain telescope with CCD camera detectors and R filters. For the lightcurves from 2007 the detector field of view was 16 arcminutes square with an image scale of 1.8 arcsec/pixel. For the lightcurves from 2016 and 2018 the field was 19 arcminutes square with image scale 1.2 arcsec/pixel. For the lightcurve from 2017 the field was 16 arcminutes square with image scale 0.94 arcsec/pixel. Observing and data reduction procedures are described by Slivan et al. (2008).

Wise – Observations were performed using the two telescopes of the Wise Observatory (Tel-Aviv University) in the Israeli desert (MPC code 097): A 1-m Ritchey-Chrétien telescope and a 0.46-m Centurion telescope (see Brosch et al. 2008), for a description of the telescope and its performance). The 1-m telescope is equipped with a cryogenically-cooled Princeton Instruments CCD. At the f/7 focus of the telescope this CCD covers a field of view of $13' \times 13'$ with 1340×1300 pixels (0.58 arcsec per pixel, unbinned). The 0.46-m telescope was used with an SBIG STL-6303E CCD at the f/2.8 prime focus. This CCD covers a field of view of $75' \times 50'$ with 3072×2048 pixels, with each pixel subtending 1.47 arcsec, unbinned. R and V filters were used on the 1-m telescope while observations with the 0.46-m telescope were unfiltered. Integration times were

120-300 s, all with auto-guider. The reduction, measurements, calibration and analysis methods of the photometric data are fully described in Polishook and Brosch (2008, 2009).

Suppl. Table 1
Observatories, Instruments and Observers/Reducers

Observatory	**Telescope**	**Diameter (m)**	**Observers/Reducers**
Abastumani		0.7	Inasaridze, Krugly, Ayvazian
Blauvac		0.4	Roy, Behrend
BOAO		1.8	Kim
Calar Alto		1.2	Ortiz, Morales
Carbuncle Hill		0.50	Pray
DSO		0.35	Pollock
IAC80		0.8	Aznar, Serra-Ricart
Kharkiv		0.7	Krugly
Leura/BMO		0.61, 0.35	Oey
La Hita		0.77	Morales, Ortiz
La Silla	Danish	1.54	Pravec, Hornoch, Kušnirák, Galád, Fatka, Kučáková
Lowell	DCT, Hall, LONEOS	4.3, 1.1, 0.55	Moskovitz, Thirouin, Fatka, Skiff
Maidanak		1.5, 0.6	Krugly, Burkhonov, Sergeev, Ergashev
Modra		0.60	Galád, Világi, Gajdoš, Kornoš, Vereš
Ondřejov		0.65	Kučáková, Hornoch, Kušnirák, Fatka, Vraštil
Pic du Midi		0.6	Colas
PROMPT		0.41	Pollock, Marchis
Réunion		0.60	Vachier
Sierra Nevada		1.5	Ortiz, Morales, Aznar
Simeiz		1.0	Gaftonyuk, Krugly
Skalnaté Pleso		0.61	Husárik, Pikler, Červák
Sozzago		0.40	Manzini
SRO		0.5	Cooney, Gross, Terrell
Sugarloaf Mountain		0.50	Pray
Whitin	Sawyer	0.61	Slivan, Levandowski, Neugent, Wasser, Zangari, Yax
Wise		0.46, 1.0	Polishook

Suppl. Table 2
Sloan color measurements from Lowell Observatory

Asteroid	Mid-observing UTC	$g-r$ [mag]	$r-i$ [mag]	$i-z$ [mag]	r [mag]
(4905)	2017-06-04.448	0.73 ± 0.03	0.23 ± 0.02	-0.01 ± 0.03	16.53 ± 0.01
(7813)	2017-03-17.477	0.64 ± 0.03	0.20 ± 0.03	-0.09 ± 0.05	17.59 ± 0.01
(23998)	2017-03-15.282	0.55 ± 0.03	0.14 ± 0.02	0.03 ± 0.03	17.60 ± 0.01
(26420)	2017-03-17.496	0.79 ± 0.06	0.13 ± 0.03	-0.54 ± 0.05	18.87 ± 0.02
(30301)	2017-03-17.457	0.67 ± 0.03	0.16 ± 0.03	-0.07 ± 0.07	18.29 ± 0.01
(42946)	2017-03-17.186	0.68 ± 0.02	0.21 ± 0.02	-0.05 ± 0.03	19.01 ± 0.01
(52773)	2017-03-17.467	0.68 ± 0.03	0.18 ± 0.03	-0.13 ± 0.05	19.25 ± 0.01
(63440)	2017-05-14.406	0.53 ± 0.03	0.14 ± 0.02	0.05 ± 0.02	18.94 ± 0.01
(69142)	2017-03-17.485	0.55 ± 0.04	0.16 ± 0.03	0.04 ± 0.05	17.29 ± 0.01
(165548)	2017-03-17.201	0.72 ± 0.02	0.19 ± 0.02	-0.06 ± 0.04	20.38 ± 0.01
(205383)	2017-03-15.272	0.57 ± 0.02	0.15 ± 0.02	0.08 ± 0.02	19.59 ± 0.01
(337181)	2017-05-14.375	0.52 ± 0.05	0.09 ± 0.03	0.01 ± 0.03	19.31 ± 0.02
(446085)	2017-03-15.309	0.70 ± 0.07	0.24 ± 0.04	-0.14 ± 0.06	20.36 ± 0.02

(1741) Giclas and (258640) 2002 ER36

We have obtained lightcurve data for the primary (1741) from 7 apparitions. Observations taken from Mauna Kea, Whitin, Palmer Divide Observatory, Leura, and Leura and Perth in 1999, 2004, 2007, 2014 and 2015, respectively, were published in Slivan et al. (2008), Warner (2008), Oey (2016) and Oey et al. (2017). We observed it from Whitin on 4 nights during 2007-11-14 to 2017-11-28, from Ondřejov and Sugarloaf Mountain on 8 nights during 2014-02-07 to 2014-04-25, from Whitin and Reunion on 10 nights during 2016-08-23 to 2016-10-03, and from Whitin, Ondřejov, La Silla, Sugarloaf Mountain and BOAO on 8 nights during 2017-12-07 to 2018-03-02. We measured $(V-R)_1 = 0.471 \pm 0.010$; the value 0.466 ± 0.010 given in Table 2 is the weighted mean of our value and the value 0.456 ± 0.015 by Slivan et al. (2008). The mean absolute magnitudes were $H_1 = 11.57 \pm 0.03, 11.70 \pm 0.03, 11.76 \pm 0.07, 11.59 \pm 0.03$ and 11.47 ± 0.13 in 2004, 2007, 2014, 2016 and 2018, respectively, assuming the phase relation slope parameter $G = 0.24 \pm 0.11$. We observed the secondary (258640) from La Silla on 4 nights during 2015-12-16 to 2016-01-09. The data did not show a clear rotational brightness variation for its low amplitude, but we derived $H_{R,2} = 15.65 \pm 0.05$, assuming $G = 0.24 \pm 0.11$. For conversion to $H_2 \equiv H_{V,2}$, we assumed the primary's color index.

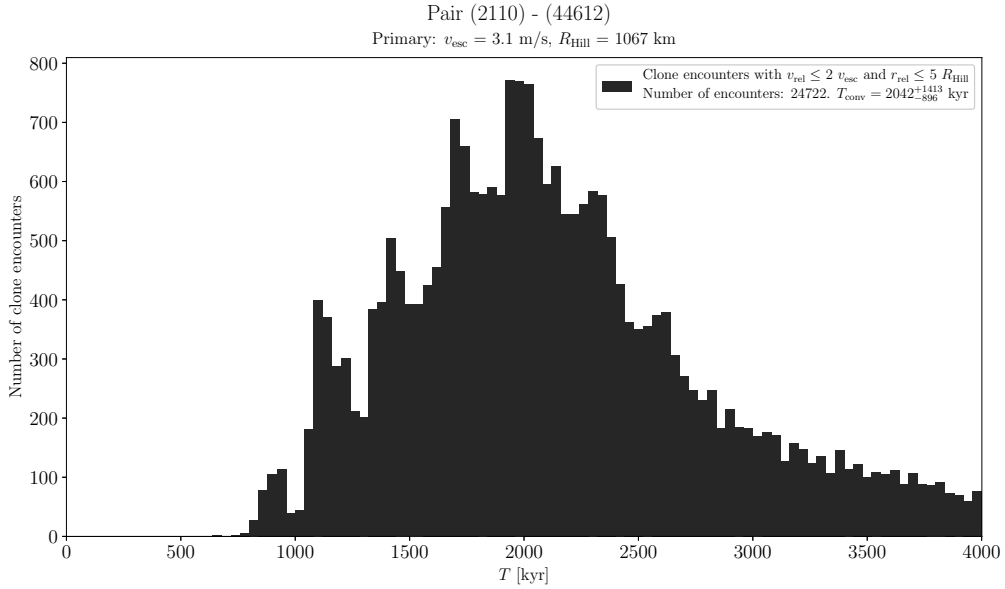

Suppl. Fig. 1. Distribution of past times of close and slow primary–secondary clone encounters for the asteroid pair 2110–44612.

(2110) Moore-Sitterly and (44612) 1999 RP27

The estimated age of this asteroid pair is about 2 Myr (Suppl. Fig. 1). We obtained lightcurve data for the primary (2110) from 5 apparitions. The observations taken in 2008-2009, 2013 from Wise, and 2014 were published in Pravec et al. (2010), Polishook (2014), and Oey (2016), respectively. We observed it from Carbuncle Hill, Ondřejov, SRO and Modra on 10 nights during 2010-03-18 to 2010-04-12, from Calar Alto and Modra on 4 nights during 2011-09-14 to 2011-09-29, and from Ondřejov, Sugarloaf Mountain and PROMPT on 6 nights during 2013-03-03 to 2013-04-04. From the Ondřejov R data, we obtained its mean absolute R magnitudes $H_{R,1} = 13.13 \pm 0.04$ and 13.09 ± 0.02 in 2010 and 2013, respectively, assuming the phase relation slope parameter $G = 0.24 \pm 0.11$. We have obtained lightcurve data for the secondary (44612) from 3 apparitions. The observations taken in 2009 and 2012 from Wise were published in Pravec et al. (2010) and Polishook (2014), respectively. We observed it from Ondřejov, La Silla and Maidanak on 6 nights during 2012-08-20 to 2012-12-12, and from La Silla on 2 nights 2014-01-25 and 2014-02-08. From our data that were taken in the Johnson-Cousins VR system, we derived its absolute magnitudes $H_2 = 15.77 \pm 0.04$ and 15.74 ± 0.06 with the slope parameters $G = 0.18 \pm 0.03$ and 0.09 ± 0.05 in the two apparitions, respectively. Suppl. Figs. 2 and 3 show the nominal spin pole solutions and the uncertainty areas for the two asteroids.

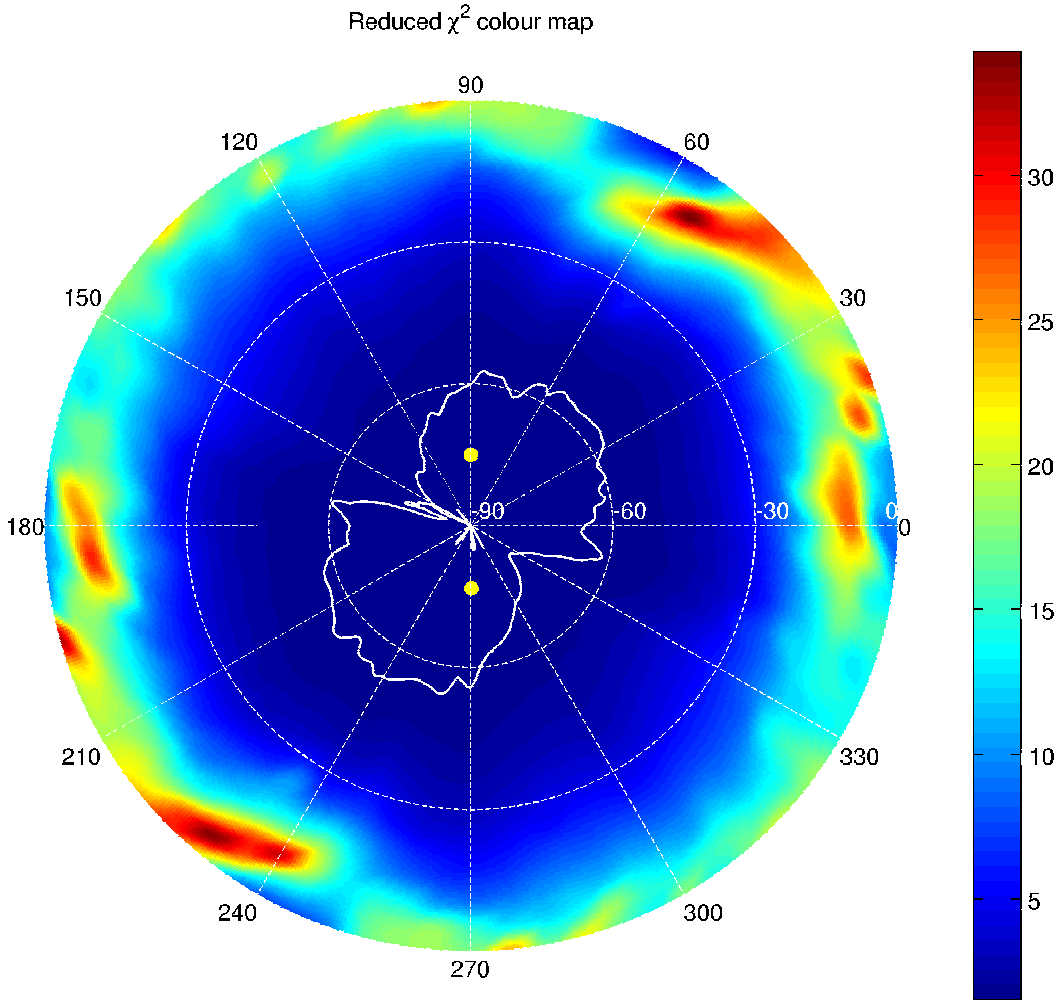

Suppl. Fig. 2. The two nominal spin pole solutions (yellow dots) and the 3-σ pole uncertainty area (white boundary) for (2110) Moore-Sitterly.

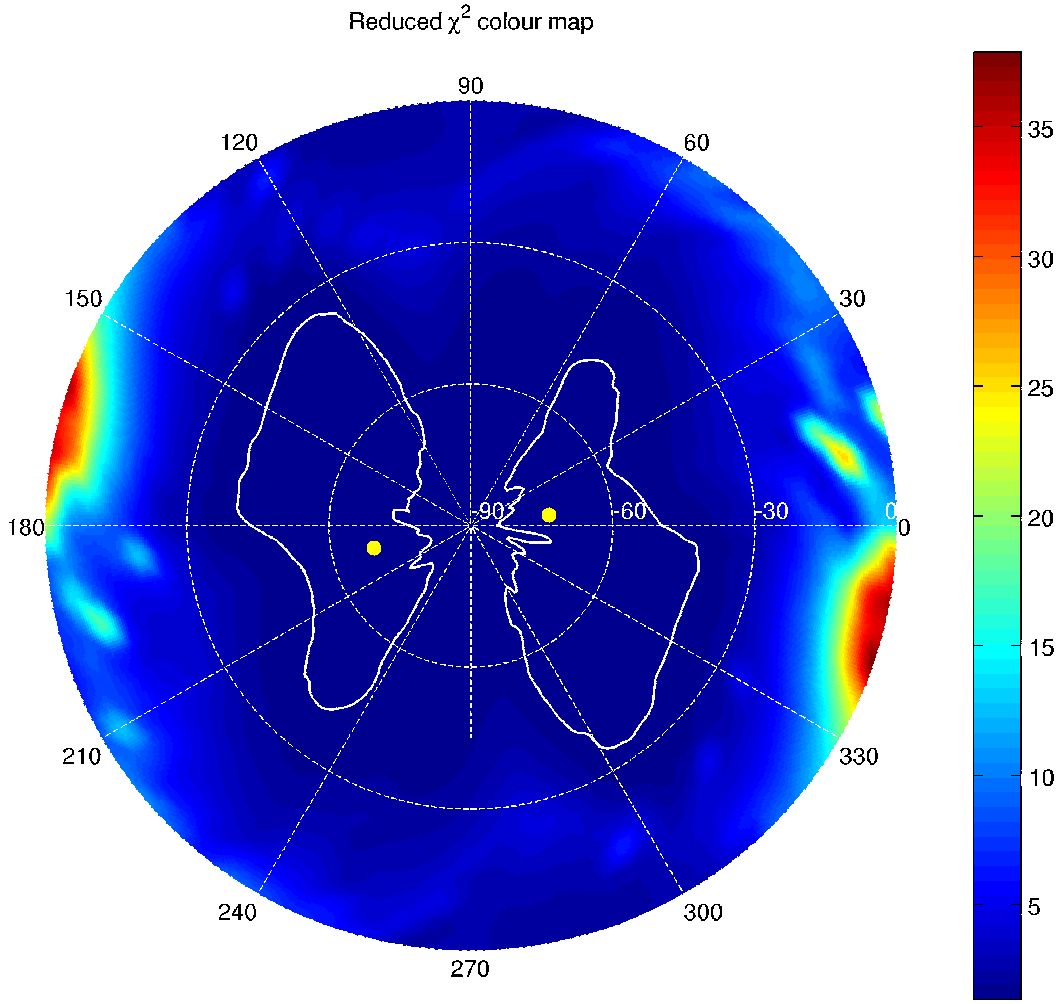

Suppl. Fig. 3. The two nominal spin pole solutions (yellow dots) and their 3-σ pole uncertainty areas (white boundaries) for (44612) 1999 RP27.

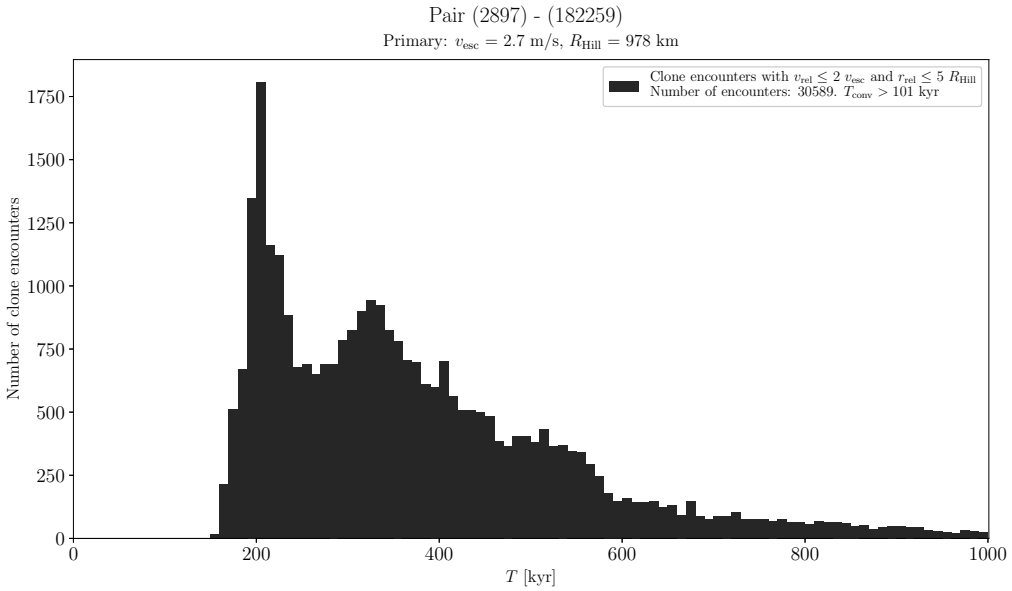

Suppl. Fig. 4. Distribution of past times of close and slow primary–secondary clone encounters for the asteroid pair 2897–182259.

(2897) Ole Romer and (182259) 2001 FZ185

A lower limit on age of this asteroid pair is about 150 kyr (Suppl. Fig. 4). We have obtained lightcurve data for the primary (2897) from 4 apparitions. Observations taken from Leura in 2010 and 2013 were published in Oey (2011, 2014). We observed it from Ondřejov and Skalnaté Pleso on 6 nights during 2011-08-24 to 2011-09-04, from Ondřejov and Sugarloaf Mountain on 5 nights during 2013-01-23 to 2013-05-05, and from Ondřejov on the night 2015-12-07 (Suppl. Figs. 5 to 7). From the Ondřejov observations that were calibrated in the Cousins R system, we derived the mean absolute R magnitudes $H_{R,1} = 13.15 \pm 0.11, 13.12 \pm 0.07$ and 12.98 ± 0.10 in the three apparitions, assuming the slope parameter $G = 0.24 \pm 0.11$ that is the mean value for S type asteroids (which is a likely spectral type of this asteroid pair). Correcting it with the secondary's color index (Table 2), the primary's weighted mean absolute magnitude is $H_1 = 13.55 \pm 0.07$. Using this H_1, we refined the WISE effective diameter and geometric albedo (Masiero et al. 2011): $D_1 = 5.2 \pm 0.5$ km and $p_{V,1} = 0.24 \pm 0.05$. We observed the secondary (182259) from La Silla on 3 nights during 2018-04-18 to 2018-04-21 (Suppl. Fig. 8). We derived its absolute magnitude $H_2 = 17.30 \pm 0.06$, assuming the slope parameter $G = 0.24 \pm 0.11$.

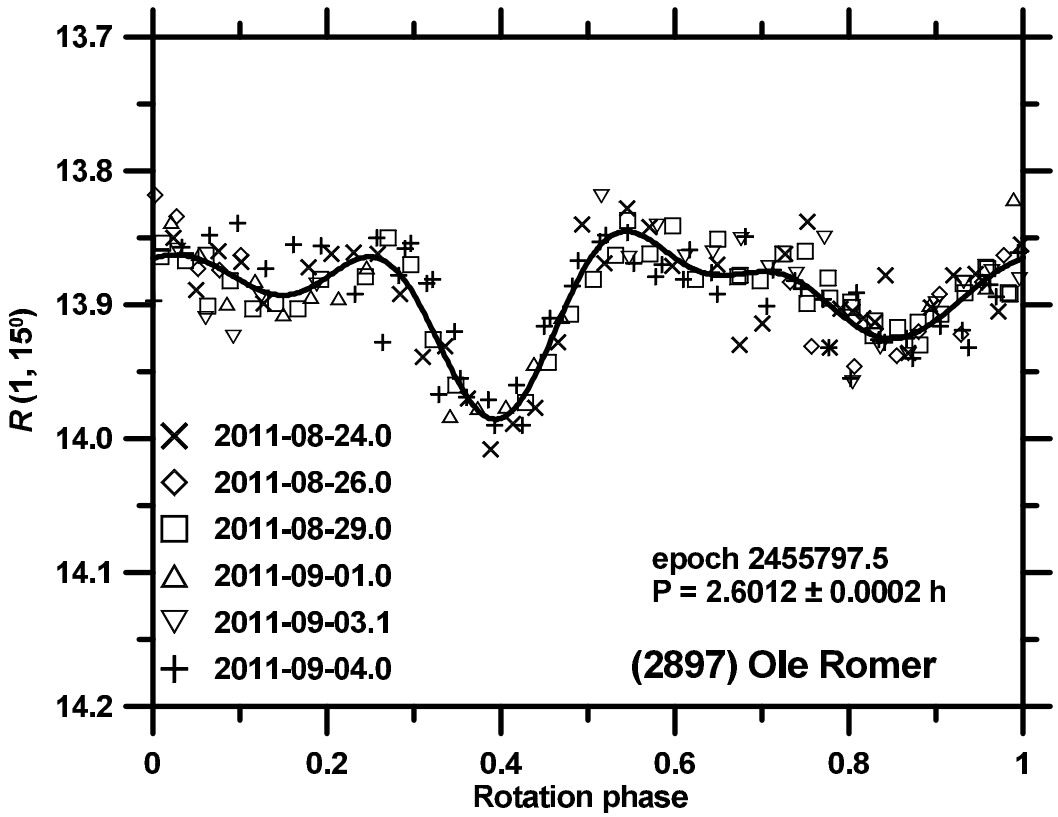

Suppl. Fig. 5. Composite lightcurve of (2897) Ole Romer from 2011.

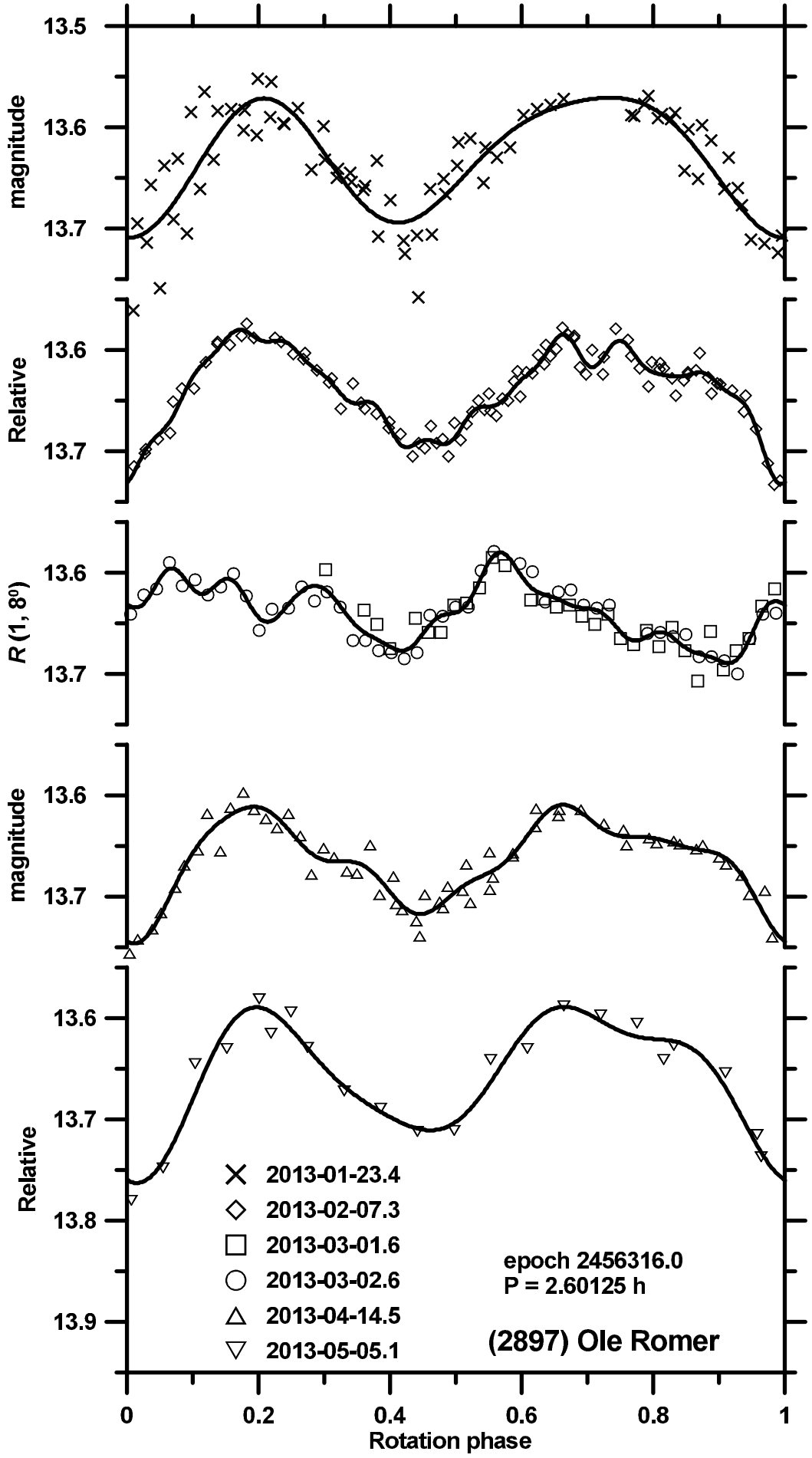

Suppl. Fig. 6. Composite lightcurves of (2897) Ole Romer from 2013.

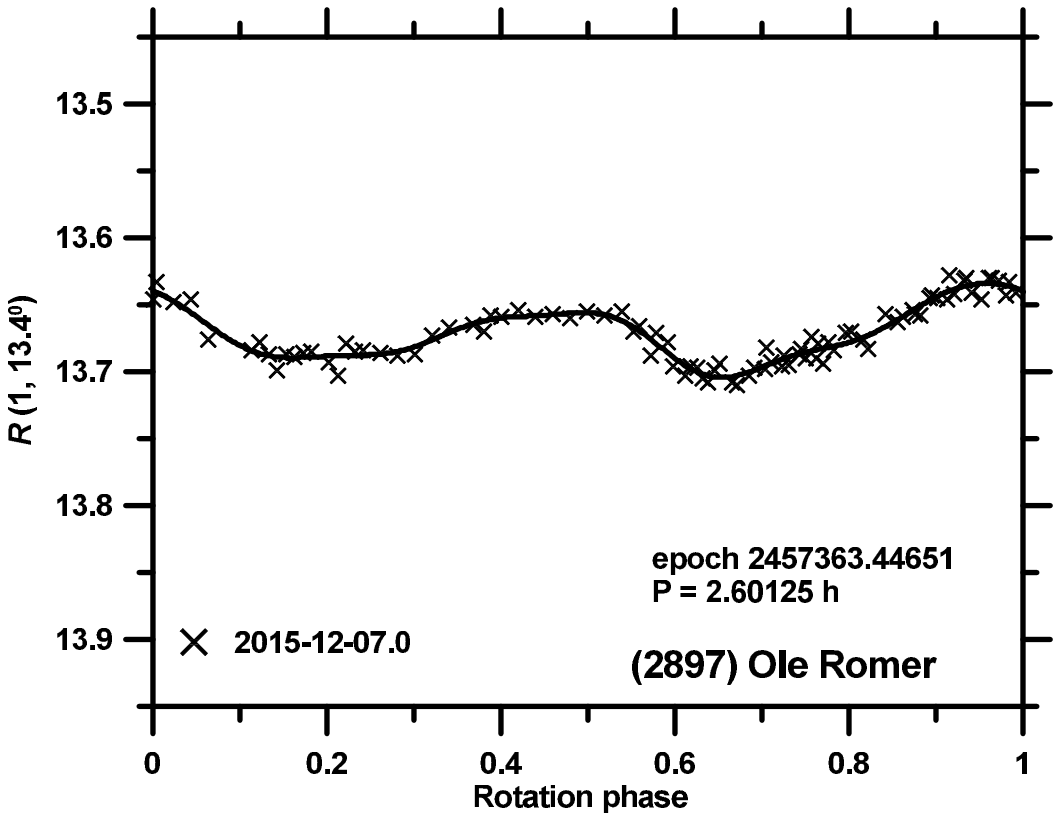

Suppl. Fig. 7. Composite lightcurve of (2897) Ole Romer from 2015.

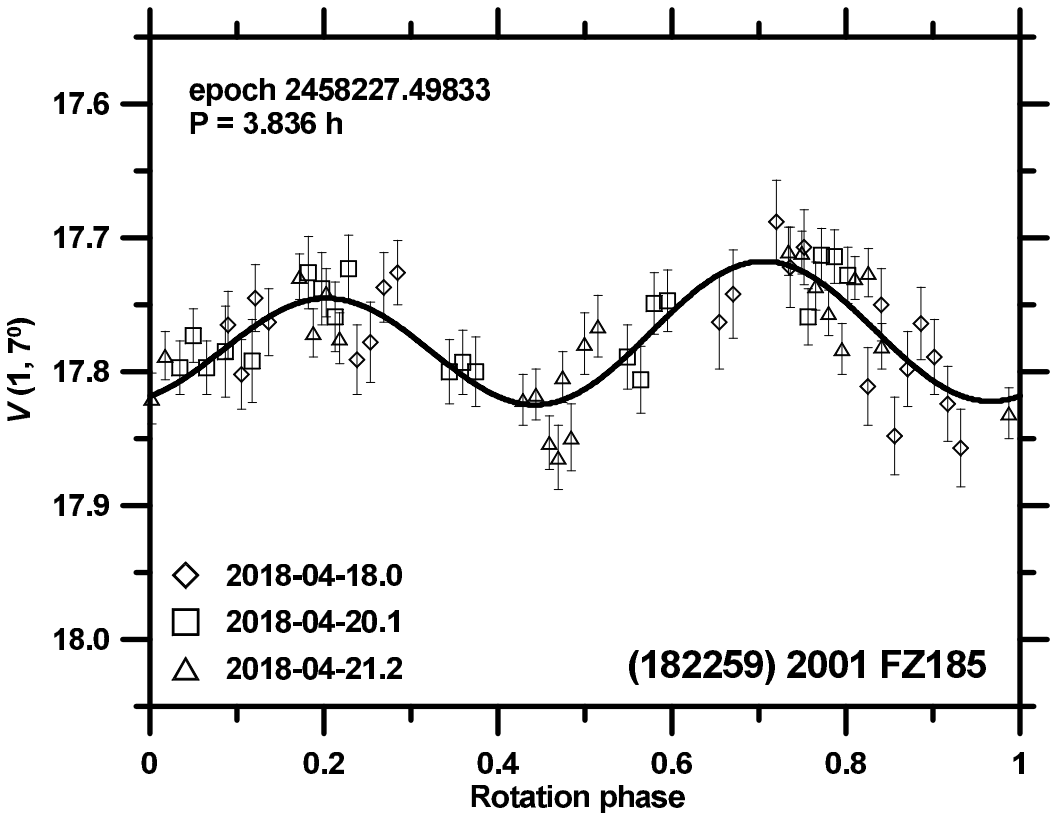

Suppl. Fig. 8. Composite lightcurve of (182259) 2001 FZ185 from 2018.

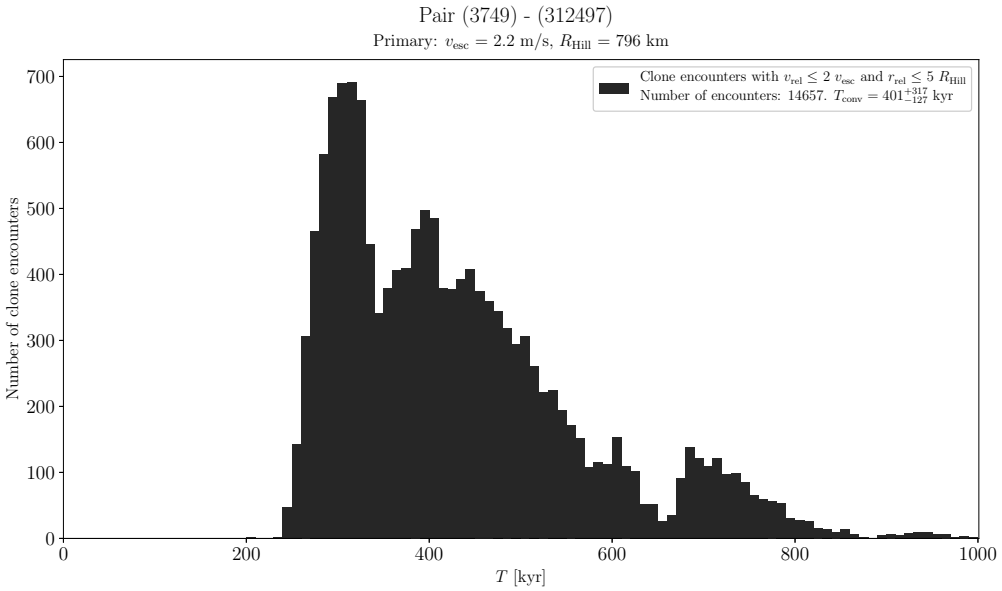

Suppl. Fig. 9. Distribution of past times of close and slow primary–secondary clone encounters for the asteroid pair 3749–312497.

(3749) Balam and (312497) 2009 BR60

This is a secure asteroid pair with an estimated age about 400 kyr (Suppl. Fig. 9). We obtained lightcurve data for the primary (3749) from 6 apparitions. Observations taken from Wise Observatory in 2007, 2009, 2010 and 2011-2012 were published in Polishook (2011, 2014), and the data from Via Capote from 2012 is available in the ALCDEF archive. We observed it with PROMPT on 10 nights during 2007-07-15 to 2007-10-07, from Ondřejov, Abastumani, PROMPT, Modra, Skalnaté Pleso and Pic du Midi on 17 nights during 2012-01-14 to 2012-03-25, from Sugarloaf Mountain, PROMPT, Blauvac, Sozzago, Ondřejov and Sierra Nevada on 14 nights during 2014-10-03 to 2014-11-22, and from Sugarloaf Mountain, Sierra Nevada, Ondřejov and IAC80 on 15 nights during 2017-09-11 to 2017-11-12 (Suppl. Figs. 10 to 17). From the Ondřejov observations that were calibrated in the Cousins R system, we derived the mean absolute R magnitude of the whole system (outside mutual events) $H_{R,1} = 13.08 \pm 0.05$ and the phase relation slope parameter $G = 0.23 \pm 0.08$. For conversion to $H_1 \equiv H_{V,1}$, we assumed the color index $(V-R) = 0.49 \pm 0.05$ that is the mean value for S type asteroids (Pravec et al. 2012b), which is a likely taxonomic type for Balam (Marchis et al. 2011).

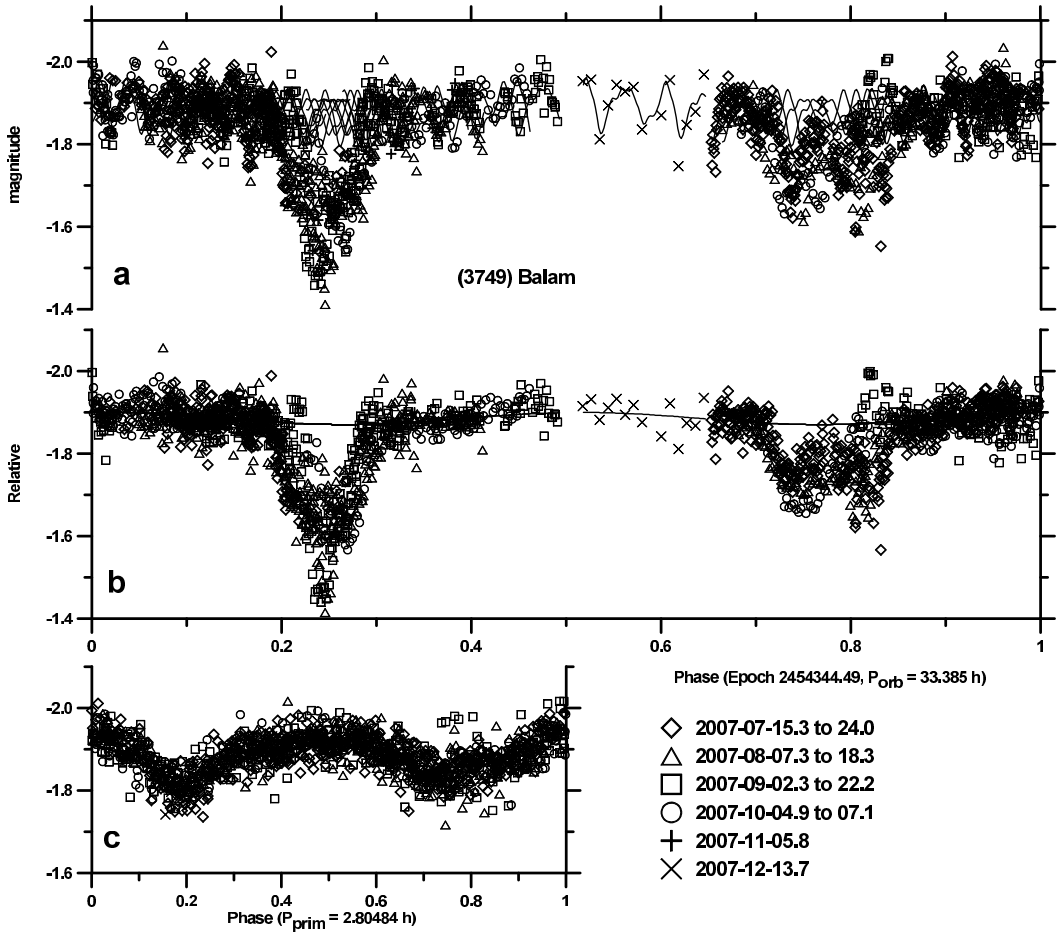

Suppl. Fig. 10. Lightcurve data of (3749) Balam from 2007. (a) The original data showing all the lightcurve components, folded with the orbital period. (b) The orbital (plus secondary rotational) lightcurve component(s), derived after subtraction of the primary lightcurve component, showing the mutual events between components of the binary system, superimposed to the secondary rotational lightcurve if present. (c) The primary lightcurve component.

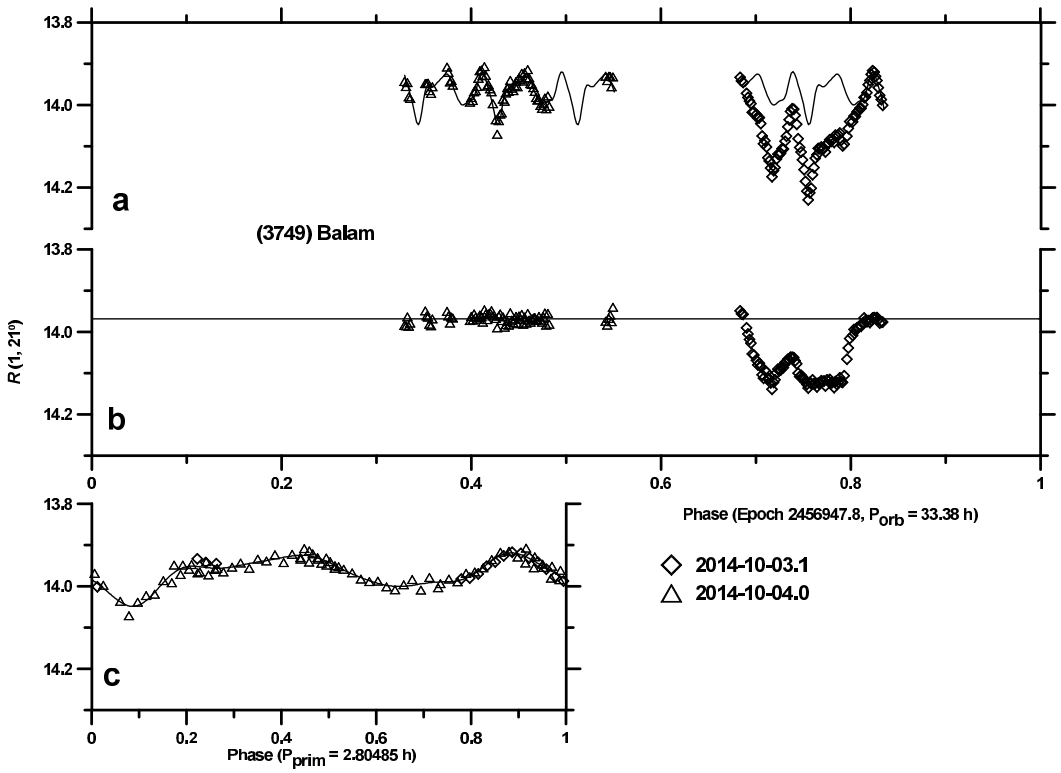

Suppl. Fig. 11. Lightcurve data of (3749) Balam from 2014 (part 1). (a) The original data showing all the lightcurve components, folded with the orbital period. (b) The orbital (plus secondary rotational) lightcurve component(s), derived after subtraction of the primary lightcurve component, showing the mutual events between components of the binary system, superimposed to the secondary rotational lightcurve if present. (c) The primary lightcurve component.

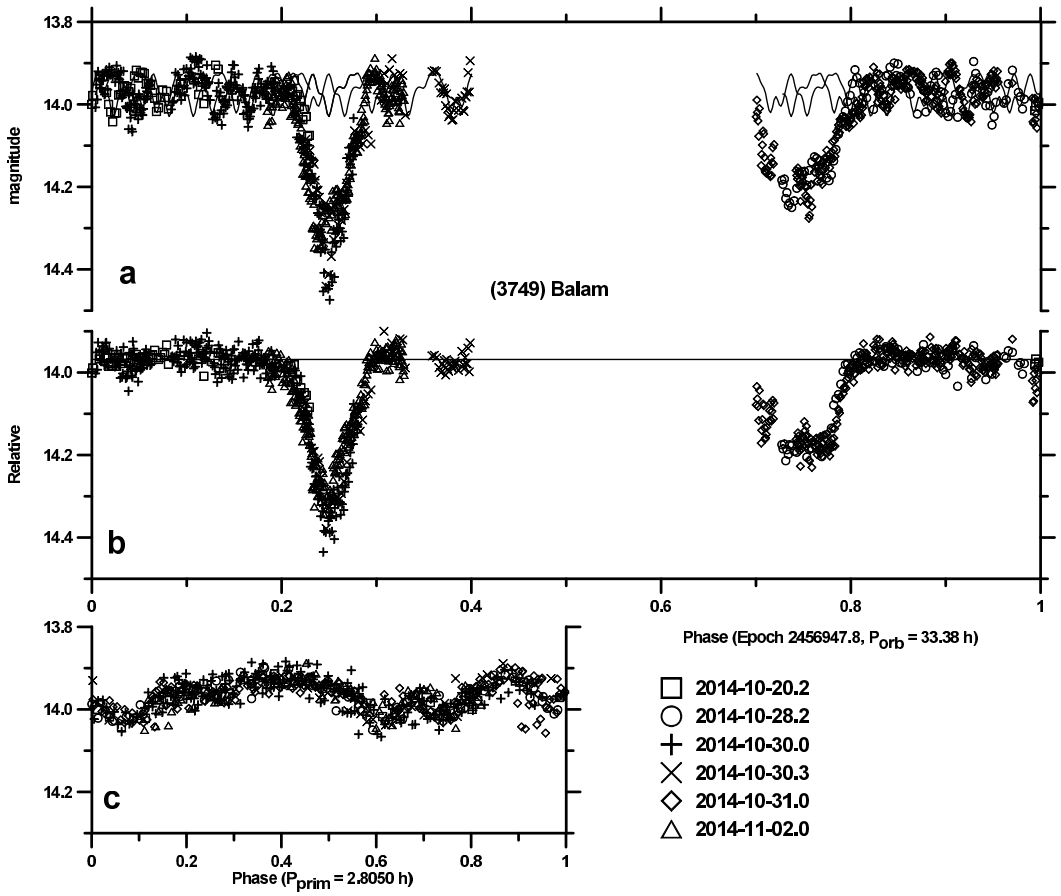

Suppl. Fig. 12. Lightcurve data of (3749) Balam from 2014 (part 2). (a) The original data showing all the lightcurve components, folded with the orbital period. (b) The orbital (plus secondary rotational) lightcurve component(s), derived after subtraction of the primary lightcurve component, showing the mutual events between components of the binary system, superimposed to the secondary rotational lightcurve if present. (c) The primary lightcurve component.

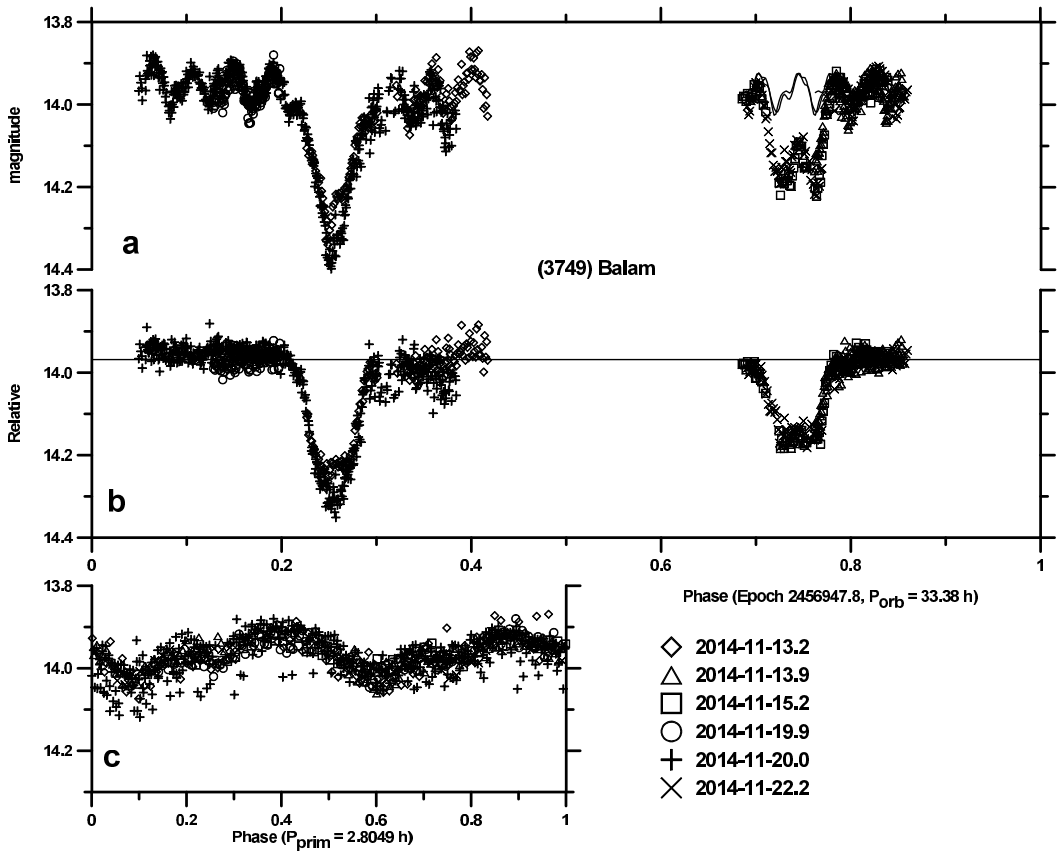

Suppl. Fig. 13. Lightcurve data of (3749) Balam from 2014 (part 3). (a) The original data showing all the lightcurve components, folded with the orbital period. (b) The orbital (plus secondary rotational) lightcurve component(s), derived after subtraction of the primary lightcurve component, showing the mutual events between components of the binary system, superimposed to the secondary rotational lightcurve if present. (c) The primary lightcurve component.

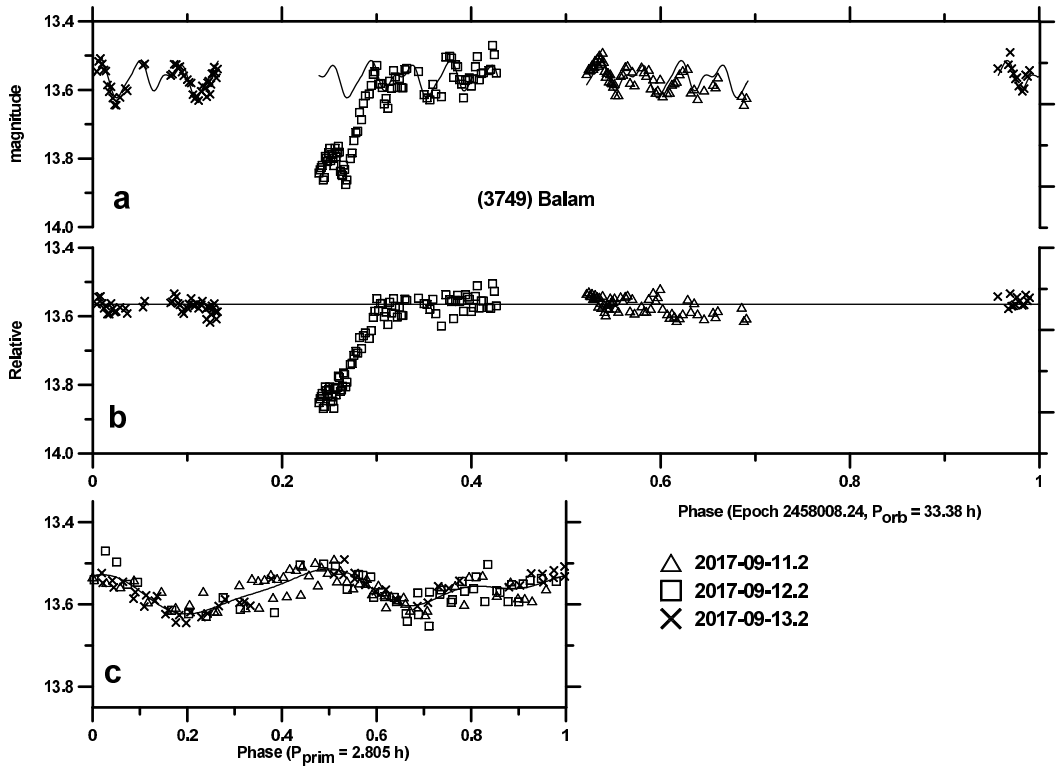

Suppl. Fig. 14. Lightcurve data of (3749) Balam from 2017 (part 1). (a) The original data showing all the lightcurve components, folded with the orbital period. (b) The orbital (plus secondary rotational) lightcurve component(s), derived after subtraction of the primary lightcurve component, showing the mutual events between components of the binary system, superimposed to the secondary rotational lightcurve if present. (c) The primary lightcurve component.

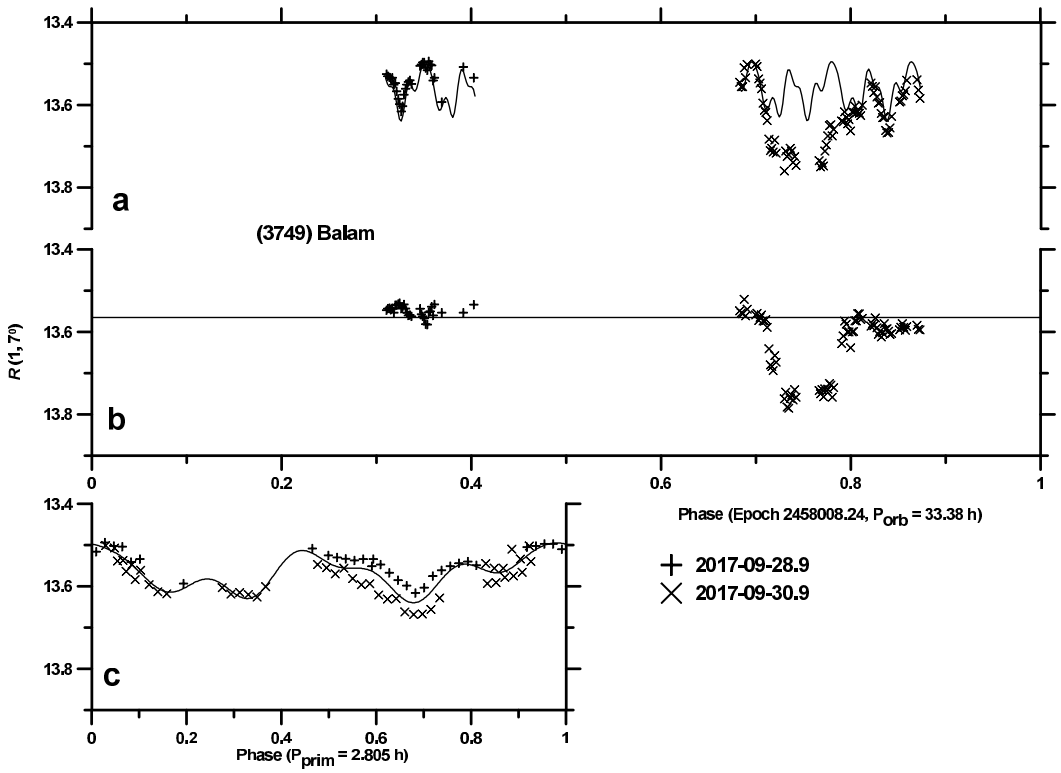

Suppl. Fig. 15. Lightcurve data of (3749) Balam from 2017 (part 2). (a) The original data showing all the lightcurve components, folded with the orbital period. (b) The orbital (plus secondary rotational) lightcurve component(s), derived after subtraction of the primary lightcurve component, showing the mutual events between components of the binary system, superimposed to the secondary rotational lightcurve if present. (c) The primary lightcurve component.

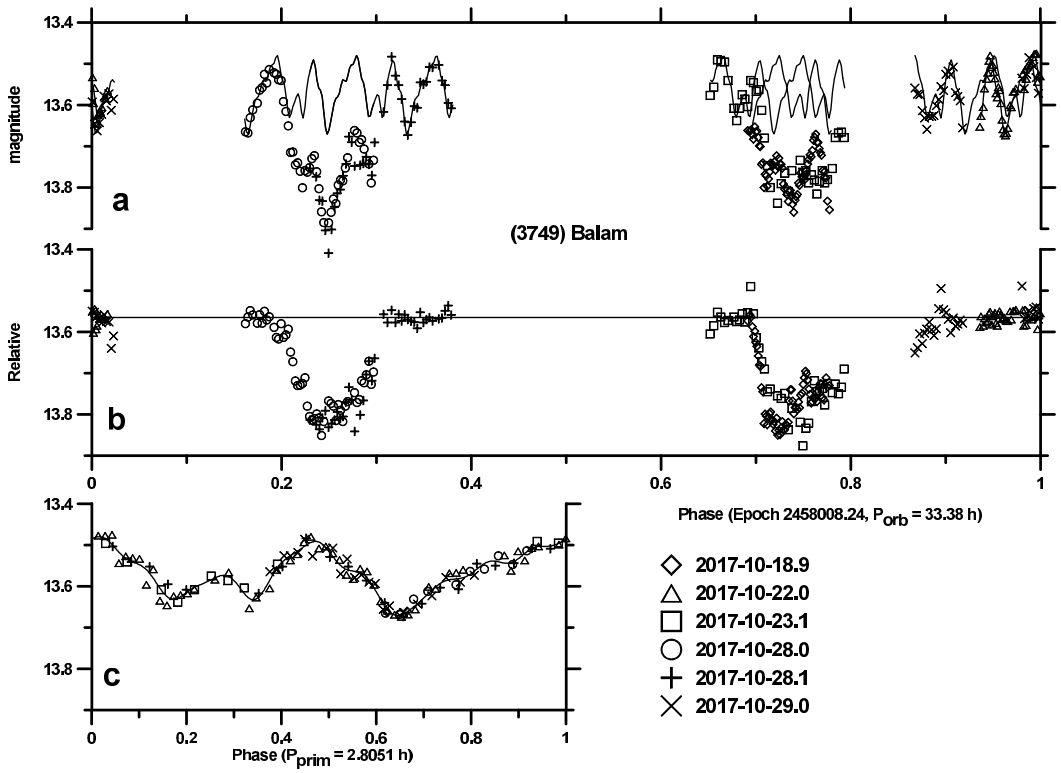

Suppl. Fig. 16. Lightcurve data of (3749) Balam from 2017 (part 3). (a) The original data showing all the lightcurve components, folded with the orbital period. (b) The orbital (plus secondary rotational) lightcurve component(s), derived after subtraction of the primary lightcurve component, showing the mutual events between components of the binary system, superimposed to the secondary rotational lightcurve if present. (c) The primary lightcurve component.

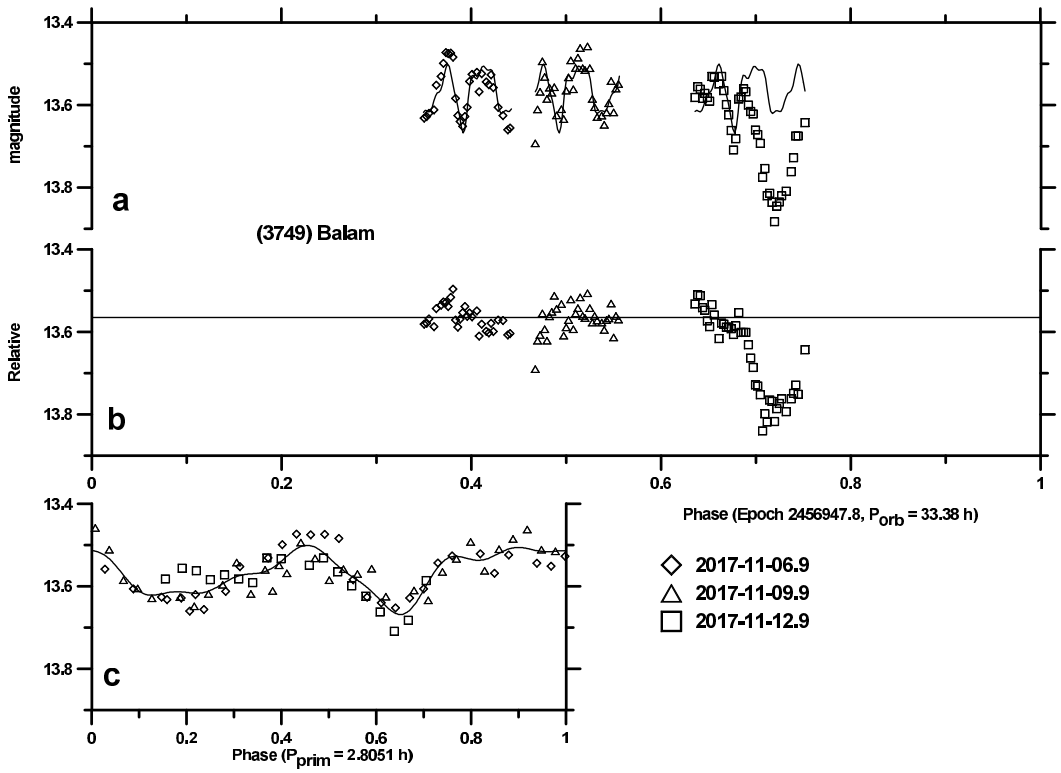

Suppl. Fig. 17. Lightcurve data of (3749) Balam from 2017 (part 4). (a) The original data showing all the lightcurve components, folded with the orbital period. (b) The orbital (plus secondary rotational) lightcurve component(s), derived after subtraction of the primary lightcurve component, showing the mutual events between components of the binary system, superimposed to the secondary rotational lightcurve if present. (c) The primary lightcurve component.

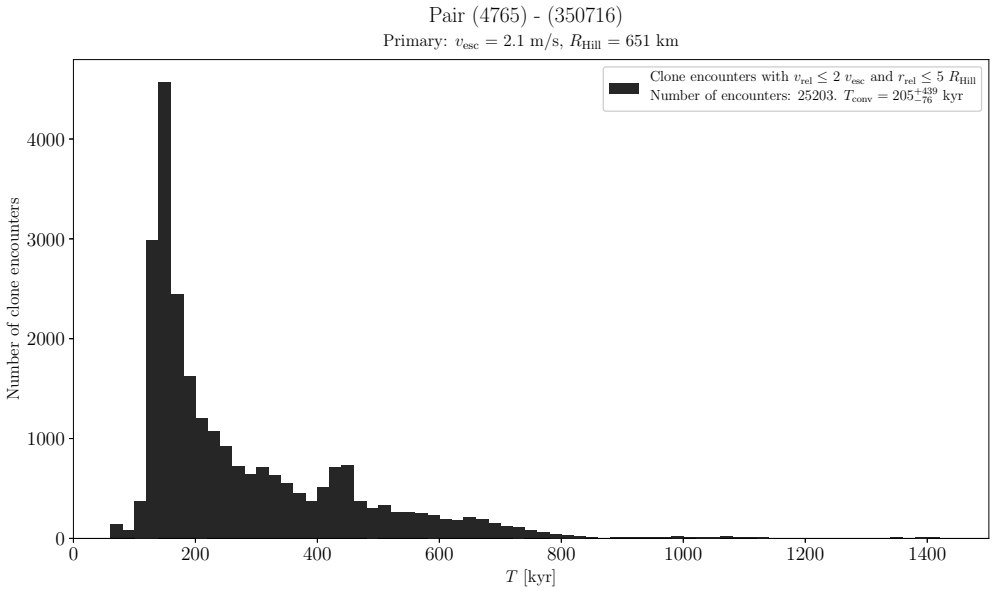

Suppl. Fig. 18. Distribution of past times of close and slow primary–secondary clone encounters for the asteroid pair 4765–350716.

(4765) Wasserburg and (350716) 2001 XO105

Backward orbital clone integrations suggest that these two asteroids separated about 200 kyr ago (Suppl. Fig. 18). We obtained lightcurve data for the primary (4765) from 6 apparitions. Observations taken from Palmer Divide Observatory and Center for Solar System Studies in 2006, 2010, 2013 and 2014 were published by Warner (2007, 2010, 2015) and Warner and Stephens (2013). Observations taken from Cerro Tololo and Modra in 2008 and 2010, respectively, were published in Pravec et al. (2010). Observations taken from Leura in 2014 were published by Oey (2016). We observed it from Sugarloaf Mountain and Wise on 8 nights during 2013-01-12 to 2013-05-05, from Sugarloaf Mountain and PROMPT on 4 nights during 2014-10-28 to 2014-11-21, and from Sugarloaf Mountain on 2 nights of 2017-12-17 and 2018-01-10. For estimation of D_1 from H_1, we assumed $p_{V,1} = 0.40$ as we assume it is an E-type Hungaria asteroid.

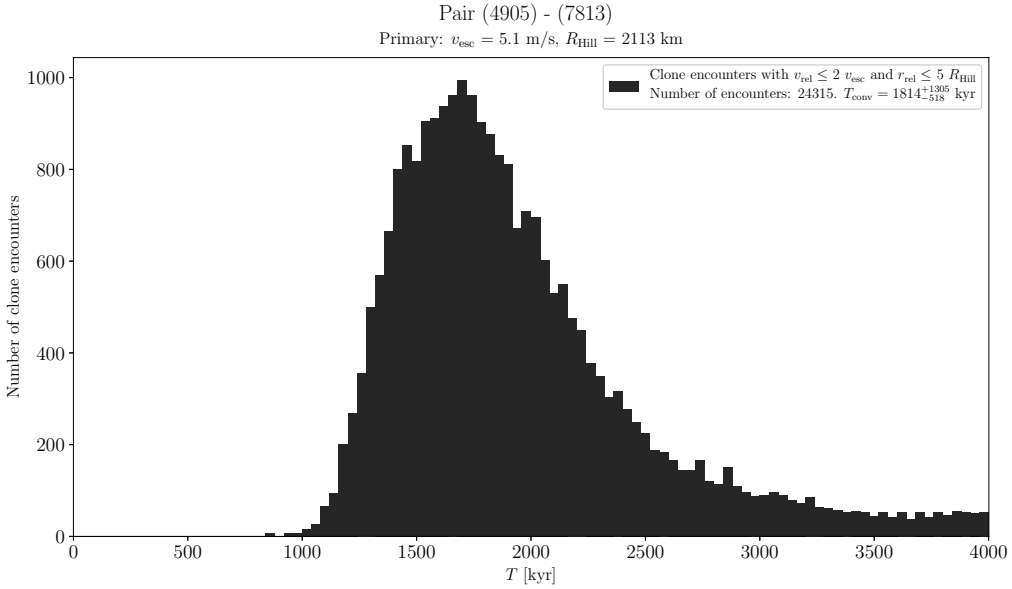

Suppl. Fig. 19. Distribution of past times of close and slow primary–secondary clone encounters for the asteroid pair 4905–7813.

(4905) Hiromi and (7813) Anderserikson

Backward orbital clone integrations suggest that these two asteroids separated about 1.8 Myr ago (Suppl. Fig. 19). We obtained lightcurve data for the primary (4905) from 4 apparitions. Observations taken from Leura and Wise in 2013 were published in Oey (2014) and Polishook (2014a). We observed it from from Sugarloaf Mountain and Lowell on 6 nights during 2013-09-24 to 2013-12-24, from Simeiz and Kharkiv on 2 nights 2012-06-17 and 2012-07-22, from Ondřejov and PROMPT on 3 nights during 2015-01-28 to 2015-02-14, and from Sugarloaf Mountain on 3 nights during 2017-08-22 to 2017-11-18. From the Ondřejov data of 2015-02-09 and -14 that were calibrated in the Cousins R system, we derived its mean absolute R magnitude $H_{R,1} = 11.94 \pm 0.06$, assuming the slope parameter $G = 0.24 \pm 0.11$. With its $(V-R)_1 = 0.49 \pm 0.03$ (Table 2), we obtained $H_1 = 12.43 \pm 0.07$. Figure 20 shows the primary's nominal spin pole solution and its uncertainty area. The second isolated area around $(L, B) = (30°, -62°)$ is also formally allowed within 3σ, but it is not considered likely as the reduced χ^2 values are substantially higher there than around the nominal pole solution. We observed the secondary (7813) from Sugarloaf Mountain and Ondřejov on 13 nights during 2014-08-20 to 2014-09-20 and derived its mean absolute R magnitude $H_{R,2} = 12.94 \pm 0.08$, assuming the slope parameter $G = 0.24 \pm 0.11$. With its $(V-R)_2 = 0.46 \pm 0.03$ (Table 2), we obtained $H_2 = 13.40 \pm 0.09$. The period $P_2 = 13.277 \pm 0.002$ h is likely, but values twice or thrice that are not ruled out (Suppl. Fig. 21).

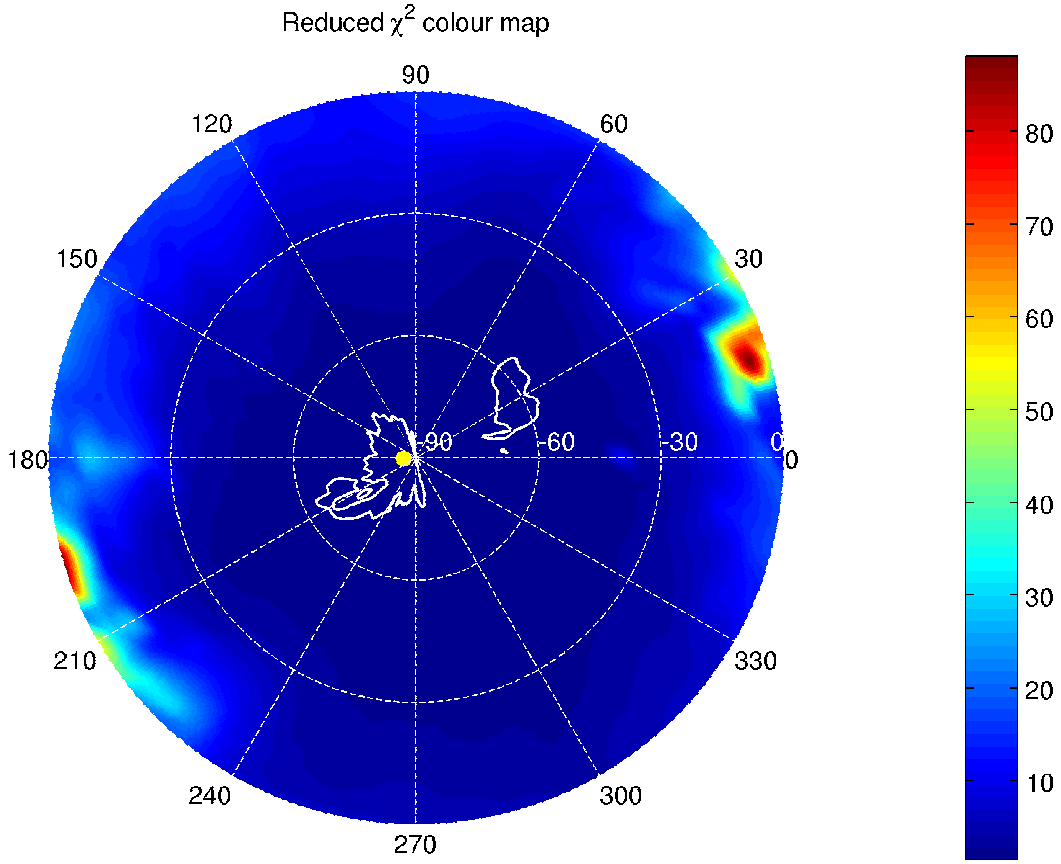

Suppl. Fig. 20. The nominal spin pole solution (yellow dot) and the 3-σ pole uncertainty area (white boundary) for (4905) Hiromi.

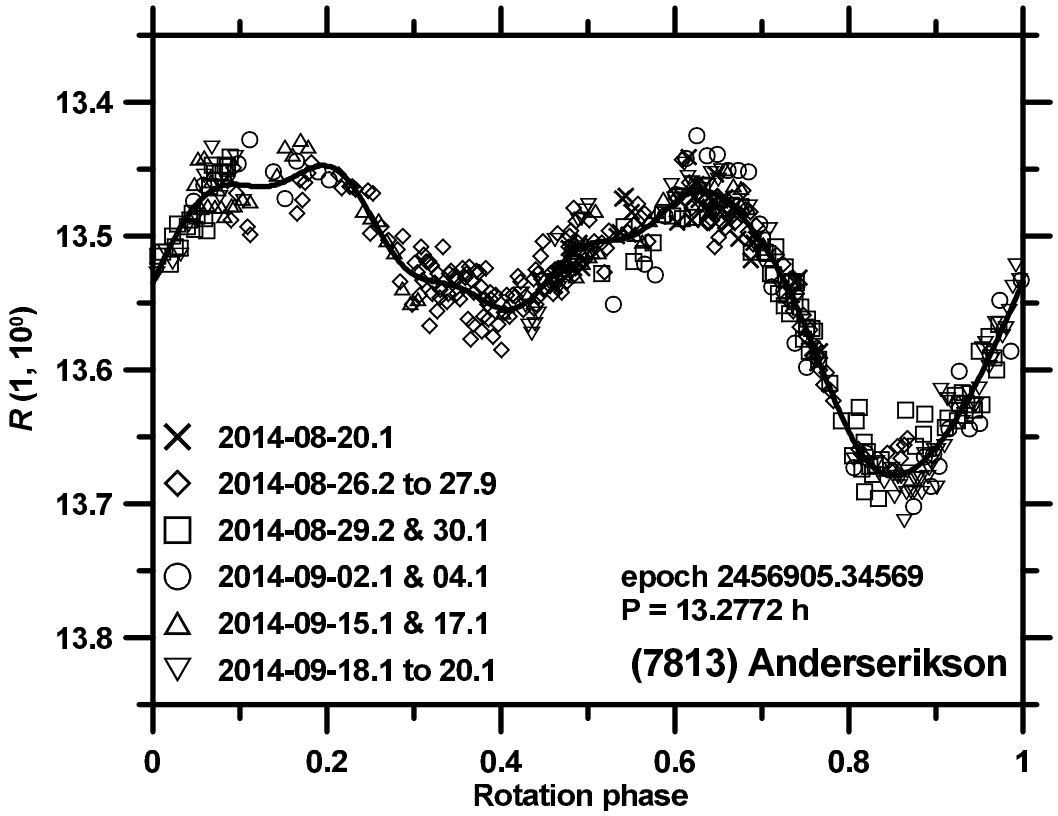

Suppl. Fig. 21. Composite lightcurves of (7813) Anderserikson from 2014.

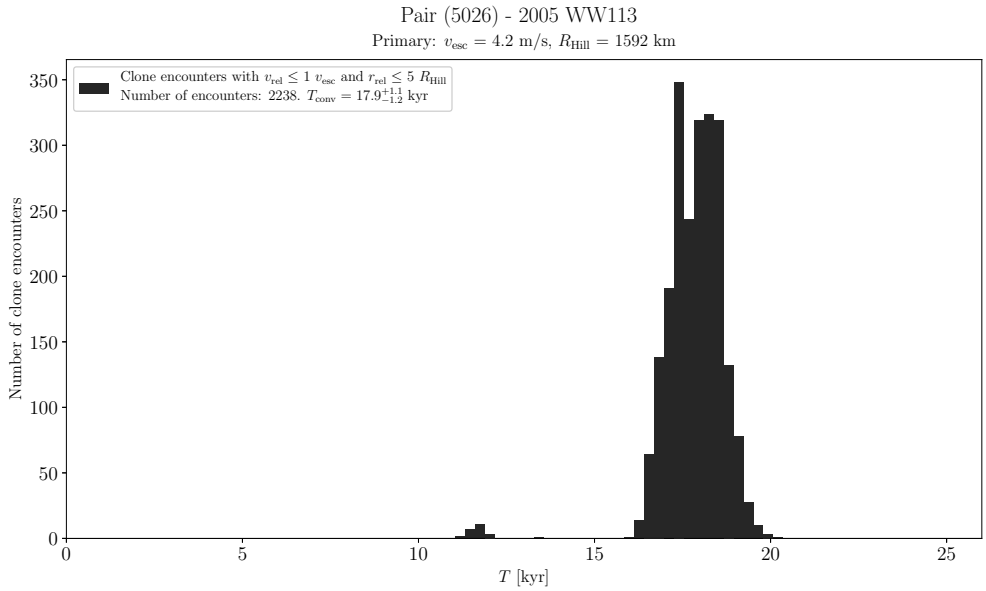

Suppl. Fig. 22. Distribution of past times of close and slow primary–secondary clone encounters for the asteroid pair 5026–2005WW113.

(5026) Martes and 2005 WW113

Backward orbital clone integrations suggest that these two asteroids separated 18 ± 1 kyr ago (Suppl. Fig. 22). We obtained lightcurve data for the primary (5026) from 6 apparitions. The observations taken in 2008-2009 and in 2011-2013 from Wise were published in Pravec et al. (2010) and Polishook (2014), respectively. We observed it from PROMPT and Dark Sky Observatory on 3 nights during 2012-04-11 to 2012-05-23, from La Hita, Sugarloaf Mountain and Simeiz on 9 nights during 2013-10-30 to 2013-12-06, and from La Silla on the night 2018-02-08. From the La Silla observations that were taken in the Johnson-Cousins VR system, we derived its mean absolute magnitude $H_1 = 14.18 \pm 0.24$, assuming $G = 0.15 \pm 0.20$.

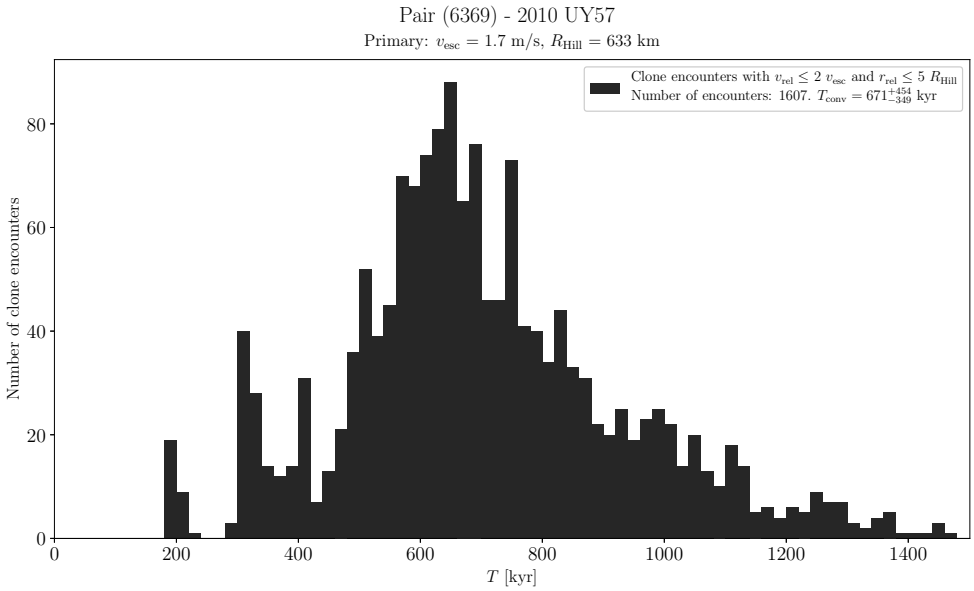

Suppl. Fig. 23. Distribution of past times of close and slow primary–secondary clone encounters for the asteroid pair 6369–510132.

(6369) 1983 UC and (510132) 2010 UY57

The estimated age of this asteroid pair is about 700 kyr (Suppl. Fig. 23). We observed the asteroid (6369) from La Silla on 8 nights during 2013-03-12 to 2003-04-17 and on 6 nights during 2016-02-02 to 2016-02-13. The lightcurve from the 2nd apparition is shown in Suppl. Fig. 24. We derived the same mean absolute magnitude $H_1 = 14.63$ in both apparitions (formal errors 0.04 and 0.06 mag) with the phase relation slope parameter $G = 0.44 \pm 0.06$ and 0.50 ± 0.10, respectively.

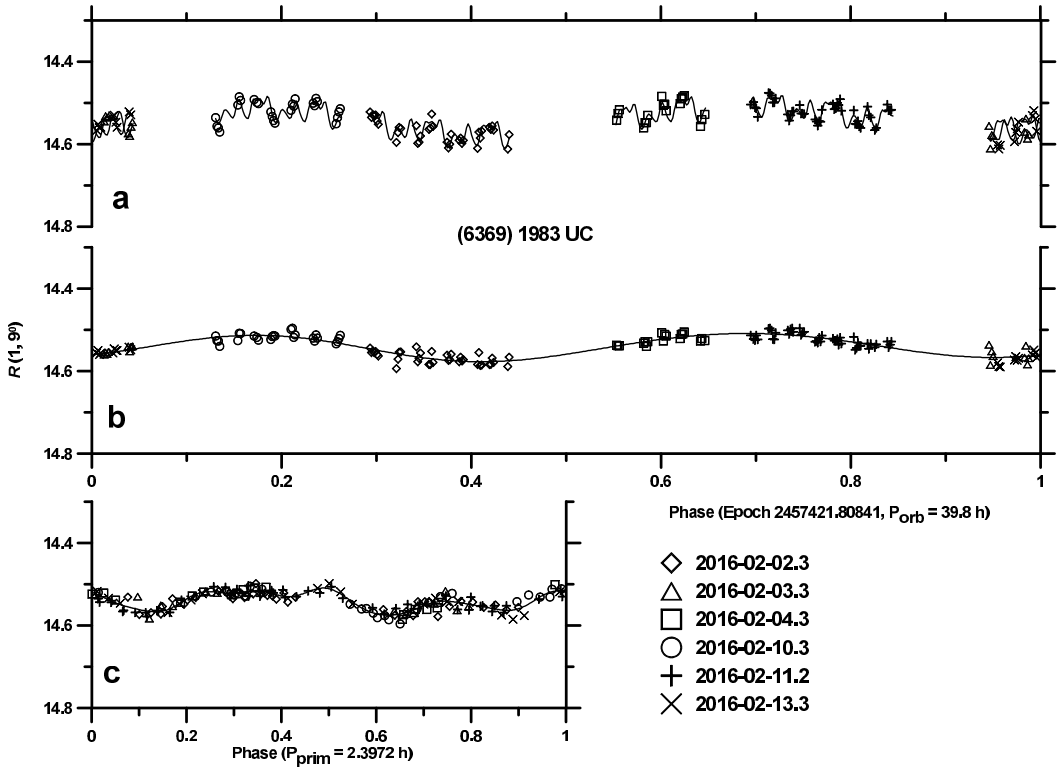

Suppl. Fig. 24. Lightcurve data of (6369) 1983 UC from 2016. (a) The original data showing all the lightcurve components, folded with the orbital period. (b) The secondary rotational lightcurve component, derived after subtraction of the primary lightcurve component; mutual events between the system's components were not present. (c) The primary lightcurve component.

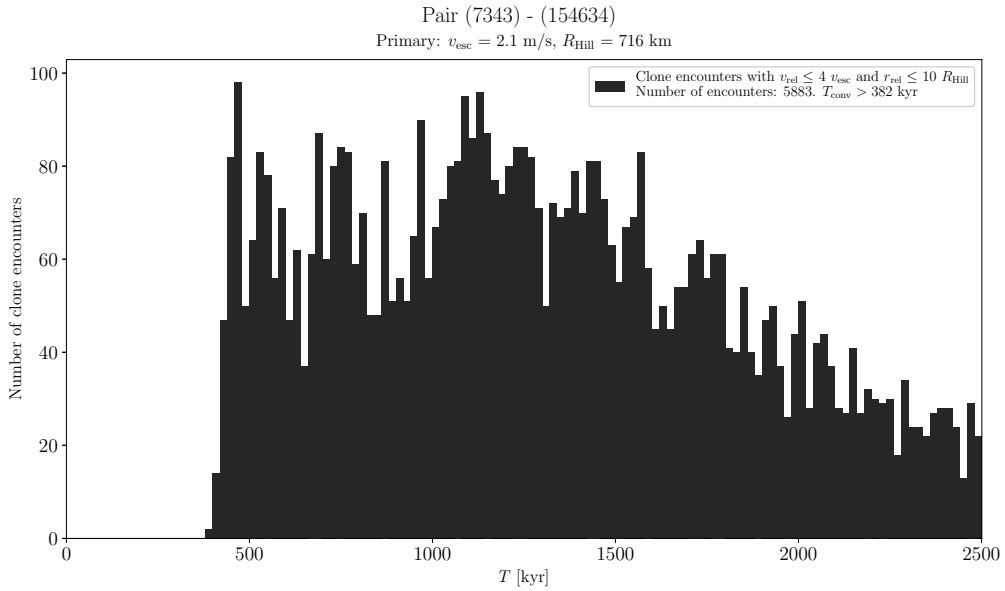

Suppl. Fig. 25. Distribution of past times of close and slow primary–secondary clone encounters for the asteroid pair 7343–154634.

(7343) Ockeghem and (154634) 2003 XX38

For this asteroid pair, we estimate a lower limit on its age of 382 kyr (Suppl. Fig. 25). We have obtained lightcurve data for (7343) from 5 apparitions. Observations taken from Wise in 2009, 2011 and 2013-2014 were published in Pravec et al. (2010) and Polishook (2014). We observed it from Modra, Skalnaté Pleso and SRO on 9 nights during 2011-01-28 to 2011-03-04.0, from Sugarloaf Mountain, La Hita, Abastumani, Simeiz and Pic du Midi on 11 nights during 2013-11-24 to 2014-02-05, from Sugarloaf Mountain on 10 nights during 2016-09-23 to 2016-12-26, and from La Silla on 4 nights 2018-03-14 to 2018-03-23. From the 2018 observations that were absolutely calibrated in the Johnson-Cousins VR system, we obtained $(V - R)_1 = 0.465 \pm 0.010$ and derived the mean absolute magnitude $H_1 = 14.31 \pm 0.11$, assuming the slope parameter $G = 0.24 \pm 0.11$ that is the mean value for S type asteroids.

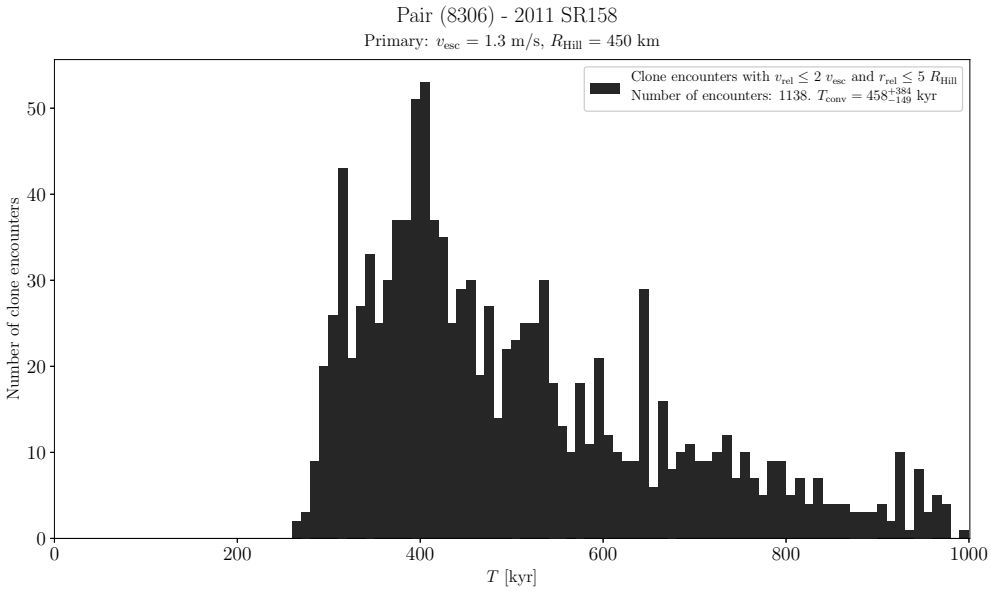

Suppl. Fig. 26. Distribution of past times of close and slow primary–secondary clone encounters for the asteroid pair 8306–2011SR158.

(8306) Shoko and 2011 SR158

The estimated age of this asteroid pair is about 400 kyr (Suppl. Fig. 26). From our observations taken in 2013–2014 and 2015, we derived the mean absolute magnitudes of the whole primary system (outside mutual events) $H_1 = 15.27 \pm 0.04$ and 15.25 ± 0.04, with the phase relation slope parameters $G = 0.19 \pm 0.03$ and 0.30 ± 0.05, respectively.

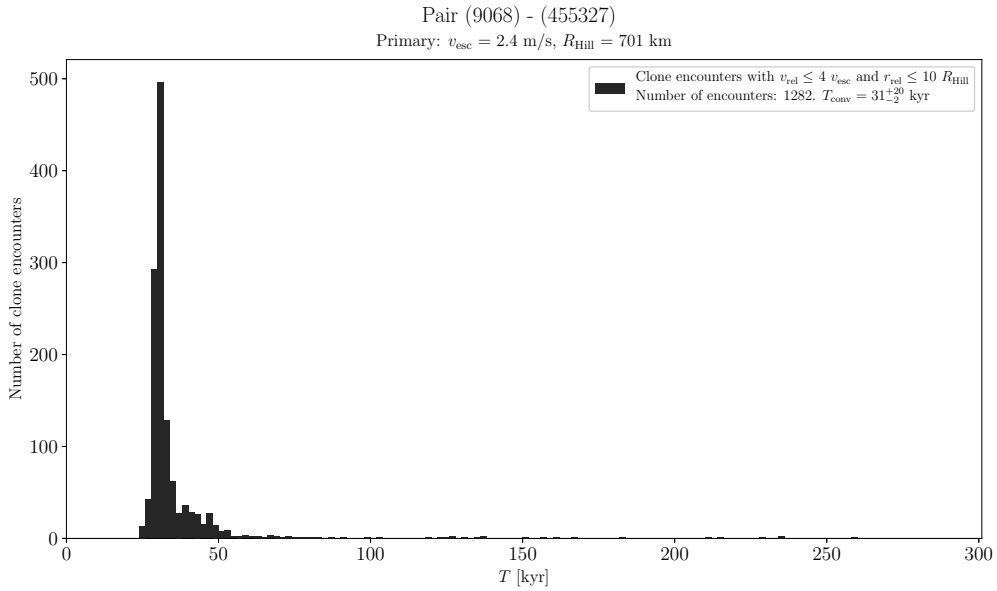

Suppl. Fig. 27. Distribution of past times of close and slow primary–secondary clone encounters for the asteroid pair 9068–455327.

(9068) 1993 OD and (455327) 2002 OP28

This is a young asteroid pair with an estimated age about 31 kyr (Suppl. Fig. 27). We have obtained lightcurve data for (9068) from 3 apparitions. The observations taken from Palmer Divide Observatory in 2008 and 2013 were published in Warner (2009, 2014). The observations taken from Leura in 2015 were published in Oey et al. (2017). We observed it from La Hita, Abastumani, Ondřejov and Skalnaté Pleso on 11 nights during 2013-10-25 to 2013-12-23 (Suppl. Fig. 28). From the two Ondřejov nights that were calibrated in the Cousins R system, we derived the mean absolute magnitude $H_{R,1} = 13.74 \pm 0.10$, assuming $G = 0.33 \pm 0.10$ that is the mean value for Hungarias. For conversion to $H_1 \equiv H_{V,1}$, we assumed $(V - R) = 0.45 \pm 0.10$.

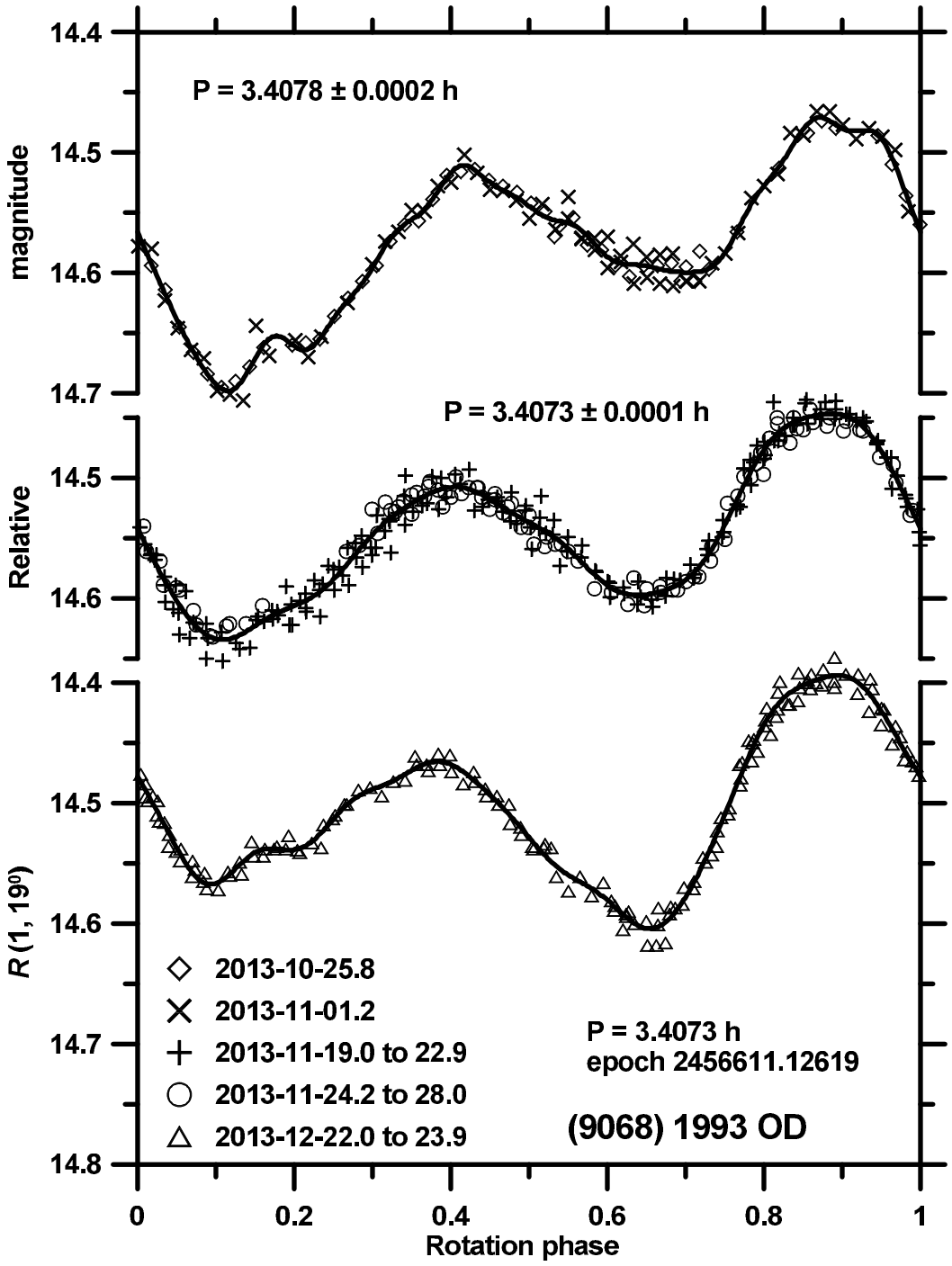

Suppl. Fig. 28. Composite lightcurves of (9068) 1993 OD from 2013.

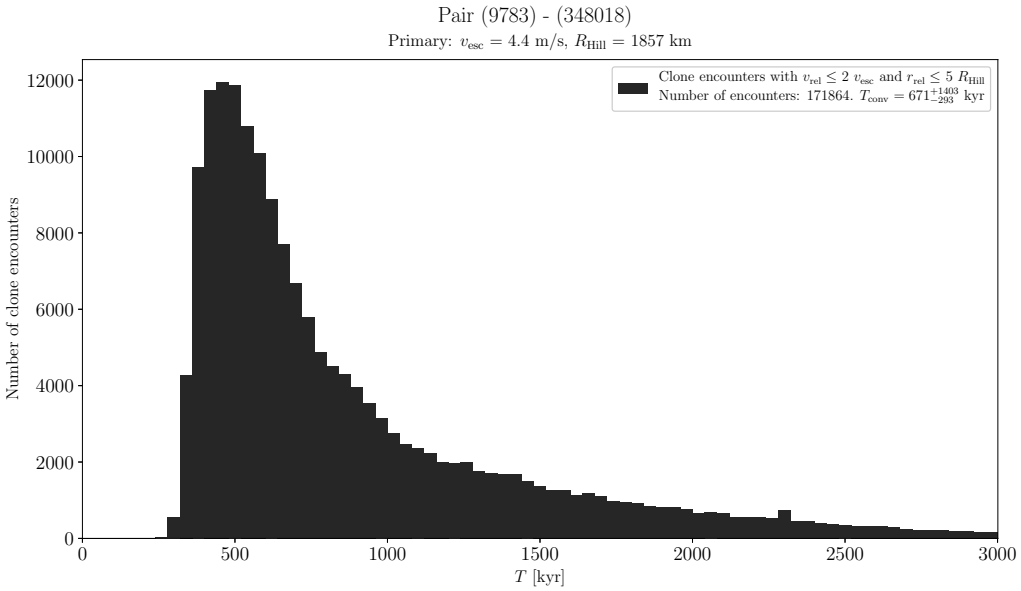

Suppl. Fig. 29. Distribution of past times of close and slow primary–secondary clone encounters for the asteroid pair 9783–348018.

(9783) Tensho-kan and (348018) 2003 SF334

The estimated age of this asteroid pair is about 600 kyr (Suppl. Fig. 29).

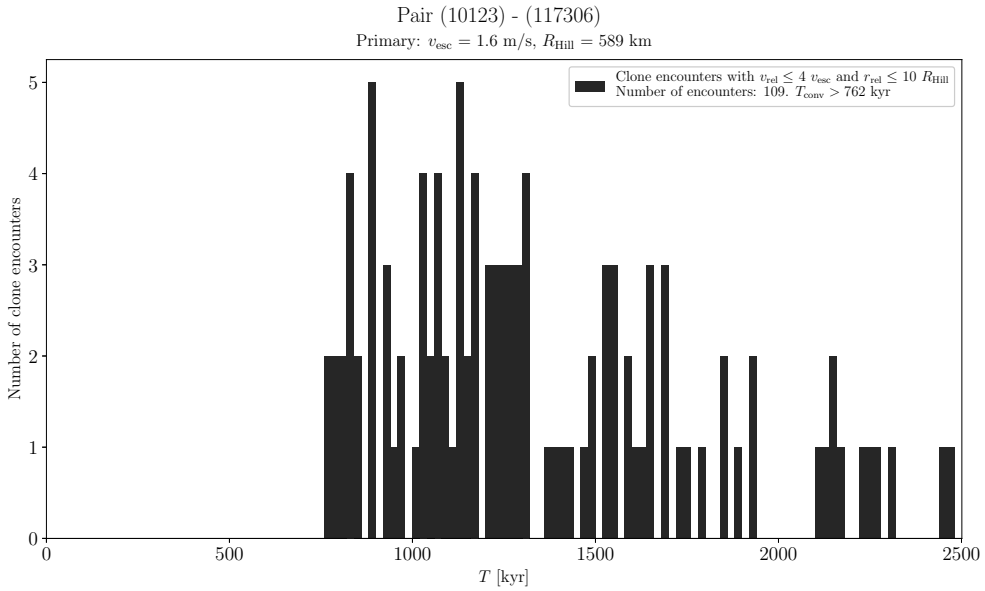

Suppl. Fig. 30. Distribution of past times of close and slow primary–secondary clone encounters for the asteroid pair 10123–117306.

(10123) Fideöja and (117306) 2004 VF21

Backward orbital clone integrations suggest that these two asteroids separated 1-2 Myr ago (Suppl. Fig. 30). For the primary (10123), we derived the mean absolute magnitudes of the whole system (outside mutual events) $H_1 = 14.54 \pm 0.03, 14.58 \pm 0.03$ and 14.54 ± 0.03 in 2010, 2013 and 2015–2016, with the phase relation slope parameter $G = 0.29 \pm 0.03$. We observed the unbound secondary (117306) from La Silla on 3 nights 2017-10-27 to 29 (Suppl. Fig. 31). We derived the mean absolute magnitude $H_2 = 16.82 \pm 0.04$, assuming the primary's $G = 0.29 \pm 0.03$.

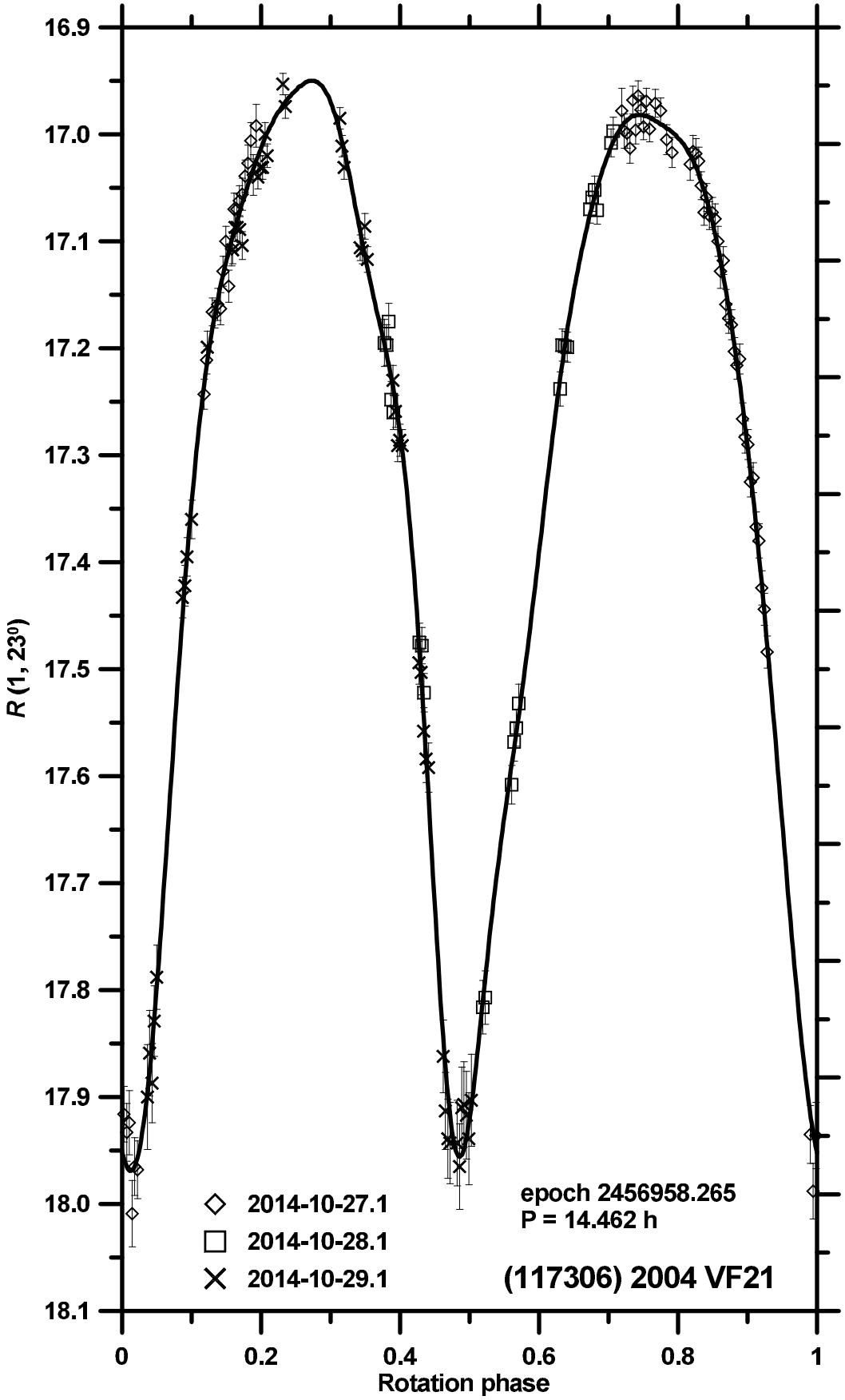

Suppl. Fig. 31. Composite lightcurve of (117306) 2004 VF21 from 2014.

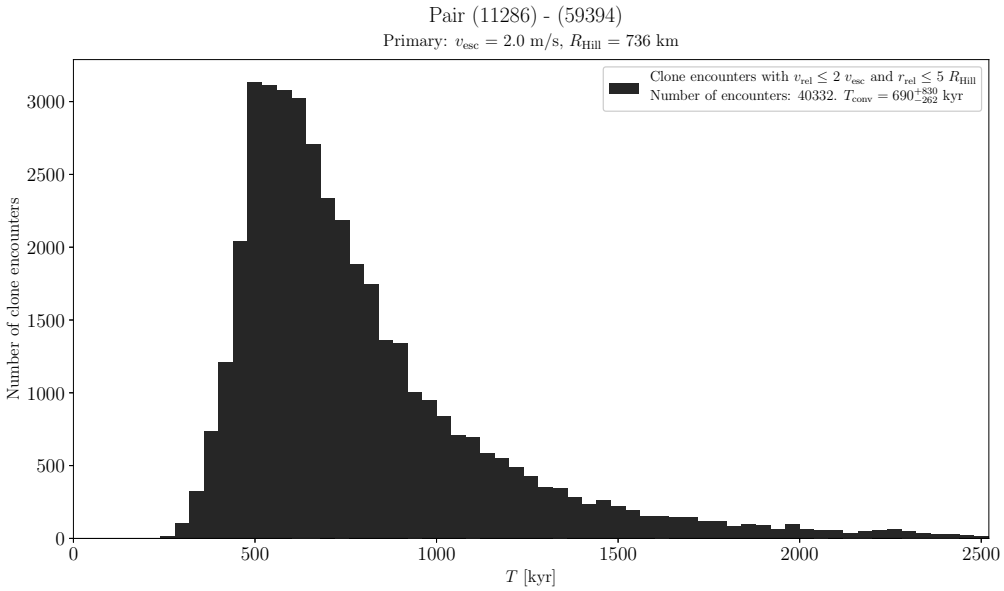

Suppl. Fig. 32. Distribution of past times of close and slow primary–secondary clone encounters for the asteroid pair 11286–59394.

(11286) 1990 RO8 and (59394) 1999 FZ23

The estimated age of this asteroid pair is about 700 kyr (Suppl. Fig. 32). We observed the primary (11286) from La Silla on 5 nights during 2016-11-08 to 2016-12-02 (Suppl. Fig. 33) and derived its mean absolute magnitude $H_1 = 14.85 \pm 0.20$, assuming the slope parameter $G = 0.15 \pm 0.20$. With this accurate H_1, we refined the WISE data by Masiero et al. (2011) and obtained $D_1 = 3.8 \pm 0.4$ km and $p_{V,1} = 0.14 \pm 0.04$. We observed the secondary (59394) from La Silla on 4 nights 2017-01-02 to -05 (Suppl. Fig. 34) and derived its mean absolute magnitude $H_2 = 15.66 \pm 0.06$, assuming the slope parameter $G = 0.15 \pm 0.20$.

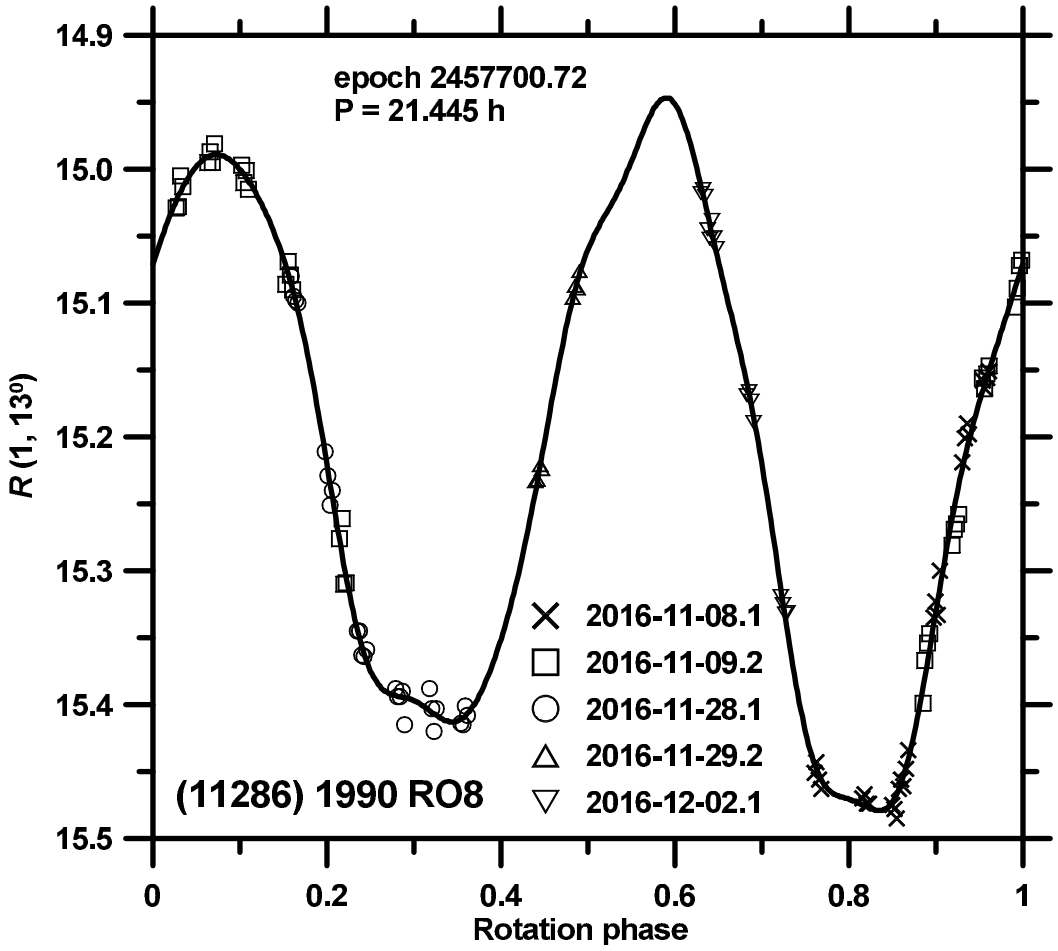

Suppl. Fig. 33. Composite lightcurve of (11286) 1990 RO8 from 2016.

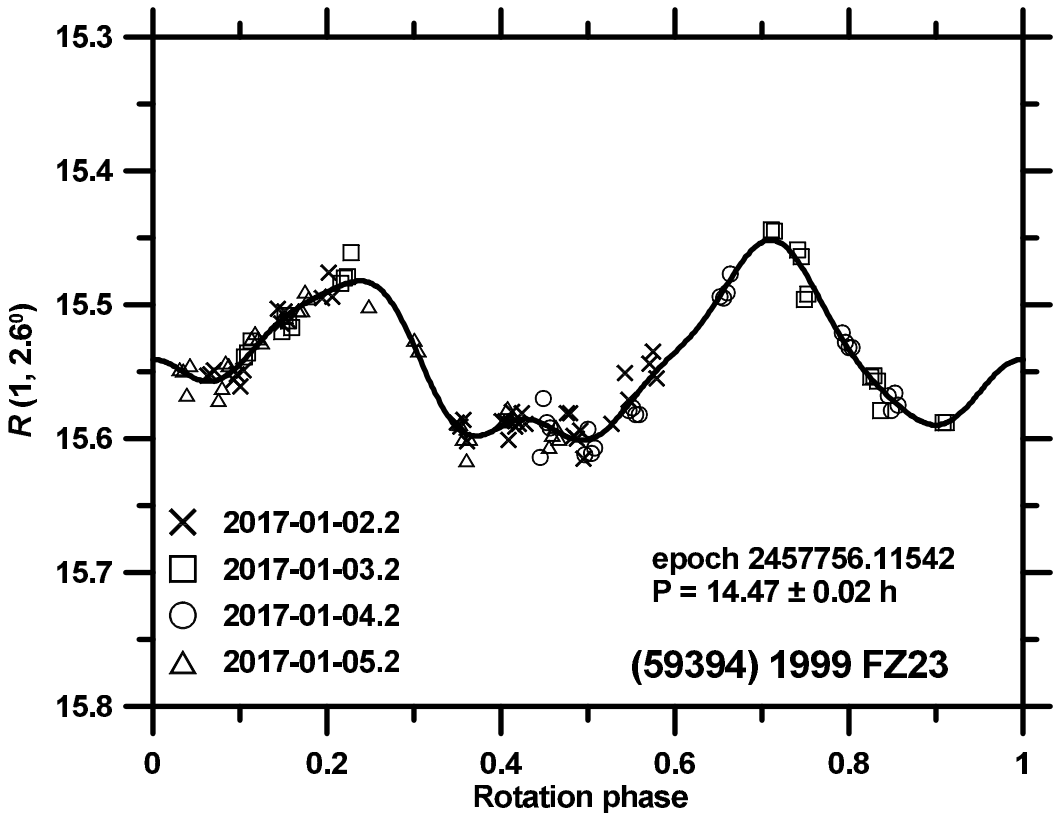

Suppl. Fig. 34. Composite lightcurve of (59394) 1999 FZ23 from 2017.

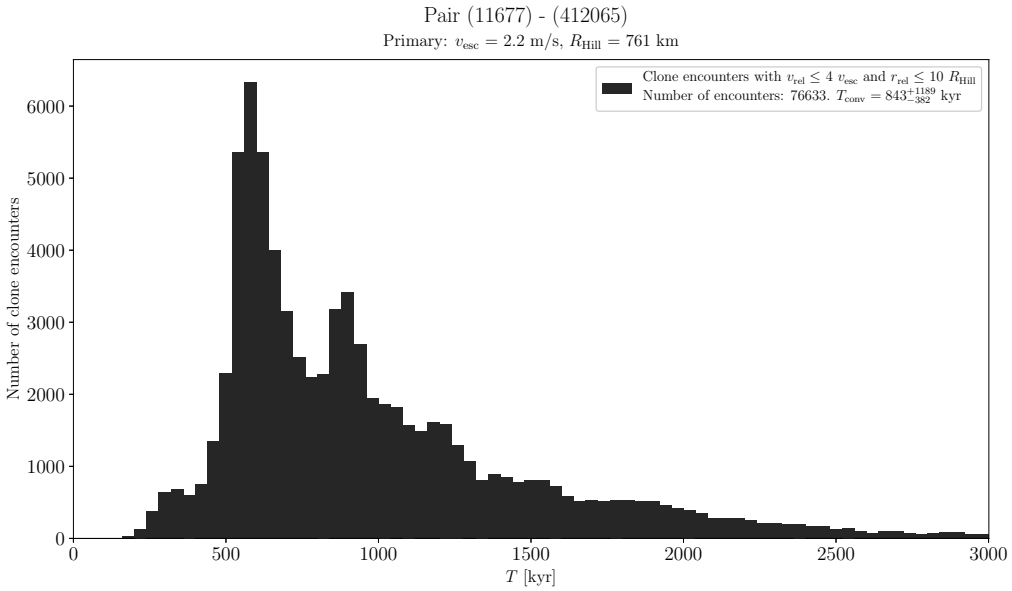

Suppl. Fig. 35. Distribution of past times of close and slow primary–secondary clone encounters for the asteroid pair 11677–412065.

(11677) 1998 DY4 and (412065) 2013 ET86

The estimated age of this asteroid pair is about 800 kyr (Suppl. Fig. 35). We have obtained lightcurve data for the primary (11677) from 3 apparitions. We observed it from Ondřejov, Sugarloaf Mountain and Abastumani on 6 nights during 2015-04-10 to 2015-05-15, and from La Silla on 2016-11-08 and 2018-02-16 (Suppl. Figs. 36 to 38). From the La Silla data that were taken in the Johnson–Cousins VR system, we derived the mean absolute magnitudes $H_1 = 14.55 \pm 0.06$ and 14.87 ± 0.09 at the two epochs, assuming the phase relation slope parameter $G = 0.24 \pm 0.11$. The absolute magnitude difference between the two epochs is real and it indicates that we observed the asteroid at a higher asterocentric latitude in 2016, which also corresponds to the much lower amplitude seen at that time.

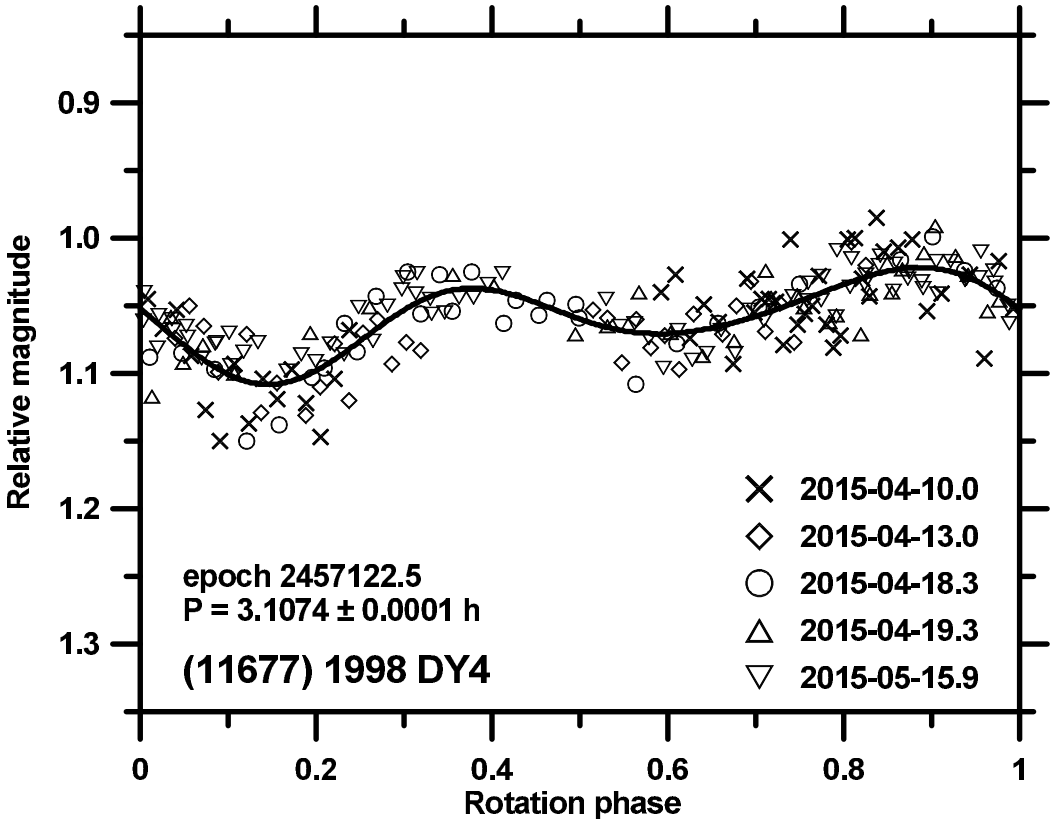

Suppl. Fig. 36. Composite lightcurve of (11677) 1998 DY4 from 2015.

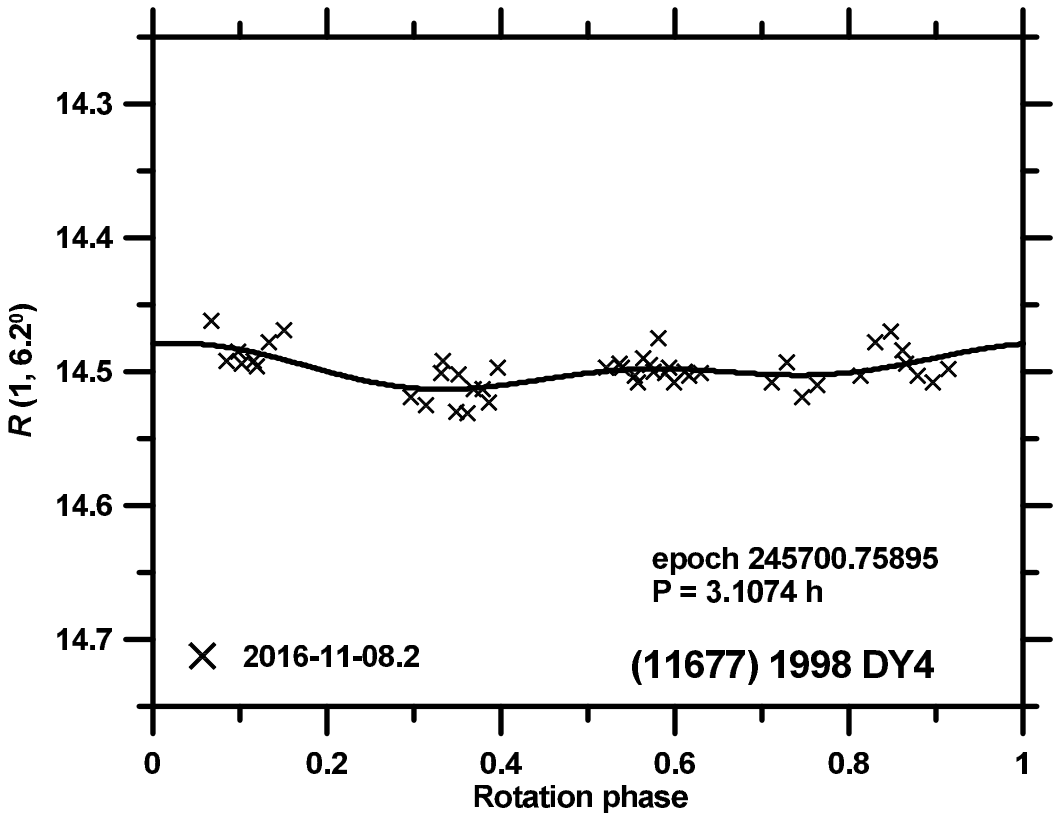

Suppl. Fig. 37. Composite lightcurve of (11677) 1998 DY4 from 2016.

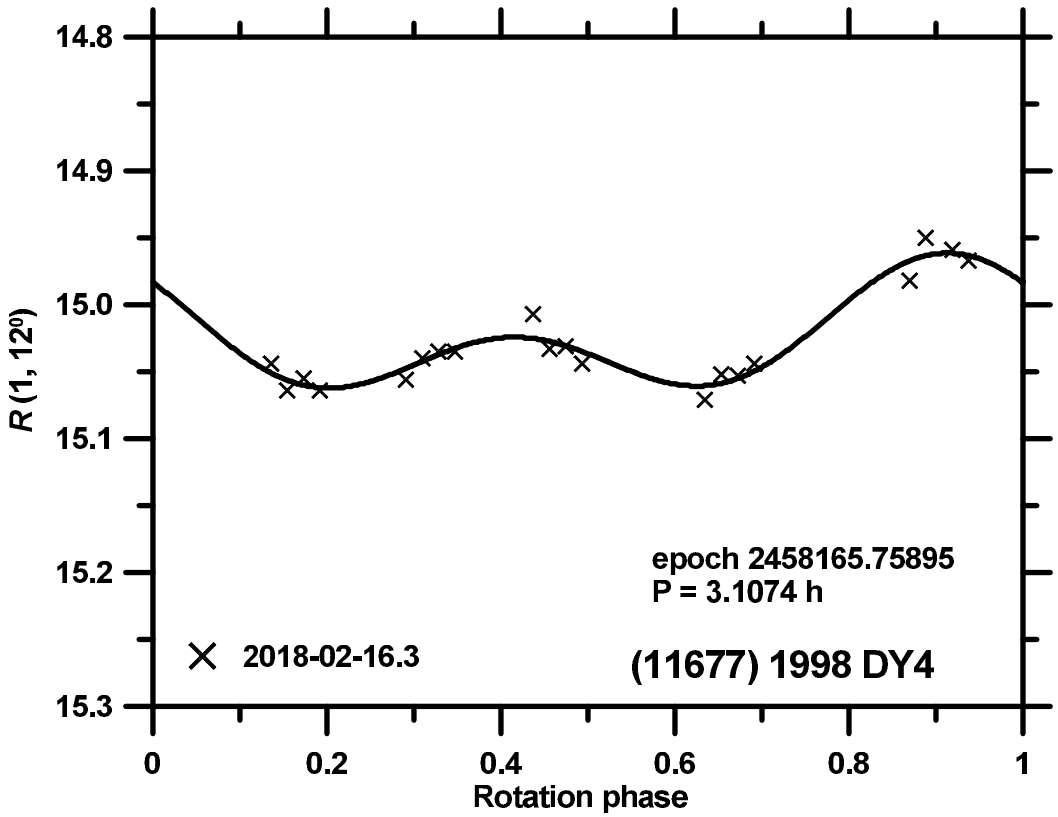

Suppl. Fig. 38. Composite lightcurve of (11677) 1998 DY4 from 2018.

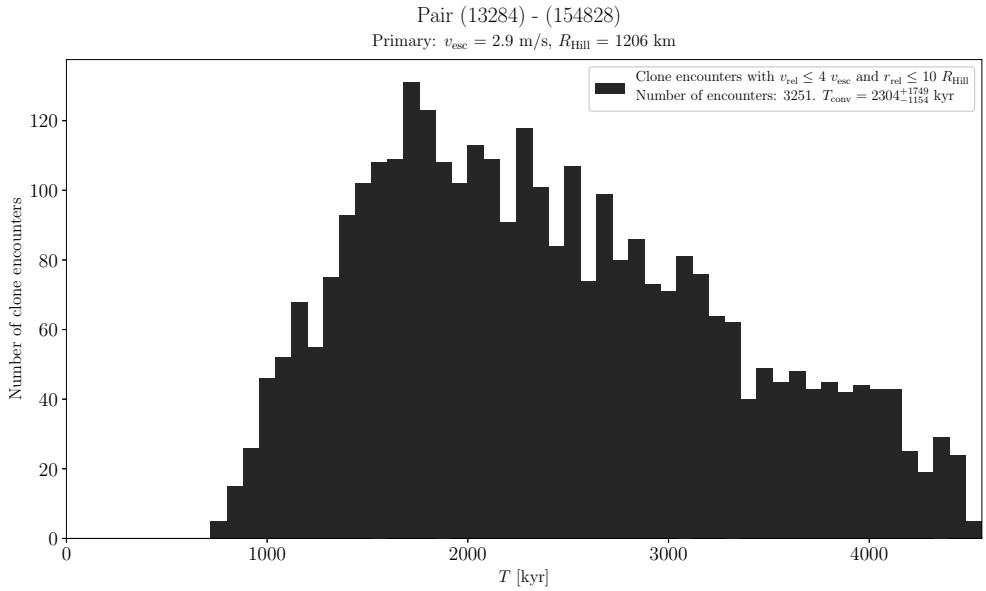

Suppl. Fig. 39. Distribution of past times of close and slow primary–secondary clone encounters for the asteroid pair 13284–154828.

(13284) 1998 QB52 and (154828) 2004 RT8

The estimated age of this asteroid pair is about 2 Myr (Suppl. Fig. 39). We have obtained lightcurve data for the primary (13284) from 3 apparitions. We observed it from Leura, Maidanak, Abastumani, Skalnaté Pleso and La Hita on 14 nights during 2011-07-23 to 2011-09-05, from La Silla on 2014-03-26, and from Ondřejov on 2 nights 2015-07-18 and -20 (Suppl. Figs. 40 to 42). From the La Silla data that were calibrated in the Johnson-Cousins VR system, we derived the mean absolute magnitude $H_1 = 13.72 \pm 0.04$, assuming the phase relation slope parameter $G = 0.15 \pm 0.20$, and refined the WISE effective diameter and geometric albedo (Masiero et al. 2011): $D_1 = 6.4 \pm 0.7$ km and $p_{V,1} = 0.14 \pm 0.03$.

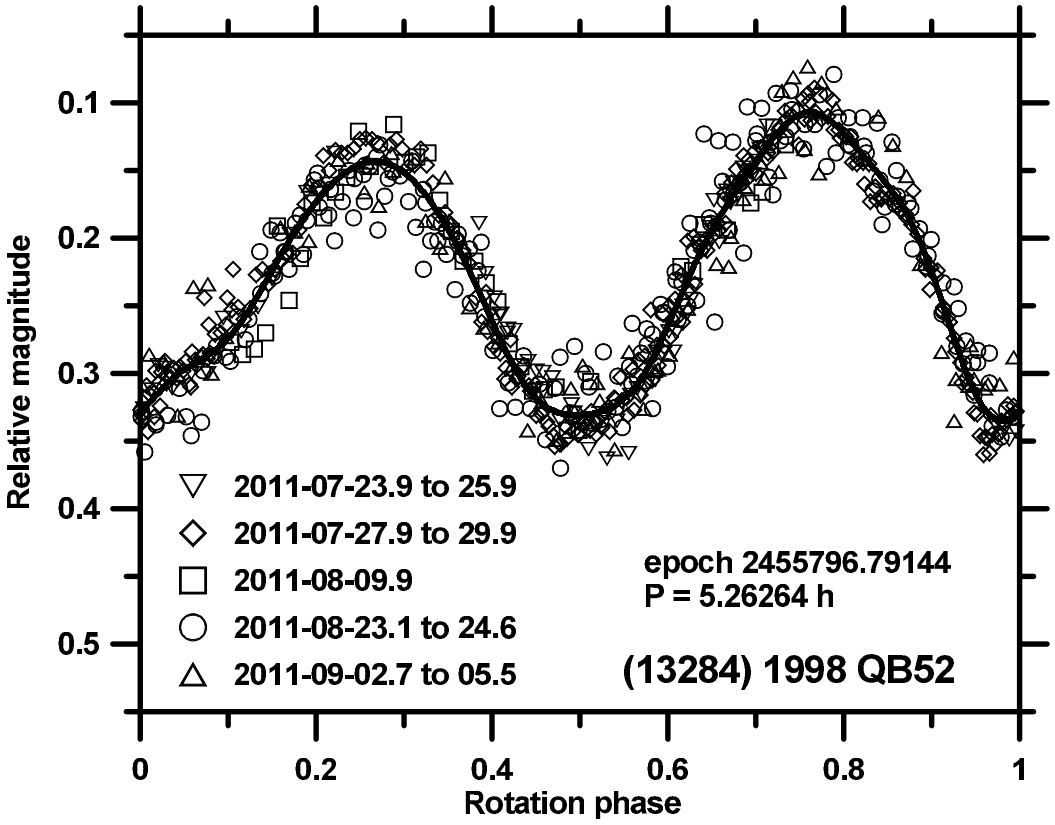

Suppl. Fig. 40. Composite lightcurve of (13284) 1998 QB52 from 2011.

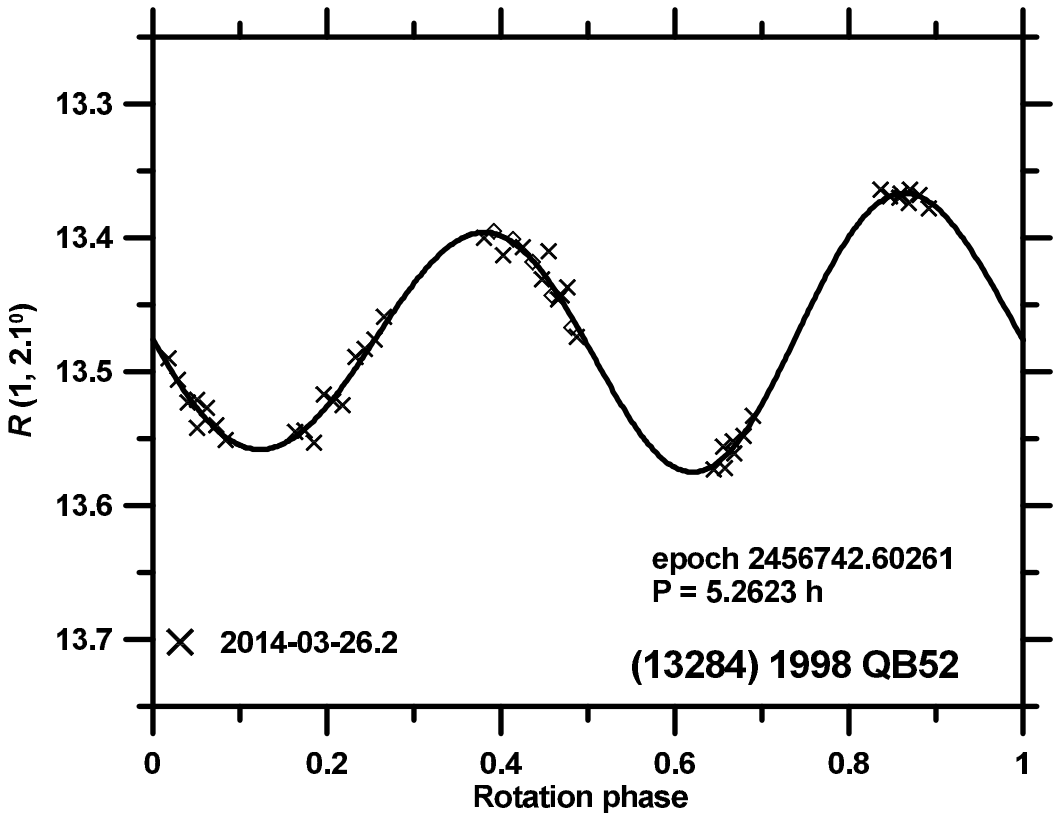

Suppl. Fig. 41. Composite lightcurve of (13284) 1998 QB52 from 2014.

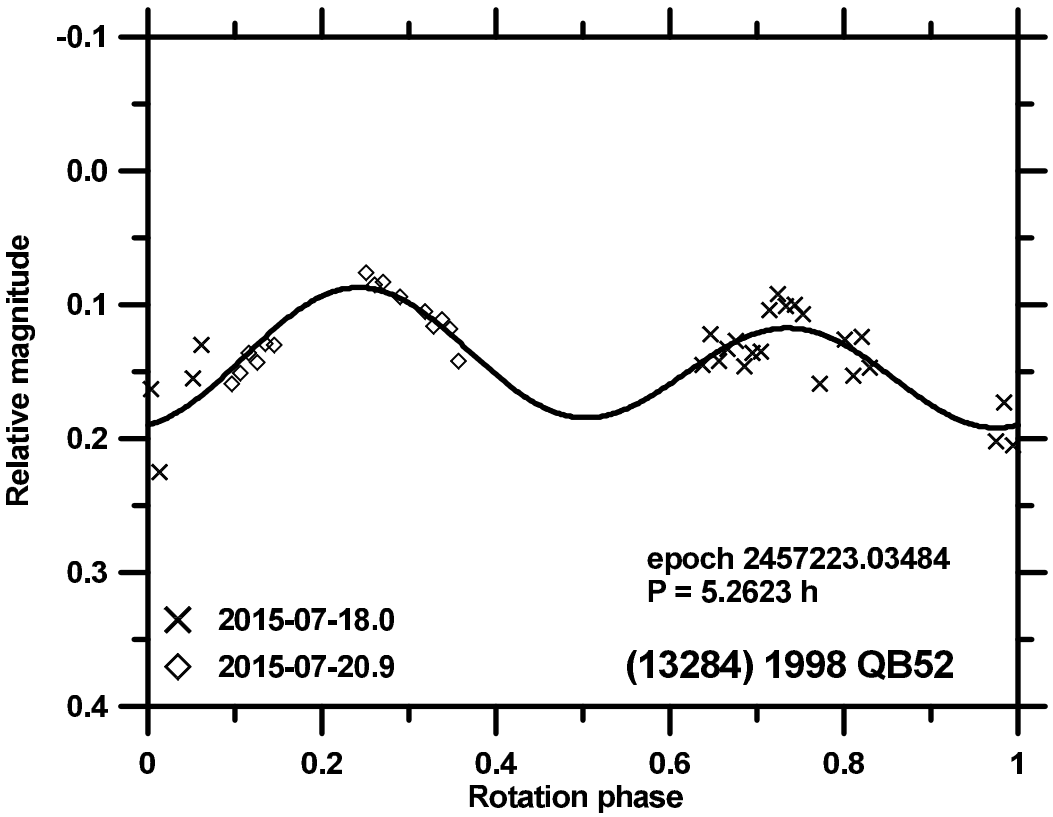

Suppl. Fig. 42. Composite lightcurve of (13284) 1998 QB52 from 2015.

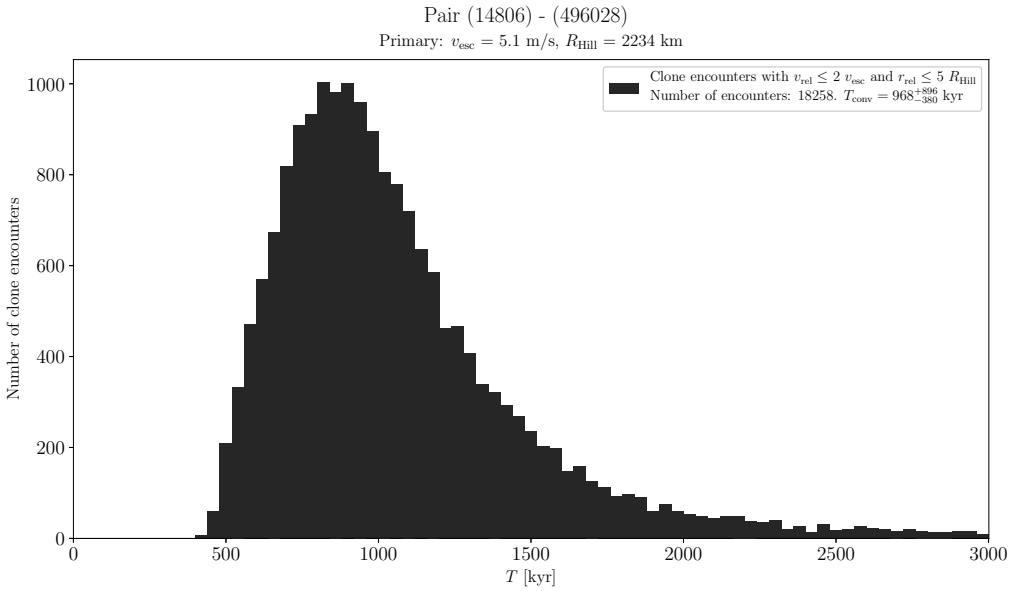

Suppl. Fig. 43. Distribution of past times of close and slow primary–secondary clone encounters for the asteroid pair 14806–496028.

(14806) 1981 EV25 and (496028) 2008 SC9

The estimated age of this asteroid pair is about 900 kyr (Suppl. Fig. 43). We observed the primary (14806) from Ondřejov on 2 nights 2015-11-02 and -03 (Suppl. Fig. 44) and derived its mean absolute magnitude in the Cousins R system $H_{R,1} = 13.64 \pm 0.08$, assuming the slope parameter $G = 0.15 \pm 0.20$. We measured $(V - R)_1 = 0.451 \pm 0.011$ from La Silla on 2018-03-15; obtained $H_1 = 14.09 \pm 0.08$. Using the H_1 value, we refined the WISE effective diameter and geometric albedo (Masiero et al. 2011): $D_1 = 4.0 \pm 0.4$ km and $p_{V,1} = 0.25 \pm 0.06$.

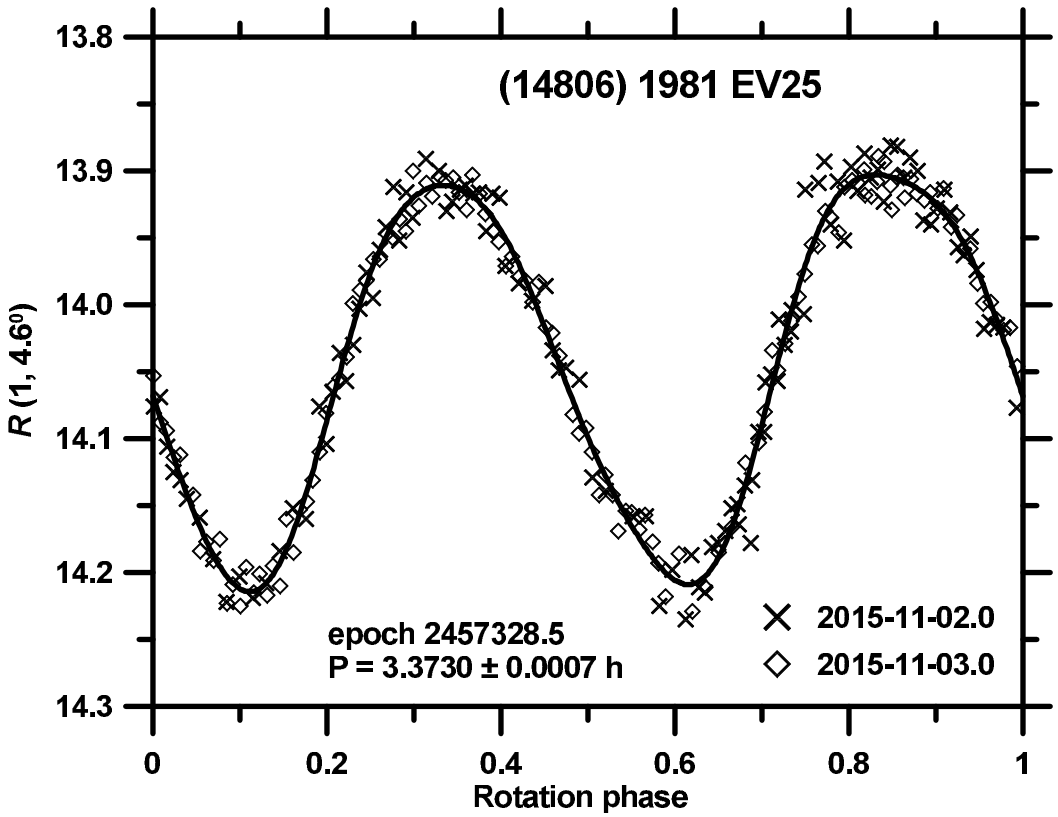

Suppl. Fig. 44. Composite lightcurve of (14806) 1981 EV25 from 2015.

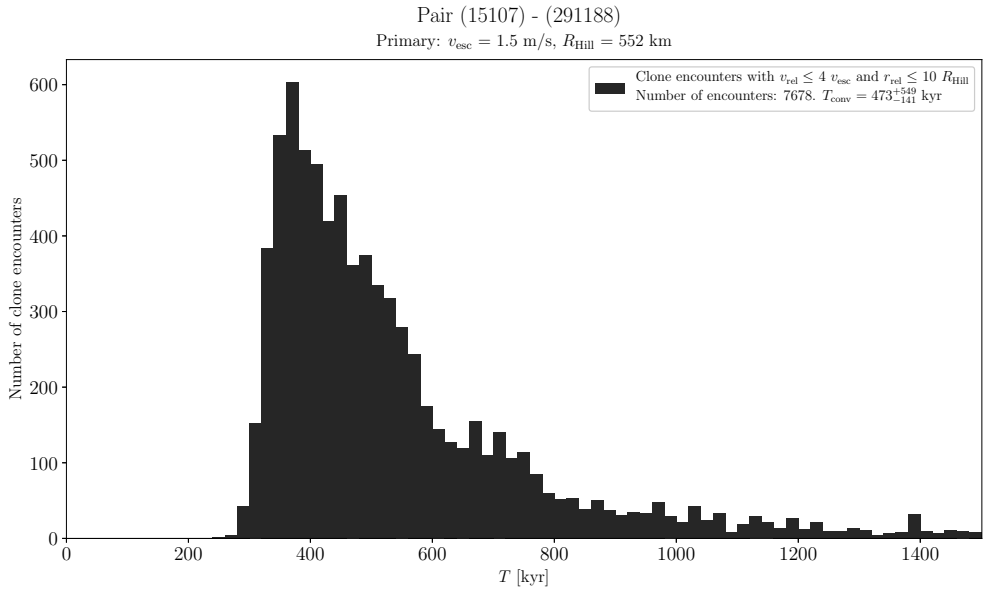

Suppl. Fig. 45. Distribution of past times of close and slow primary–secondary clone encounters for the asteroid pair 15107–291188.

(15107) Toepperwein and (291188) 2006 AL54

The estimated age of this asteroid pair is about 500 kyr (Suppl. Fig. 45). We have obtained lightcurve data for (15107) from 2 apparitions. The observations from 2008 were published in Pravec et al. (2010). We observed it from La Silla on 6 nights during 2015-11-03.2 to 2015-11-18.1 (Suppl. Fig. 46), refining the period $P_1 = 2.5321 \pm 0.0001$ h and deriving the mean absolute magnitude $H_1 = 14.82 \pm 0.03$ and the phase relation slope parameter $G = 0.27 \pm 0.03$. Using the accurate H_1 value, we refined the WISE effective diameter and geometric albedo (Masiero et al. 2011): $D_1 = 2.8 \pm 0.4$ km and $p_{V,1} = 0.27 \pm 0.08$. Our additional observations of the primary (15107) taken in the Fall 2018 suggest presence of a satellite, but it has to be confirmed with thorough observations in the future.

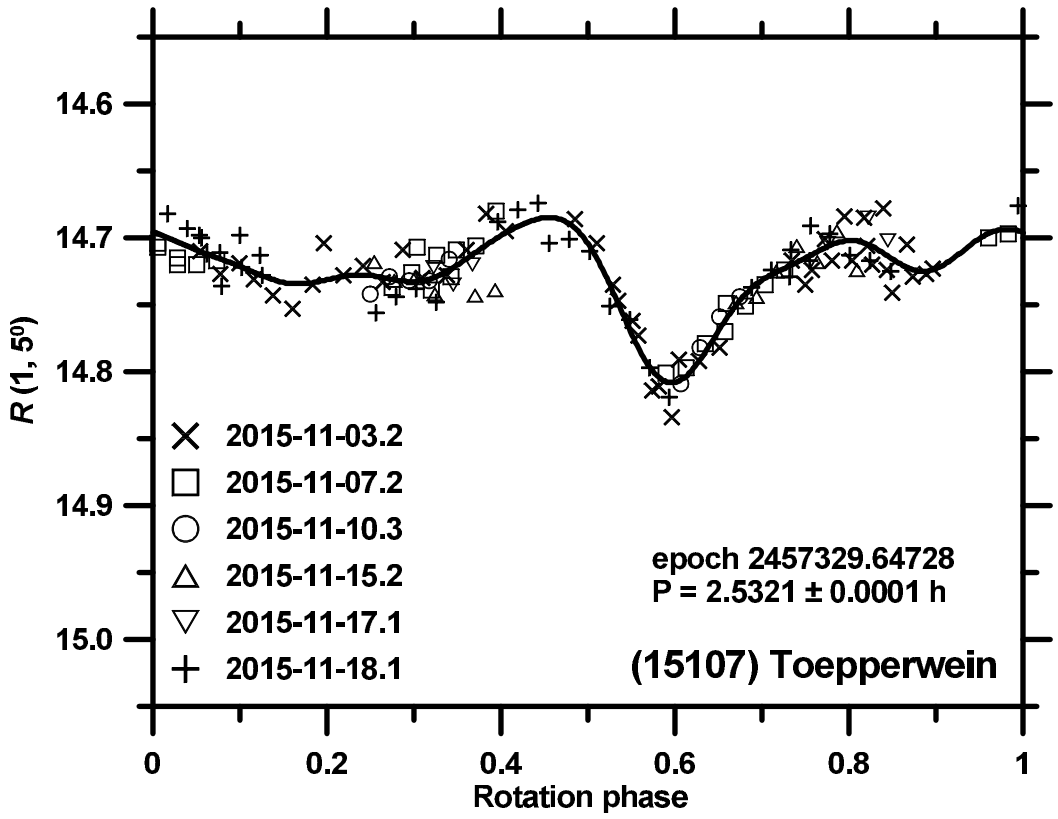

Suppl. Fig. 46. Composite lightcurve of (15107) Toepperwein from 2015.

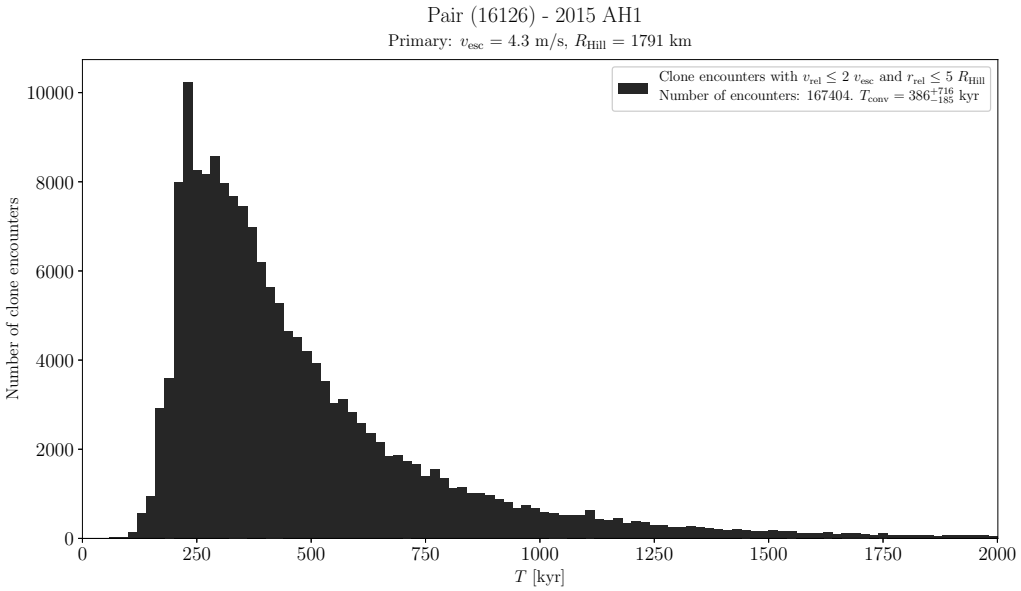

Suppl. Fig. 47. Distribution of past times of close and slow primary–secondary clone encounters for the asteroid pair 16126–2015AH1.

(16126) 1999 XQ86 and 2015 AH1

The estimated age of this asteroid pair is about 400 kyr (Suppl. Fig. 47). We have obtained lightcurve data for (16126) from 2 apparitions. The observations from 2015 were published in Oey et al. (2017). We observed it from La Silla on 3 nights of 2018-02-10 to 12 (Suppl. Fig. 48). We measured $(V-R)_1 = 0.444 \pm 0.011$ and derived $H_1 = 13.03 \pm 0.24$, assuming $G = 0.15 \pm 0.20$. Using the H_1 value, we refined the WISE effective diameter and geometric albedo (Masiero et al. 2011): $D_1 = 6.5 \pm 0.7$ km and $p_{V,1} = 0.26 \pm 0.08$.

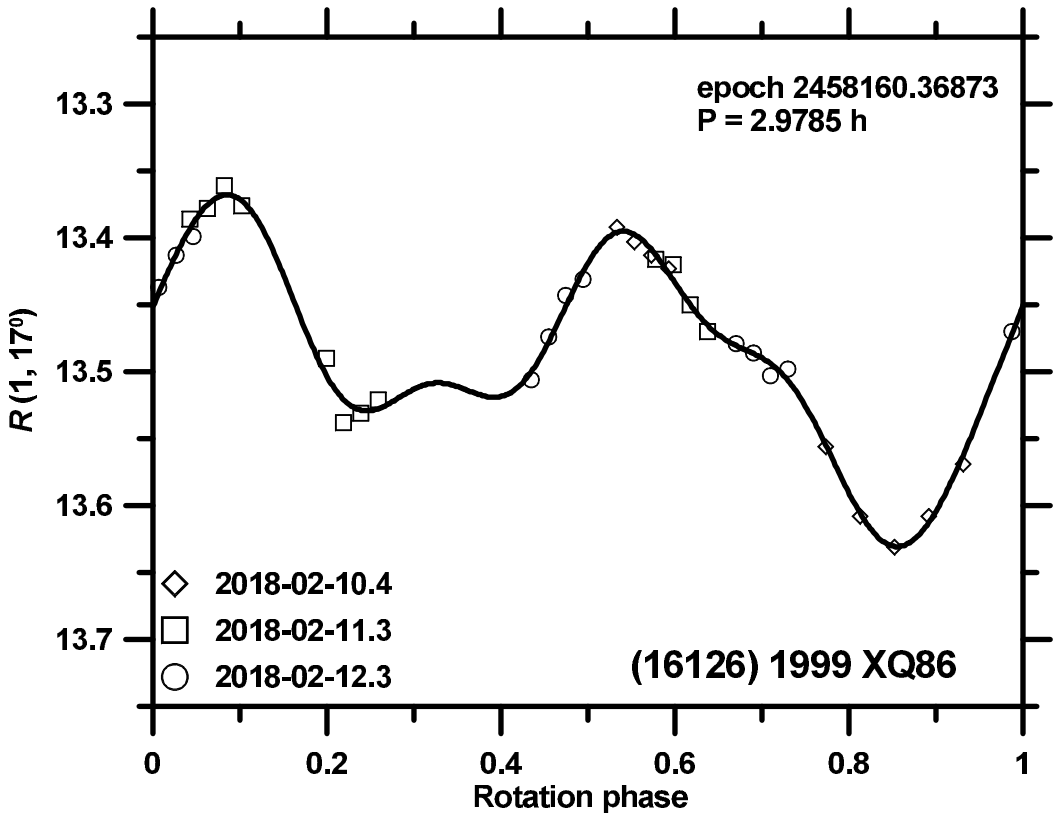

Suppl. Fig. 48. Composite lightcurve of (16126) 1999 XQ86 from 2018.

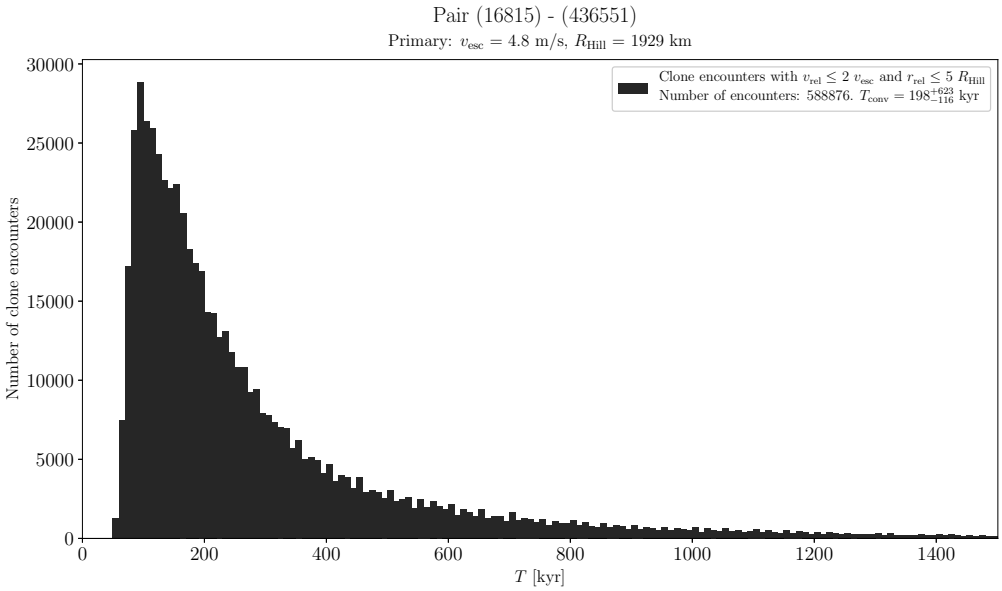

Suppl. Fig. 49. Distribution of past times of close and slow primary–secondary clone encounters for the asteroid pair 16815–436551.

(16815) 1997 UA9 and (436551) 2011 GD83

The estimated age of this asteroid pair is about 200 kyr (Suppl. Fig. 49). We have obtained lightcurve data for (16815) from 3 apparitions. The observations taken from Wise on 2013-10-30 were published in Polishook (2014). We observed it from Sugarloaf Mountain and Ondřejov on 6 nights during 2013-09-27 to 2013-10-02 and on 4 nights during 2015-01-23 to 2015-02-15, and from Leura on 3 nights during 2017-09-16 to 2017-11-24 (Suppl. Figs. 50 to 52). The Ondřejov nights taken in 2013 and 2015 were calibrated in the Cousins R system and we derived the mean absolute magnitudes $H_{R,1} = 12.56 \pm 0.07$ and 12.51 ± 0.08 in the two years, assuming $G = 0.24 \pm 0.11$. For conversion of $H_{R,1}$ to $H_1 \equiv H_{V,1}$, we assumed $(V - R) = 0.45 \pm 0.10$.

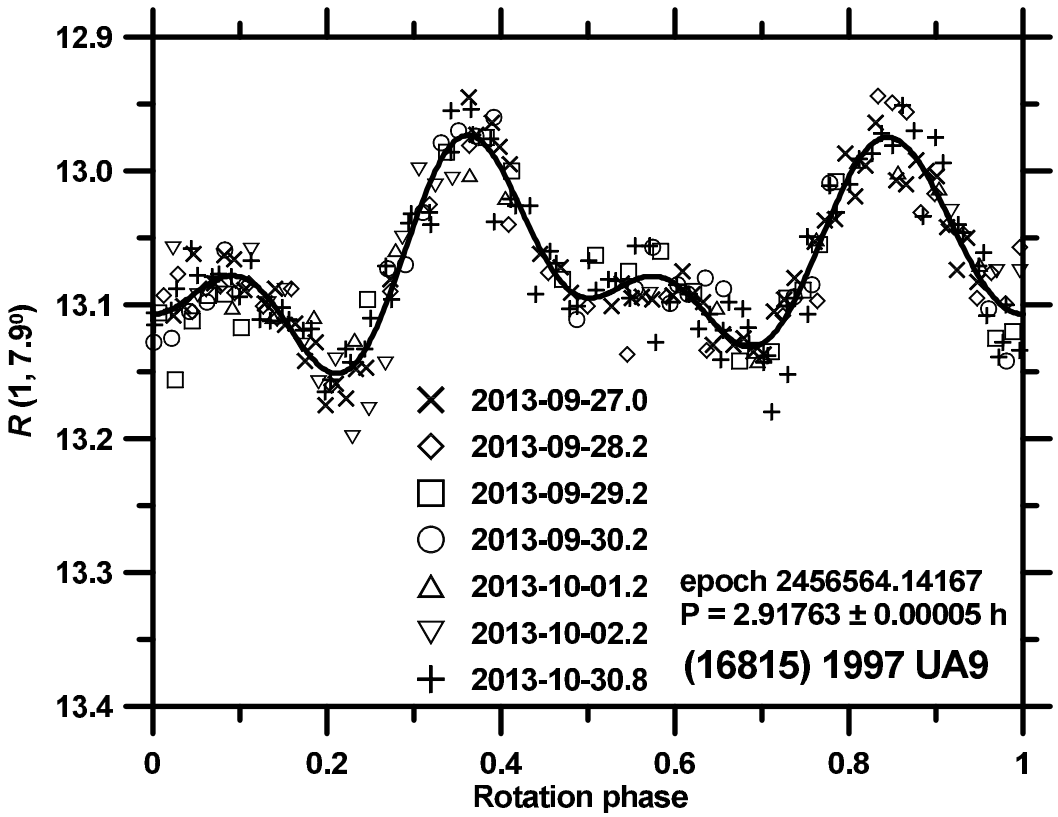

Suppl. Fig. 50. Composite lightcurve of (16815) 1997 UA9 from 2013.

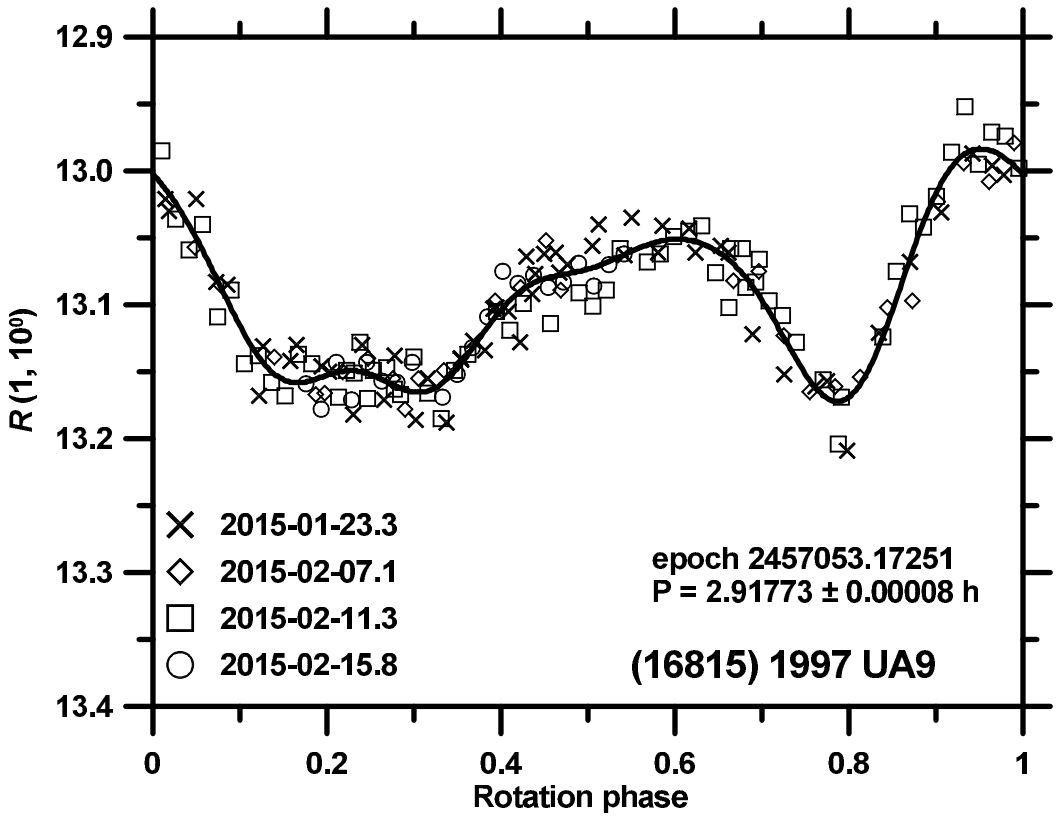

Suppl. Fig. 51. Composite lightcurve of (16815) 1997 UA9 from 2015.

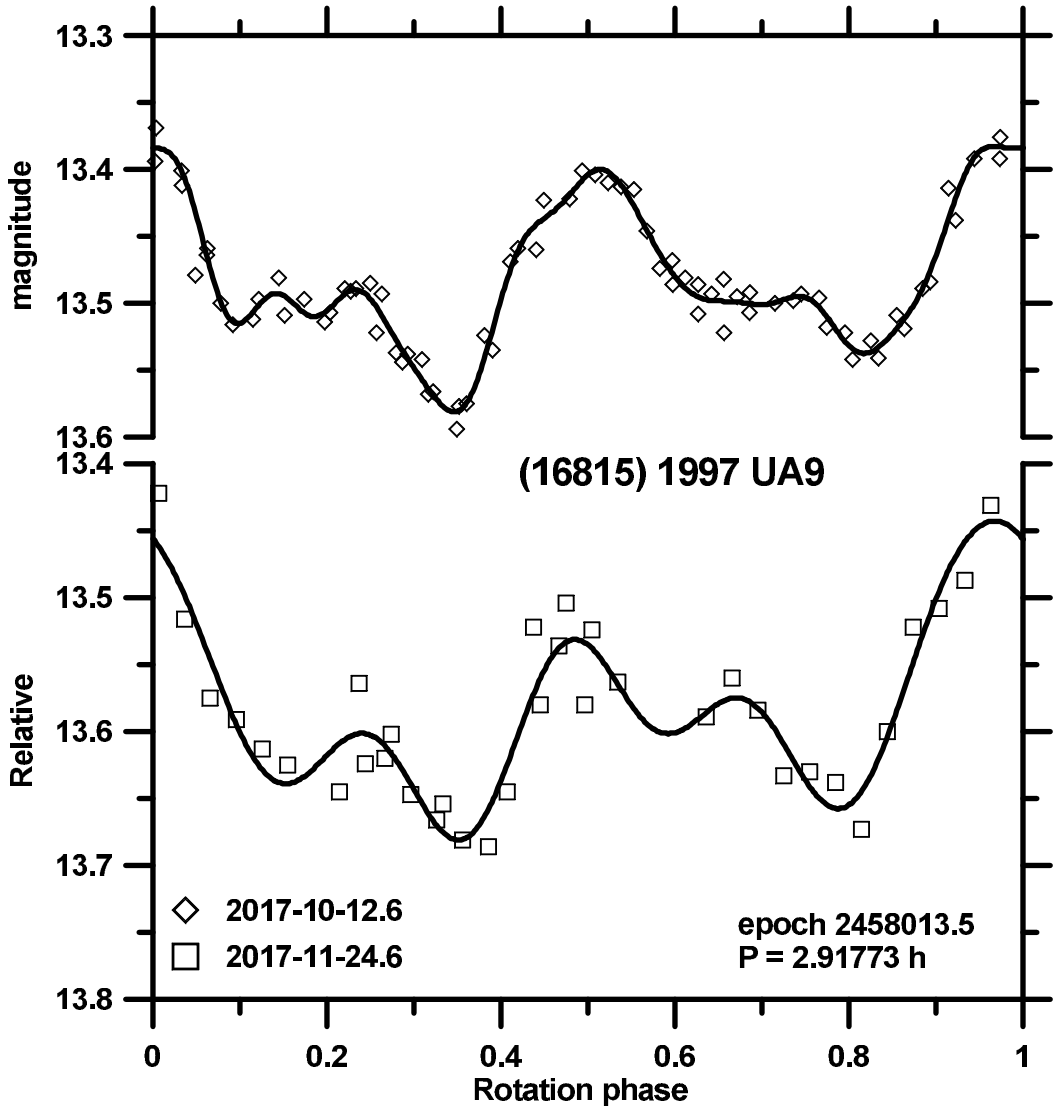

Suppl. Fig. 52. Composite lightcurves of (16815) 1997 UA9 from 2017.

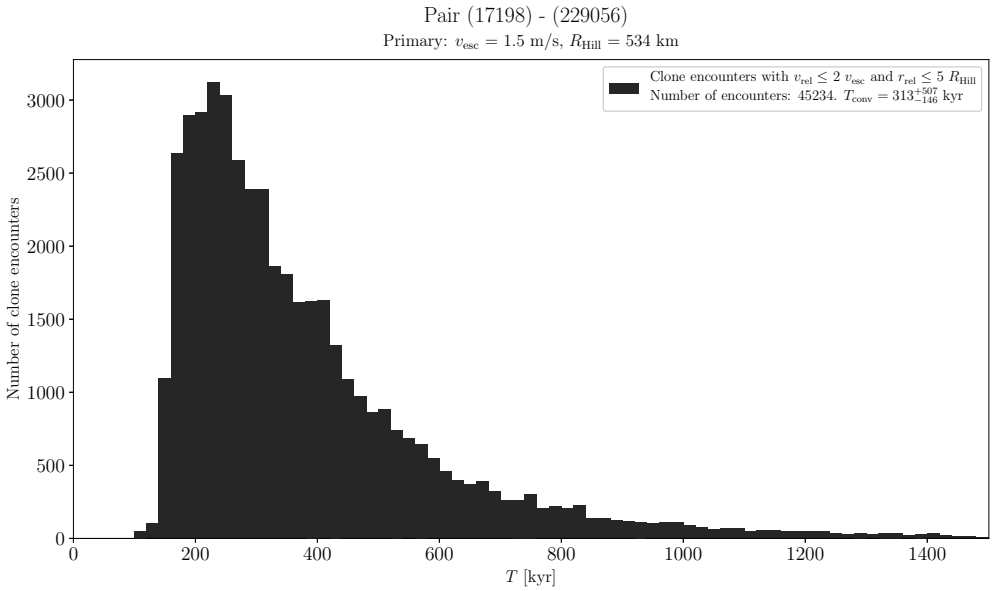

Suppl. Fig. 53. Distribution of past times of close and slow primary–secondary clone encounters for the asteroid pair 17198–229056.

(17198) Gorjup and (229056) 2004 FC126

The estimated age of this asteroid pair is about 300 kyr (Suppl. Fig. 53). We have obtained lightcurve data for (17198) from 2 apparitions. The observations taken from Wise and Cerro Tololo in 2008 were published in Pravec et al. (2010). We observed it from La Silla and Maidanak on 11 nights during 2012-10-18 to 2012-11-07 (Suppl. Fig. 54). We derived the mean absolute magnitude $H_1 = 15.32 \pm 0.02$ and the phase relation slope parameter $G = 0.26 \pm 0.02$.

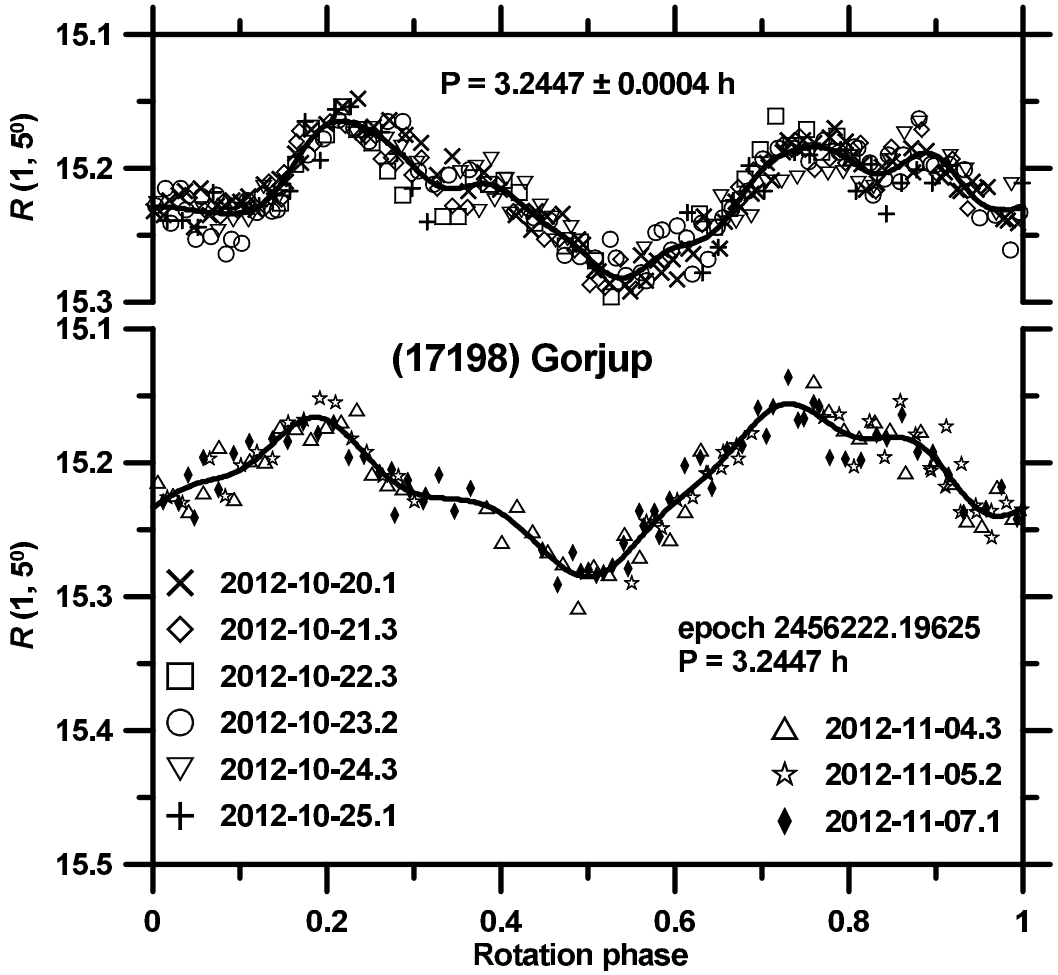

Suppl. Fig. 54. Composite lightcurves of (17198) Gorjup from 2012.

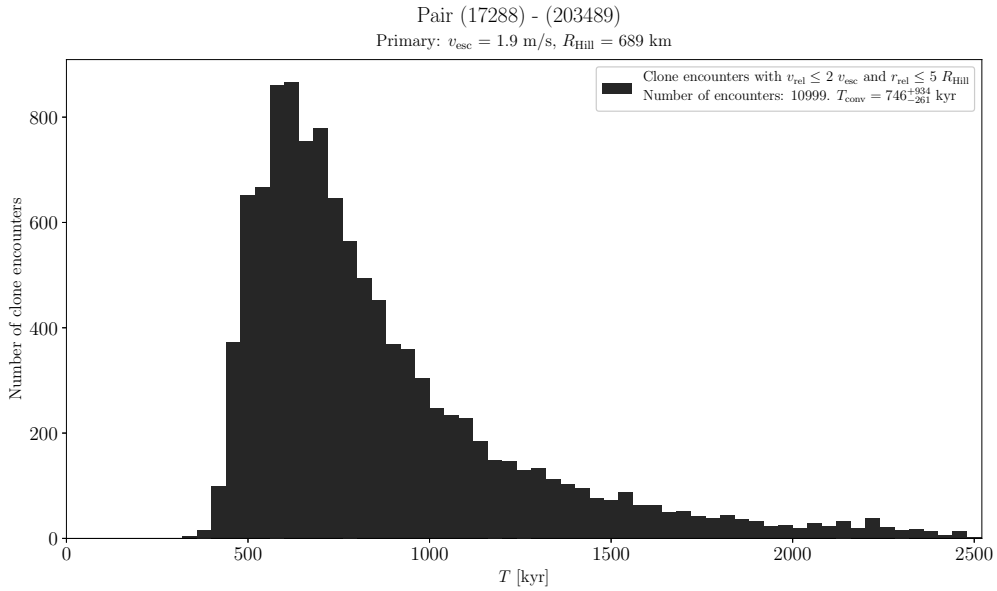

Suppl. Fig. 55. Distribution of past times of close and slow primary–secondary clone encounters for the asteroid pair 17288–203489.

(17288) 2000 NZ10 and (203489) 2002 AL80

The estimated age of this asteroid pair is about 700 kyr (Suppl. Fig. 55). We observed the primary (17288) from Sierra Nevada on 3 nights 2014-08-19 to -21 (Suppl. Fig. 56). Masiero et al. (2011) measured its effective diameter $D_1 = 3.6 \pm 0.6$ km.

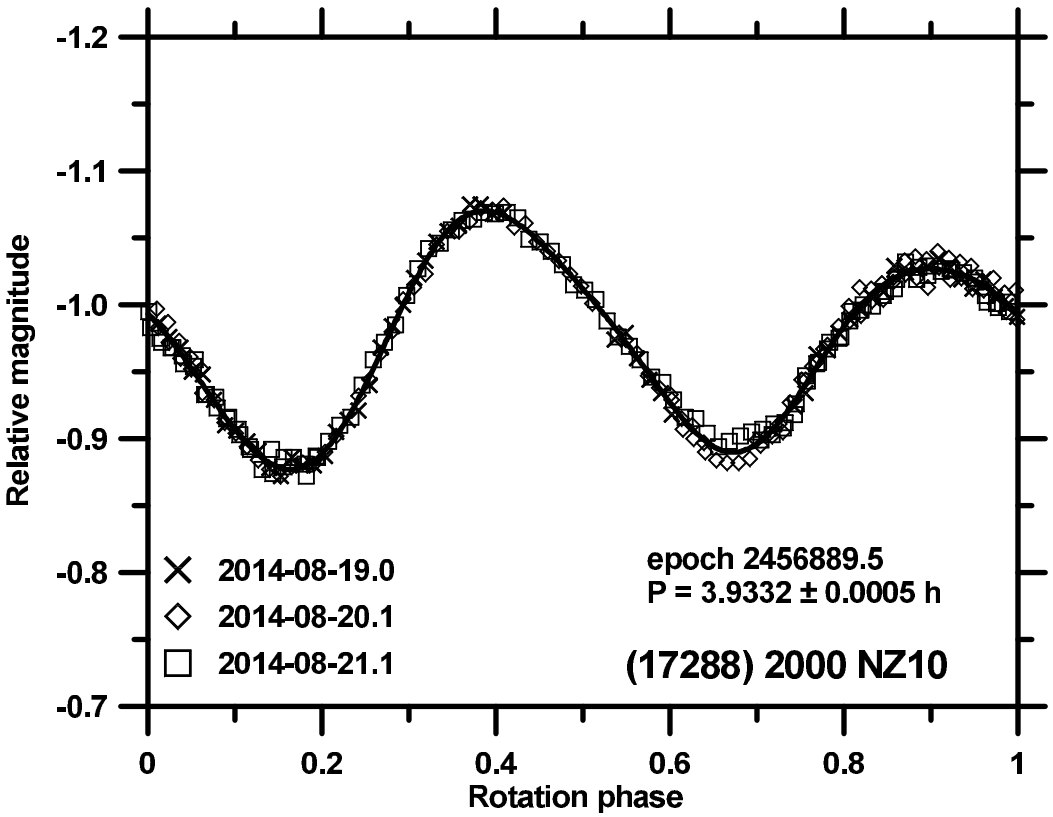

Suppl. Fig. 56. Composite lightcurve of (17288) 2000 NZ10 from 2014.

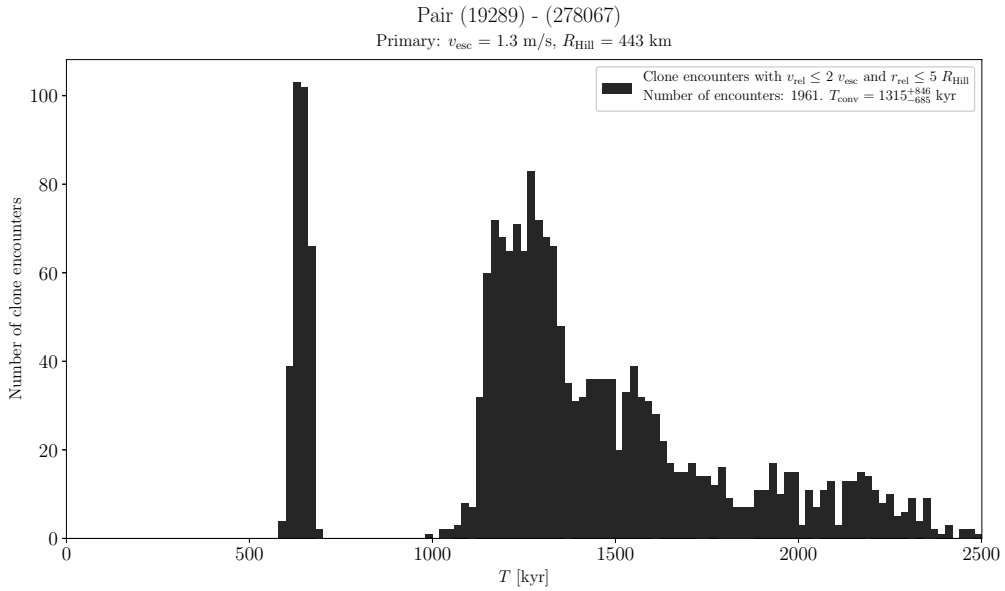

Suppl. Fig. 57. Distribution of past times of close and slow primary–secondary clone encounters for the asteroid pair 19289–278067.

(19289) 1996 HY12 and (278067) 2006 YY40

The estimated age of this asteroid pair is about 1300 kyr, though an younger age of $\sim$ 600 kyr is also possible (Suppl. Fig. 57). We obtained lightcurve data for (19289) from 4 apparitions. The observations taken in 2009 were published in Pravec et al. (2010). The observations taken from Leura in 2015 were published in Oey (2017). We observed it from Deep Sky Observatory, PROMPT and Abastumani on 3 nights during 2012-09-11 to 12, from La Silla on 6 nights during 2014-01-26 to 2014-02-08, and from Abastumani, Maidanak and Sugarloaf Mountain on 7 nights during 2015-08-14 to 2015-09-14 (Suppl. Figs. 58 to 60). From the VR data taken at La Silla, we derived $(V-R)_1 = 0.473 \pm 0.010, H_1 = 15.73 \pm 0.03$ and $G_1 = 0.31 \pm 0.03$.

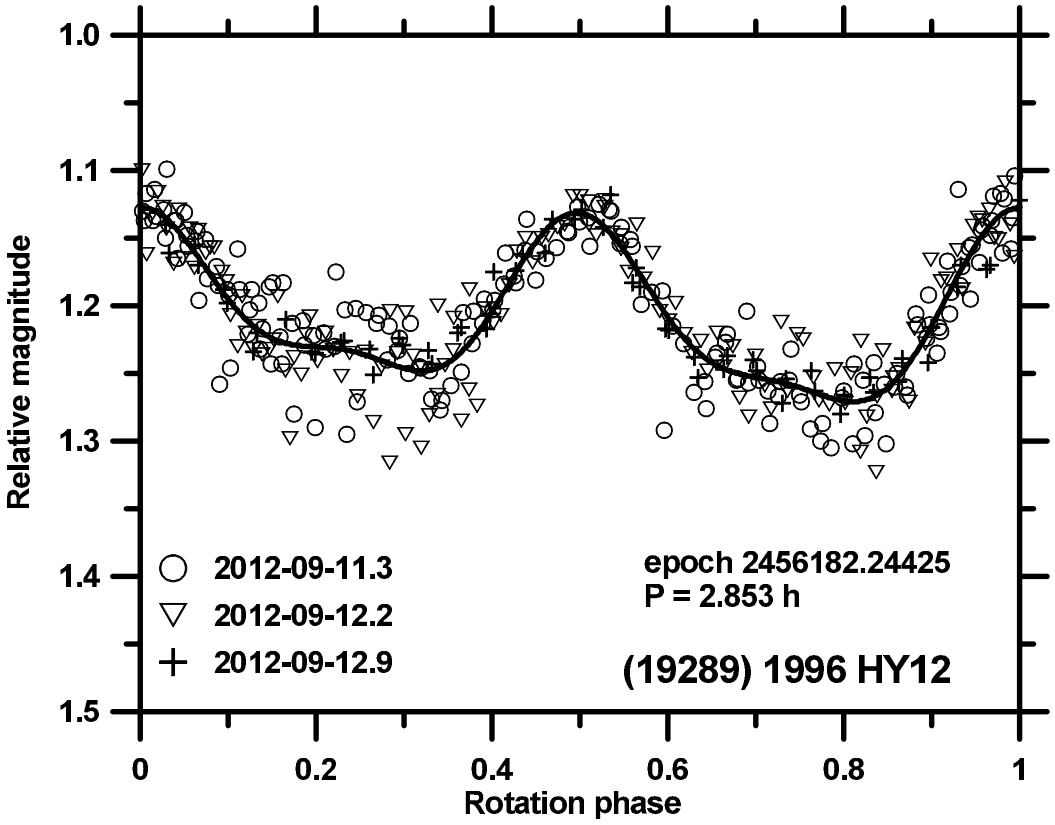

Suppl. Fig. 58. Composite lightcurve of (19289) 1996 HY12 from 2012.

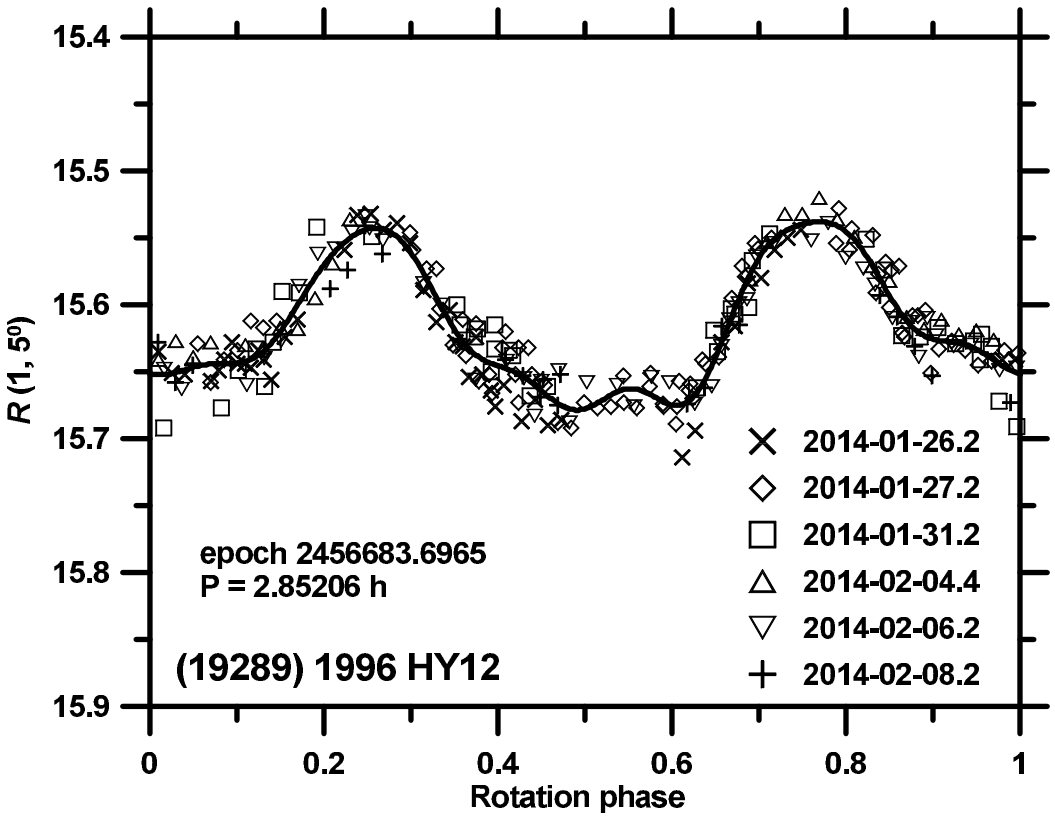

Suppl. Fig. 59. Composite lightcurve of (19289) 1996 HY12 from 2014.

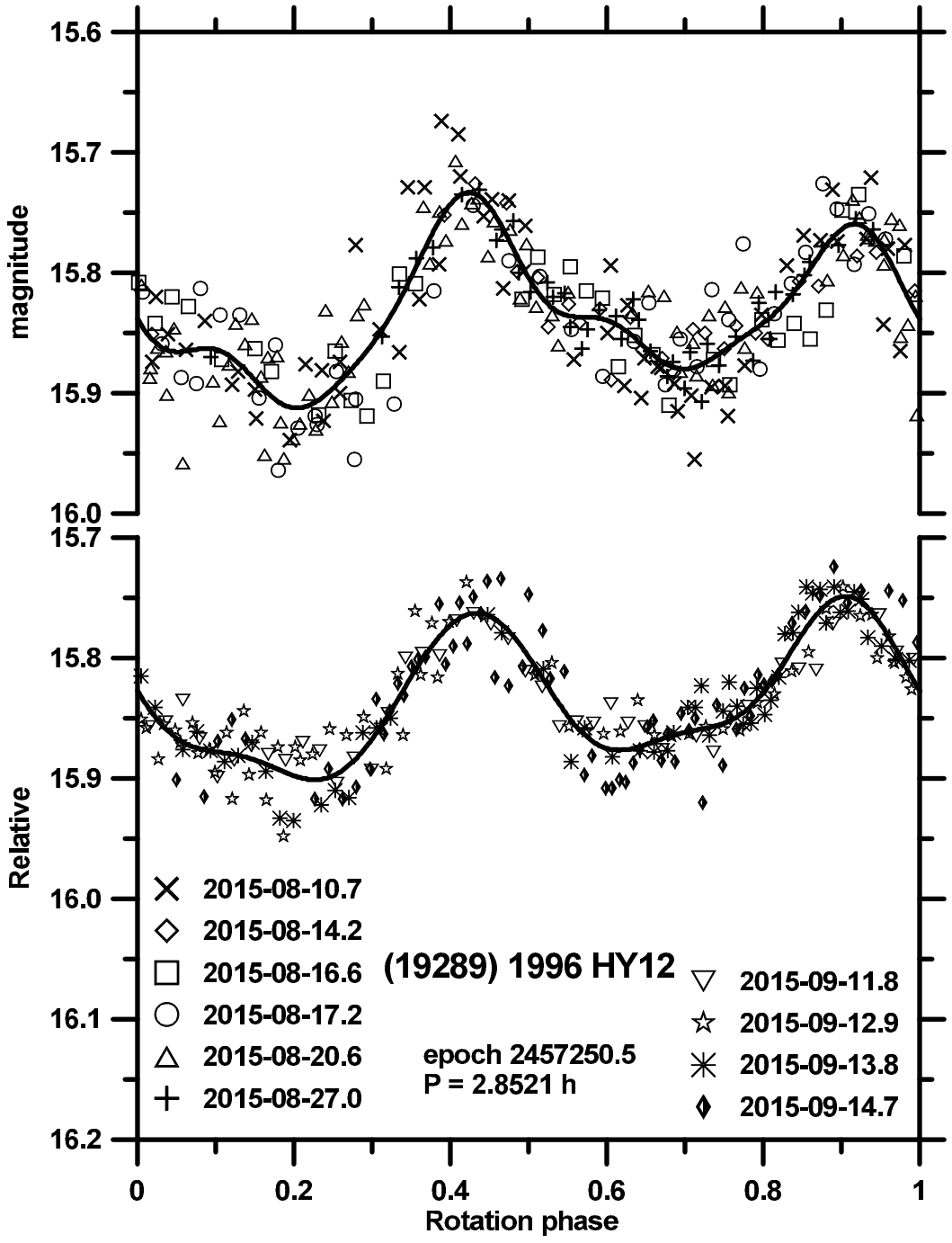

Suppl. Fig. 60. Composite lightcurves of (19289) 1996 HY12 from 2015.

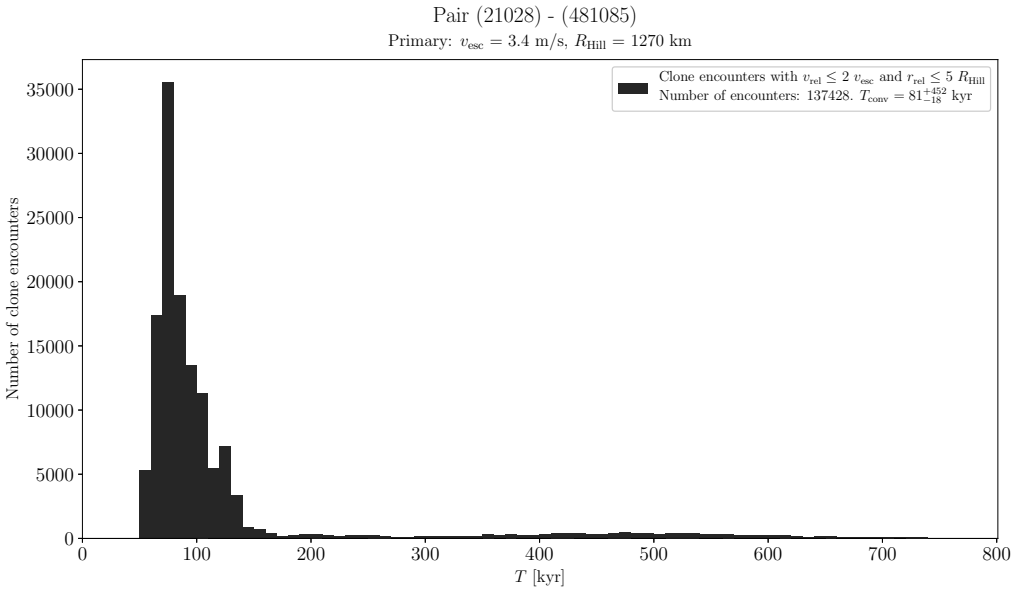

Suppl. Fig. 61. Distribution of past times of close and slow primary–secondary clone encounters for the asteroid pair 21028–481085.

(21028) 1989 TO and (481085) 2005 SA135

The estimated age of this asteroid pair is about 80 kyr (Suppl. Fig. 61). We have obtained lightcurve data for (21028) from 2 apparitions. The observations taken from Palmer Divide Observatory in 2007 and from Center for Solar System Studies in 2014 were published in Warner et al. (2008) and Stephens and Warner (2015), respectively. We observed it from Skalnaté Pleso and Ondřejov on 7 nights during 2007-11-28 to 2007-12-19 and from Sugarloaf Mountain on 6 nights during 2014-09-15 to 2014-12-16 (Suppl. Figs. 62 and 63). The mean absolute magnitude $H_1 = 13.29 \pm 0.16$ was published in Pravec et al. (2012b).

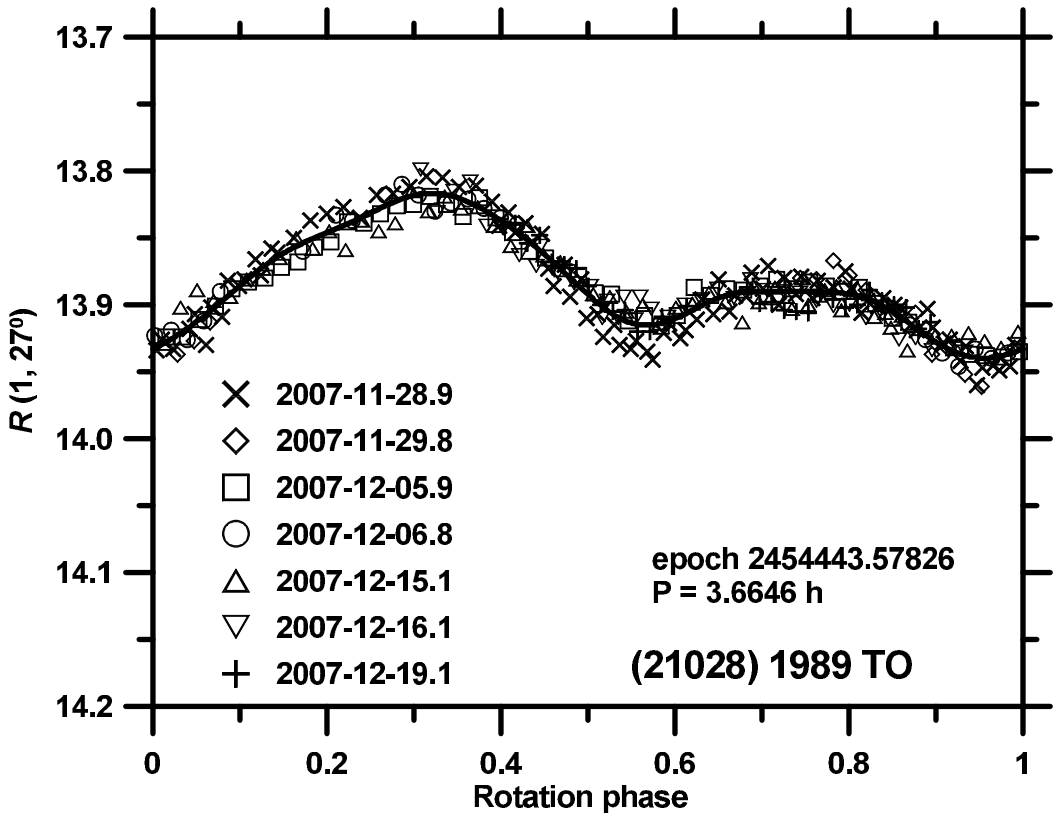

Suppl. Fig. 62. Composite lightcurve of (21028) 1989 TO from 2007.

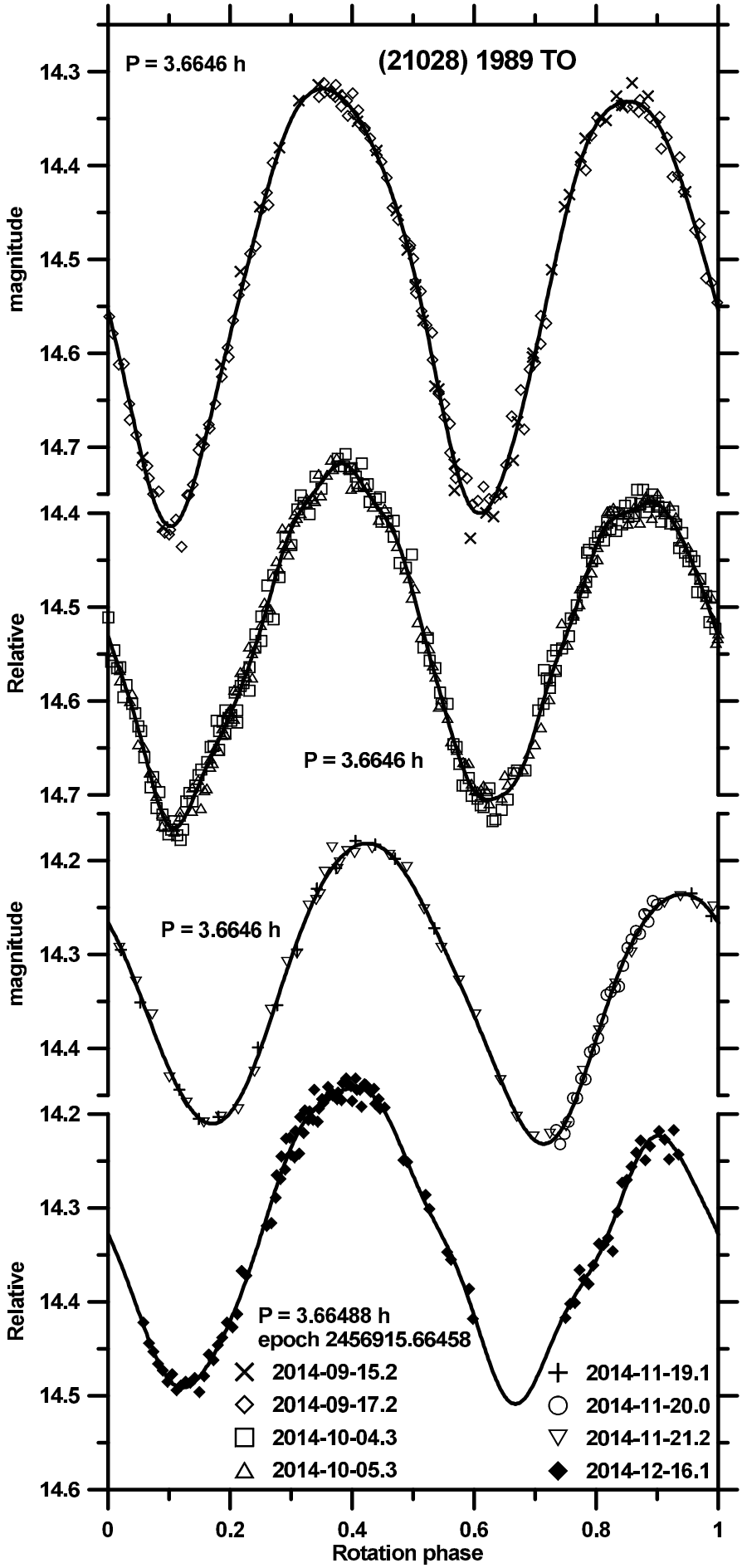

Suppl. Fig. 63. Composite lightcurves of (21028) 1989 TO from 2014.

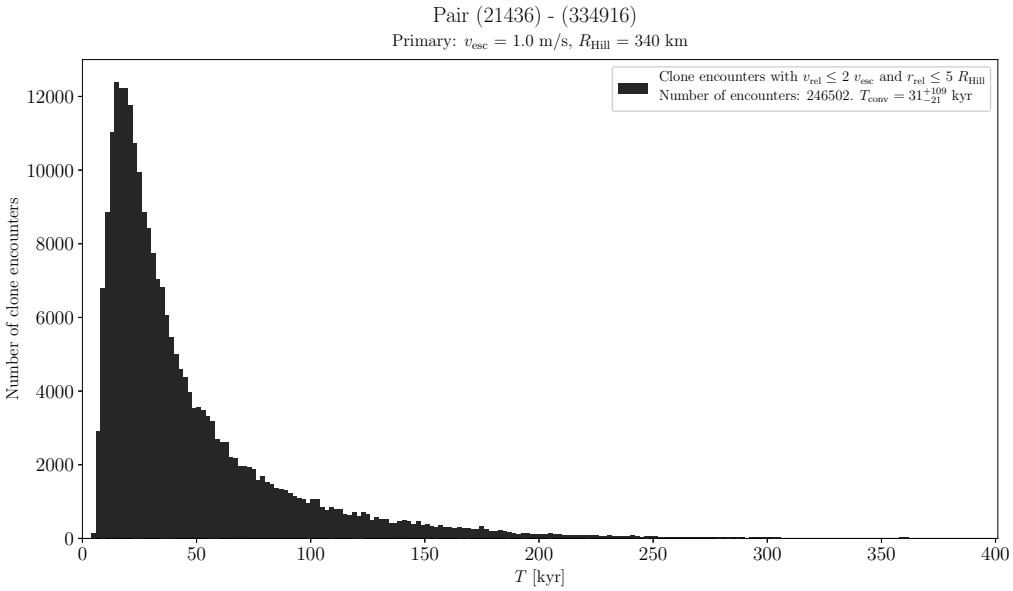

Suppl. Fig. 64. Distribution of past times of close and slow primary–secondary clone encounters for the asteroid pair 21436–334916.

(21436) Chaoyichi and (334916) 2003 YK39

This is a young asteroid pair, showing an orbital convergence about 30 kyr ago (Suppl. Fig. 64). We obtained lightcurve data for (21436) from 4 apparitions. The observations from 2009-11-16 were published in Pravec et al. (2010). We observed it from La Silla and Sierra Nevada on 20 nights during 2014-02-23 to 2014-05-04, and from La Silla on 2 nights 2015-10-08 and -13 and on 16 nights during 2016-10-28 to 2016-12-23. The primary period $P_{1,p} = 2.8655 \pm 0.0002$ h is likely; while a period twice or thrice that long is formally not ruled out, it appears unlikely due to the complex lightcurve shape observed on the four apparitions repeating well with the 2.8655-h period. We derived the mean absolute magnitude of the whole system (outside events) $H_1 = 15.66 \pm 0.03$ and the slope parameter $G = 0.24 \pm 0.02$ in 2014, 15.56 ± 0.07 and 0.14 ± 0.05 in 2016, and 15.65 ± 0.07 with assuming $G = 0.19 \pm 0.05$ in 2015.

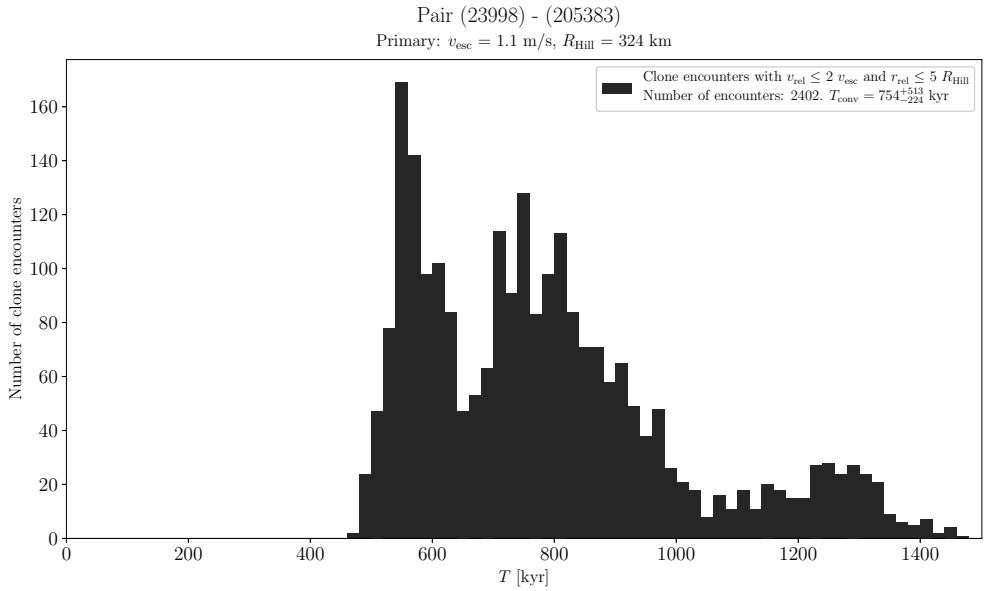

Suppl. Fig. 65. Distribution of past times of close and slow primary–secondary clone encounters for the asteroid pair 23998–205383.

(23998) 1999 RP29 and (205383) 2001 BV47

The estimated age of this asteroid pair is about 800 kyr (Suppl. Fig. 65).

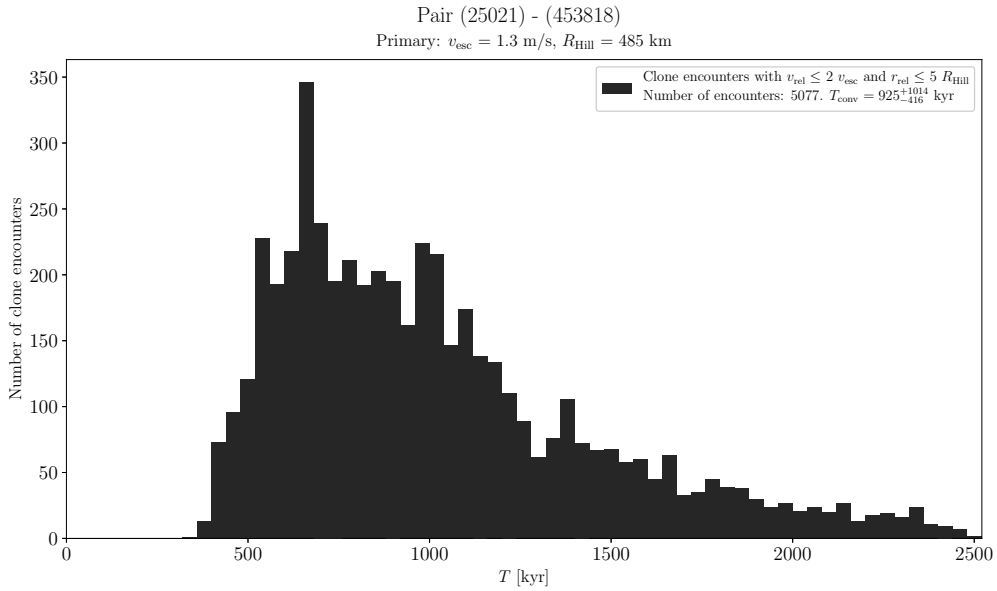

Suppl. Fig. 66. Distribution of past times of close and slow primary–secondary clone encounters for the asteroid pair 25021–453818.

(25021) Nischaykumar and (453818) 2011 SJ109

The estimated age of this asteroid pair is about 900 kyr (Suppl. Fig. 66). We have obtained lightcurve data for (25021) from 3 apparitions. We observed it from La Silla on 6 nights during 2015-03-14 to 2015-03-20, on 10 nights during 2016-09-06 to 2016-10-08, and on 9 nights during 2018-02-13 to 2018-03-24. We measured $(V-R)_1 = 0.507 \pm 0.013$. We derived the mean absolute magnitudes $H_1 = 15.96 \pm 0.04, 15.92 \pm 0.03$ and 15.95 ± 0.03 in the three apparitions, with the phase relation slope parameter $G = 0.11 \pm 0.03$. Using the mean $H_1 = 15.94 \pm 0.03$, we refined the WISE effective diameter and geometric albedo (Masiero et al. 2011): $D_1 = 2.1 \pm 0.6$ km and $p_{V,1} = 0.16 \pm 0.08$.

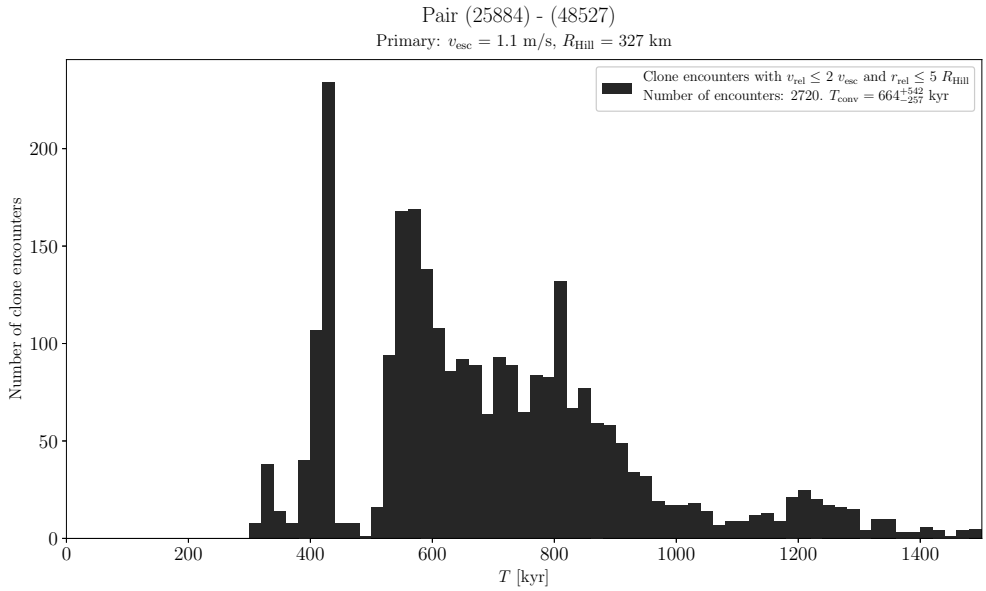

Suppl. Fig. 67. Distribution of past times of close and slow primary–secondary clone encounters for the asteroid pair 25884–48527.

(25884) Asai and (48527) 1993 LC1

The estimated age of this asteroid pair is about 700 kyr (Suppl. Fig. 67). We have obtained lightcurve data for (25884) from 4 apparitions. The observations from Wise in 2010 and 2013 were published in Polishook et al. (2011) and Polishook and Aharonson (2019), respectively. The observations from Palmer Divide Observatory in 2011 were published in Warner et al. (2012). Data taken from Via Capote in 2011 are available in the ALCDEF archive. We observed it from Modra on 7 nights during 2010-03-08 to 2010-04-07, from Ondřejov and Modra on 4 nights during 2011-11-15 to 2011-11-28, from PROMPT on night 2013-04-04, and from Leura on 3 nights during 2016-07-02 to 2016-08-27. From the two Ondřejov nights taken in November 2011, we derived the mean absolute magnitude in the Cousins R system $H_{R,1} = 14.60 \pm 0.07$, assuming $G = 0.33 \pm 0.10$ that is the mean value for Hungarias. For conversion to $H_1 \equiv H_{V,1}$, we assumed $(V - R) = 0.45 \pm 0.10$.

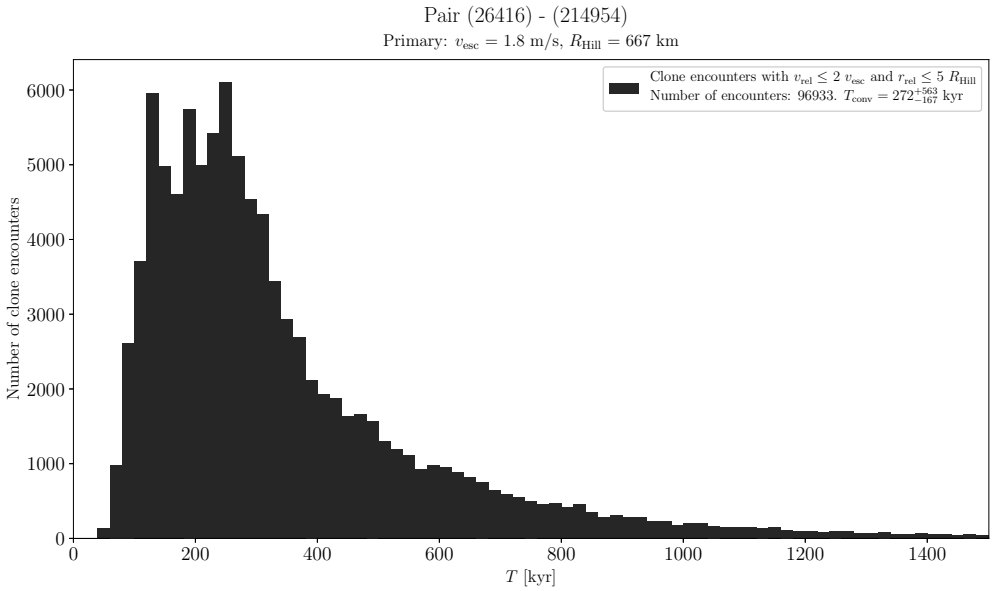

Suppl. Fig. 68. Distribution of past times of close and slow primary–secondary clone encounters for the asteroid pair 26416–214954.

(26416) 1999 XM84 and (214954) 2007 WO58

The estimated age of this asteroid pair is about 300 kyr (Suppl. Fig. 68). We obtained lightcurve data for (26416) from 4 apparitions. The observations from Wise in 2011 were published in Polishook (2014b). We observed it from La Silla on 3 nights 2009-11-13 to 15, on 9 nights during 2015-03-16 to 2015-04-15, and on 13 nights during 2016-09-01 to 2016-12-03. From the 2015 and 2016 data that were absolutely calibrated in the Johnson-Cousins VR system, we derived $(V-R)_1 = 0.495 \pm 0.011$ and the mean absolute magnitudes of the whole system $H_1 = 14.62 \pm 0.03$ and 14.58 ± 0.03 with the slope parameters $G_1 = 0.23 \pm 0.03$ and 0.20 ± 0.02, respectively. We observed the unbound secondary (214954) from La Silla on 5 nights during 2016-03-08 to 2016-03-15 (Suppl. Fig. 69) and derived its mean absolute magnitude $H_{R,2} = 16.64 \pm 0.04$ and the slope parameter $G = 0.24 \pm 0.06$.

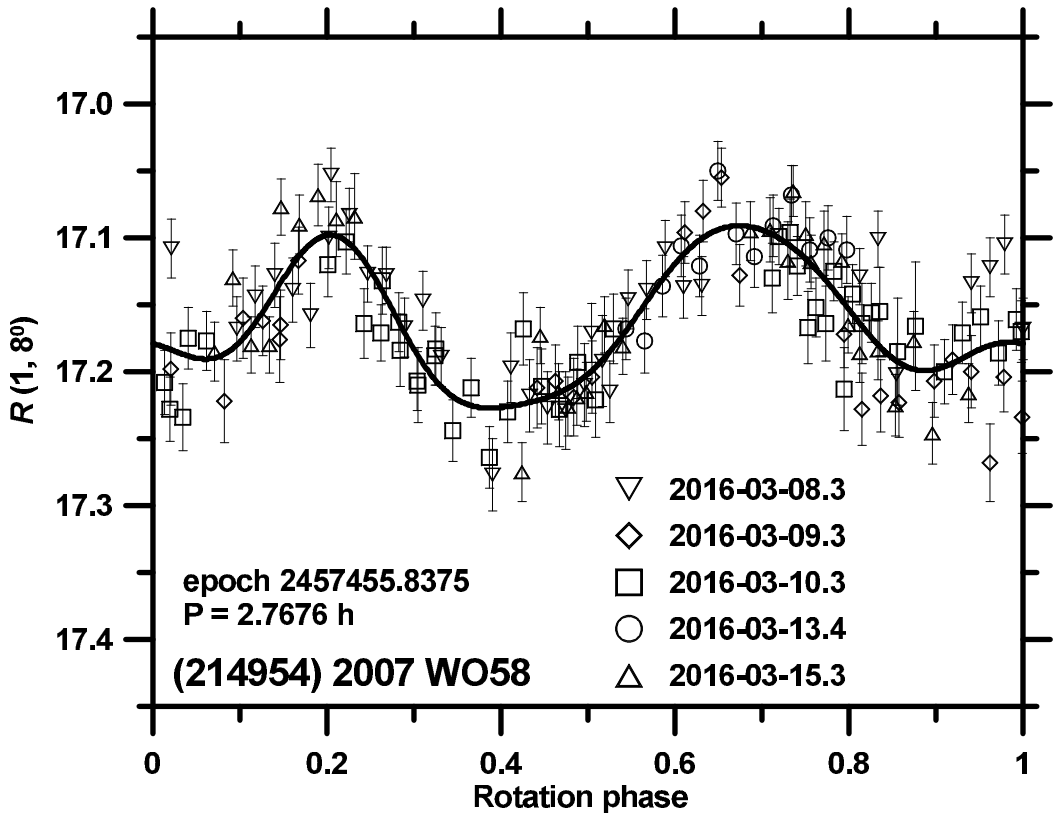

Suppl. Fig. 69. Composite lightcurve of (214954) 2007 WO58 from 2016.

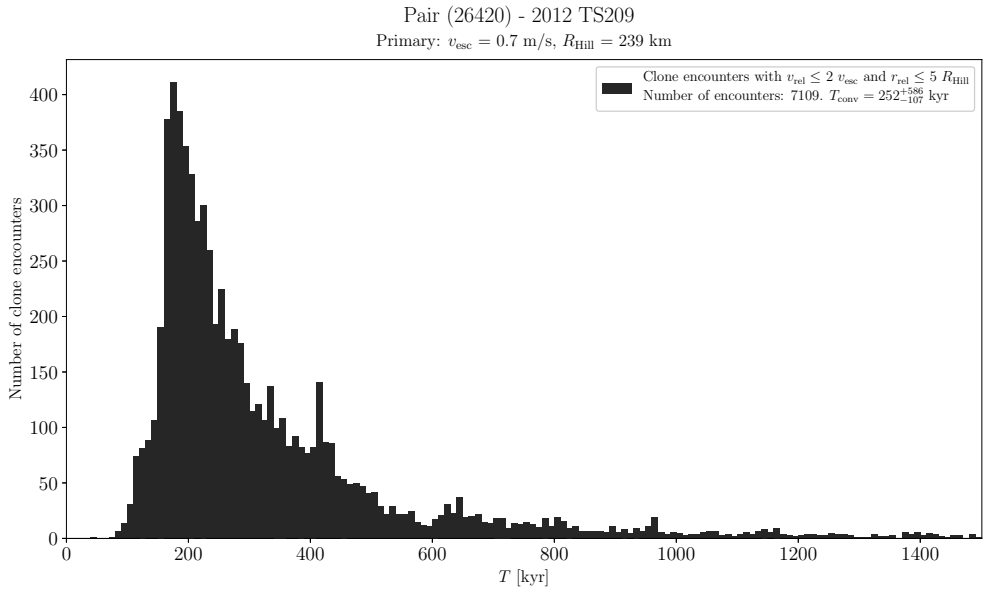

Suppl. Fig. 70. Distribution of past times of close and slow primary–secondary clone encounters for the asteroid pair 26420–2012TS209.

(26420) 1999 XL103 and 2012 TS209

The estimated age of this asteroid pair is about 250 kyr (Suppl. Fig. 70). We observed (26420) from La Silla on 10 nights during 2015-12-11 to 2016-02-10 and on 5 nights during 2017-03-26 to 2017-04-02 (Suppl. Figs. 71 and 72). We derived the mean absolute magnitudes of the whole system (outside mutual events) $H_1 = 16.11 \pm 0.05$ and 16.03 ± 0.04 in the two apparitions, with the slope parameter $G = 0.52 \pm 0.06$ in 2015–2016 and assuming $G = 0.43 \pm 0.08$ for the 2017 observations.

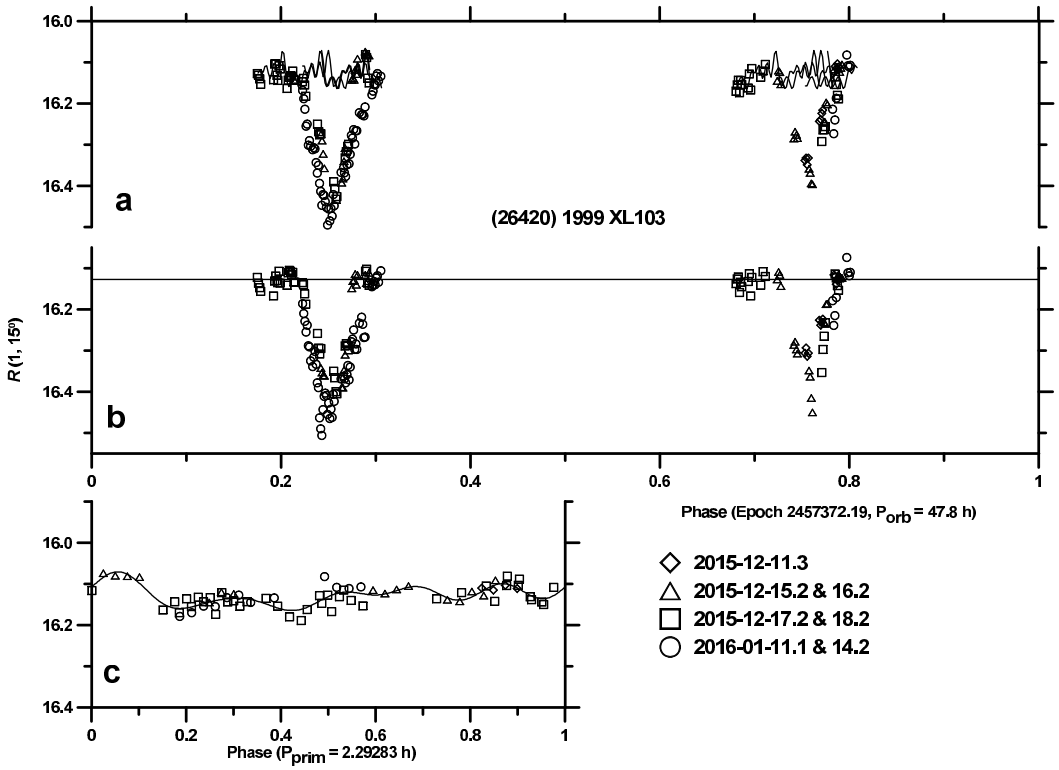

Suppl. Fig. 71. Lightcurve data of (26420) 1999 XL103 from 2015–2016. (a) The original data showing all the lightcurve components, folded with the orbital period. (b) The orbital lightcurve component, derived after subtraction of the primary lightcurve component, showing the mutual events between components of the binary system. (c) The primary lightcurve component.

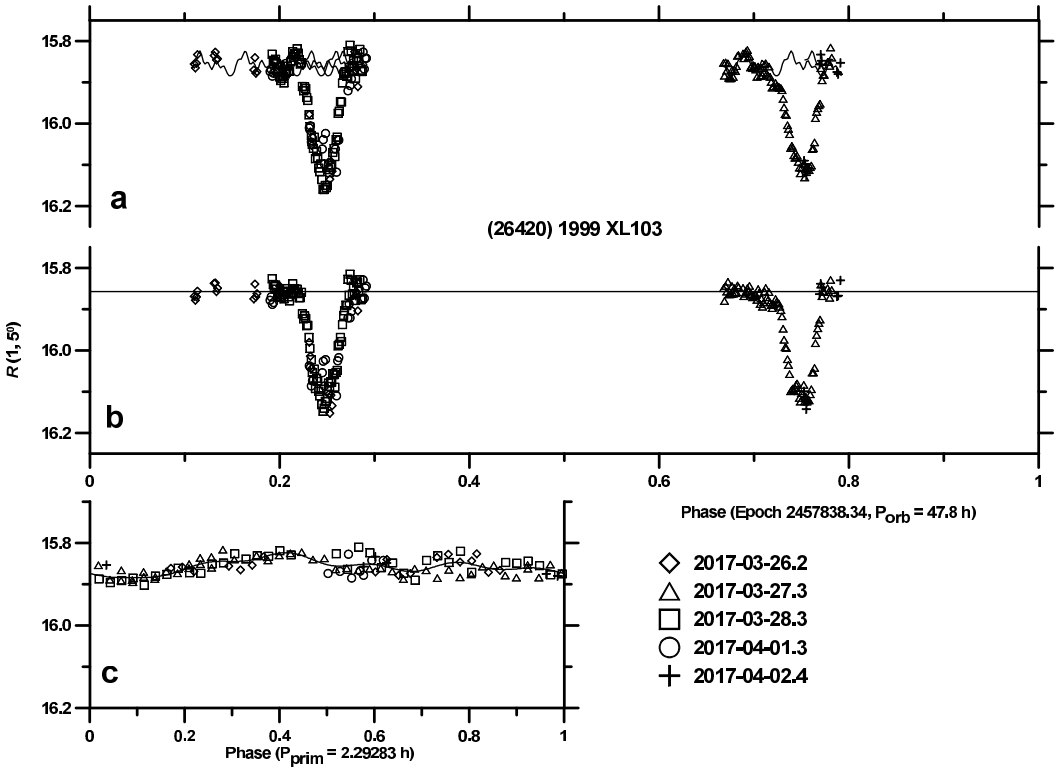

Suppl. Fig. 72. Lightcurve data of (26420) 1999 XL103 from 2017. (a) The original data showing all the lightcurve components, folded with the orbital period. (b) The orbital lightcurve component, derived after subtraction of the primary lightcurve component, showing the mutual events between components of the binary system. (c) The primary lightcurve component.

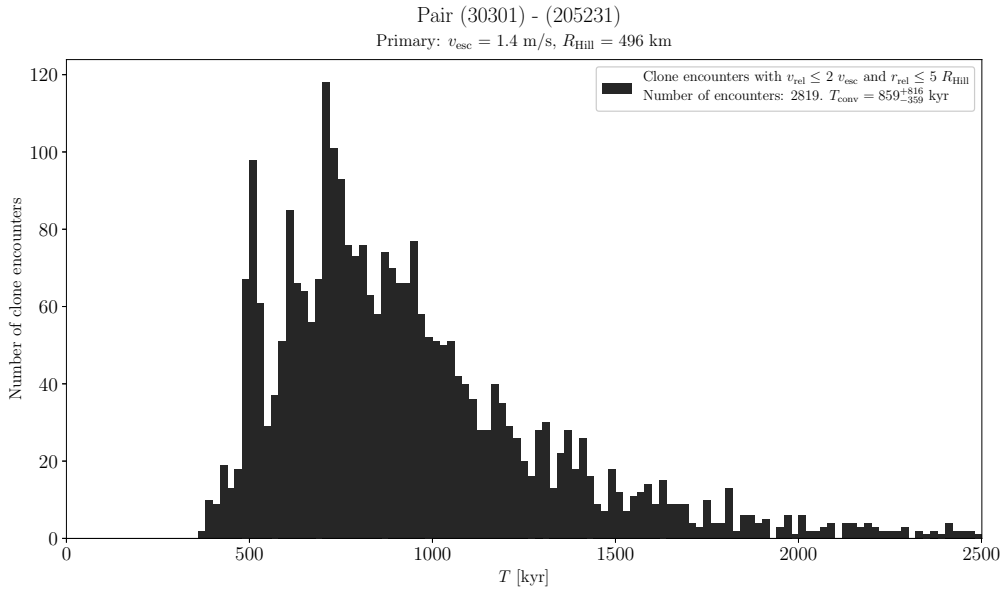

Suppl. Fig. 73. Distribution of past times of close and slow primary–secondary clone encounters for the asteroid pair 30301–205231.

(30301) Kuditipudi and (205231) 2000 QY110

The estimated age of this asteroid pair is about 900 kyr (Suppl. Fig. 73). We observed (30301) from La Silla on 3 nights during 2013-01-19 to 22 (Suppl. Fig. 74). We derived the mean absolute magnitude in the Cousins R system $H_{R,1} = 14.76 \pm 0.03$, assuming the slope parameter $G = 0.24 \pm 0.11$. For conversion to $H_1 \equiv H_{V,1}$, we assumed the color index $(V - R) = 0.49 \pm 0.05$; these assumed values are means for S type asteroids (Pravec et al. 2012b).

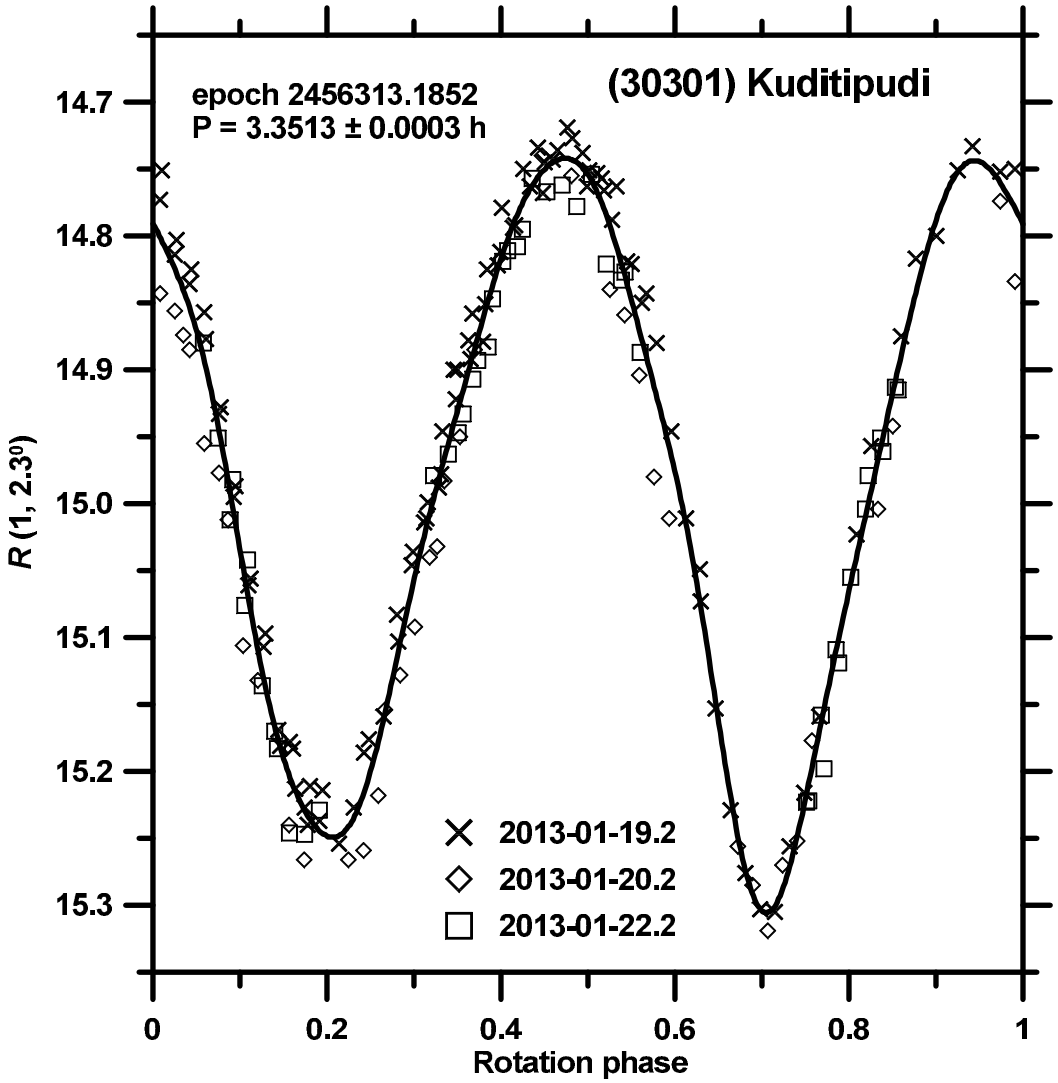

Suppl. Fig. 74. Composite lightcurve of (30301) Kuditipudi from 2013.

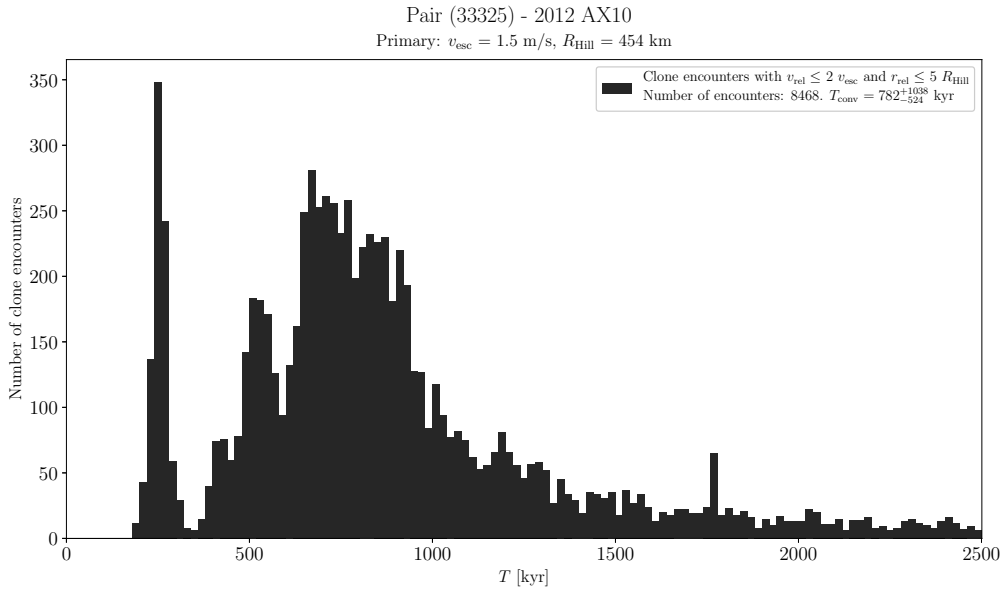

Suppl. Fig. 75. Distribution of past times of close and slow primary–secondary clone encounters for the asteroid pair 33325–2012AX10.

(33325) 1998 RH3 and 2012 AX10

The estimated age of this asteroid pair is about 800 kyr (Suppl. Fig. 75). We observed (33325) from La Silla on 3 nights during 2016-02-27 to 2016-03-06 (Suppl. Fig. 76). We derived the mean absolute magnitude in the Cousins R system $H_{R,1} = 14.81 \pm 0.03$, assuming the slope parameter $G = 0.33 \pm 0.10$ that is the mean value for Hungaria asteroids. For conversion to $H_1 \equiv H_{V,1}$, we assumed the color index $(V - R) = 0.45 \pm 0.10$. With our H_1, we refined the WISE effective diameter and geometric albedo (Masiero et al. 2011): $D_1 = 1.6 \pm 0.3$ km and $p_{V,1} = 0.51 \pm 0.17$.

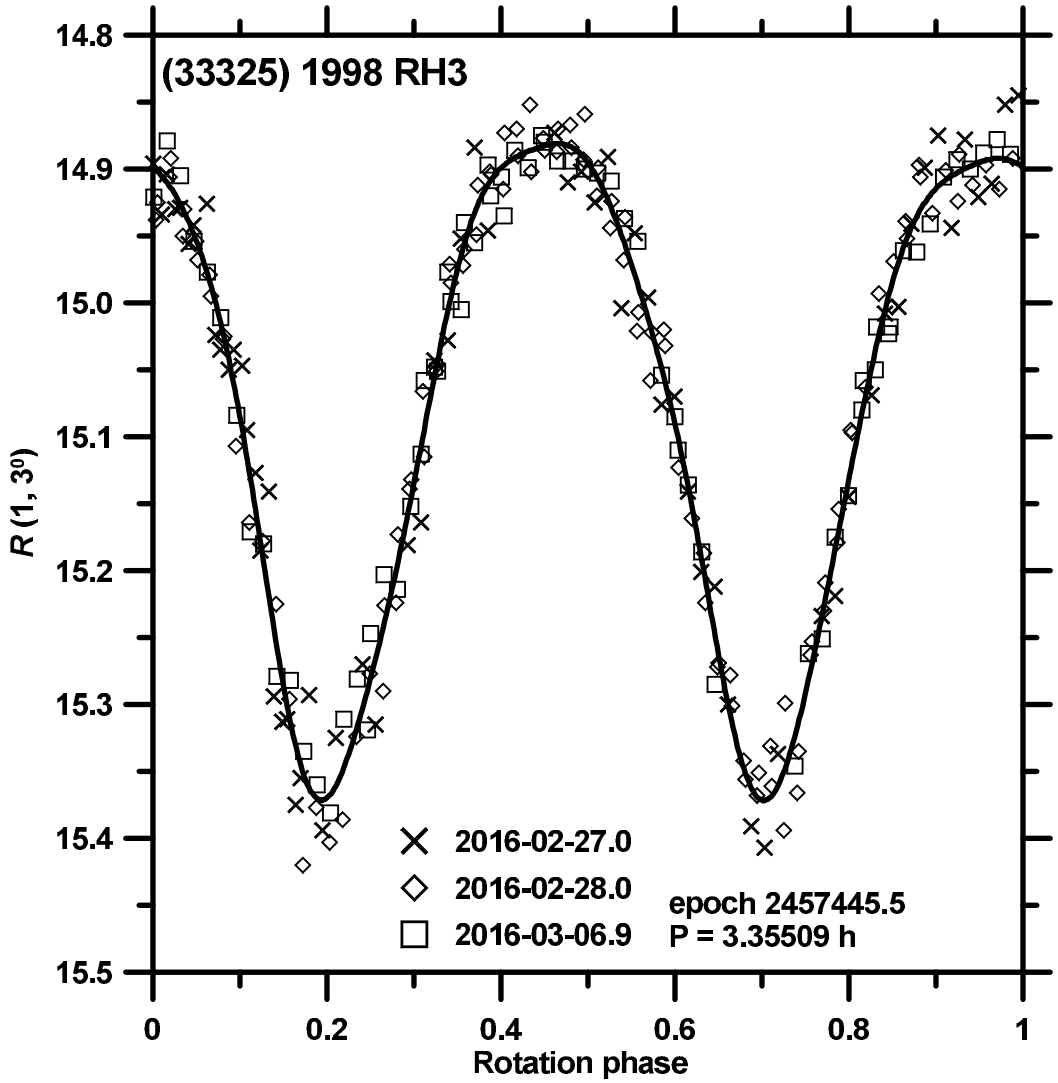

Suppl. Fig. 76. Composite lightcurve of (33325) 1998 RH3 from 2016.

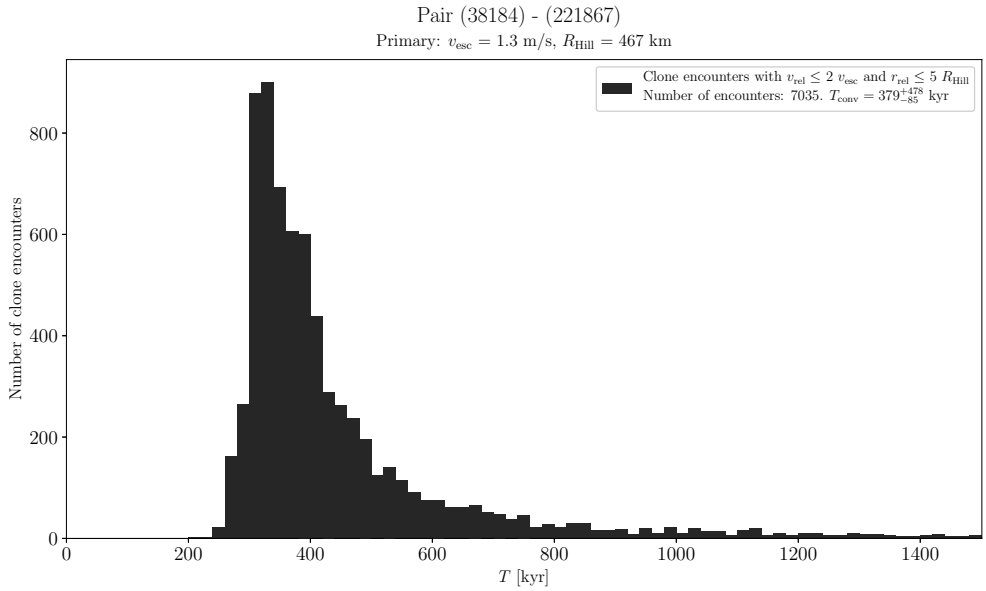

Suppl. Fig. 77. Distribution of past times of close and slow primary–secondary clone encounters for the asteroid pair 38184–221867.

(38184) 1999 KF and (221867) 2008 GR90

The estimated age of this asteroid pair is about 400 kyr (Suppl. Fig. 77). We have obtained lightcurve data for (38184) from 3 apparitions. We observed it from Simeiz on 2010-07-15, and from La Silla on 3 nights during 2013-04-11 to 2013-04-15 and on 4 nights during 2014-11-18 to 2014-11-25 (Suppl. Figs. 78 to 80). From the 2014 data, we derived the mean absolute magnitude $H_1 = 15.50 \pm 0.03$ and the phase relation slope parameter $G = 0.22 \pm 0.05$, and refined the WISE effective diameter and geometric albedo (Masiero et al. 2011): $D_1 = 1.9 \pm 0.4$ km and $p_{V,1} = 0.32 \pm 0.13$.

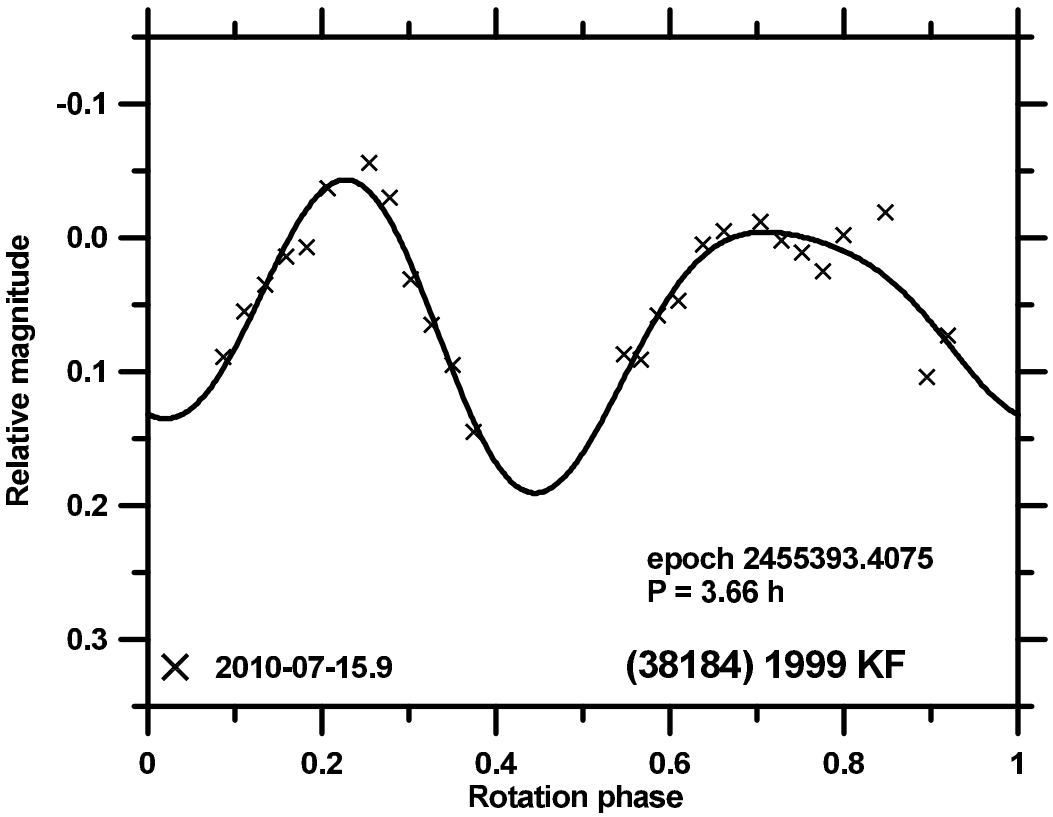

Suppl. Fig. 78. Composite lightcurve of (38184) 1999 KF from 2010.

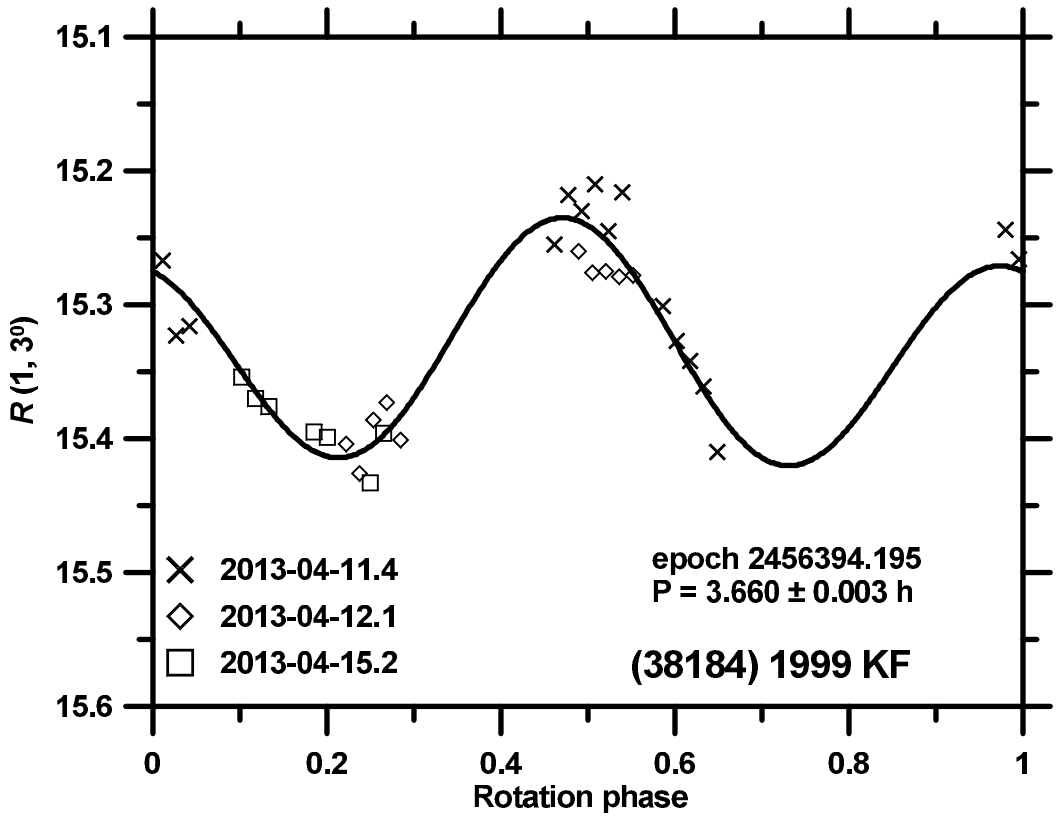

Suppl. Fig. 79. Composite lightcurve of (38184) 1999 KF from 2013.

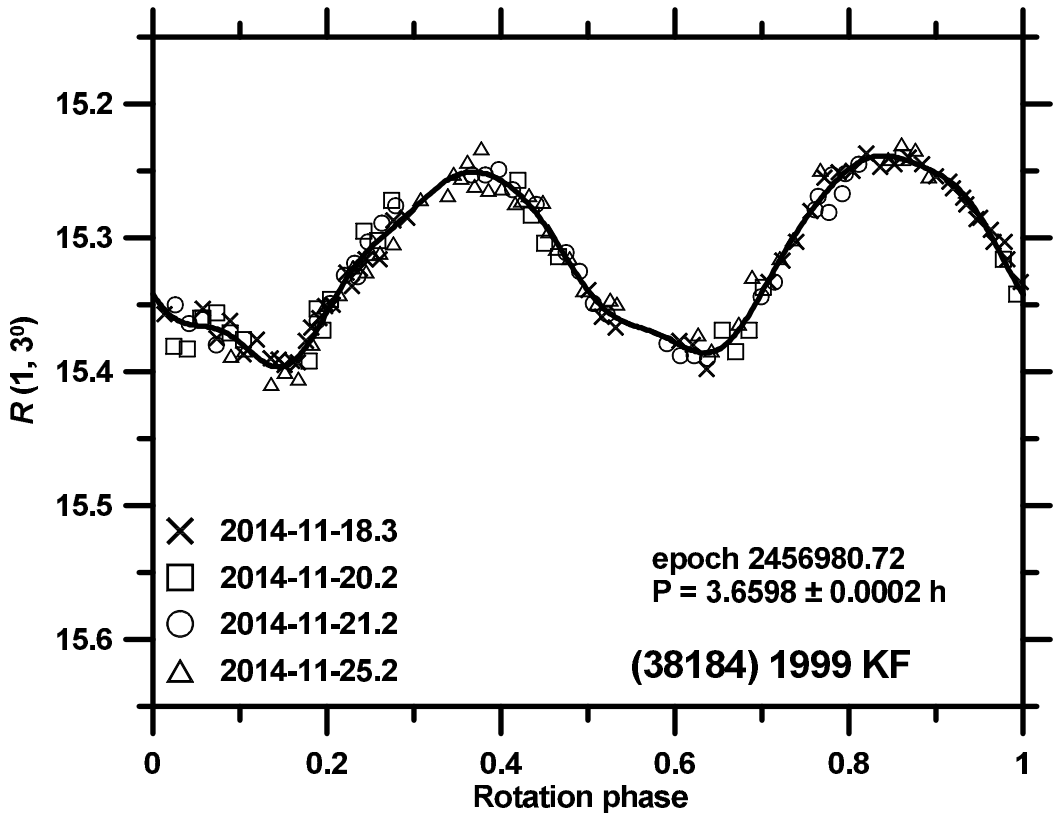

Suppl. Fig. 80. Composite lightcurve of (38184) 1999 KF from 2014.

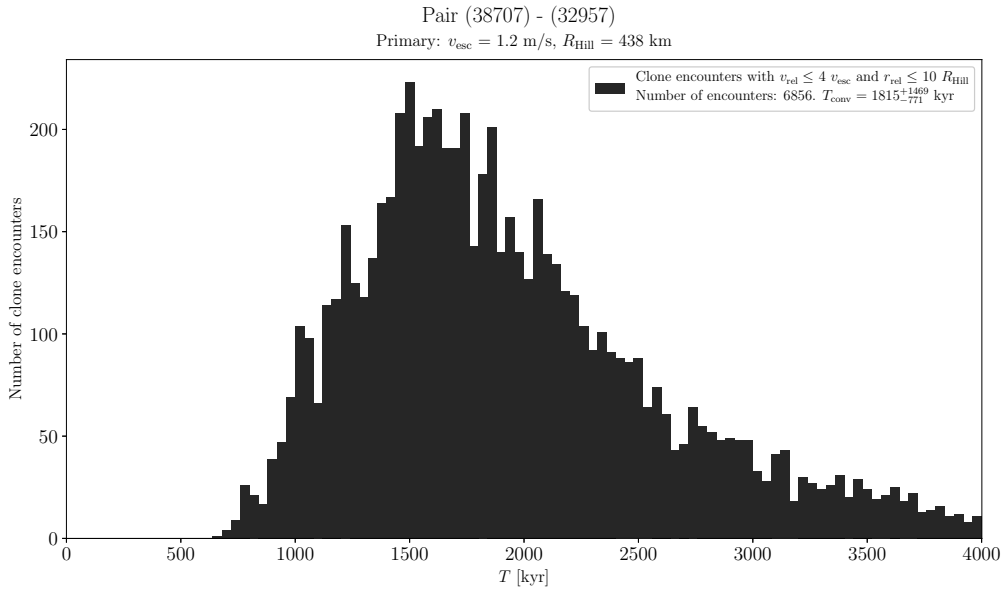

Suppl. Fig. 81. Distribution of past times of close and slow primary–secondary clone encounters for the asteroid pair 38707–32957.

(38707) 2000 QK89 and (32957) 1996 HX20

The estimated age of this asteroid pair is about 1800 kyr (Suppl. Fig. 81). Masiero et al. (2011) measured the primary's effective diameter $D_1 = 2.3 \pm 0.3$ km.

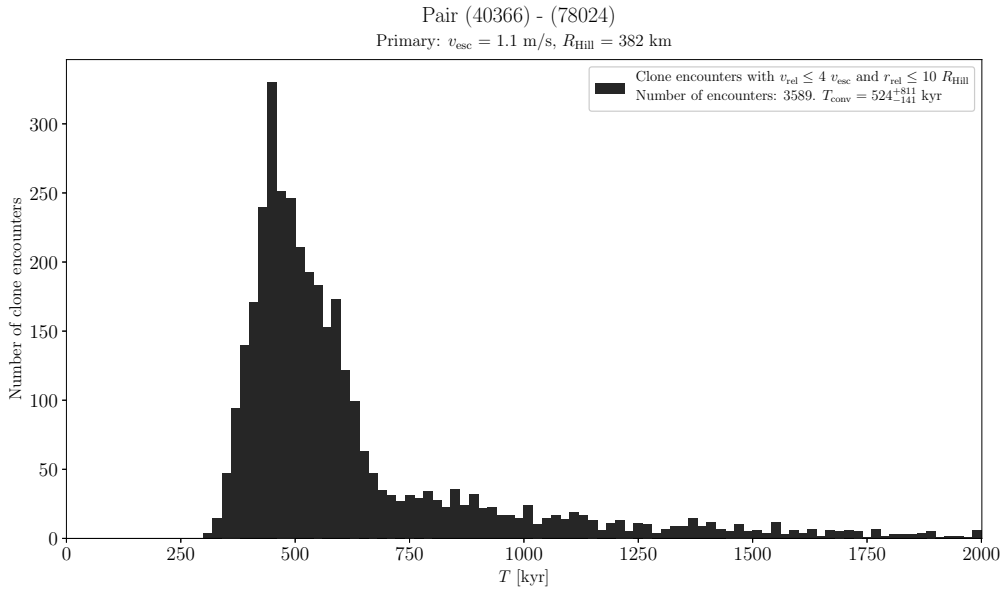

Suppl. Fig. 82. Distribution of past times of close and slow primary–secondary clone encounters for the asteroid pair 40366–78024.

(40366) 1999 NF27 and (78024) 2002 JO70

The estimated age of this asteroid pair is about 500 kyr (Suppl. Fig. 82). We observed the primary (40366) from La Silla on 2 nights 2018-04-23 and -24 (Suppl. Fig. 83). We derived its mean absolute magnitude $H_1 = 16.17 \pm 0.08$, assuming the phase relation slope parameter $G = 0.24 \pm 0.11$. The lightcurve data for the secondary were published in Pravec et al. (2010).

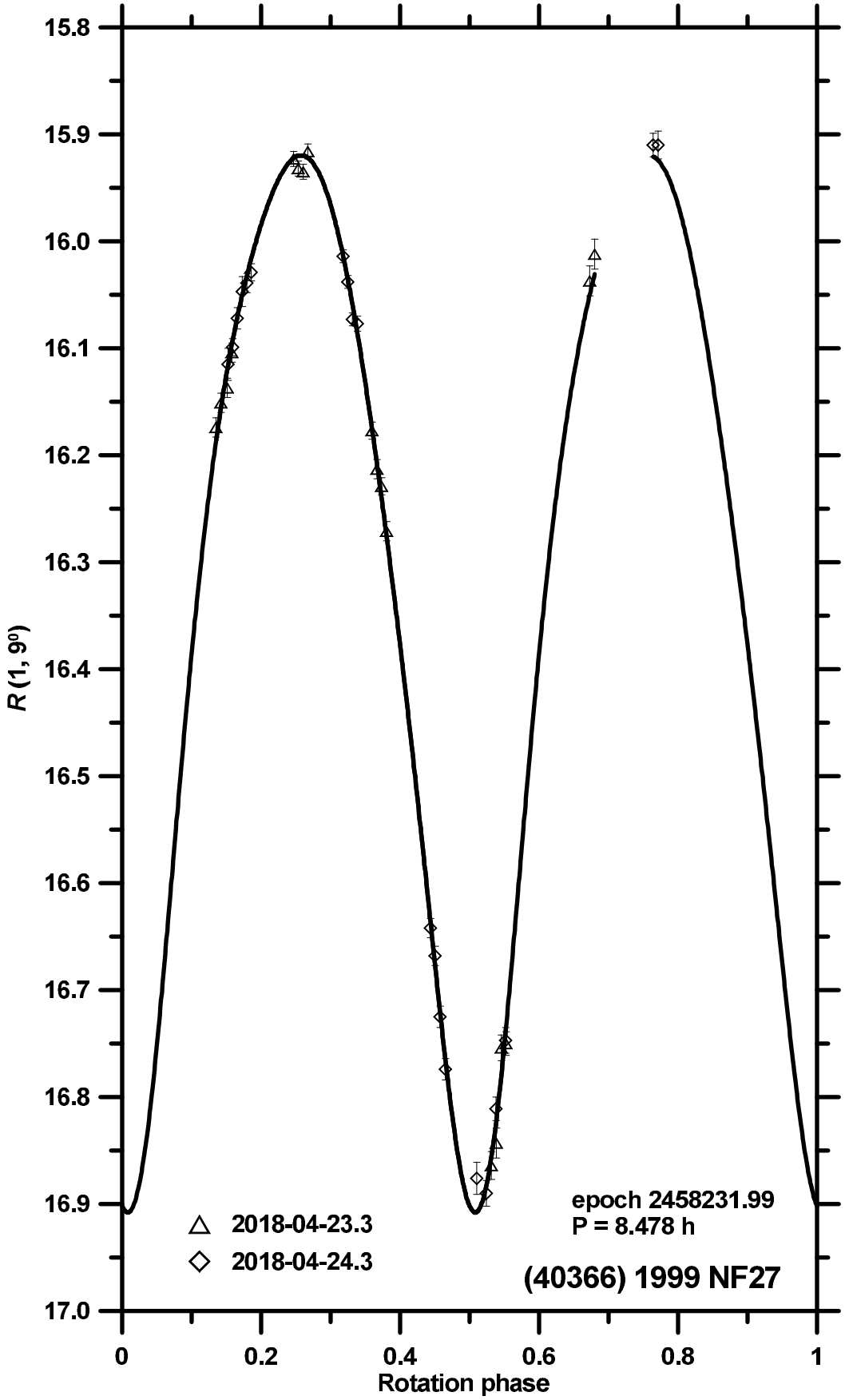

Suppl. Fig. 83. Composite lightcurve of (40366) 1999 NF27 from 2018.

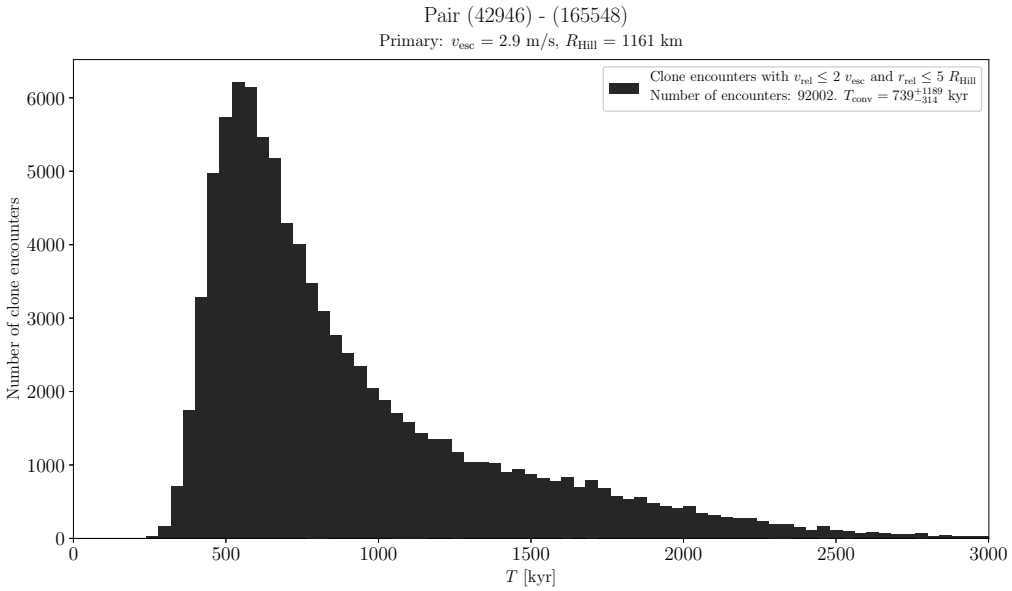

Suppl. Fig. 84. Distribution of past times of close and slow primary–secondary clone encounters for the asteroid pair 42946–165548.

(42946) 1999 TU95 and (165548) 2001 DO37

The estimated age of this asteroid pair is about 700 kyr (Suppl. Fig. 84). We obtained lightcurve data for the primary (42946) from 3 apparitions. The observations from Wise in 2014 were published in Polishook and Aharonson (2019). We observed it from Maidanak and Sugarloaf Mountain on 7 nights during 2012-12-03 to 2012-12-14, from Ondřejov on night 2014-04-23, and from La Silla and Ondřejov on 3 nights during 2018-02-19 to 2018-03-22 (Suppl. Figs. 85 to 87). We derived its mean absolute magnitudes $H_1 = 14.02 \pm 0.04$ and 14.08 ± 0.05 in 2014 and 2018, respectively, with the phase relation slope parameter $G = 0.22 \pm 0.05$ measured in 2018. With the weighted mean $H_1 = 14.05 \pm 0.04$, we refined the WISE effective diameter and geometric albedo (Masiero et al. 2011): $D_1 = 4.8 \pm 0.5$ km and $p_{V,1} = 0.19 \pm 0.04$. We observed the secondary (165548) from La Silla on two nights 2018-04-23 and -24. We estimated its period $P_2 = 7.9 \pm 0.1$ h, but it is not a unique solution, other values are also possible. We derived its mean absolute magnitude $H_2 = 15.90 \pm 0.03$, assuming the primary's $G = 0.22 \pm 0.05$.

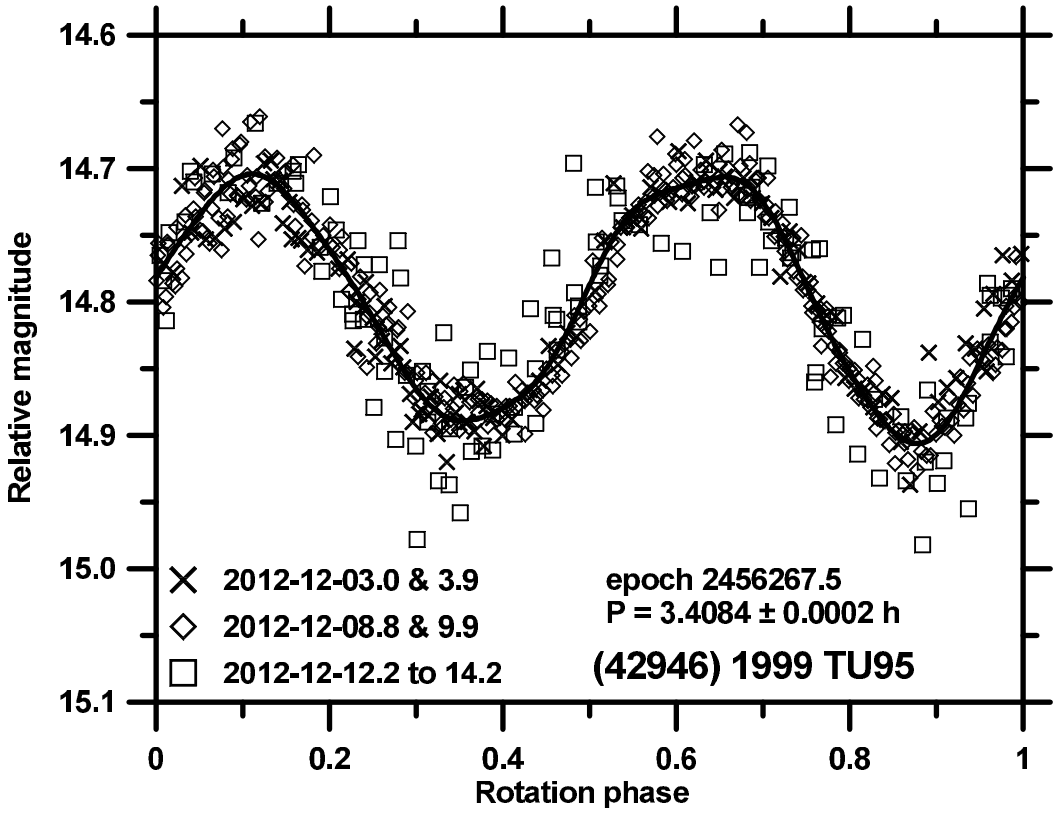

Suppl. Fig. 85. Composite lightcurve of (42946) 1999 TU95 from 2012.

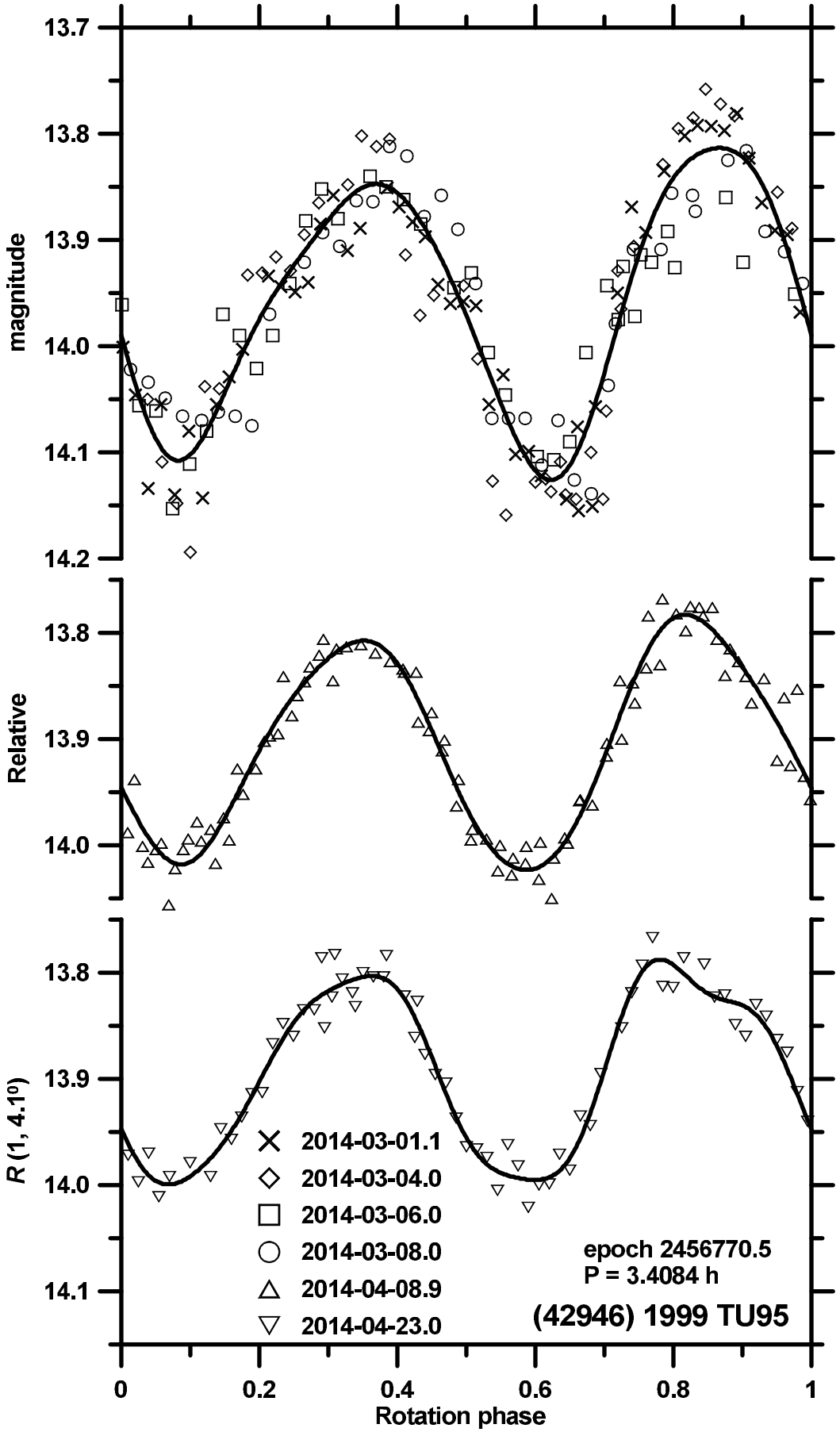

Suppl. Fig. 86. Composite lightcurves of (42946) 1999 TU95 from 2014.

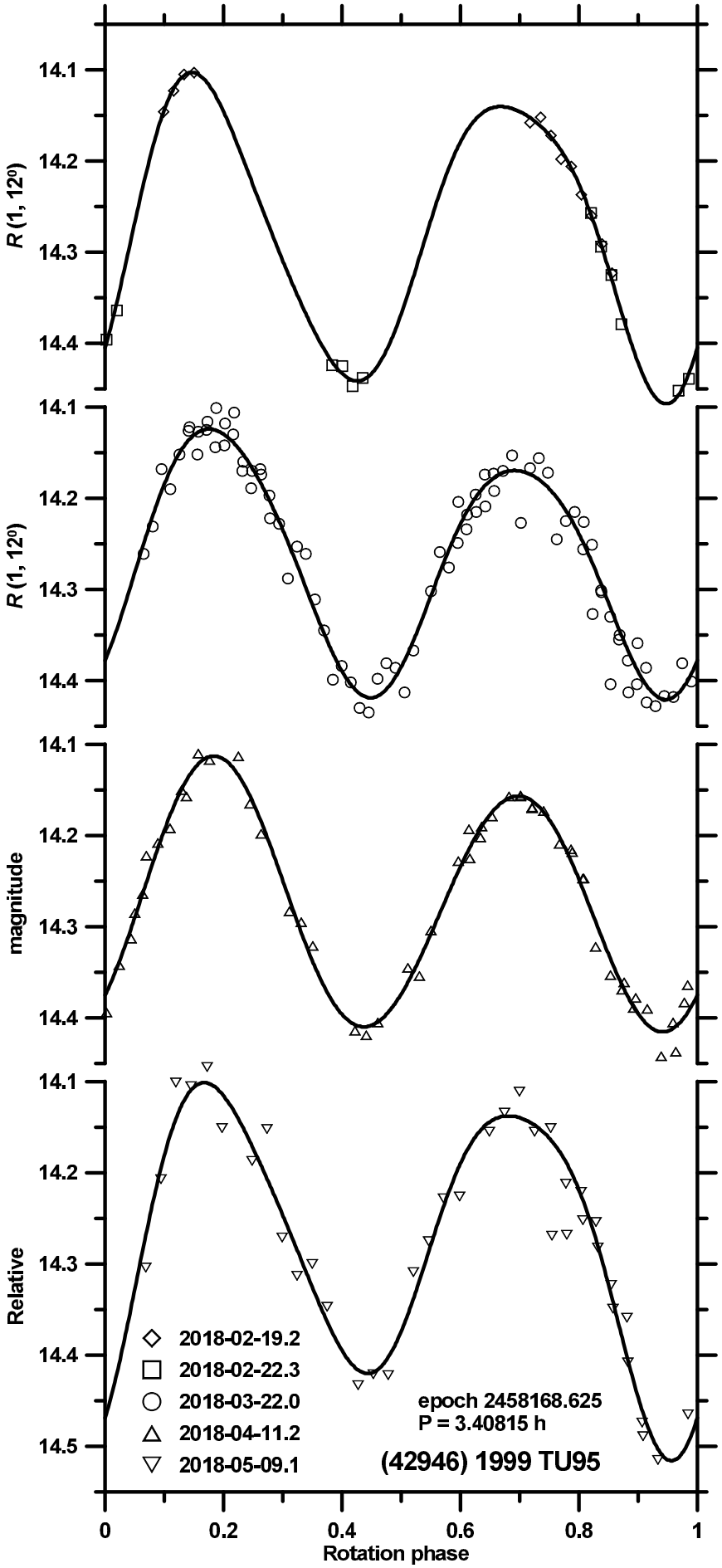

Suppl. Fig. 87. Composite lightcurves of (42946) 1999 TU95 from 2018.

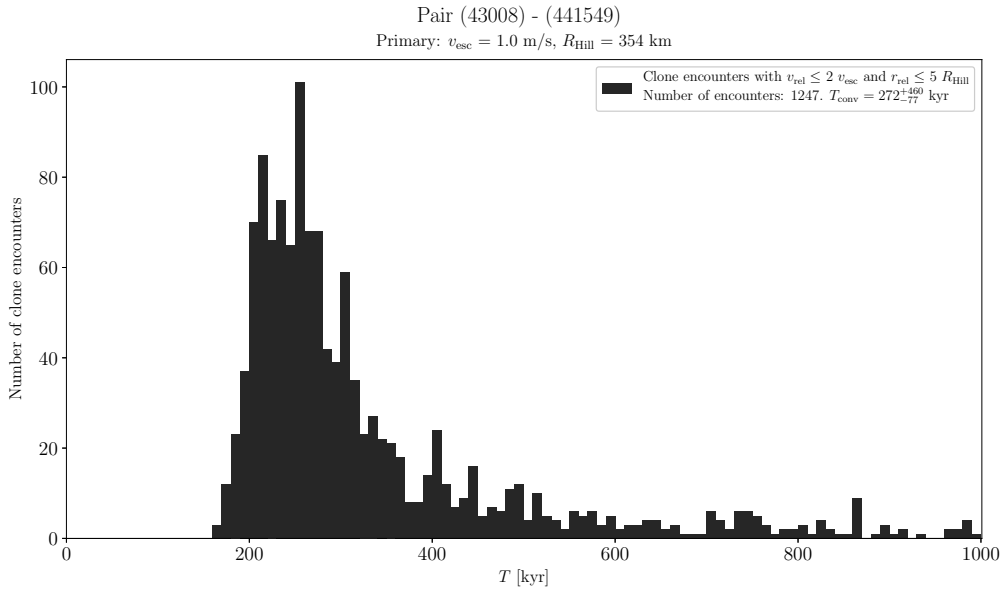

Suppl. Fig. 88. Distribution of past times of close and slow primary–secondary clone encounters for the asteroid pair 43008–441549.

(43008) 1999 UD31 and (441549) 2008 TM68

Backward orbital clone integrations suggest that these two asteroids separated about 270 kyr ago (Suppl. Fig. 88). We observed (43008) from La Silla on 16 nights during 2014-12-14 to 2015-01-25 and on 4 nights during 2016-04-01 to 2016-04-06, and from Lowell Observatory on 6 nights during 2017-09-21 to 2017-10-01 (Figs. 26 to 28). From the 2014-2015 data, we derived the mean absolute magnitude of the whole system (outside mutual events) $H_1 = 15.93 \pm 0.05$ and the slope parameter $G = 0.24 \pm 0.08$. We observed (441549) from La Silla on 3 nights during 2015-10-12 to 18 (Suppl. Fig. 89). Assuming the primary's $G = 0.24 \pm 0.08$ and $(V - R) = 0.458 \pm 0.02$, we derived $H_2 = 17.91 \pm 0.08$.

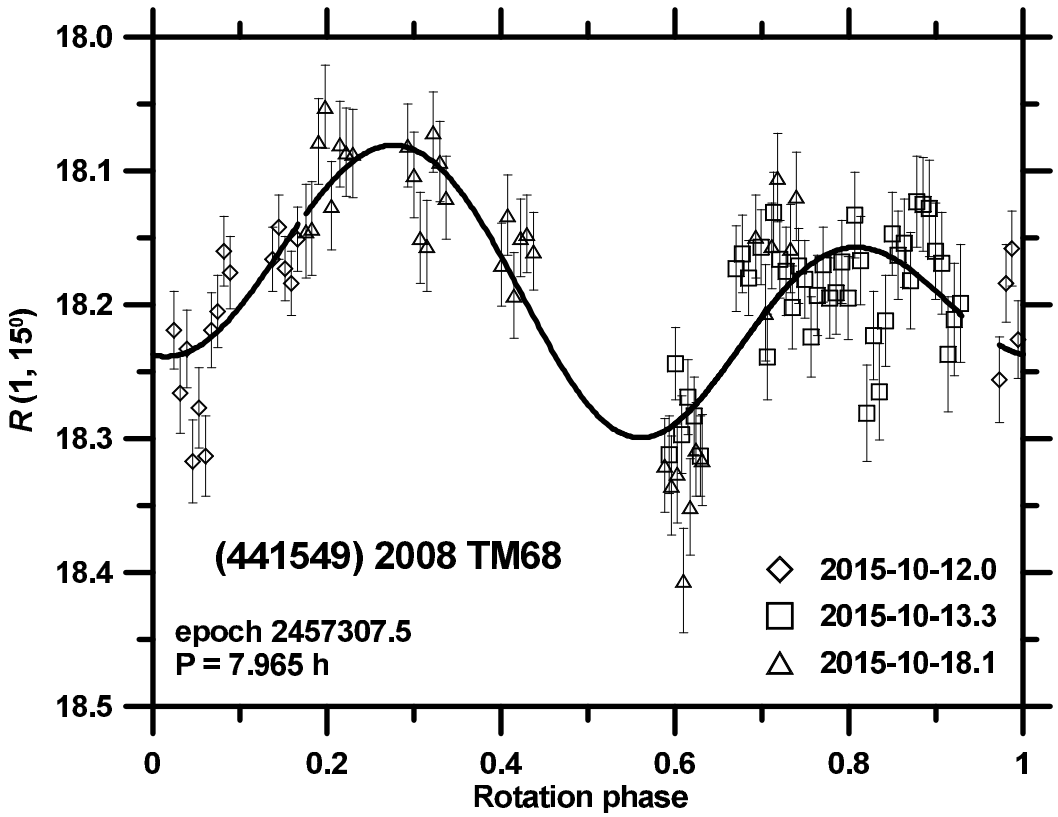

Suppl. Fig. 89. Composite lightcurve of (441549) 2008 TM68 from 2015.

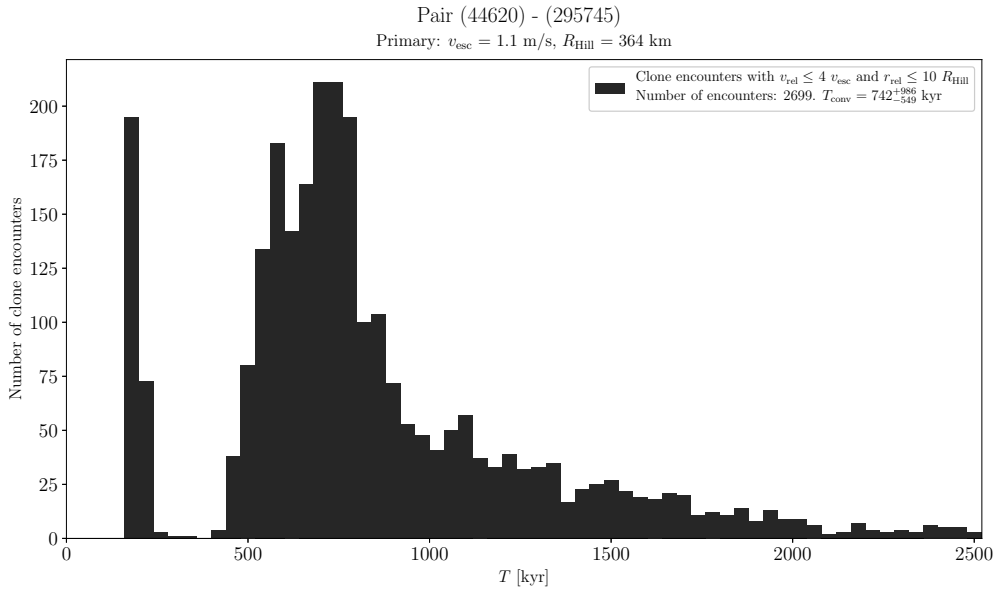

Suppl. Fig. 90. Distribution of past times of close and slow primary–secondary clone encounters for the asteroid pair 44620–295745.

(44620) 1999 RS43 and (295745) 2008 UH98

The estimated age of this asteroid pair is about 700 kyr, though an younger age of about 220 kyr is also possible (Suppl. Fig. 90). We observed (44620) from La Silla and Sierra Nevada on 16 nights during 2014-03-26 to 2014-05-06, from La Silla and Ondřejov on 15 nights during 2015-10-24 to 2016-01-14, and from Ondřejov on 4 nights during 2018-08-12 to 2018-08-23. We derived the mean absolute magnitudes of the whole system (outside mutual events) $H_1 = 15.78 \pm 0.04, 15.79 \pm 0.04$ and 15.78 ± 0.04 in the three apparitions, with the slope parameter $G = 0.24 \pm 0.02$.

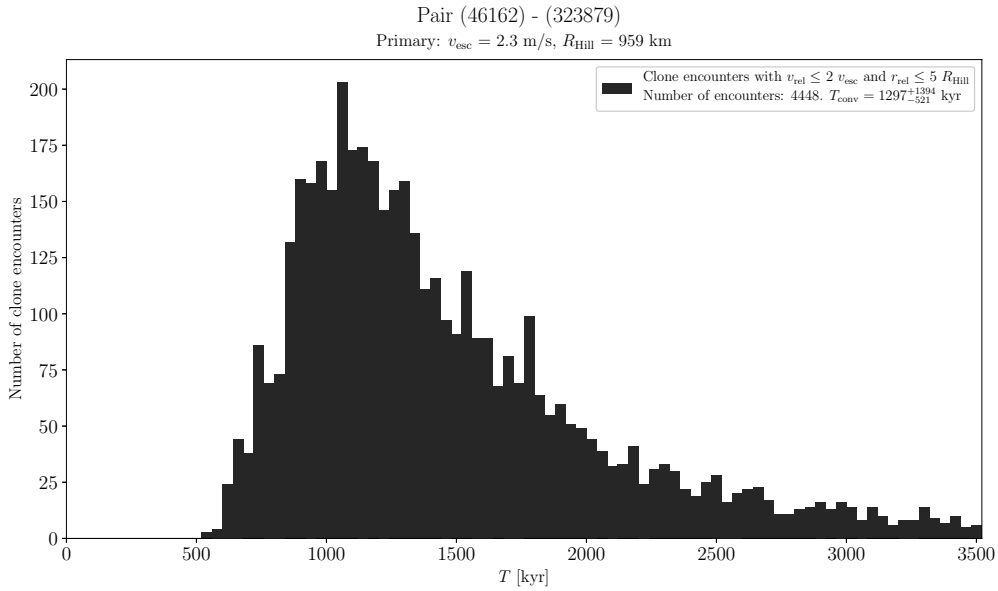

Suppl. Fig. 91. Distribution of past times of close and slow primary–secondary clone encounters for the asteroid pair 46162–323879.

(46162) 2001 FM78 and (323879) 2005 SA204

The estimated age of this asteroid pair is about 1300 kyr (Suppl. Fig. 91). We observed the primary (46162) from La Silla on 3 nights 2013-02-13 to -15 (Suppl. Fig. 92) and derived its mean absolute magnitude $H_1 = 14.90 \pm 0.10$, assuming the slope parameter $G = 0.15 \pm 0.20$, and refined the WISE effective diameter and geometric albedo (Masiero et al. 2011): $D_1 = 2.8 \pm 0.6$ km and $p_{V,1} = 0.24 \pm 0.10$.

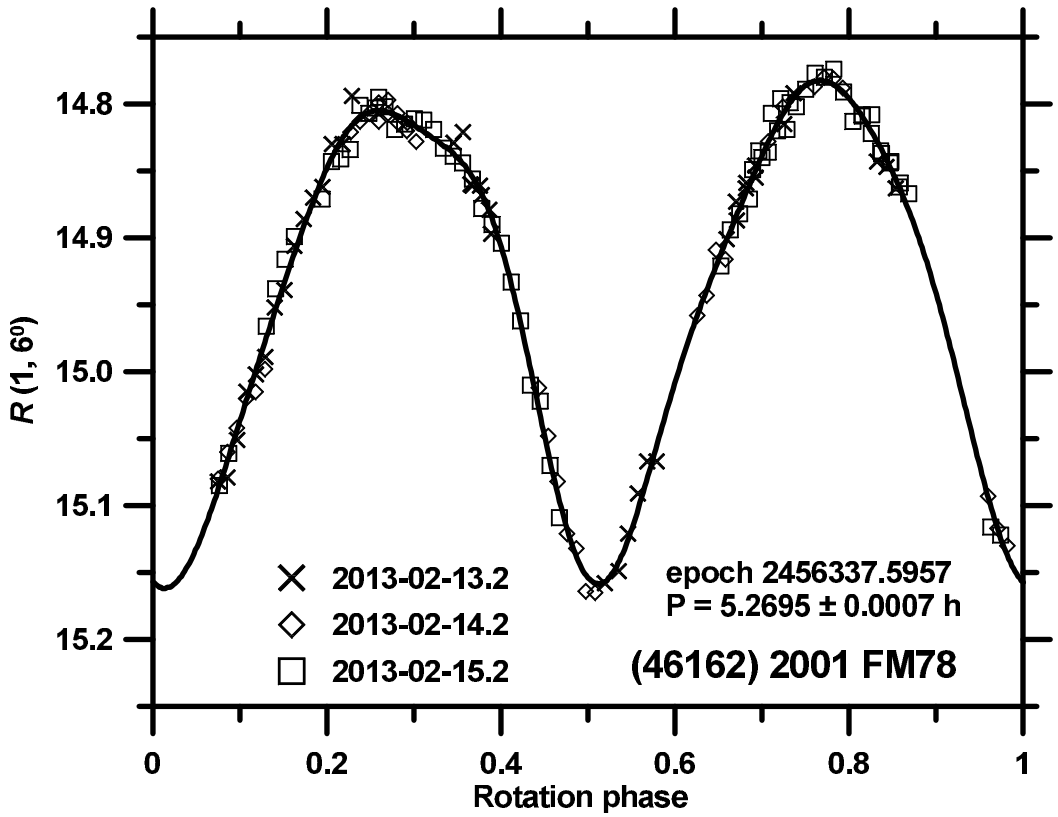

Suppl. Fig. 92. Composite lightcurve of (46162) 2001 FM78 from 2013.

(46829) McMahon and 2014 VR4

We observed (46829) from La Silla on 12 nights during 2015-02-12 to 2015-03-18. We derived the mean absolute magnitude of the whole system (outside mutual events) $H_1 = 15.25 \pm 0.03$ and the slope parameter $G = 0.30 \pm 0.02$.

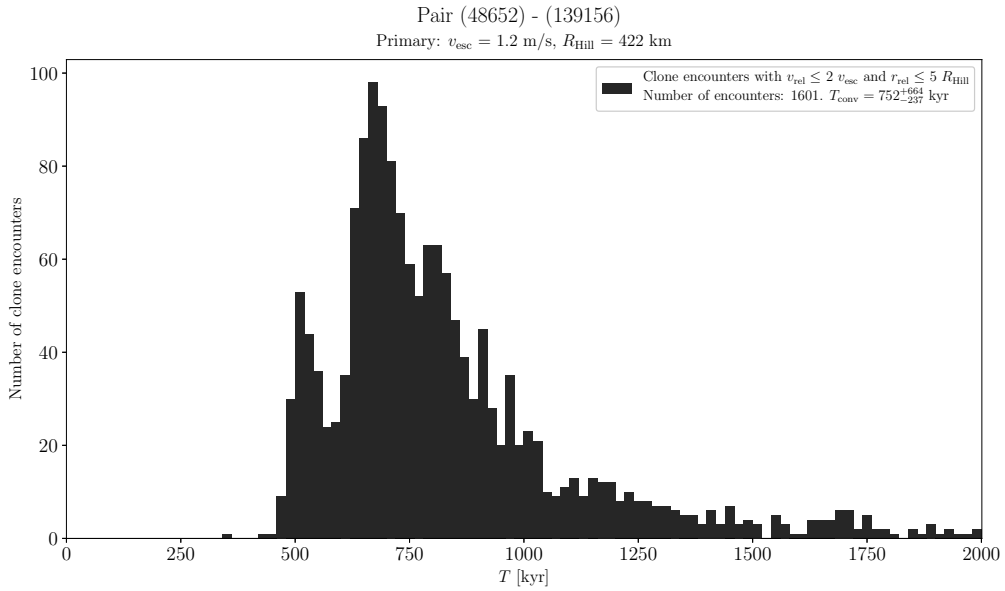

Suppl. Fig. 93. Distribution of past times of close and slow primary–secondary clone encounters for the asteroid pair 48652–139156.

(48652) 1995 VB and (139156) 2001 FP106

The estimated age of this asteroid pair is about 700 kyr (Suppl. Fig. 93). Masiero et al. (2011) measured the primary's effective diameter $D_1 = 2.2 \pm 0.2$ km.

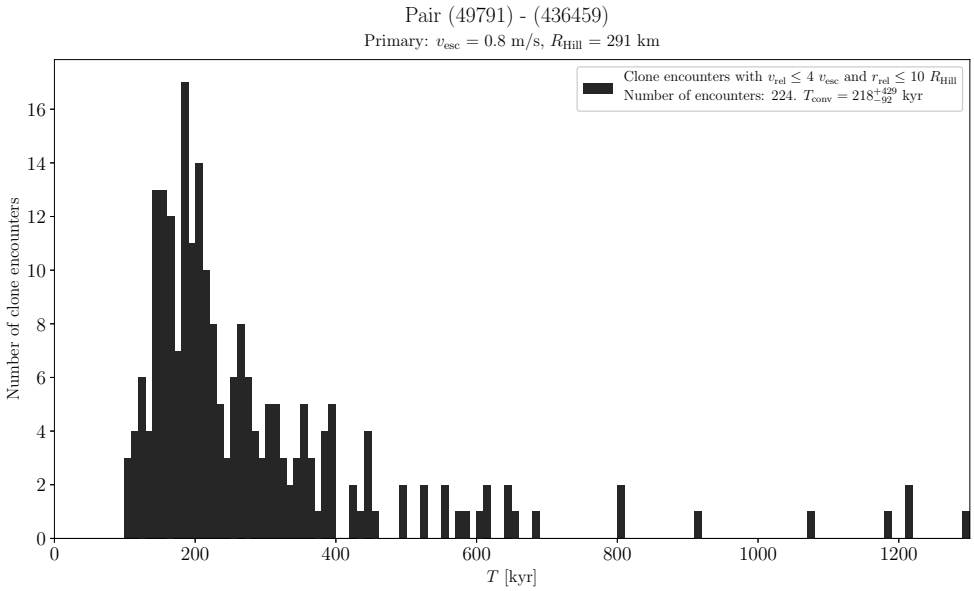

Suppl. Fig. 94. Distribution of past times of close and slow primary–secondary clone encounters for the asteroid pair 49791–436459.

(49791) 1999 XF31 and (436459) 2011 CL97

The estimated age of this asteroid pair is about 200 kyr (Suppl. Fig. 94). We observed (49791) from La Silla on 8 nights during 2013-11-25 to 2013-12-10 (Suppl. Fig. 95). We derived the mean absolute magnitude $H_1 = 16.07 \pm 0.05$ and the slope parameter $G = 0.37 \pm 0.08$.

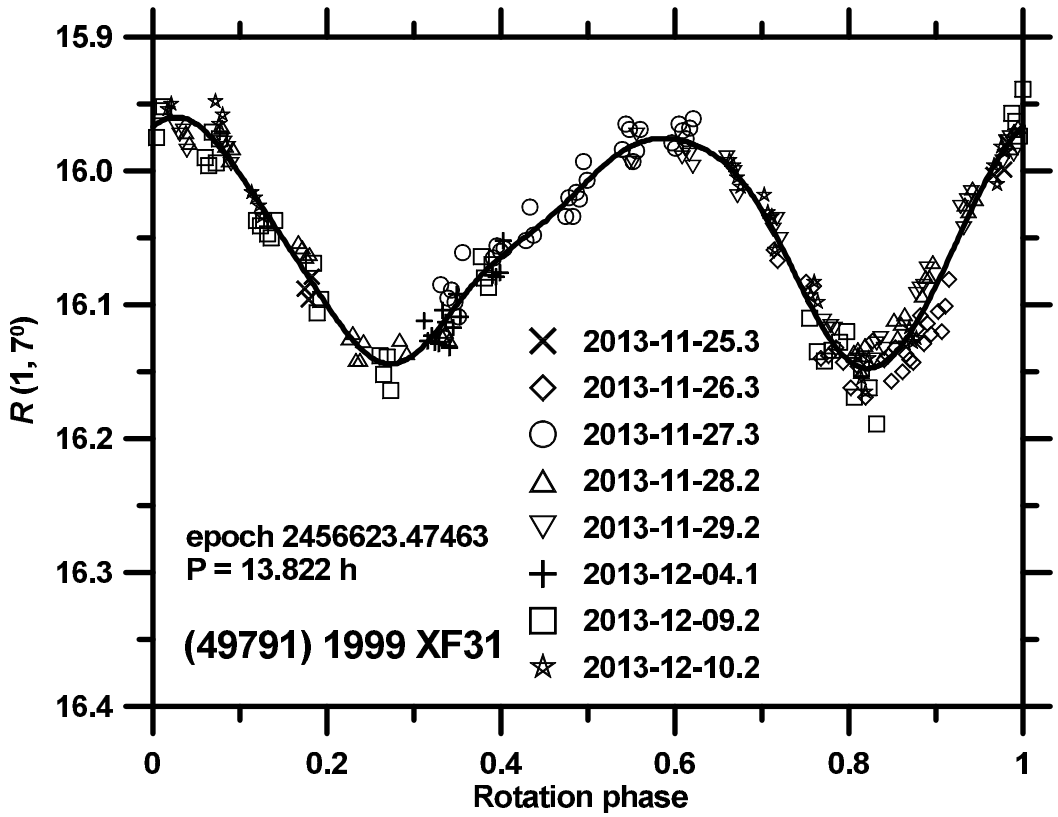

Suppl. Fig. 95. Composite lightcurve of (49791) 1999 XF31 from 2013.

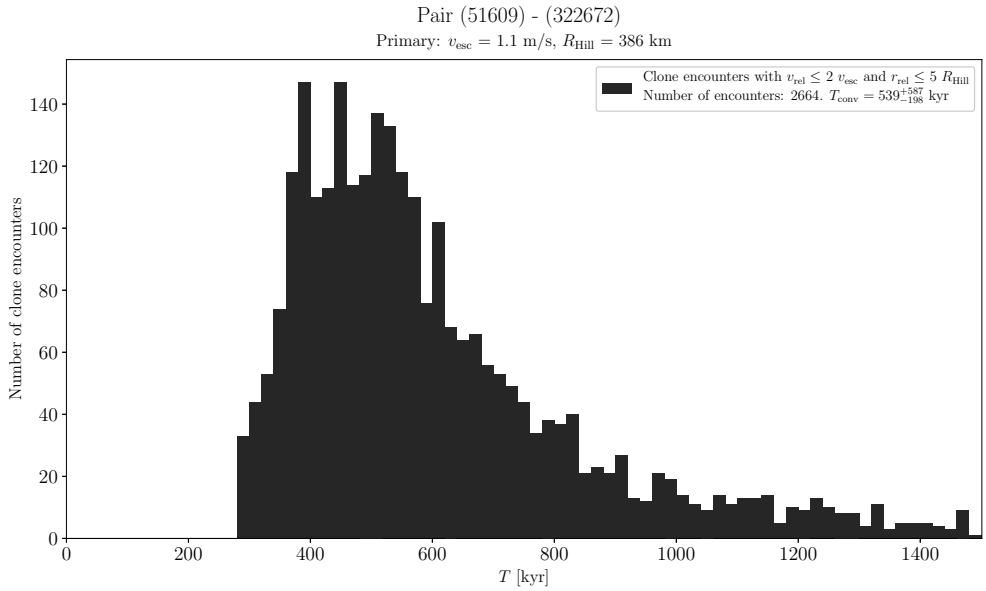

Suppl. Fig. 96. Distribution of past times of close and slow primary–secondary clone encounters for the asteroid pair 51609-322672.

(51609) 2001 HZ32 and (322672) 1999 TE221

The estimated age of this asteroid pair is about 500 kyr (Suppl. Fig. 96). The observations of (51609) in 2009 were published in Pravec et al. (2010). We observed it from La Silla on 2 nights of 2018-03-12 and 20 (Suppl. Fig. 97). We measured $(V-R)_1 = 0.421 \pm 0.013$. We derived the mean absolute magnitude $H_1 = 15.45 \pm 0.14$, assuming the slope parameter $G = 0.15 \pm 0.20$. With this H_1, we refined the WISE effective diameter and geometric albedo (Masiero et al. 2011): $D_1 = 1.9 \pm 0.7$ km and $p_{V,1} = 0.32 \pm 0.23$.

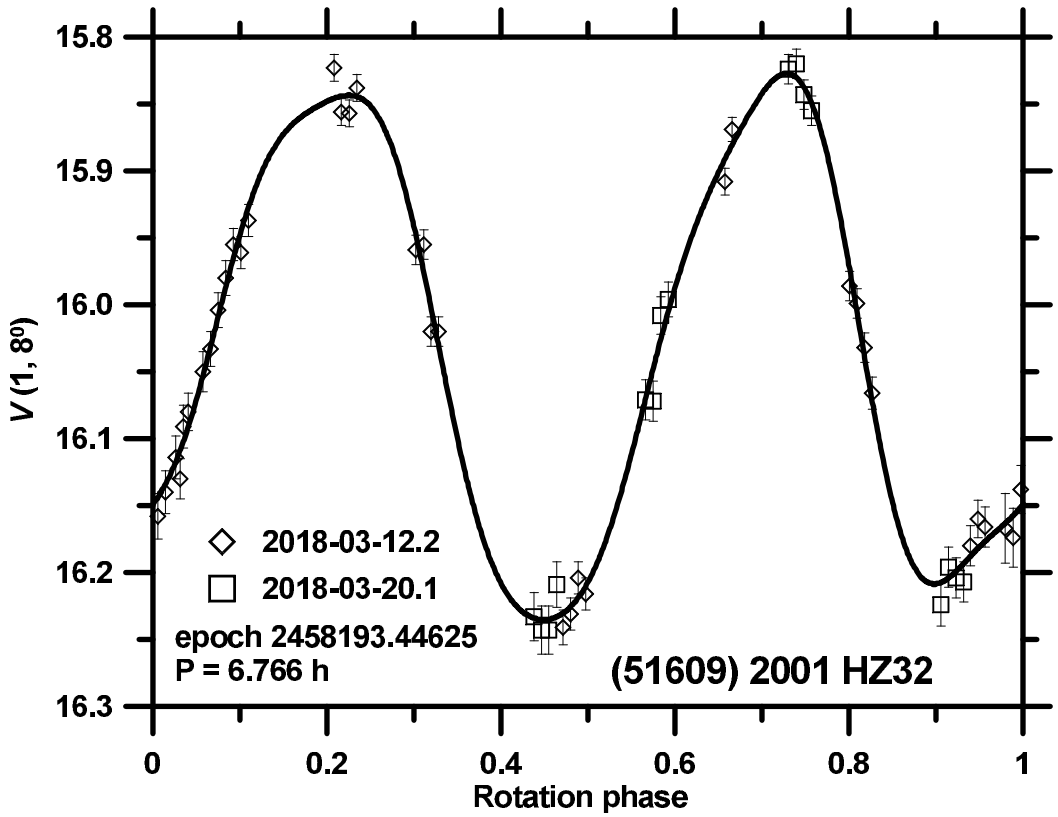

Suppl. Fig. 97. Composite lightcurve of (51609) 2001 HZ32 from 2018.

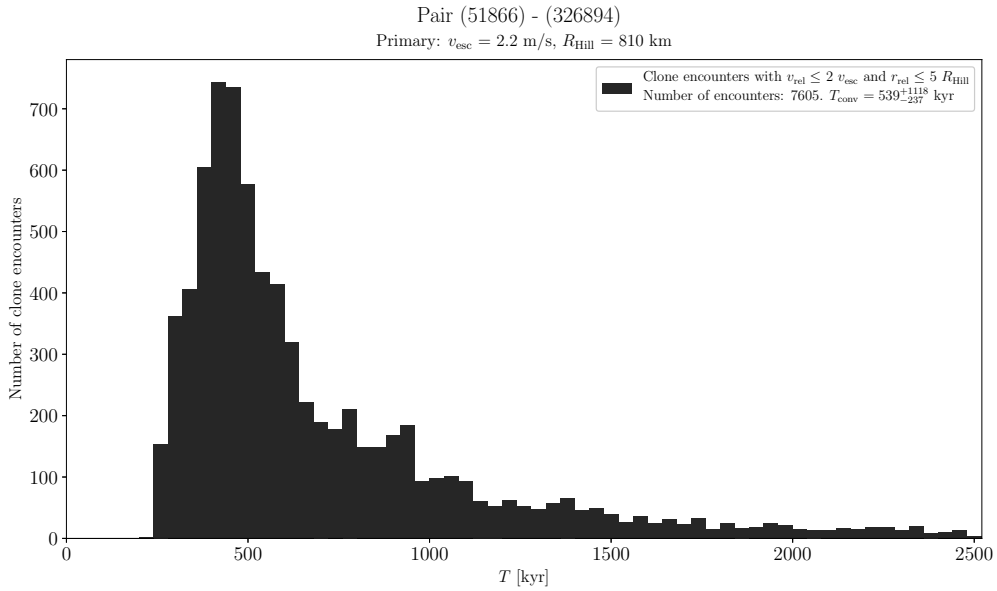

Suppl. Fig. 98. Distribution of past times of close and slow primary–secondary clone encounters for the asteroid pair 51866–326894.

(51866) 2001 PH3 and (326894) 2003 WV25

The estimated age of this asteroid pair is about 500 kyr (Suppl. Fig. 98). We observed the primary (51866) with PROMPT and from La Silla on 10 nights during 2013-12-27 to 2014-02-04 (Suppl. Fig. 99). From the La Silla observations, we derived its mean absolute magnitude $H_1 = 14.31 \pm 0.12$, assuming $G = 0.24 \pm 0.11$, and refined the WISE effective diameter and geometric albedo (Masiero et al. 2011): $D_1 = 4.0 \pm 0.4$ km and $p_{V,1} = 0.21 \pm 0.05$.

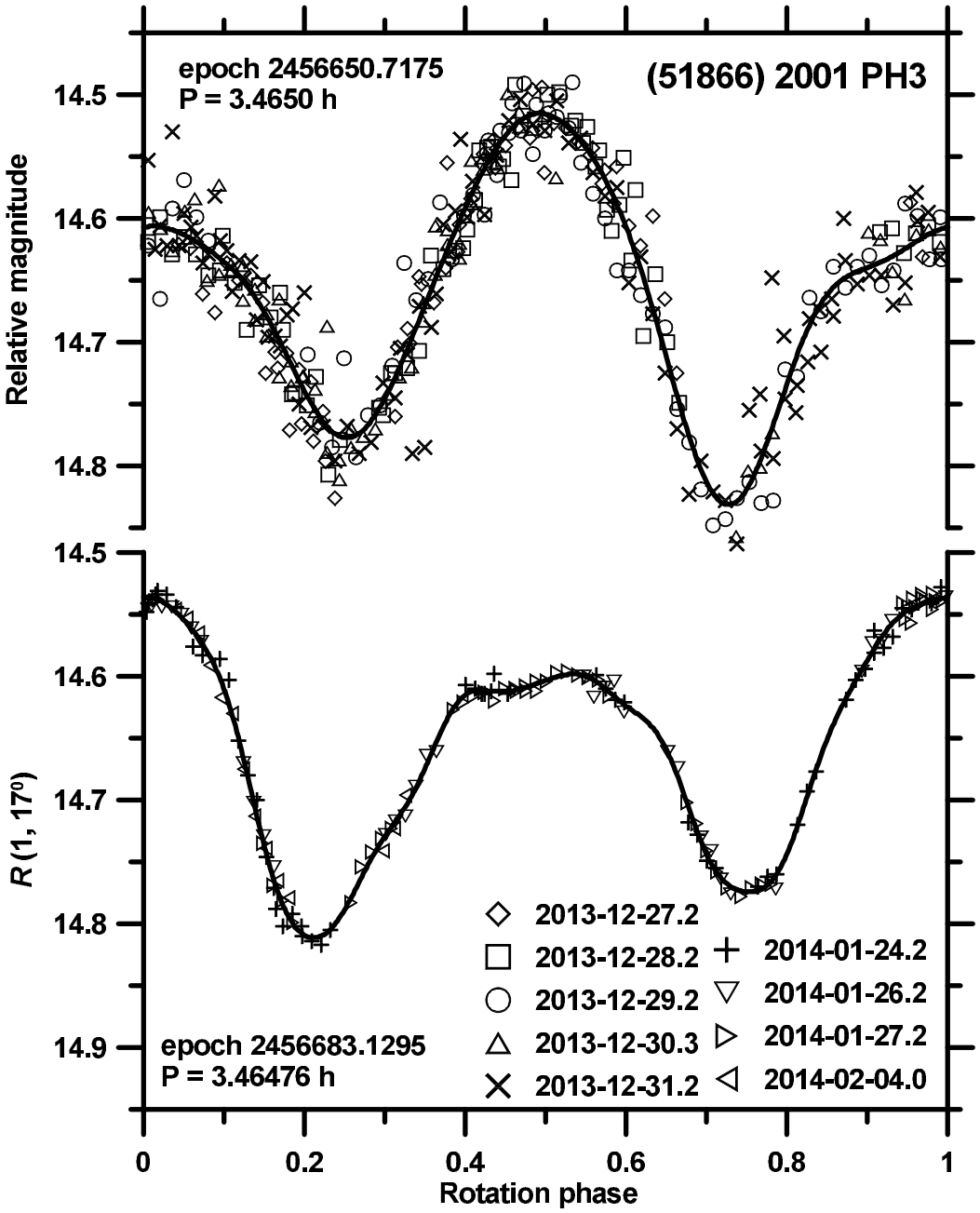

Suppl. Fig. 99. Composite lightcurves of (51866) 2001 PH3 from 2013–2014.

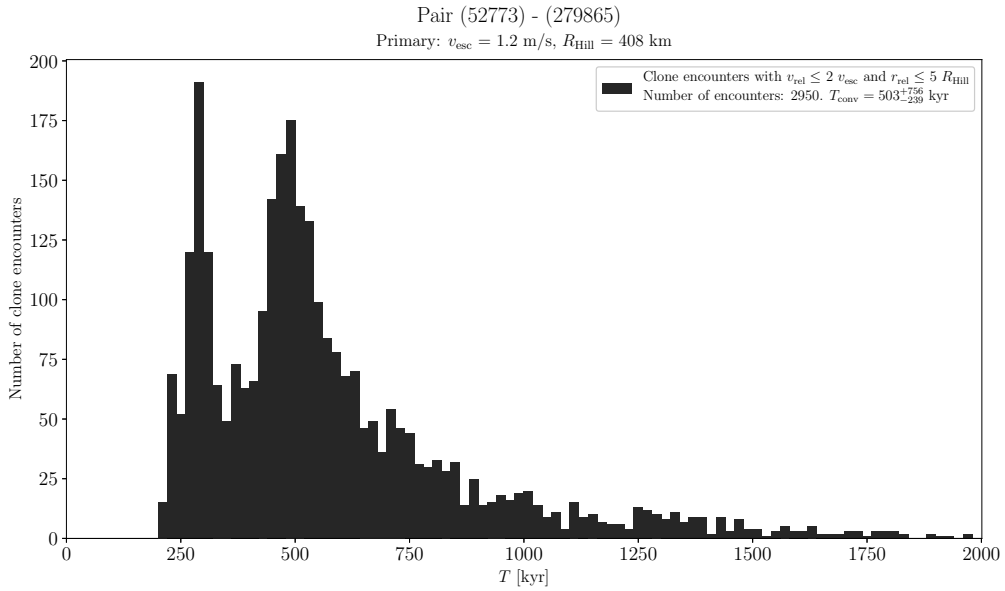

Suppl. Fig. 100. Distribution of past times of close and slow primary–secondary clone encounters for the asteroid pair 52773–279865.

(52773) 1998 QU12 and (279865) 2001 HU24

The estimated age of this asteroid pair is about 500 kyr (Suppl. Fig. 100). The observations of (52773) in 2008 were published in Pravec et al. (2010). We observed it from Ondřejov on 2018-09-08 and -10 (Suppl. Fig. 101). We derived $H_{R,1} = 15.39 \pm 0.13$, assuming the slope parameter $G = 0.24 \pm 0.11$. With $(V - R)_1 = 0.44 \pm 0.03$ derived from Lowell SDSS color measurements, it is $H_1 = 15.83 \pm 0.13$.

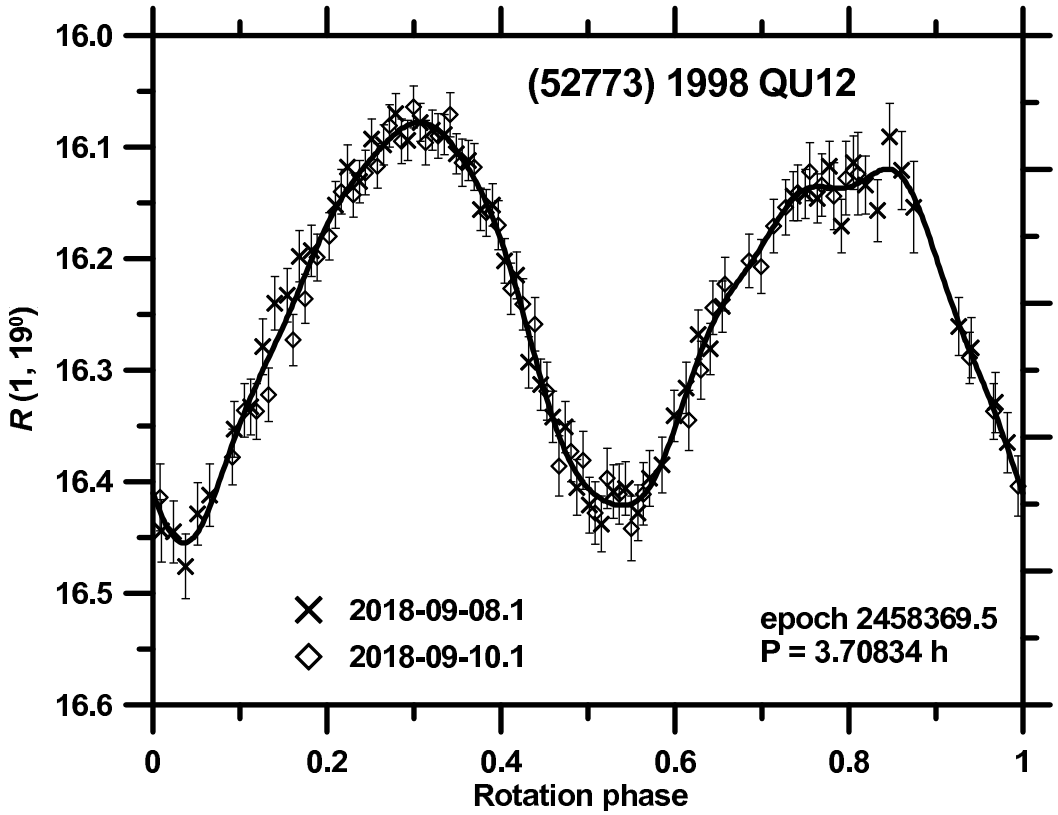

Suppl. Fig. 101. Composite lightcurve of (52773) 1998 QU12 from 2018.

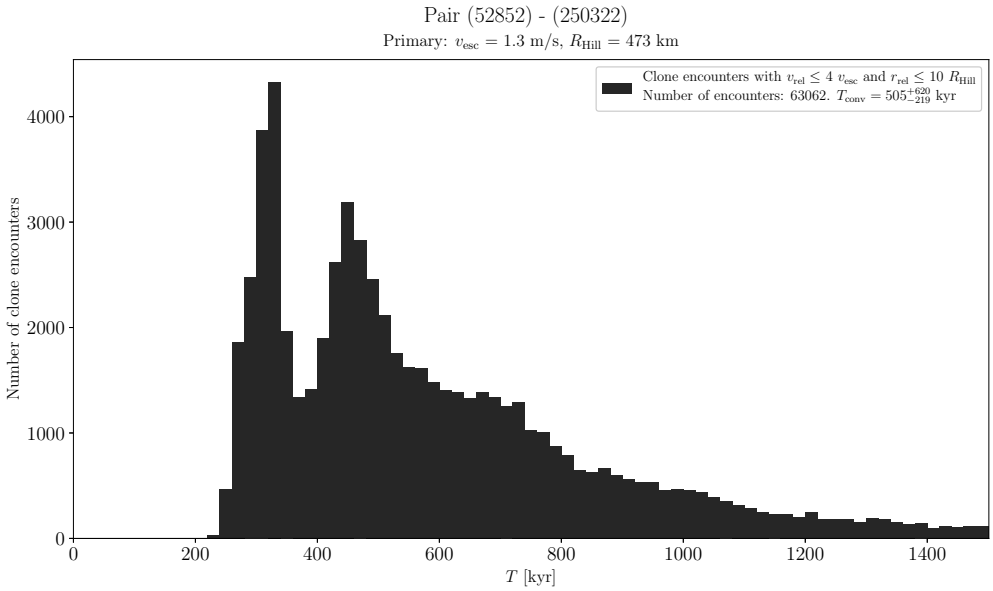

Suppl. Fig. 102. Distribution of past times of close and slow primary–secondary clone encounters for the asteroid pair 52852–250322.

(52852) 1998 RB75 and (250322) 2003 SC7

The estimated age of this asteroid pair is about 500 kyr (Suppl. Fig. 102). The observations of (52852) in 2008 were published in Pravec et al. (2010). We observed it from Sugarloaf Mountain and Ondřejov on 18 nights during 2015-09-15 to 2015-10-19. From the two Ondřejov nights that were calibrated in the Cousins R system, we derived $H_{R,1} = 14.48 \pm 0.06$, assuming the slope parameter $G = 0.24 \pm 0.11$. For conversion to $H_1 \equiv H_{V,1}$, we assumed the color index $(V - R) = 0.49 \pm 0.05$; these assumed values are means for S type asteroids (Pravec et al. 2012b). With the H_1 value, we refined the WISE data by Masiero et al. (2011) and obtained $D_1 = 2.5 \pm 0.5$ km and $p_{V,1} = 0.29 \pm 0.11$.

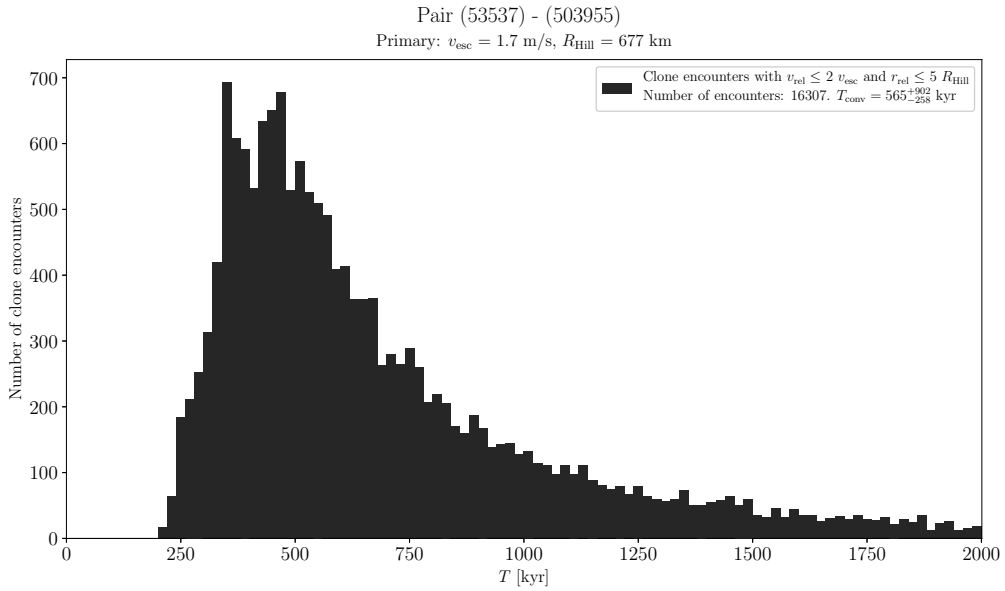

Suppl. Fig. 103. Distribution of past times of close and slow primary–secondary clone encounters for the asteroid pair 53537–503955.

(53537) 2000 AZ239 and (503955) 2004 ED107

Backward orbital clone integrations suggest that these two asteroids separated about 500 kyr ago (Suppl. Fig. 103). We observed the primary (53537) from La Silla on 28 nights during 2013-10-27 to 2014-01-04 and derived its mean absolute R magnitude $H_{R,1} = 14.29 \pm 0.07$ and the slope parameter $G = 0.26 \pm 0.08$. For conversion to $H_1 \equiv H_{V,1}$, we assumed the color index $(V-R) = 0.49 \pm 0.05$.

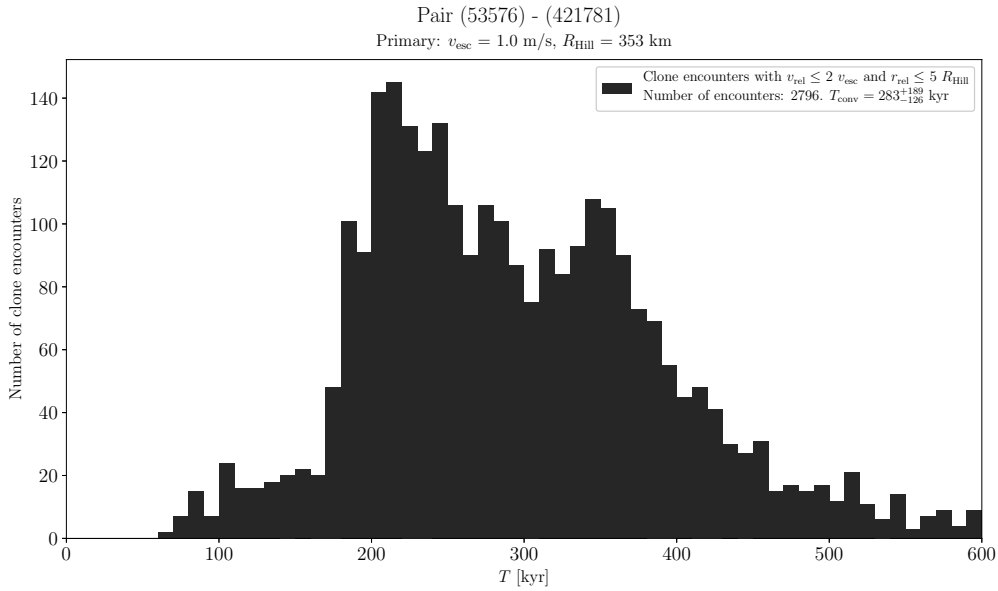

Suppl. Fig. 104. Distribution of past times of close and slow primary–secondary clone encounters for the asteroid pair 53576–421781.

(53576) 2000 CS47 and (421781) 2014 QG22

Backward orbital clone integrations suggest that these two asteroids separated about 300 kyr ago (Suppl. Fig. 104). We observed the primary (53576) from La Silla on 7 nights during 2015-12-05 to 2015-12-16 (Suppl. Fig. 105). We derived the mean absolute magnitude $H_1 = 15.95 \pm 0.03$ and the phase relation slope parameter $G = 0.16 \pm 0.05$. With the H_1 value, we refined the WISE data by Masiero et al. (2011) and obtained $D_1 = 1.8 \pm 0.5$ km and $p_{V,1} = 0.23 \pm 0.12$.

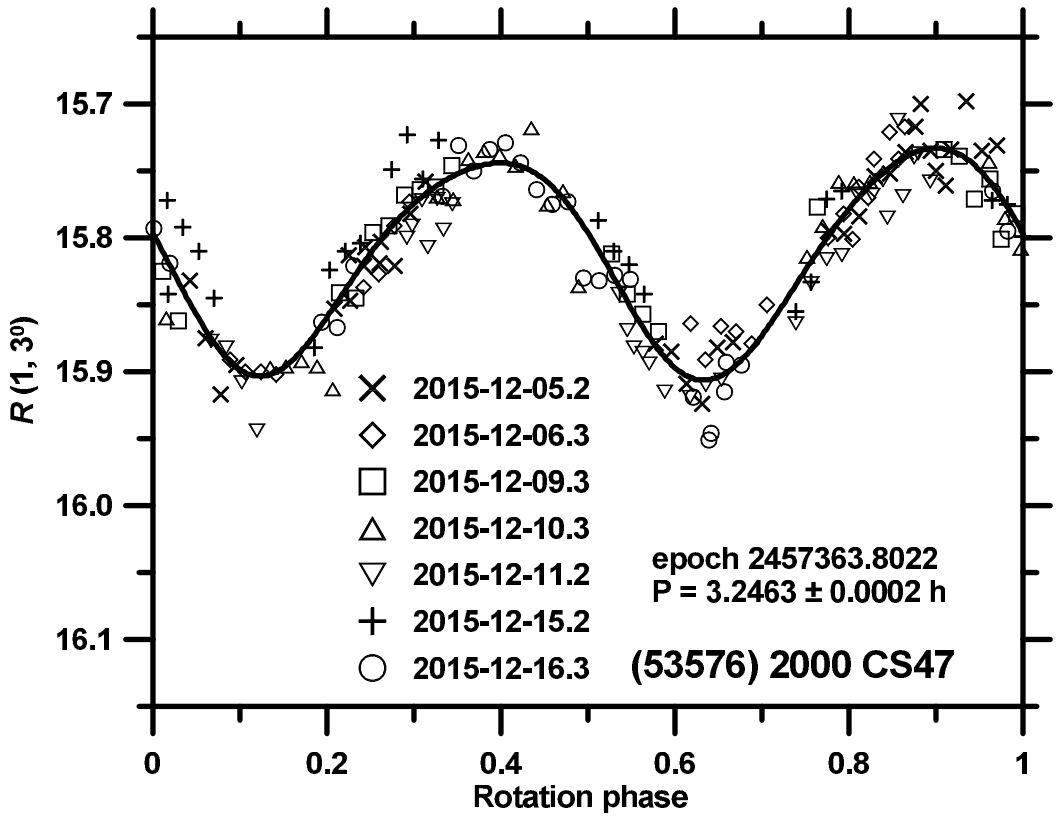

Suppl. Fig. 105. Composite lightcurve of (53576) 2000 CS47 from 2015.

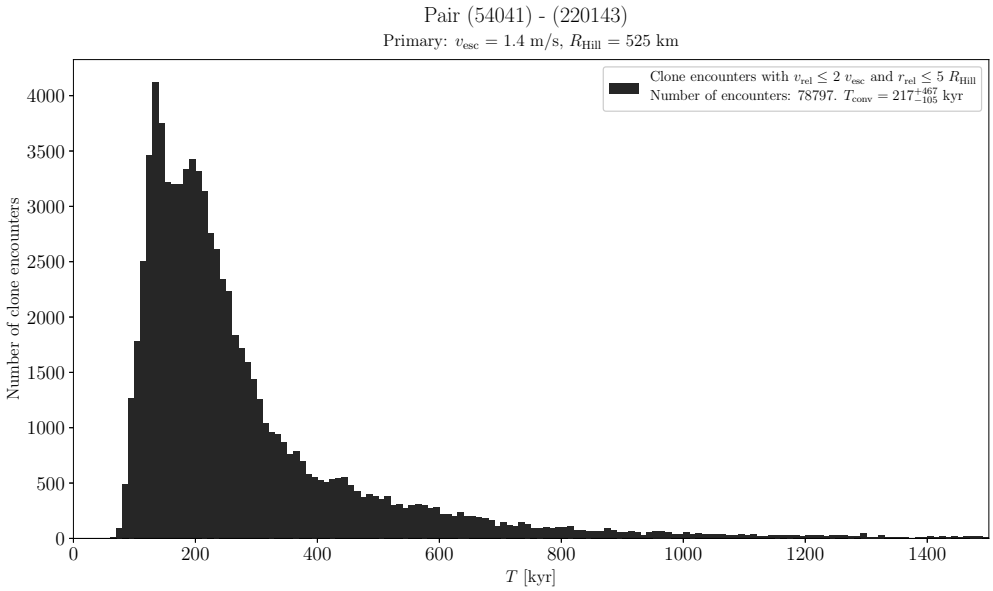

Suppl. Fig. 106. Distribution of past times of close and slow primary–secondary clone encounters for the asteroid pair 54041–220143.

(54041) 2000 GQ113 and (220143) 2002 TO134

The estimated age of this asteroid pair is about 200 kyr (Suppl. Fig. 106). The observations of the primary (54041) in 2008 were published in Pravec et al. (2010). We observed it from La Silla on 4 nights during 2012-11-06 to 2012-12-15, on 7 nights during 2014-02-06 to 2014-04-05, and on the night 2018-02-20, from Maidanak on 2 nights 2012-11-07 and 08, and from Ondřejov on 2 nights of 2015-05-10 and 12 (Suppl. Figs. 107 to 109). We measured $(V-R)_1 = 0.495 \pm 0.015$ and 0.490 ± 0.010 in 2014 and 2018, respectively. We derived the mean absolute magnitudes $H_1 = 15.02 \pm 0.03$ and 15.03 ± 0.03 in 2012 and 2014, respectively, with the phase relation slope parameter $G = 0.28 \pm 0.02$. With the mean H_1 value, we refined the WISE effective diameter and geometric albedo (Masiero et al. 2011): $D_1 = 2.6 \pm 0.8$ km and $p_{V,1} = 0.25 \pm 0.14$. The observations of the secondary (220143) in 2009 were published in Pravec et al. (2010). We observed it from La Silla on 2 nights 2013-12-28 and 2014-01-06, on 4 nights during 2015-03-14 to 2015-03-23, and on 6 nights during 2016-09-01 to 2016-11-05 (Suppl. Figs. 110 to 112). We measured $(V-R)_2 = 0.447 \pm 0.018$ on 2016-09-02. We derived the mean absolute magnitudes $H_2 = 16.79 \pm 0.03, 16.95 \pm 0.03$ and 16.95 ± 0.04 in the three apparitions, with the slope parameter $G = 0.26 \pm 0.03$; the value 16.90 ± 0.05 in Table 1 is the weighted mean of the three values.

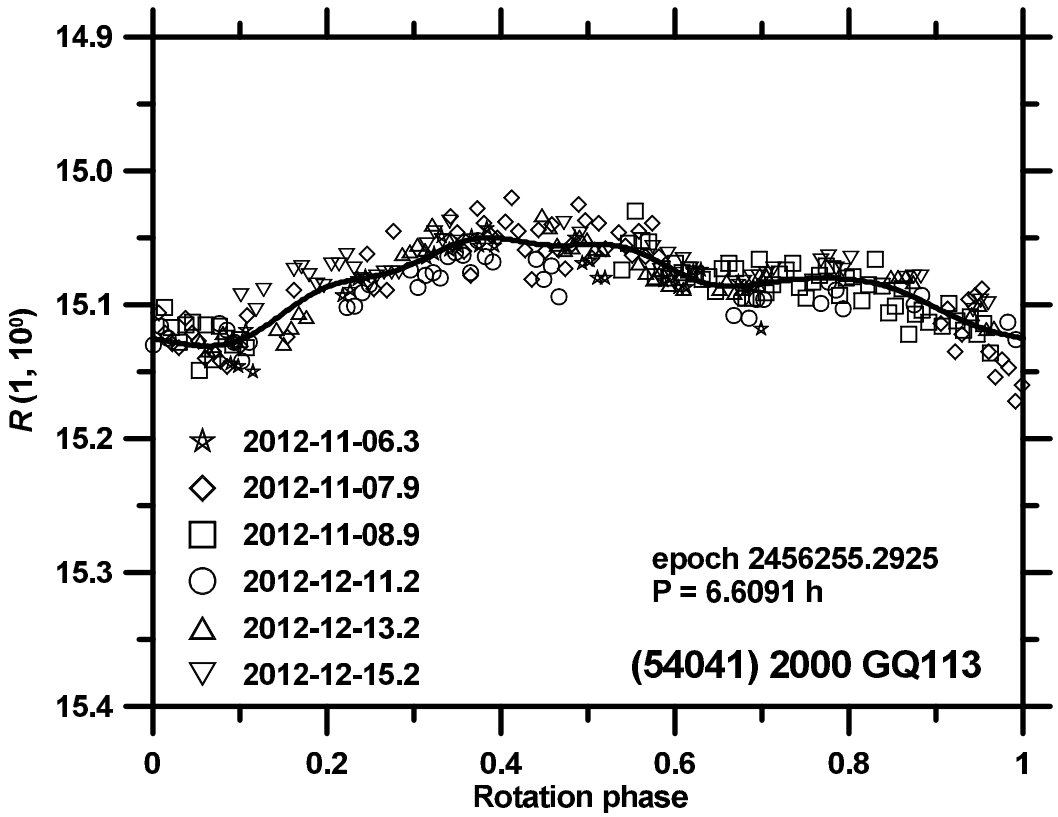

Suppl. Fig. 107. Composite lightcurve of (54041) 2000 GQ113 from 2012.

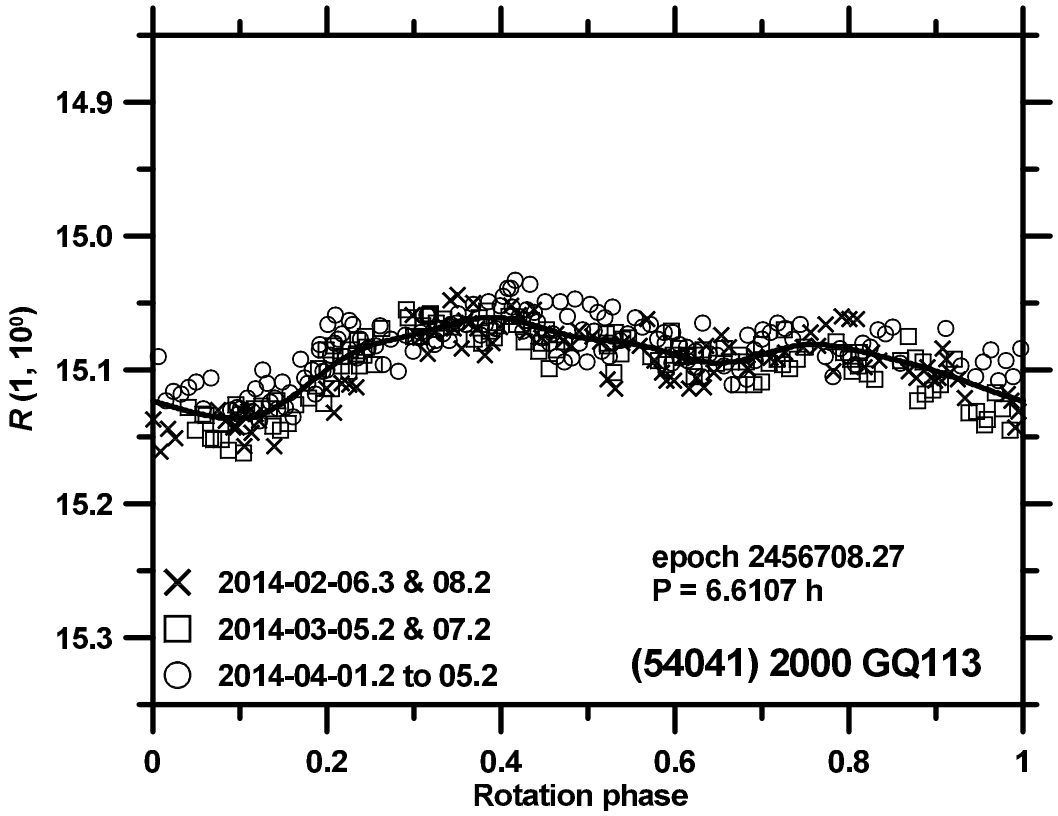

Suppl. Fig. 108. Composite lightcurve of (54041) 2000 GQ113 from 2014.

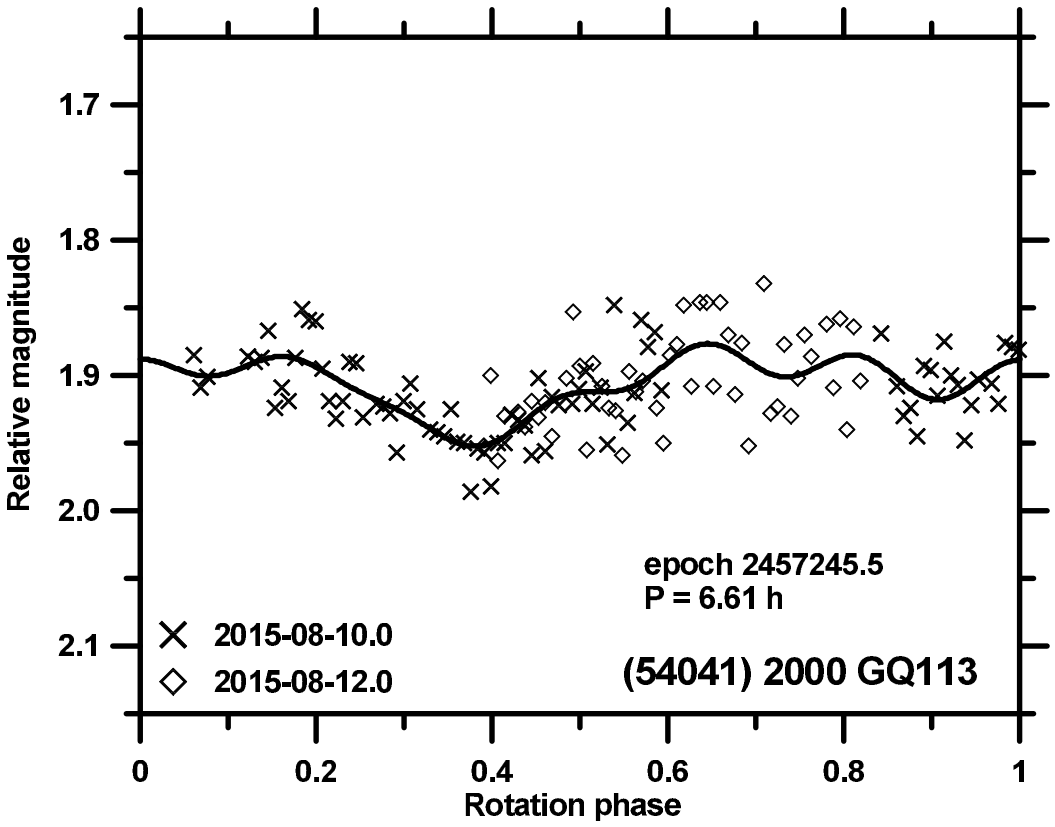

Suppl. Fig. 109. Composite lightcurve of (54041) 2000 GQ113 from 2015.

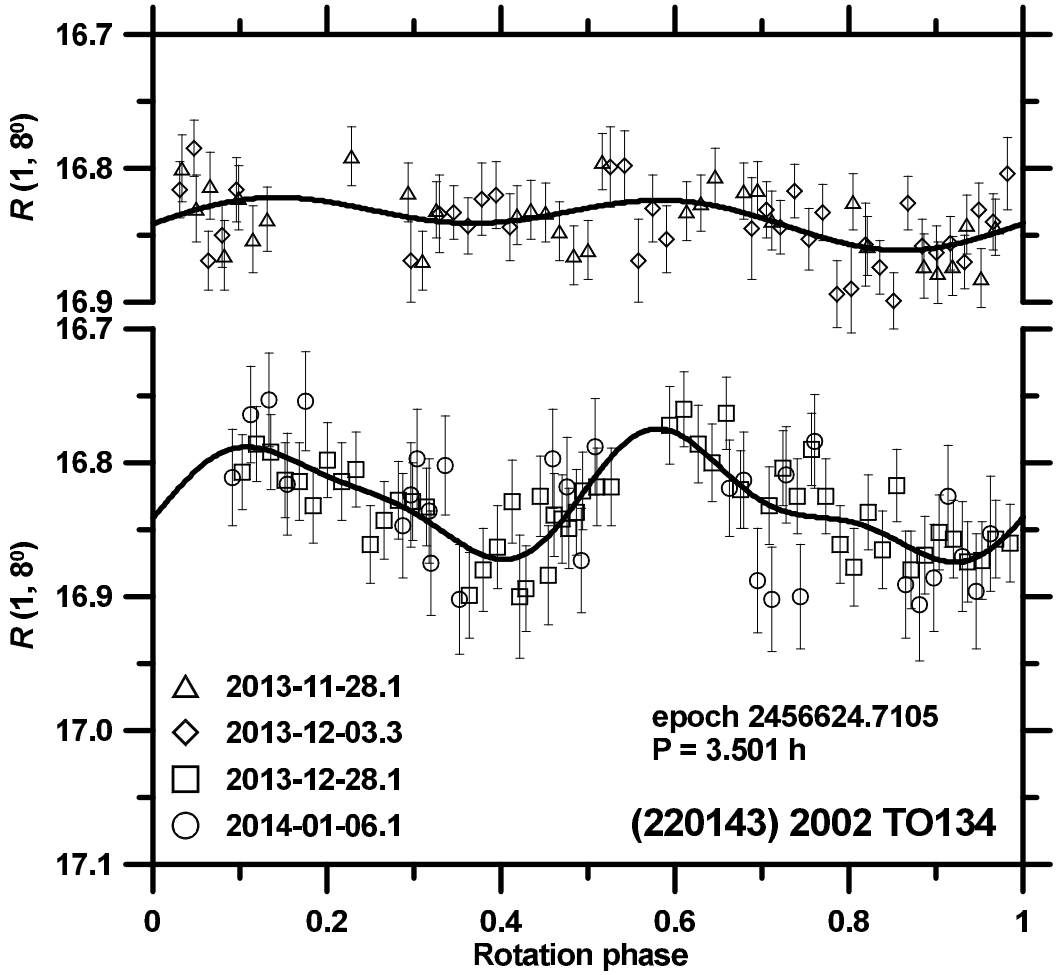

Suppl. Fig. 110. Composite lightcurves of (220143) 2002 TO134 from 2013–2014.

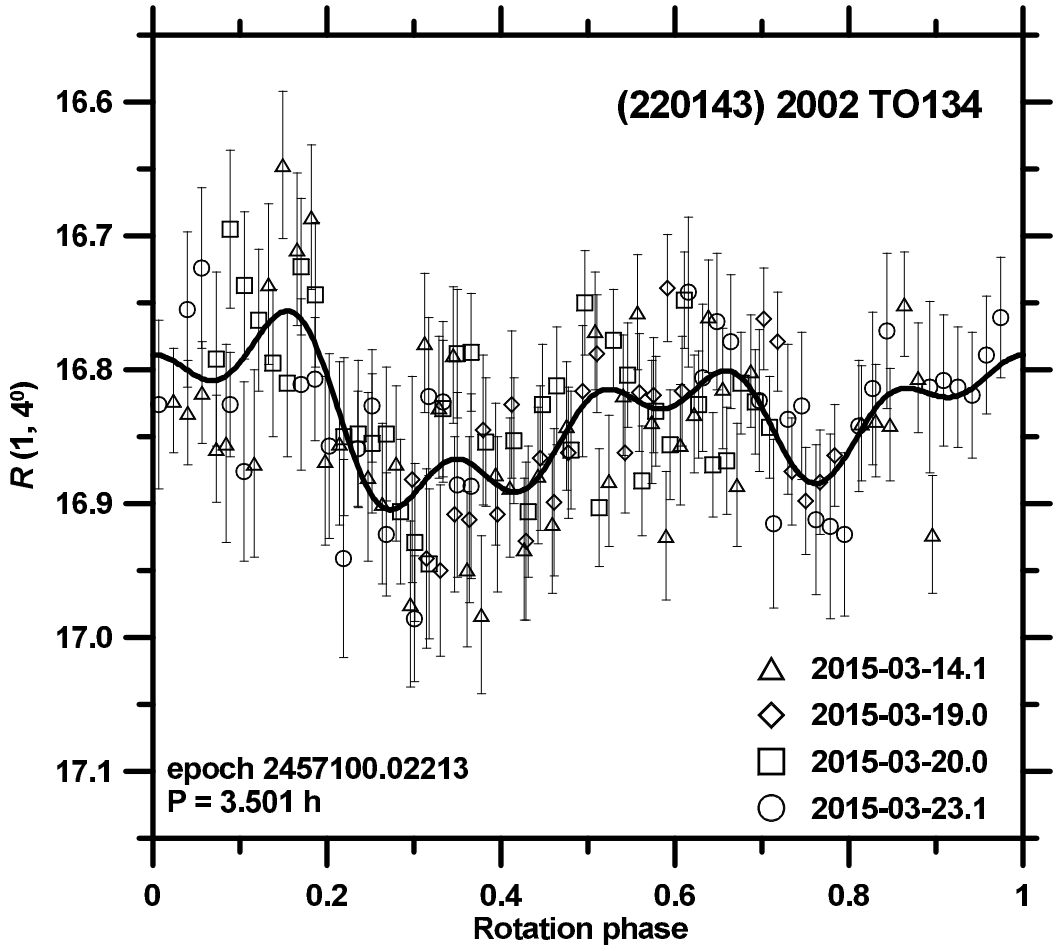

Suppl. Fig. 111. Composite lightcurve of (220143) 2002 TO134 from 2015.

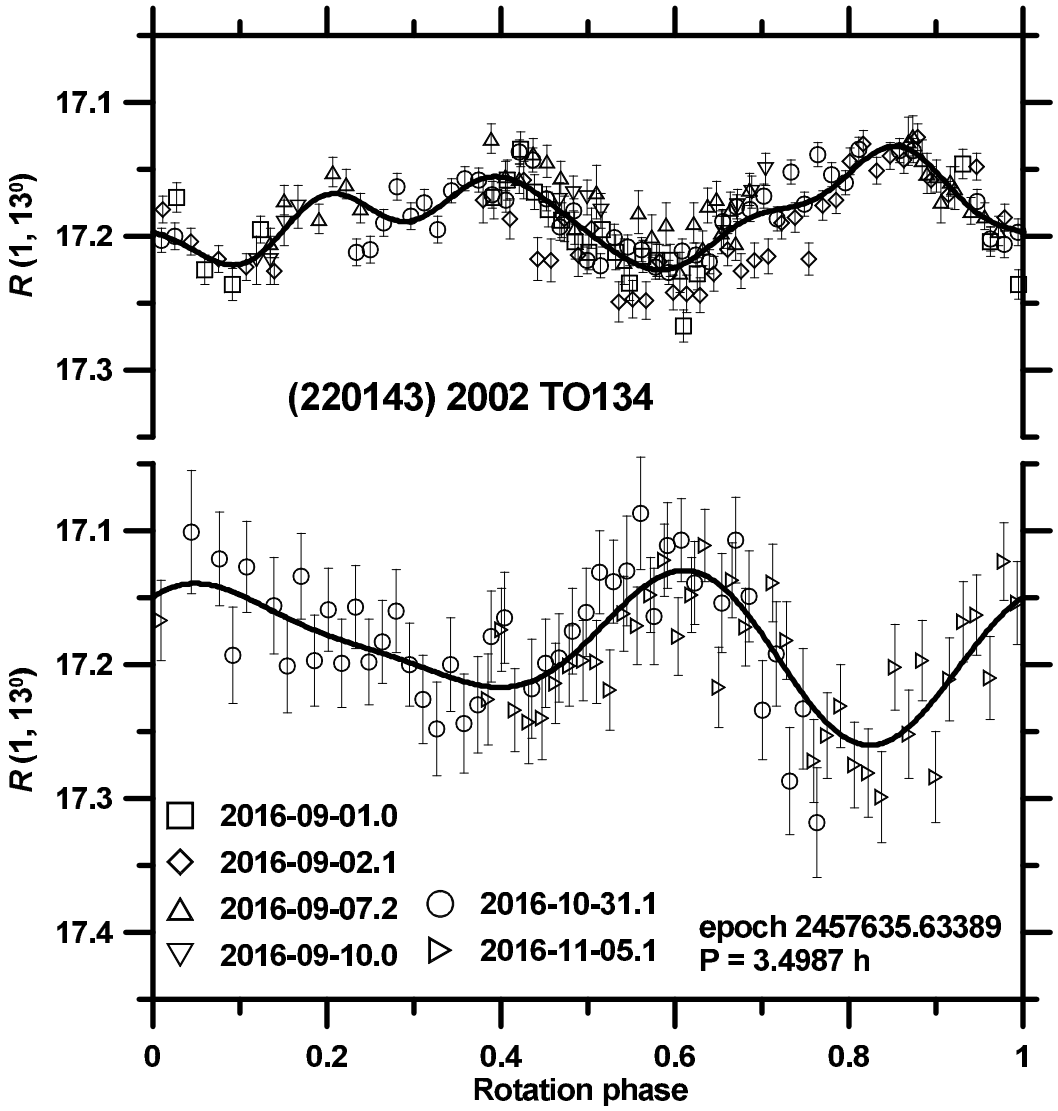

Suppl. Fig. 112. Composite lightcurves of (220143) 2002 TO134 from 2016.

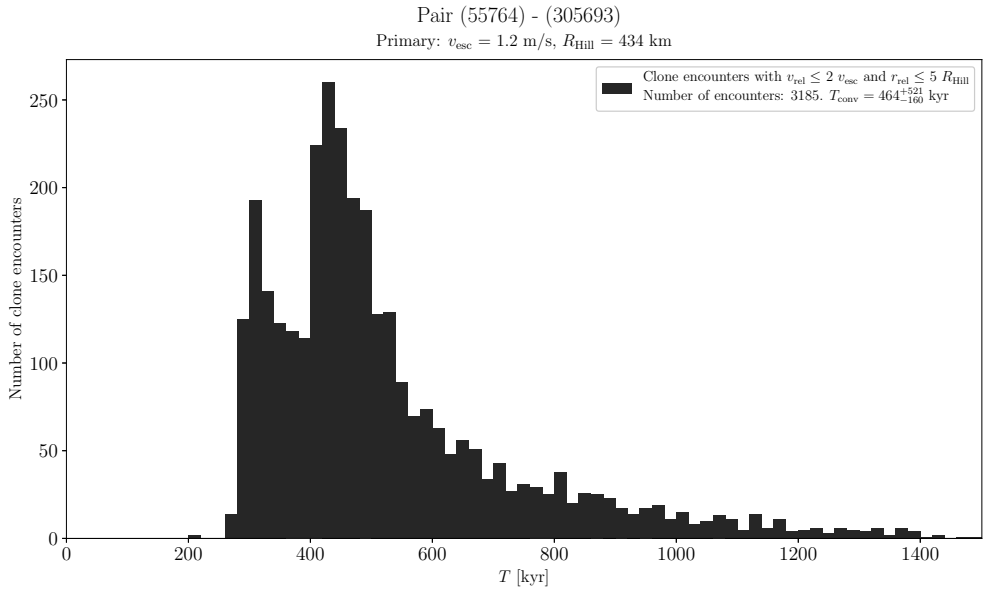

Suppl. Fig. 113. Distribution of past times of close and slow primary–secondary clone encounters for the asteroid pair 55764–305693.

(55764) 1992 DG12 and (305693) 2009 BB131

The estimated age of this asteroid pair is about 500 kyr (Suppl. Fig. 113). We observed (55764) from La Silla on 3 nights during 2012-11-16 to 2012-11-18 and on 2016-12-31 (Suppl. Fig. 114 and 115). We derived the mean absolute magnitudes $H_1 = 15.63 \pm 0.06$ and 15.65 ± 0.06 in 2012 and 2016, respectively, assuming $G = 0.24 \pm 0.11$.

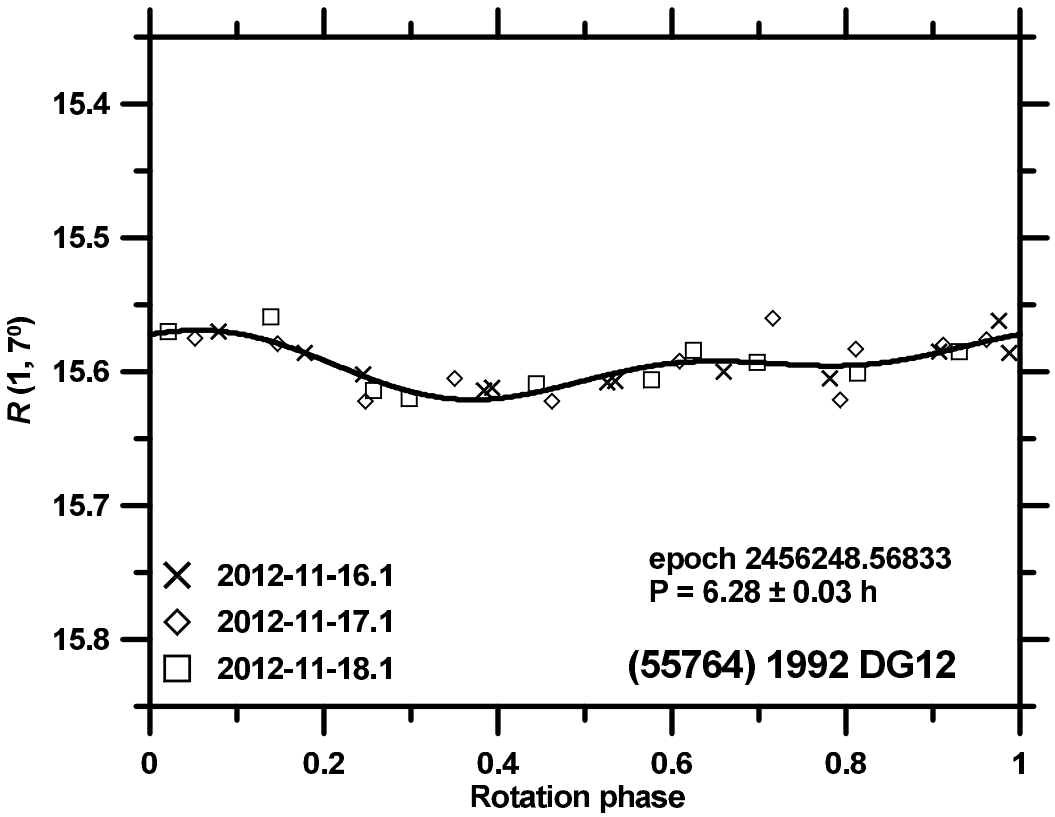

Suppl. Fig. 114. Composite lightcurve of (55764) 1992 DG12 from 2012.

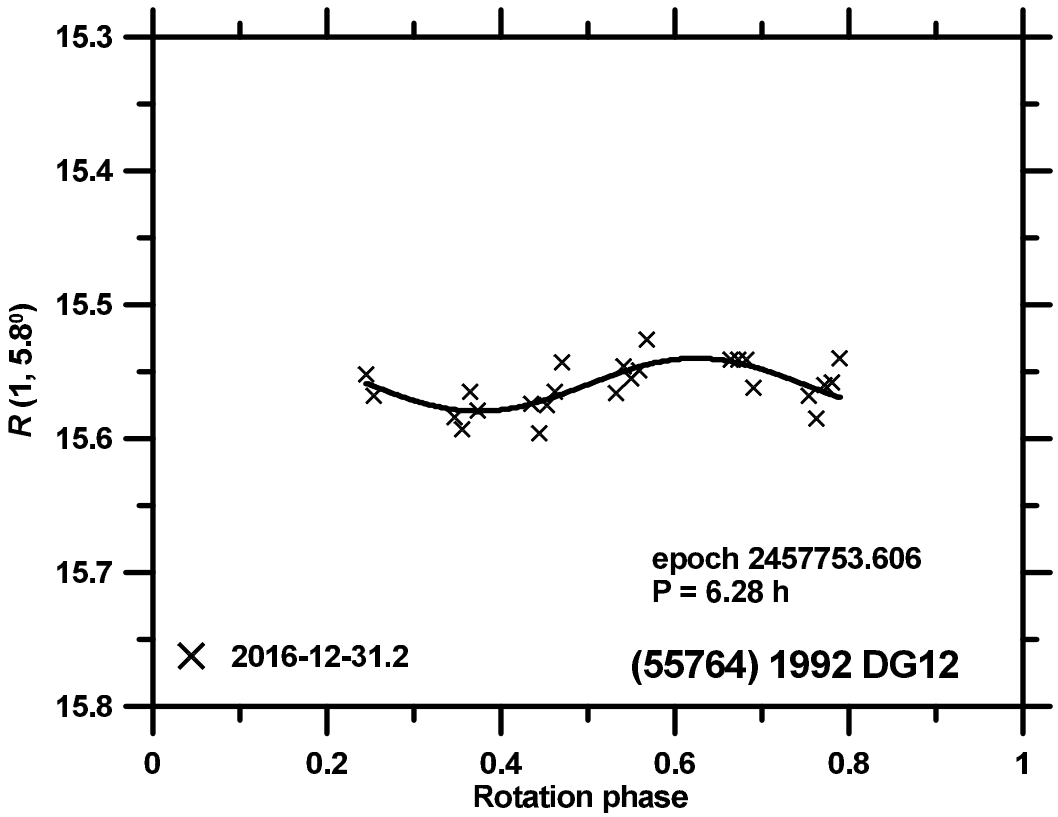

Suppl. Fig. 115. Composite lightcurve of (55764) 1992 DG12 from 2016.

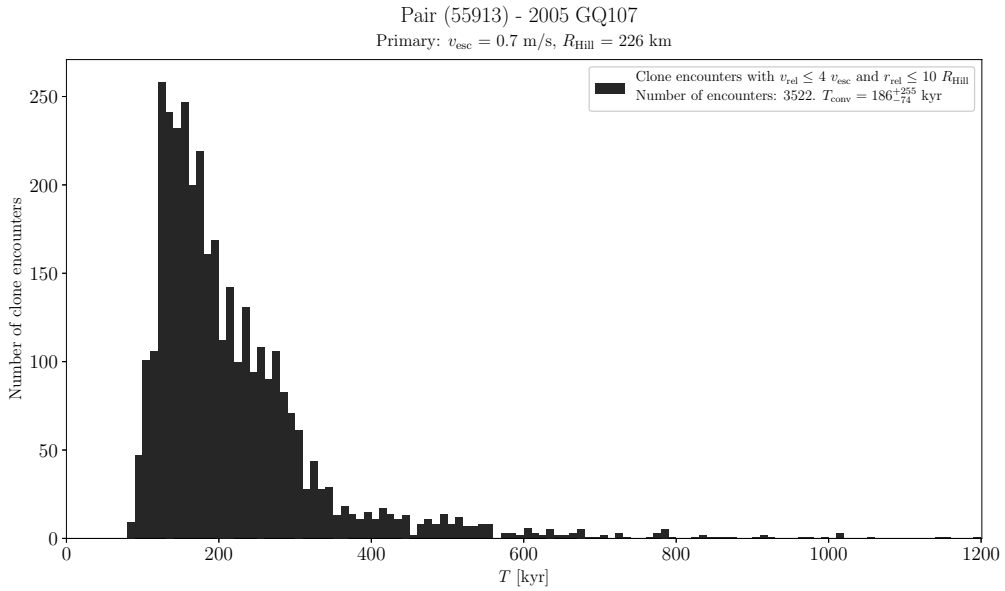

Suppl. Fig. 116. Distribution of past times of close and slow primary–secondary clone encounters for the asteroid pair 55913–2005GQ107.

(55913) 1998 FL12 and 2005 GQ107

The estimated age of this asteroid pair is about 200 kyr (Suppl. Fig. 116). We observed the primary (55913) from Ondřejov on 4 nights during 2014-03-21 to 2014-03-30 and from La Silla on 4 nights during 2015-11-06 to 2015-11-16 (Suppl. Figs. 117 and 118). We derived the mean absolute magnitudes $H_1 = 15.68 \pm 0.04$ and 15.83 ± 0.07 with slope parameters $G = 0.53 \pm 0.06$ and 0.45 ± 0.10 in 2014 and 2015, respectively. The absolute magnitude difference between the two years is real and it indicates that we observed the asteroid at a higher asterocentric latitude in 2014, which also corresponds to the much lower amplitude seen at that time.

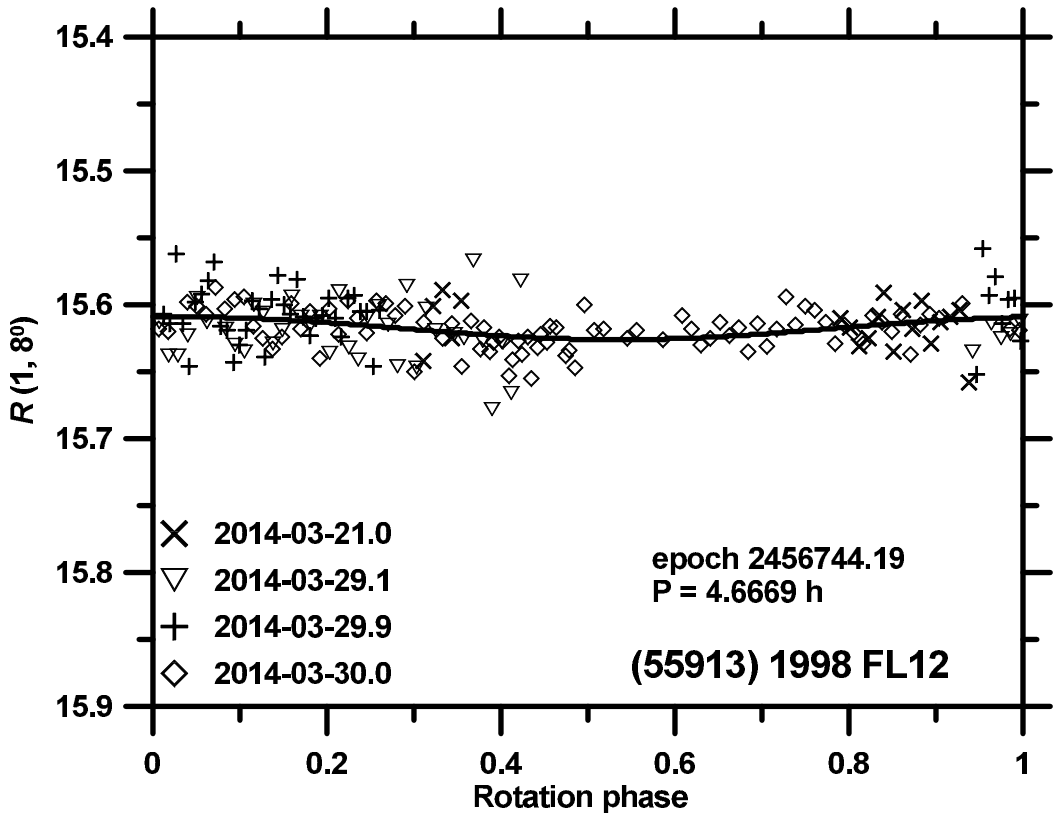

Suppl. Fig. 117. Composite lightcurve of (55913) 1998 FL12 from 2014.

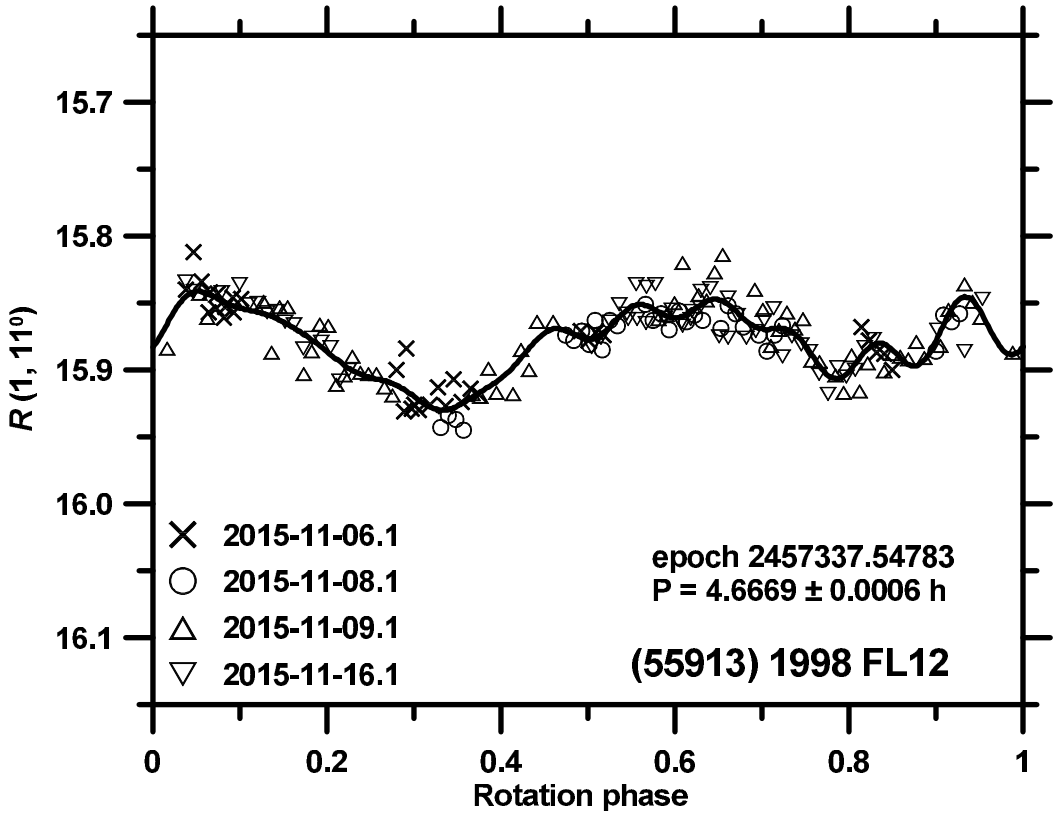

Suppl. Fig. 118. Composite lightcurve of (55913) 1998 FL12 from 2015.

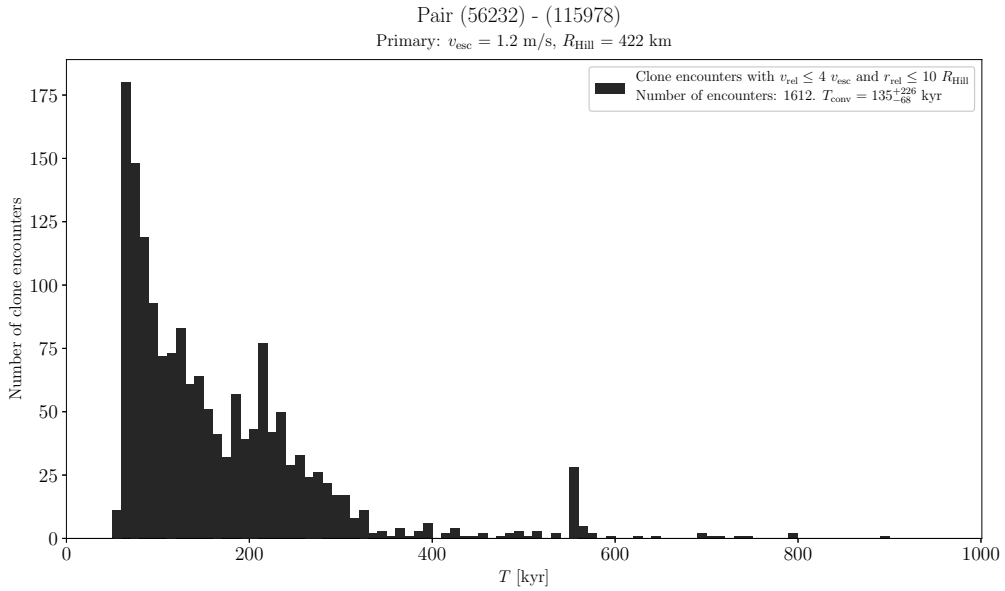

Suppl. Fig. 119. Distribution of past times of close and slow primary–secondary clone encounters for the asteroid pair 56232–115978.

(56232) 1999 JM31 and (115978) 2003 WQ56

The estimated age of this asteroid pair is about 130 kyr (Suppl. Fig. 119). The observations of the primary (56232) in 2009 were published in Pravec et al. (2010). We observed it from La Silla on 5 nights during 2013-11-28 to 2014-01-25, on 5 nights during 2015-02-18 to 2015-04-13, on 4 nights during 2016-10-28 to 2016-11-29, and on 3 nights during 2018-02-17 to 2018-02-20. We derived the mean absolute magnitudes $H_1 = 15.57 \pm 0.04, 15.50 \pm 0.05, 15.57 \pm 0.04$ and 15.51 ± 0.04 in the four apparitions, with the phase relation slope parameters $G = 0.27 \pm 0.04, 0.19 \pm 0.04$ and 0.30 ± 0.06, respectively. Figure 120 shows the primary's nominal spin pole solution and its uncertainty area. We observed the secondary (115978) from La Silla on 6 nights during 2013-12-10 to 2014-01-10, on 3 nights during 2015-03-14 to 2015-03-30, and on 11 nights during 2016-11-06 to 2016-12-07 (Suppl. Figs. 121 to 123). Its period $P_2 = 9.4380 \pm 0.0009$ h is likely, but we cannot entirely rule out a period twice that with four pairs of maxima/minima per rotation. We derived the mean absolute magnitudes $H_2 = 16.74 \pm 0.03, 16.82 \pm 0.03$ and 16.70 ± 0.03 in the three apparitions, with the slope parameter $G = 0.35 \pm 0.02$.

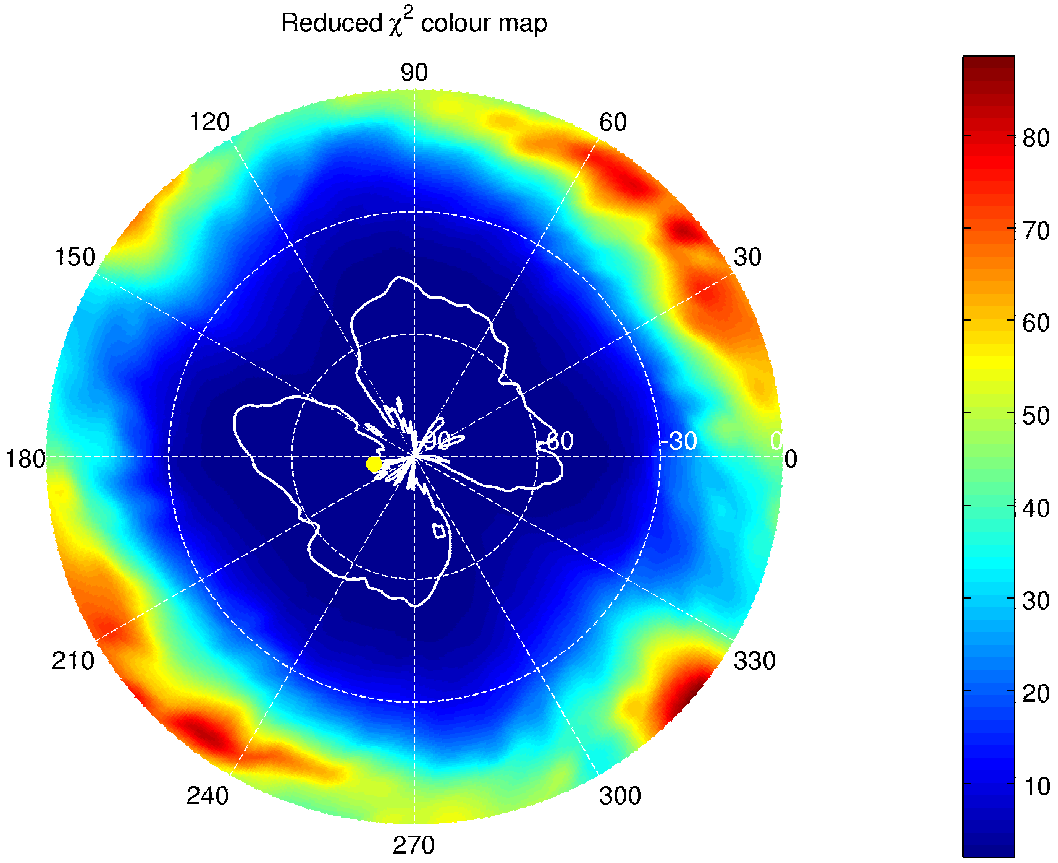

Suppl. Fig. 120. The nominal spin pole solution (yellow dot) and the 3-σ pole uncertainty area (white boundary) for (56232) 1999 JM31.

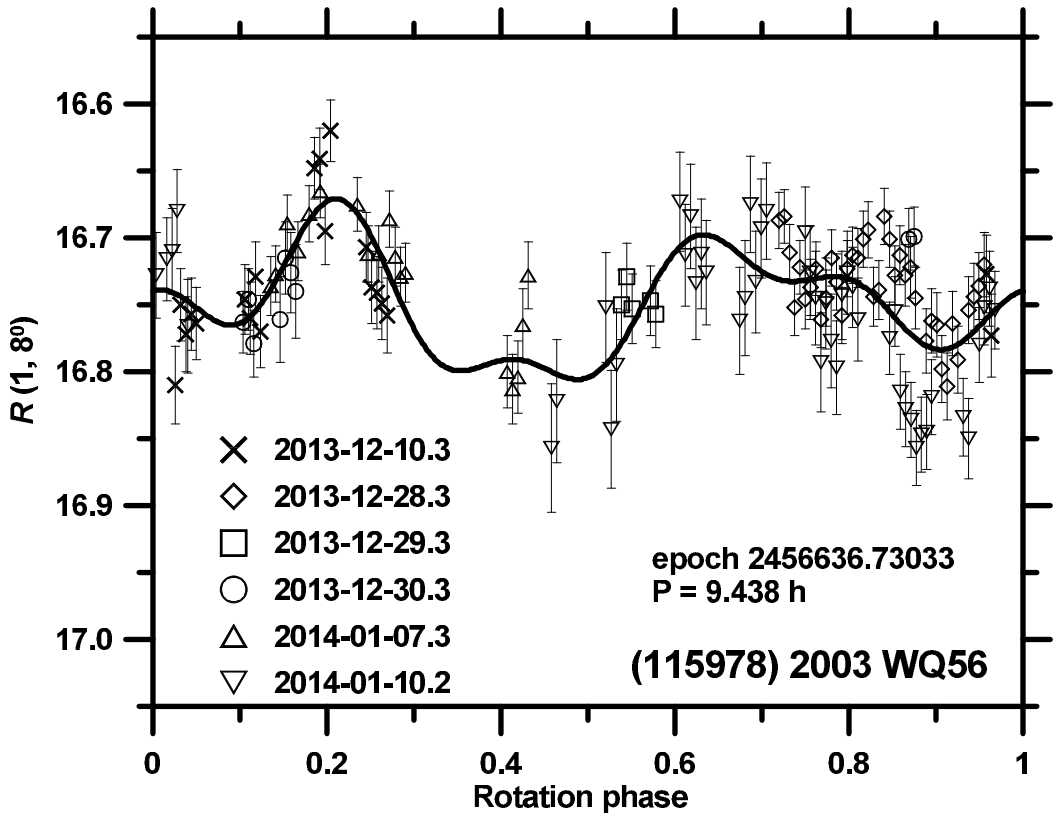

Suppl. Fig. 121. Composite lightcurve of (115978) 2003 WQ56 from 2013–2014.

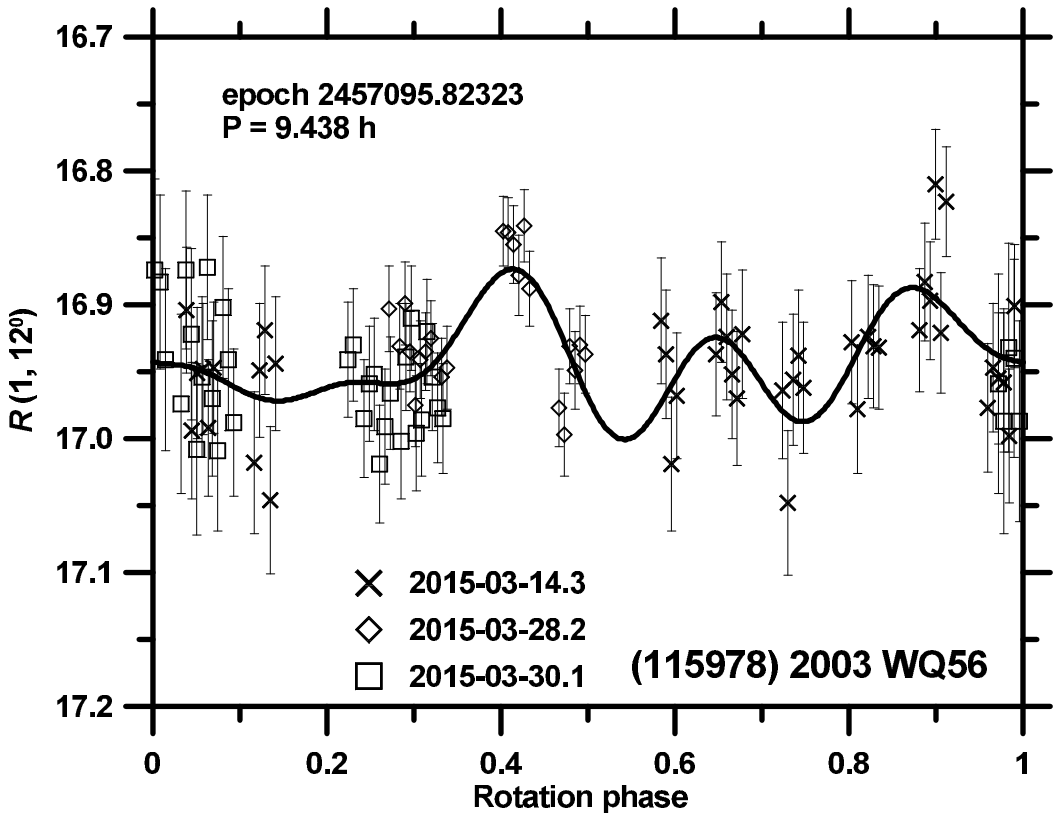

Suppl. Fig. 122. Composite lightcurve of (115978) 2003 WQ56 from 2015.

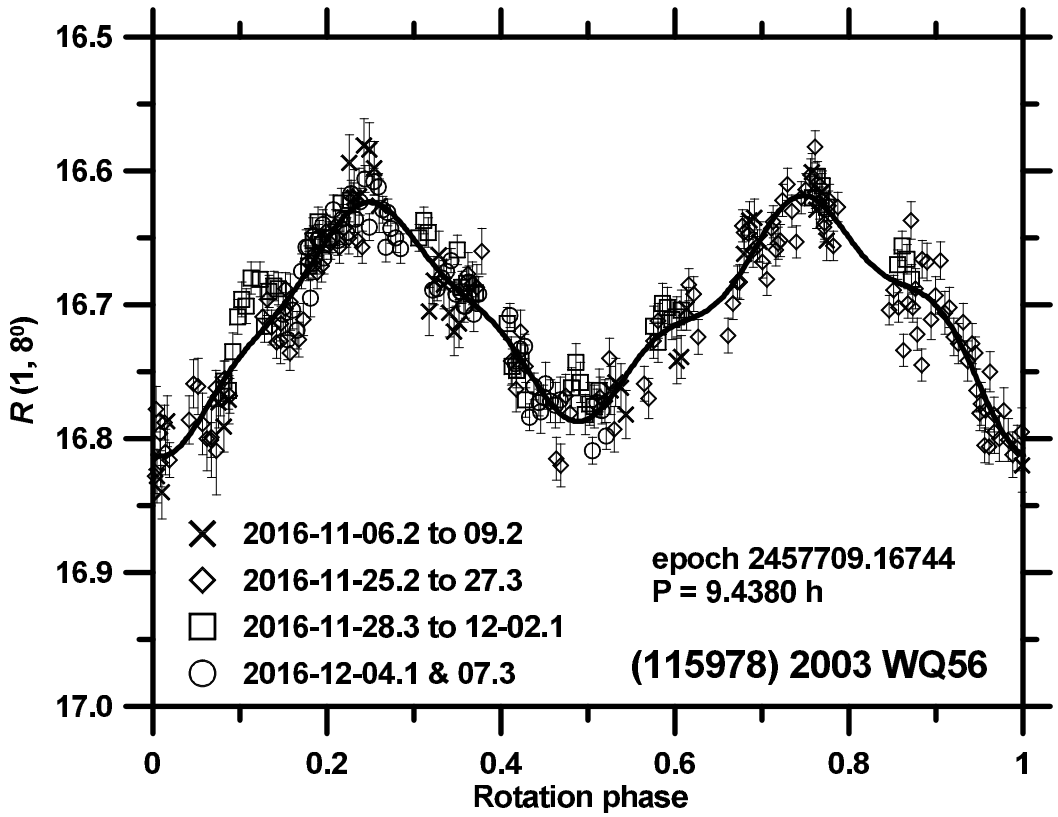

Suppl. Fig. 123. Composite lightcurve of (115978) 2003 WQ56 from 2016.

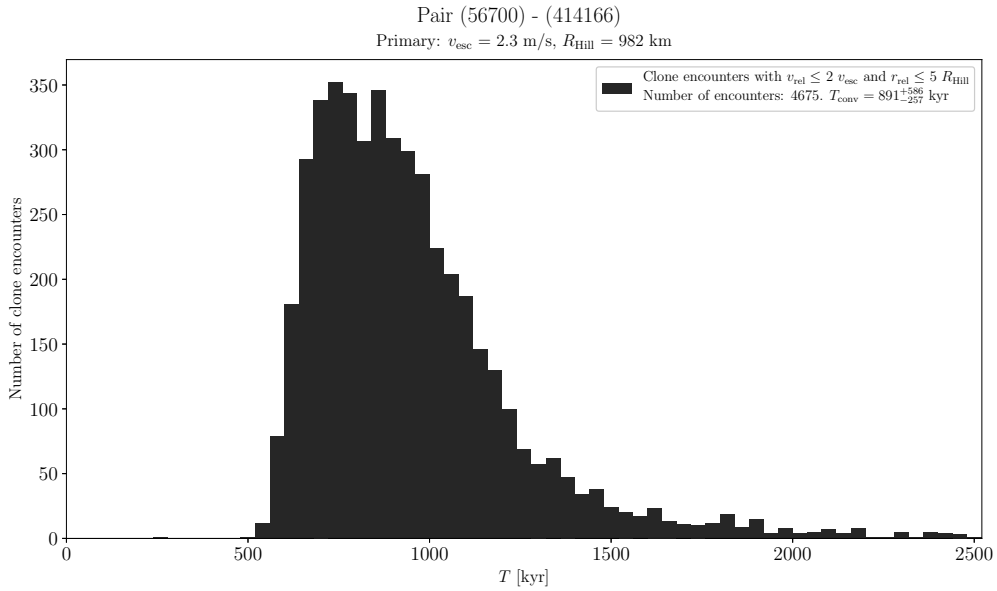

Suppl. Fig. 124. Distribution of past times of close and slow primary–secondary clone encounters for the asteroid pair 56700–414166.

(56700) 2000 LL28 and (414166) 2008 AU67

The estimated age of this asteroid pair is about 900 kyr (Suppl. Fig. 124). We observed the primary (56700) from La Silla on 5 nights during 2016-01-30 to 2016-02-12 (Suppl. Fig. 125) and derived its mean absolute magnitude $H_1 = 14.16 \pm 0.03$ and the slope parameter $G = 0.27 \pm 0.05$.

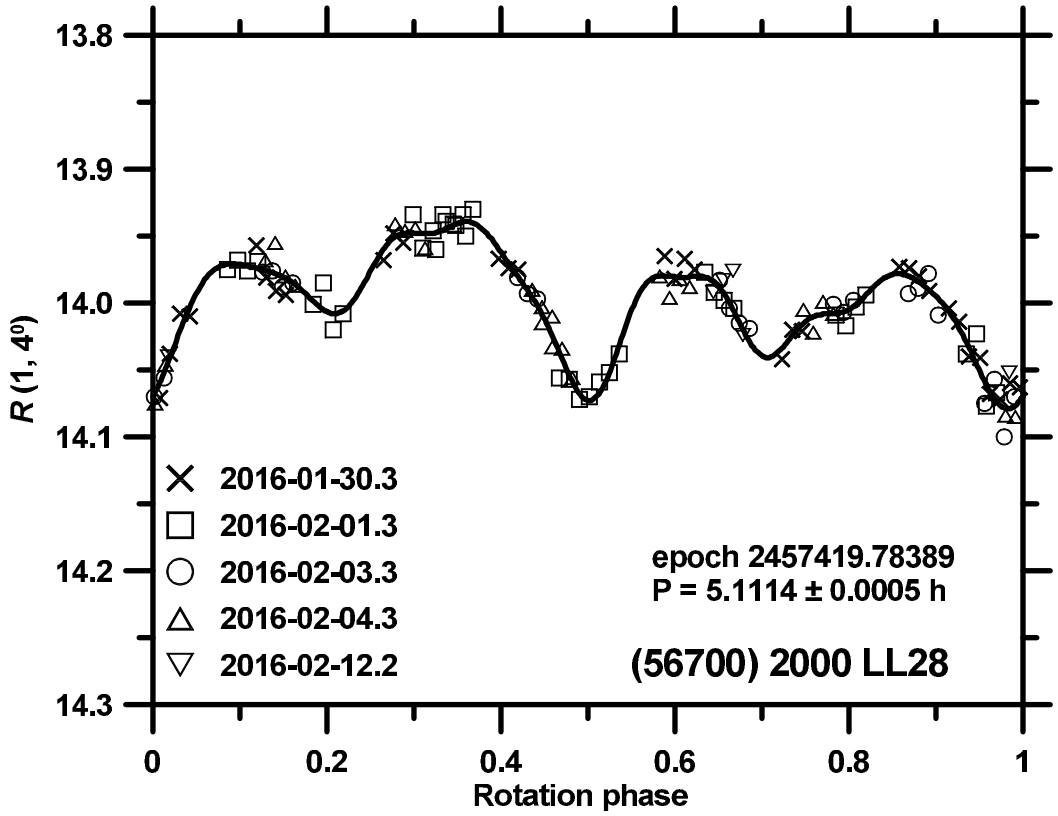

Suppl. Fig. 125. Composite lightcurve of (56700) 2000 LL28 from 2016.

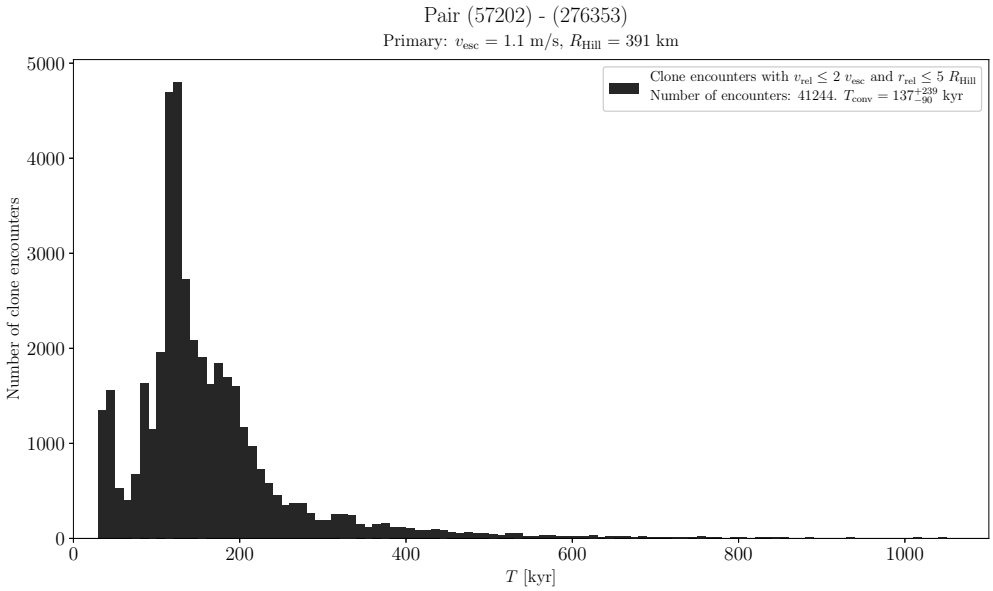

Suppl. Fig. 126. Distribution of past times of close and slow primary–secondary clone encounters for the asteroid pair 57202–276353.

(57202) 2001 QJ53 and (276353) 2002 UY20

The estimated age of this asteroid pair is about 140 kyr (Suppl. Fig. 126). We observed (57202) from La Silla on 8 nights during 2014-02-24 to 2014-04-05 and on 12 nights during 2016-12-22 to 2017-02-02 (Suppl. Figs. 127 and 128). We derived the mean absolute magnitudes $H_1 = 15.83 \pm 0.04$ and 15.83 ± 0.03 in the two apparitions, with the slope parameter $G = 0.22 \pm 0.03$.

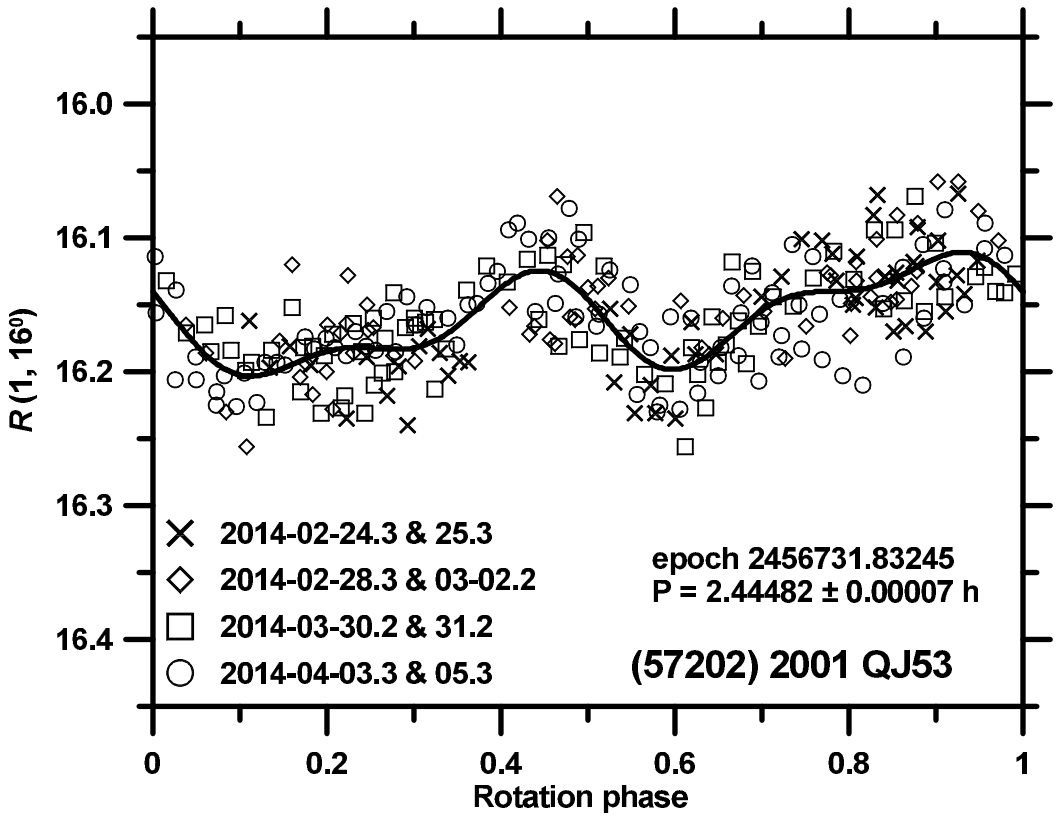

Suppl. Fig. 127. Composite lightcurve of (57202) 2001 QJ53 from 2014.

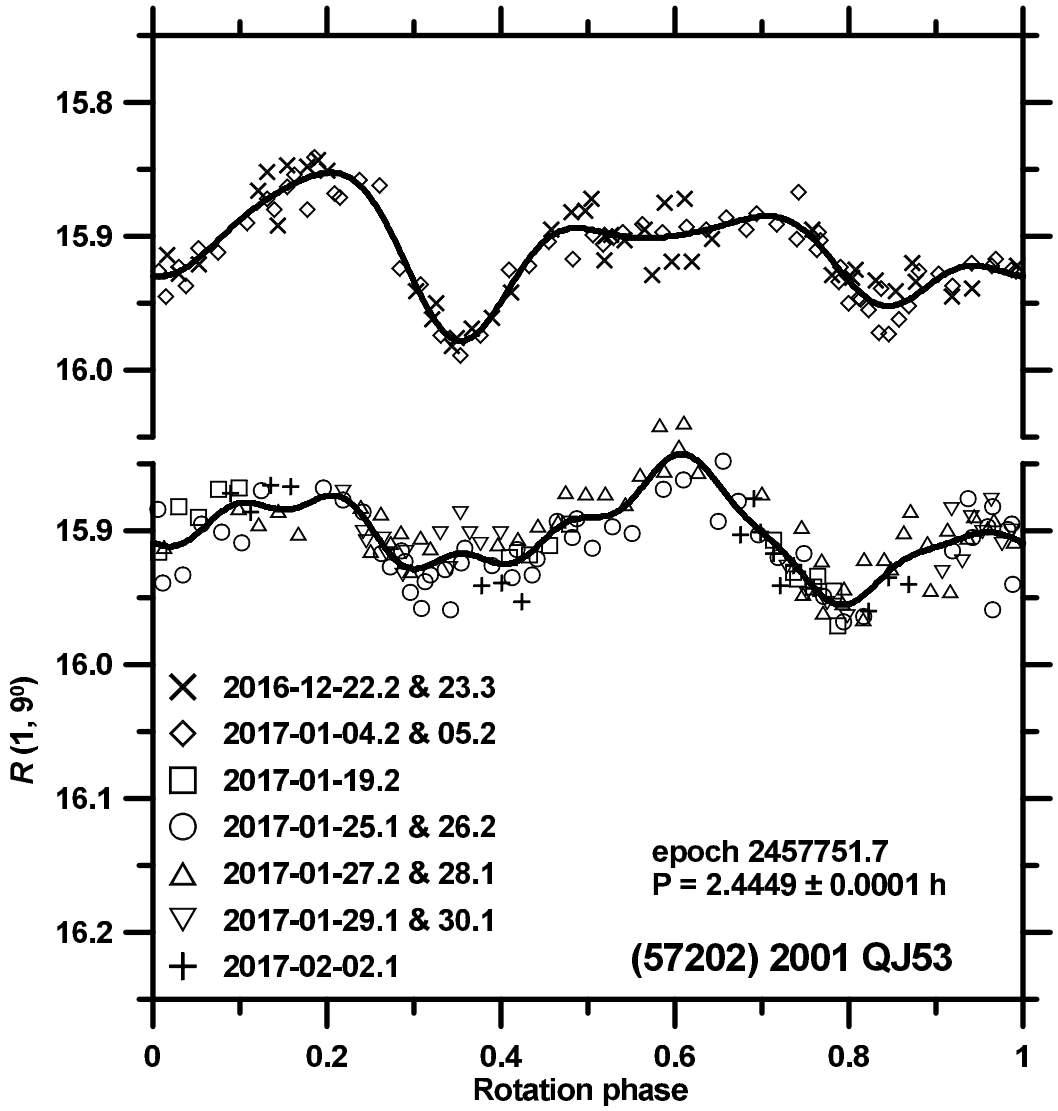

Suppl. Fig. 128. Composite lightcurves of (57202) 2001 QJ53 from 2016–2017.

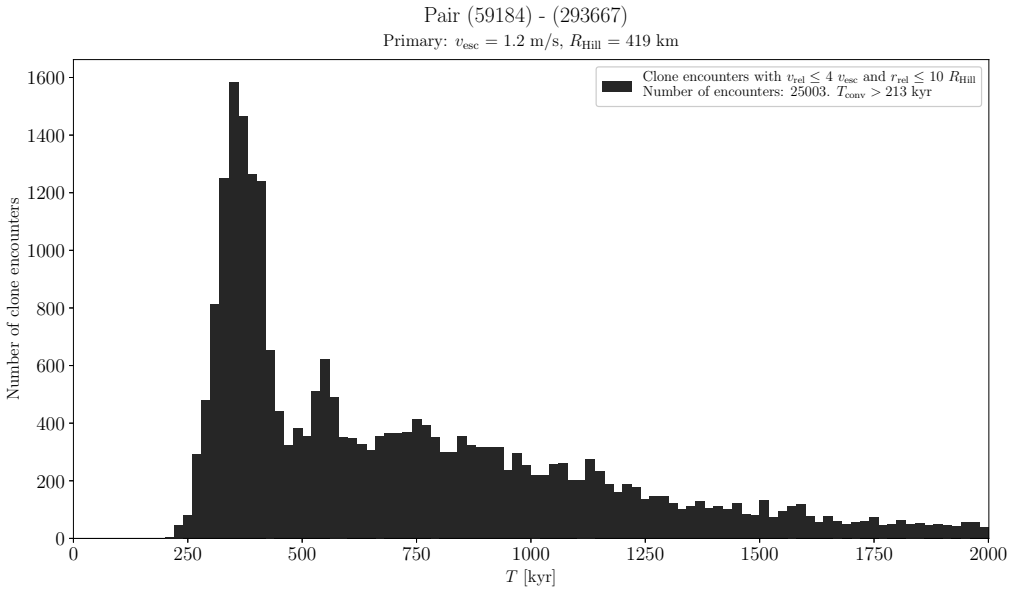

Suppl. Fig. 129. Distribution of past times of close and slow primary–secondary clone encounters for the asteroid pair 59184–293667.

(59184) 1999 AR15 and (293667) 2007 PD19

A lower limit on age of this asteroid pair is estimated to be 213 kyr (Suppl. Fig. 129). We observed the primary (59184) from La Silla on 3 nights from 2013-02-05 to -07 (Suppl. Fig. 130). We derived $H_{R,1} = 15.12 \pm 0.03$, assuming the slope parameter $G = 0.24 \pm 0.11$. For conversion to $H_1 \equiv H_{V,1}$, we assumed the color index $(V - R) = 0.49 \pm 0.05$; these assumed values are means for S type asteroids (Pravec et al. 2012b). With the H_1 value, we refined the WISE data by Masiero et al. (2011) and obtained $D_1 = 2.5 \pm 0.3$ km and $p_{V,1} = 0.16 \pm 0.04$.

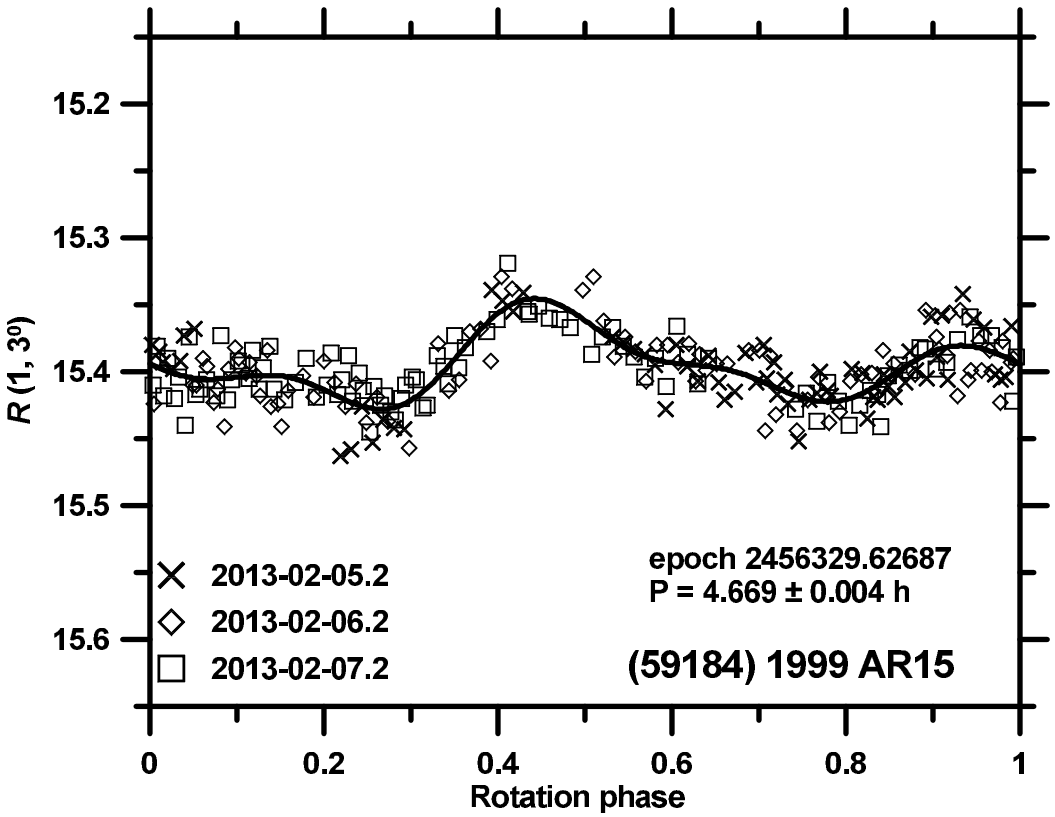

Suppl. Fig. 130. Composite lightcurve of (59184) 1999 AR15 from 2013.

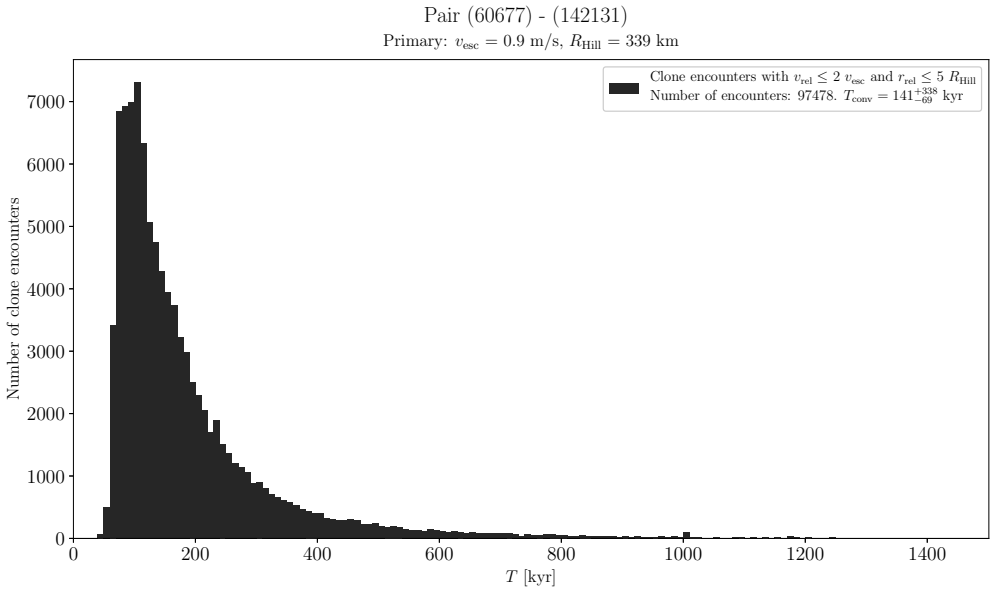

Suppl. Fig. 131. Distribution of past times of close and slow primary–secondary clone encounters for the asteroid pair 60677–142131.

(60677) 2000 GO18 and (142131) 2002 RV11

Backward orbital clone integrations suggest that these two asteroids separated about 140 kyr ago (Suppl. Fig. 131). We observed the primary (60677) from La Silla on 3 nights 2012-10-17 to -19 and on 2 nights 2018-02-19 and -20, and from Maidanak on 2 nights 2012-10-20 and -21. We derived $H_1 = 16.20 \pm 0.04$ and 16.17 ± 0.02 in the two apparitions, assuming the slope parameter $G = 0.24 \pm 0.11$. We observed the secondary (142131) from La Silla on 2 nights 2016-04-01 and -02. We derived $H_{R,2} = 15.99 \pm 0.05$, assuming the slope parameter $G = 0.24 \pm 0.11$. For conversion to $H_2 \equiv H_{V,2}$, we assumed the primary's color index $(V - R) = 0.457 \pm 0.010$.

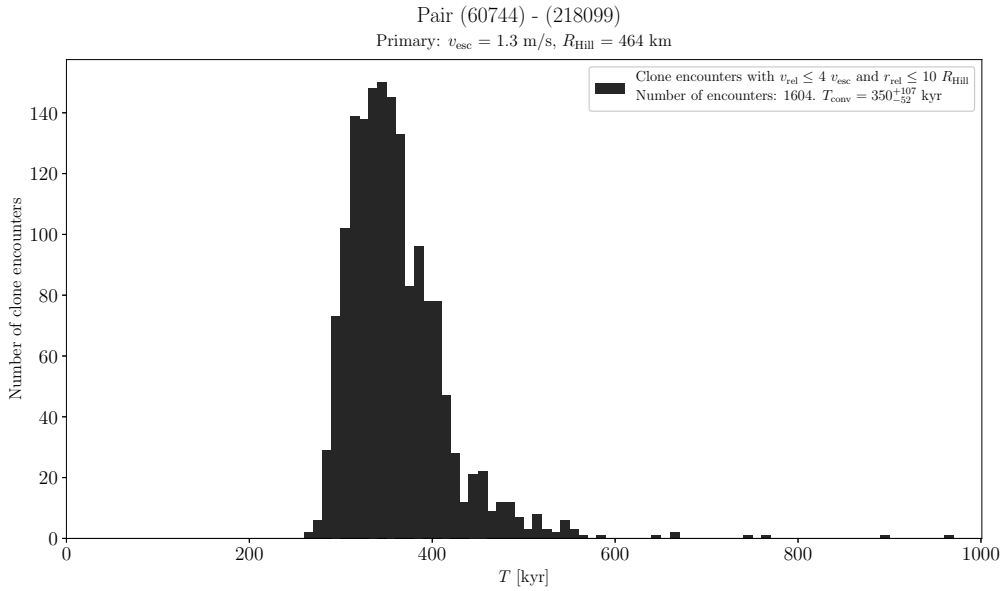

Suppl. Fig. 132. Distribution of past times of close and slow primary–secondary clone encounters for the asteroid pair 60744–218099.

(60744) 2000 GB93 and (218099) 2002 MH3

The estimated age of this asteroid pair is about 350 kyr (Suppl. Fig. 132). Figure 133 shows the primary's nominal spin pole solution and its uncertainty area. The second isolated area around $(L, B) = (0°, -80°)$ is also formally allowed within 3σ, but it is not considered likely as the reduced χ^2 values are substantially higher there than around the nominal pole solution. Data for the secondary (218099) from 2009 were published in Pravec et al. (2010). We observed the secondary from La Silla on 6 nights during 2013-12-06 to 2014-01-09, on 2 nights 2015-03-12 and -18, and on 9 nights during 2016-09-02 to 2016-11-02 (Suppl. Figs. 134 to 136). We measured the primary's mean absolute magnitudes $H_1 = 15.44 \pm 0.04, 15.40 \pm 0.04, 15.42 \pm 0.03$ and 15.48 ± 0.04 in 2012–2013, 2014, 2015 and 2018, respectively, with the phase relation slope parameter $G = 0.27 \pm 0.04$ measured in 2012–2013. We measured the secondary's mean absolute magnitudes $H_2 = 16.46 \pm 0.03, 16.46 \pm 0.03$ and 16.41 ± 0.03 in 2013–2014, 2015 and 2016, respectively, with the phase relation slope parameter $G = 0.21 \pm 0.02$ measured in 2016.

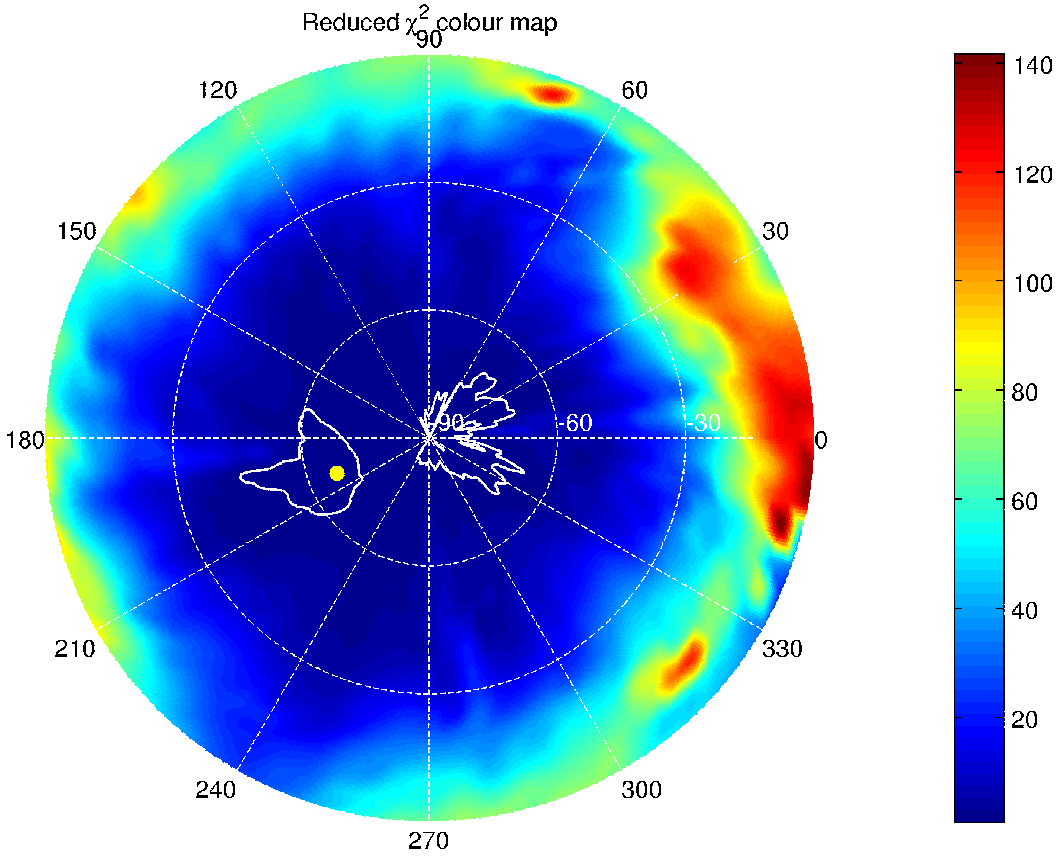

Suppl. Fig. 133. The nominal spin pole solution (yellow dot) and the 3-σ pole uncertainty area (white boundary) for (60744) 2000 GB93.

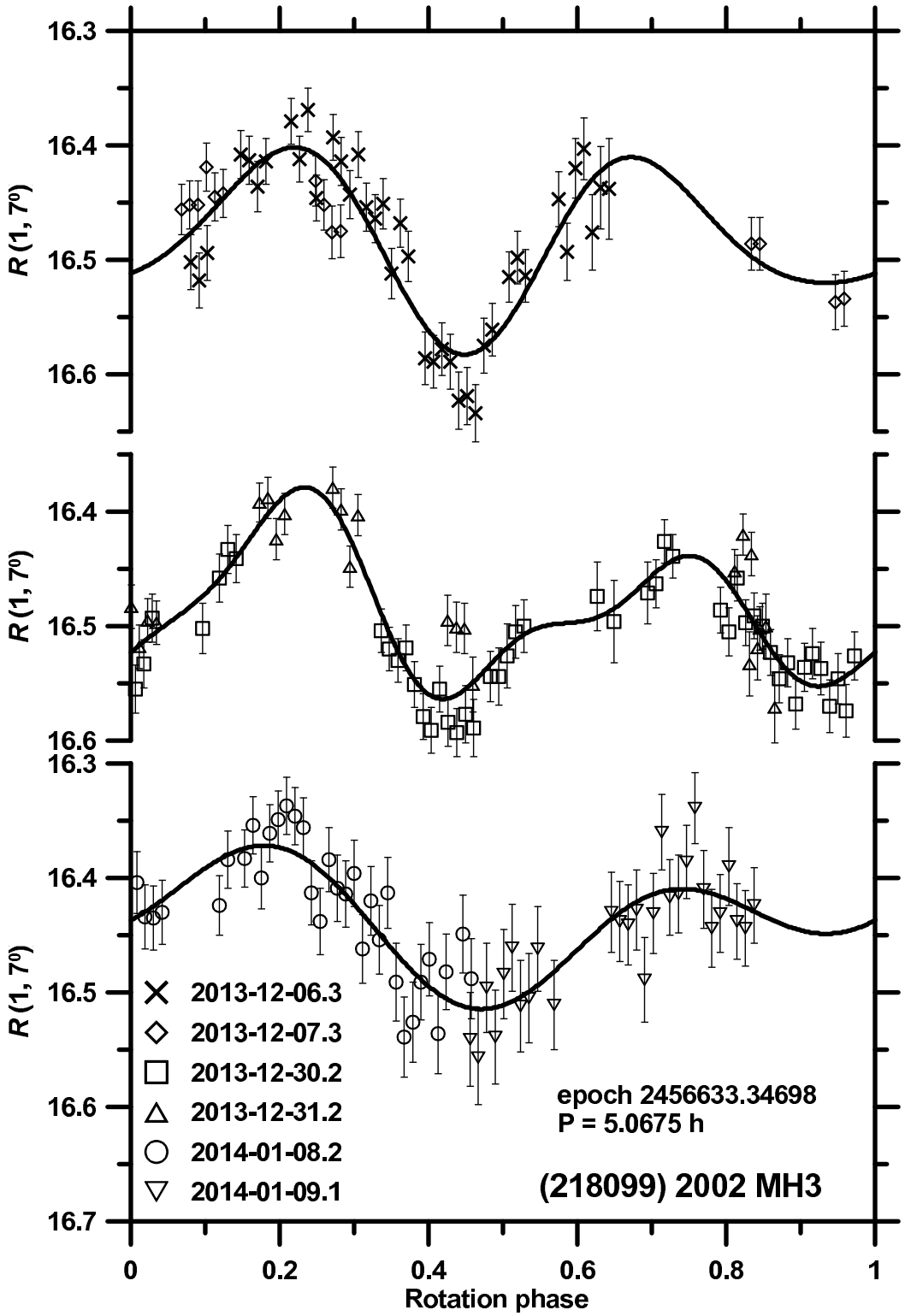

Suppl. Fig. 134. Composite lightcurves of (218099) 2002 MH3 from 2013–2014.

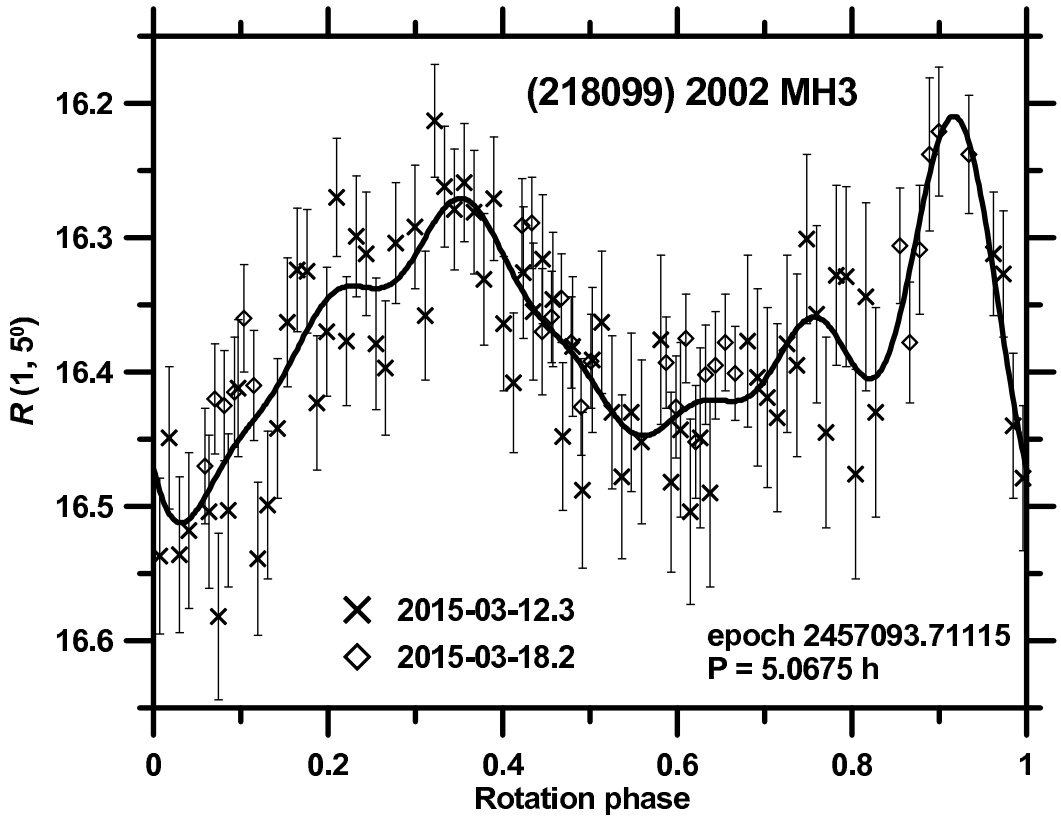

Suppl. Fig. 135. Composite lightcurve of (218099) 2002 MH3 from 2015.

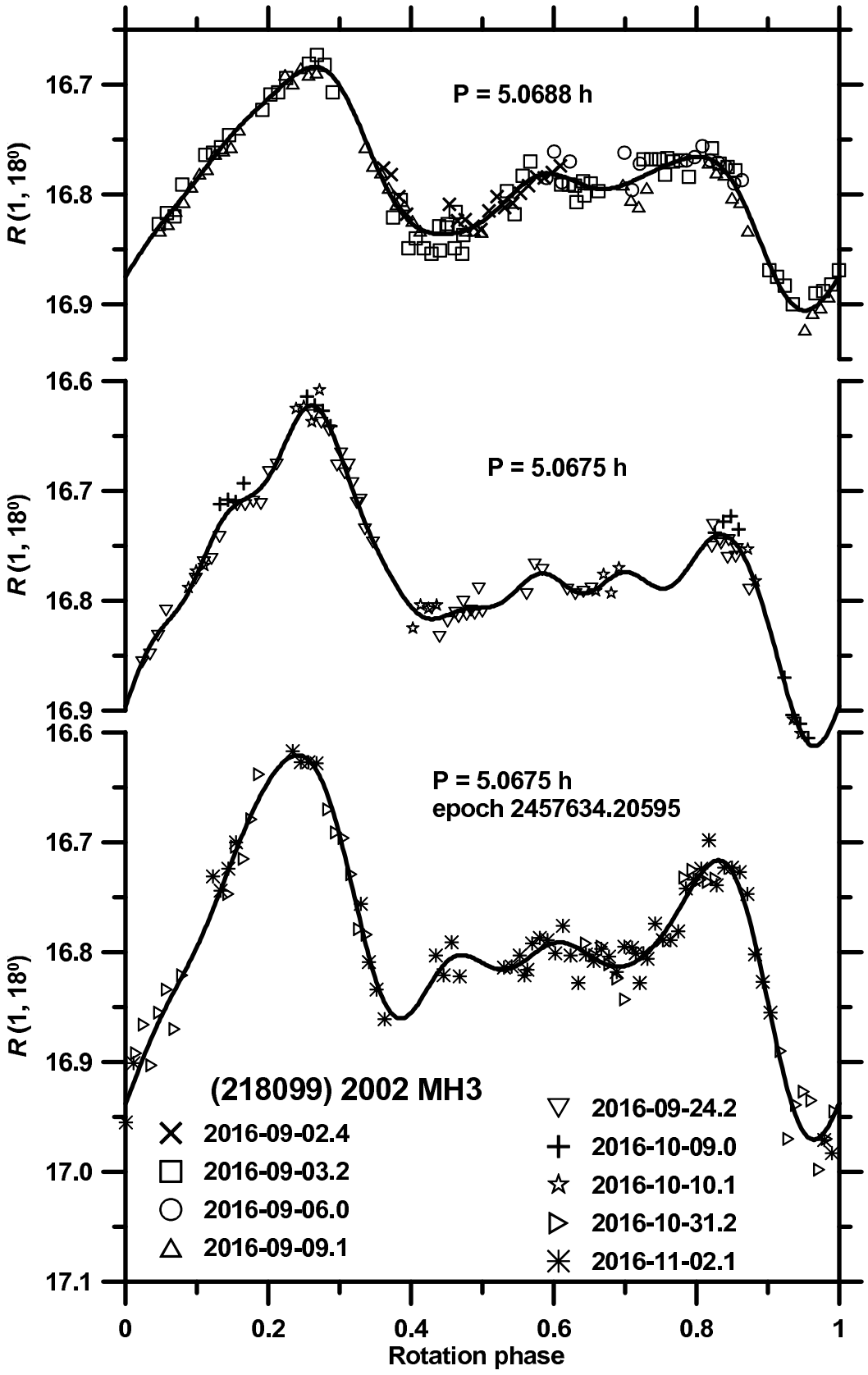

Suppl. Fig. 136. Composite lightcurves of (218099) 2002 MH3 from 2016.

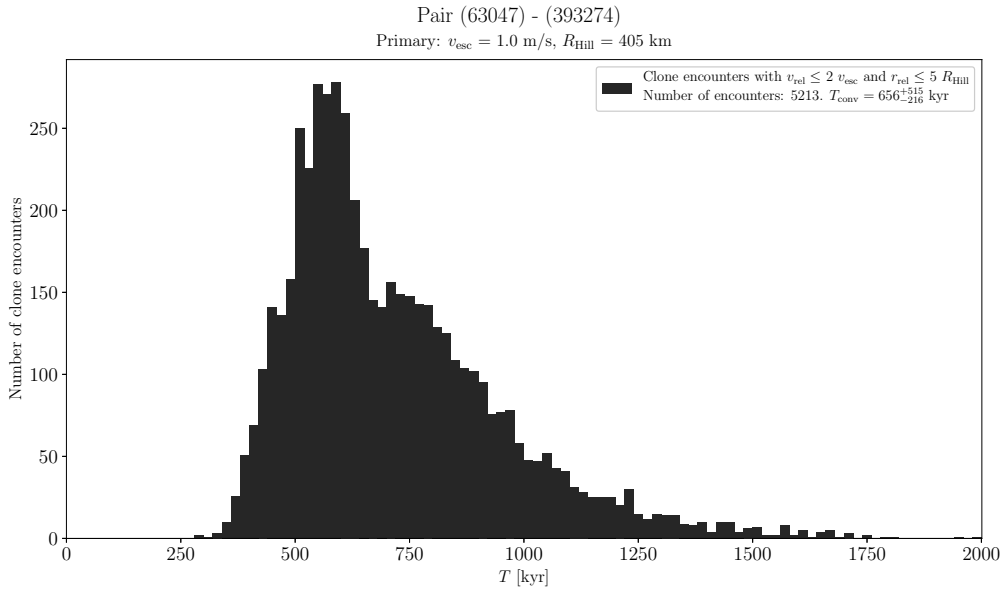

Suppl. Fig. 137. Distribution of past times of close and slow primary–secondary clone encounters for the asteroid pair 63047–393274.

(63047) 2000 WQ93 and (393274) 2013 WJ82

The estimated age of this asteroid pair is about 600 kyr (Suppl. Fig. 137). We observed the primary (63047) from La Silla on 4 nights 2016-10-24 to 27 (Suppl. Fig. 138). We derived its mean absolute magnitude $H_1 = 15.92 \pm 0.03$, assuming the phase relation slope parameter $G = 0.24 \pm 0.11$.

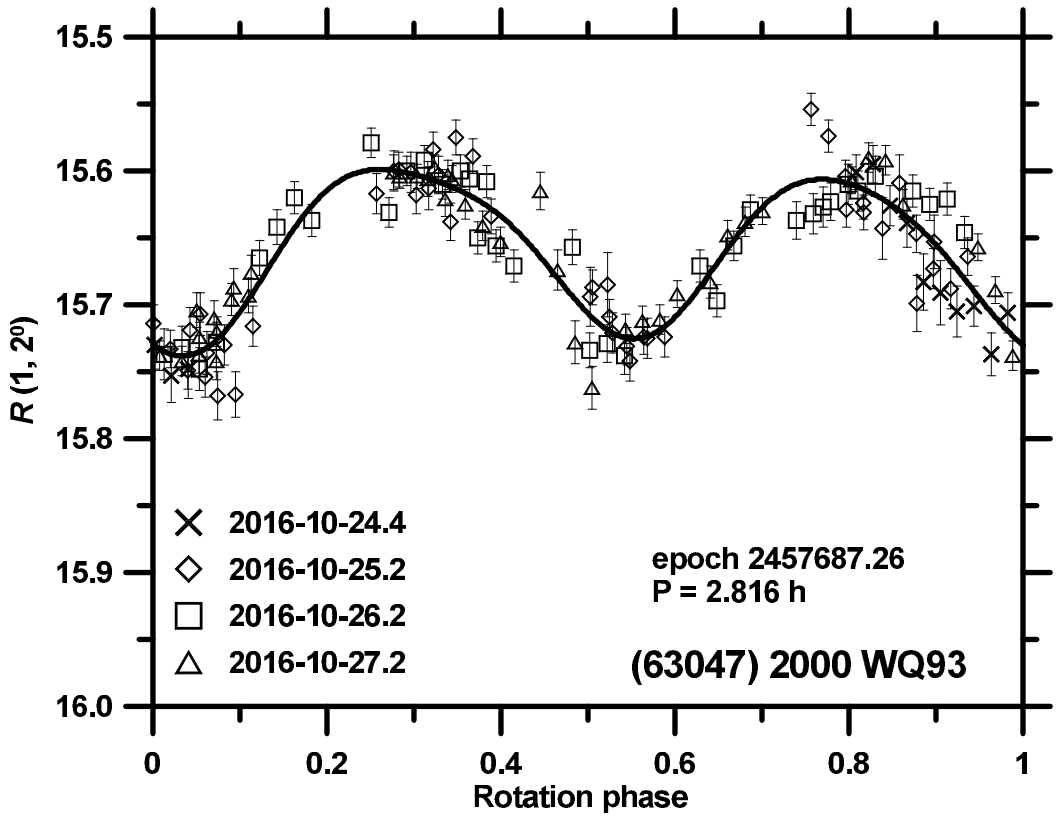

Suppl. Fig. 138. Composite lightcurves of (63047) 2000 WQ93 from 2016.

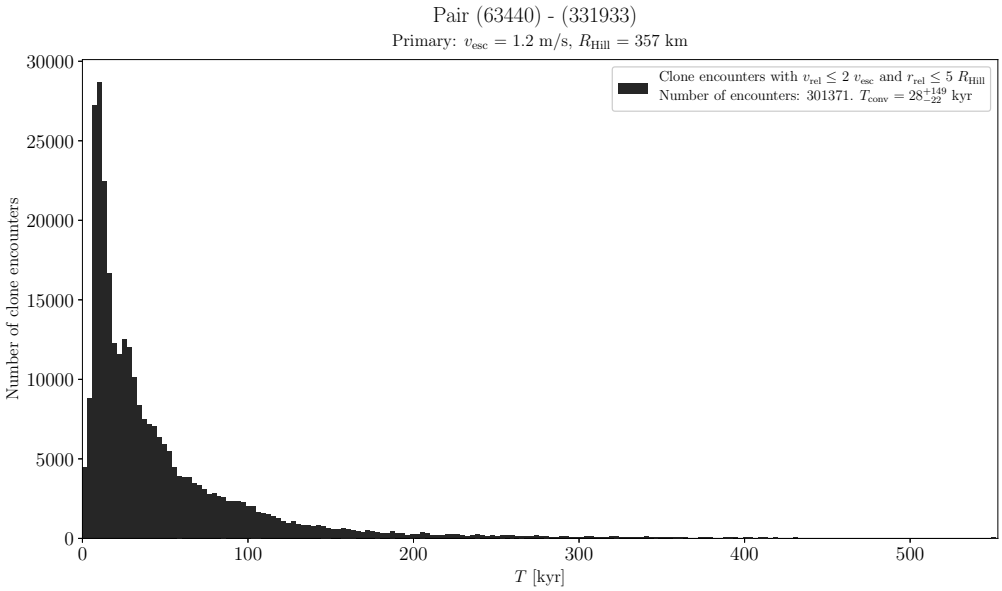

Suppl. Fig. 139. Distribution of past times of close and slow primary–secondary clone encounters for the asteroid pair 63440–331933.

(63440) 2001 MD30 and (331933) 2004 TV14

This is probably a young asteroid pair, see Suppl. Fig. 139. We have obtained lightcurve data for (63440) from 2 apparitions. The observations taken in 2009 were published in Pravec et al. (2010). We observed it from Ondřejov and Wise on 7 nights during 2012-10-09 to 2012-12-06 (Suppl. Fig. 140). From the Ondřejov data, we derived the mean absolute magnitude in the Cousins R system $H_{R,1} = 15.18 \pm 0.09$, assuming $G = 0.33 \pm 0.10$ that is the mean value for Hungarias. For conversion to $H_1 \equiv H_{V,1}$, we assumed $(V-R) = 0.45 \pm 0.10$.

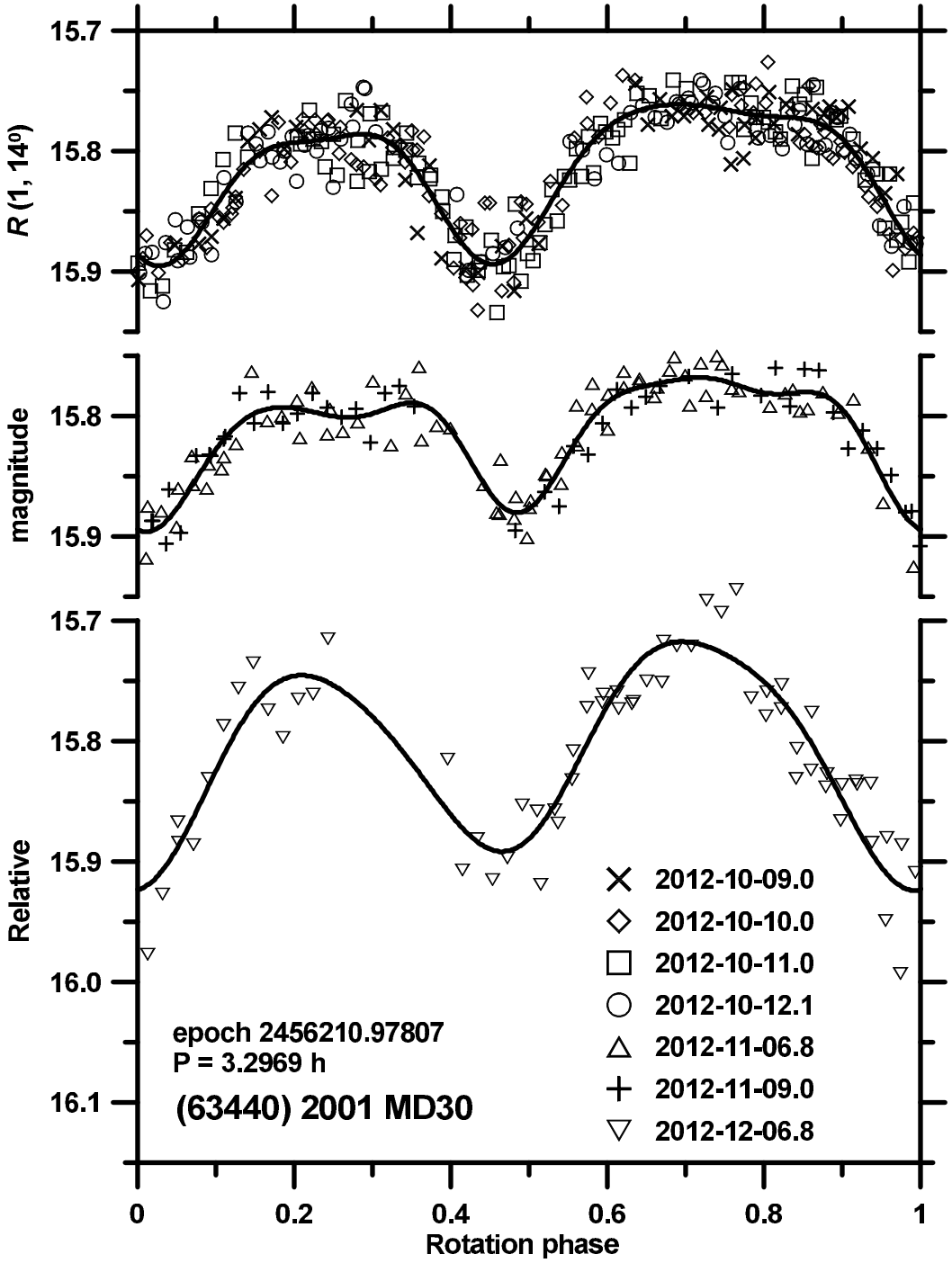

Suppl. Fig. 140. Composite lightcurves of (63440) 2001 MD30 from 2012.

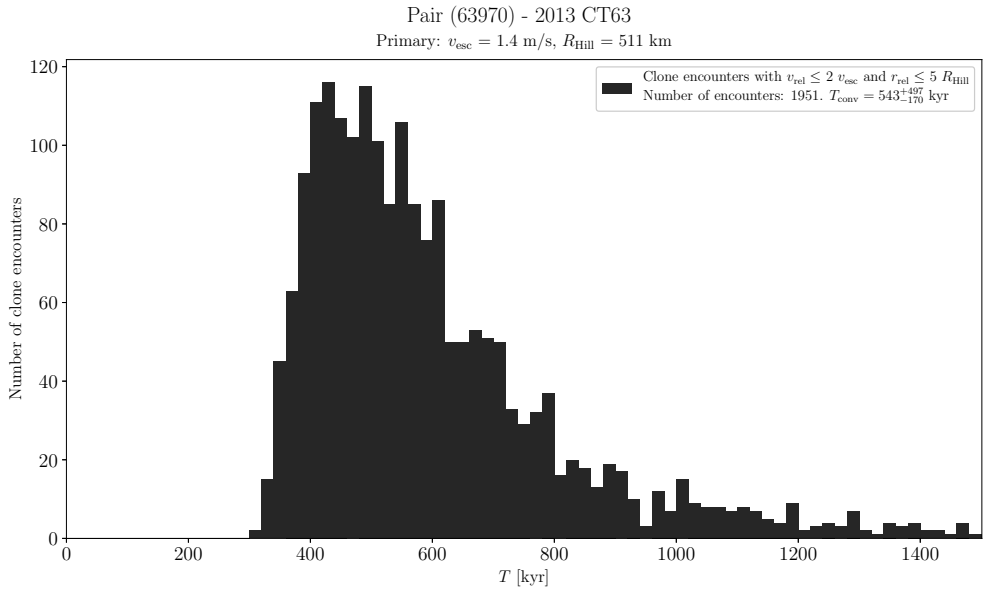

Suppl. Fig. 141. Distribution of past times of close and slow primary–secondary clone encounters for the asteroid pair 63970–2013CT63.

(63970) 2001 SG72 and 2013 CT63

The estimated age of this asteroid pair is about 500 kyr (Suppl. Fig. 141). We observed the primary (63970) from La Silla on 4 nights during 2015-10-10 to 2015-10-20 (Suppl. Fig. 142). We derived the mean absolute magnitude $H_1 = 15.30 \pm 0.07$, assuming $G = 0.24 \pm 0.11$, and refined the WISE effective diameter and geometric albedo (Masiero et al. 2011): $D_1 = 2.1 \pm 0.5$ km and $p_{V,1} = 0.31 \pm 0.16$.

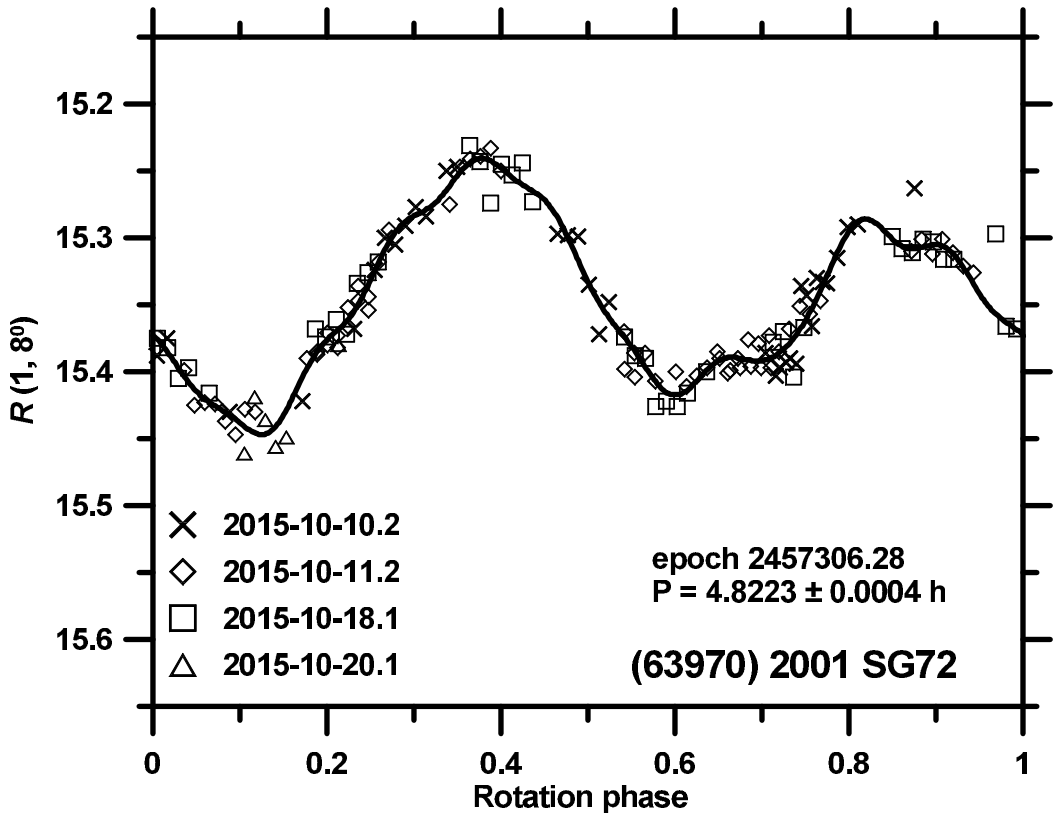

Suppl. Fig. 142. Composite lightcurve of (63970) 2001 SG72 from 2015.

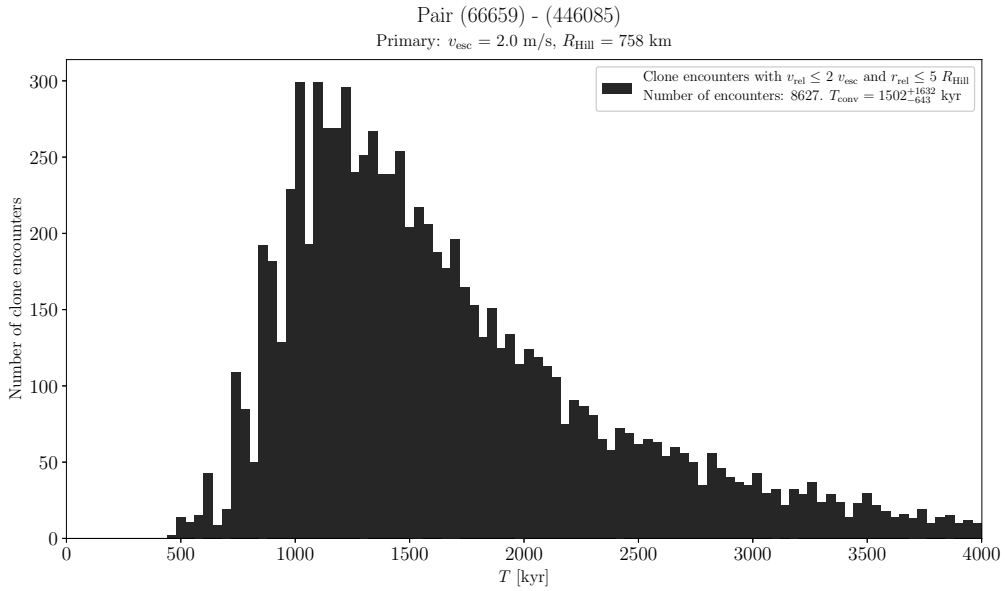

Suppl. Fig. 143. Distribution of past times of close and slow primary–secondary clone encounters for the asteroid pair 66659–446085.

(66659) 1999 TJ1 and (446085) 2013 CW179

The estimated age of this asteroid pair is about 1.5 Myr (Suppl. Fig. 143). We observed the primary (66659) from La Silla on 5 nights during 2016-01-08 to 2016-01-13 (Suppl. Fig. 144) and derived its mean absolute magnitude $H_1 = 14.51 \pm 0.06$, assuming the slope parameter $G = 0.24 \pm 0.11$, and refined the WISE effective diameter and geometric albedo (Masiero et al. 2011): $D_1 = 3.9 \pm 0.4$ km and $p_{V,1} = 0.18 \pm 0.04$.

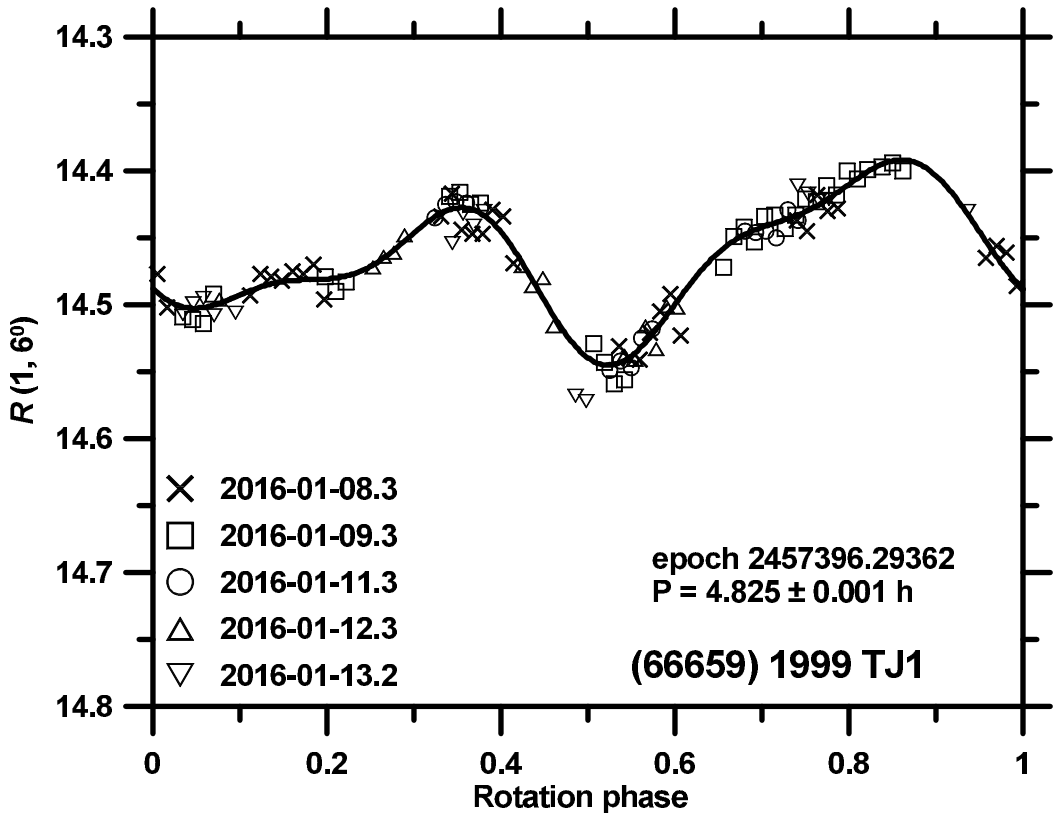

Suppl. Fig. 144. Composite lightcurve of (66659) 1999 TJ1 from 2016.

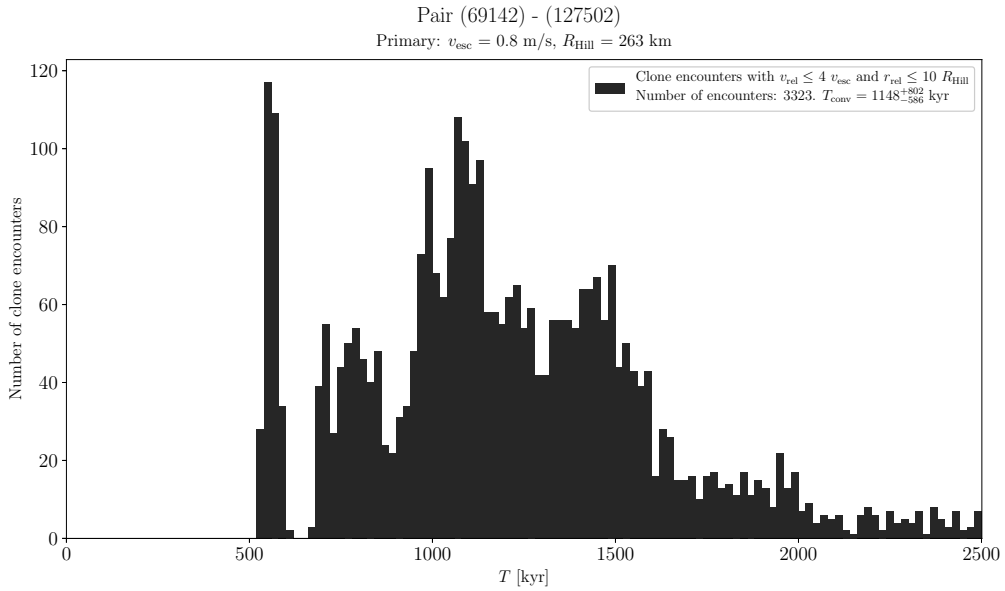

Suppl. Fig. 145. Distribution of past times of close and slow primary–secondary clone encounters for the asteroid pair 69142–127502.

(69142) 2003 FL115 and (127502) 2002 TP59

Despite the somewhat increased distance between these two asteroids ($d_{\mathrm{mean}} =$ 17.1 m/s) and its relatively high estimated about 1 Myr (Suppl. Fig. 145), it appears to be a real pair. We have obtained lightcurve data for the primary (69142) from 4 apparitions. The observations taken from Wise and Pic du Midi in 2009 and from Center for Solar System Studies in 2014 were published in Pravec et al. (2010) and Warner (2014b), respectively. We observed it from La Silla on 3 nights during 2014-02-09 to 2014-03-28, on 7 nights during 2015-10-10 to 2015-12-11, and on 2 nights 2018-10-06 and 2018-11-06. We derived the mean absolute magnitudes $H_1 = 15.83 \pm 0.10$, 15.76 ± 0.13 and 15.81 ± 0.11 in the three apparitions, with the slope parameter $G = 0.18 \pm 0.10$. We observed the secondary (127502) on 2 nights of 2015-03-15 and -17 and on 13 nights during 2016-10-08 to 2016-11-29. Its period $P_2 = 23.150 \pm 0.008$ h is well established despite that 30% of the lightcurve was not covered (Suppl. Fig. 146). We derived the mean absolute magnitudes $H_2 = 17.26 \pm 0.11$ and 17.34 ± 0.10 in the two apparitions, assuming $G = 0.33 \pm 0.10$ that is the mean value for Hungarias.

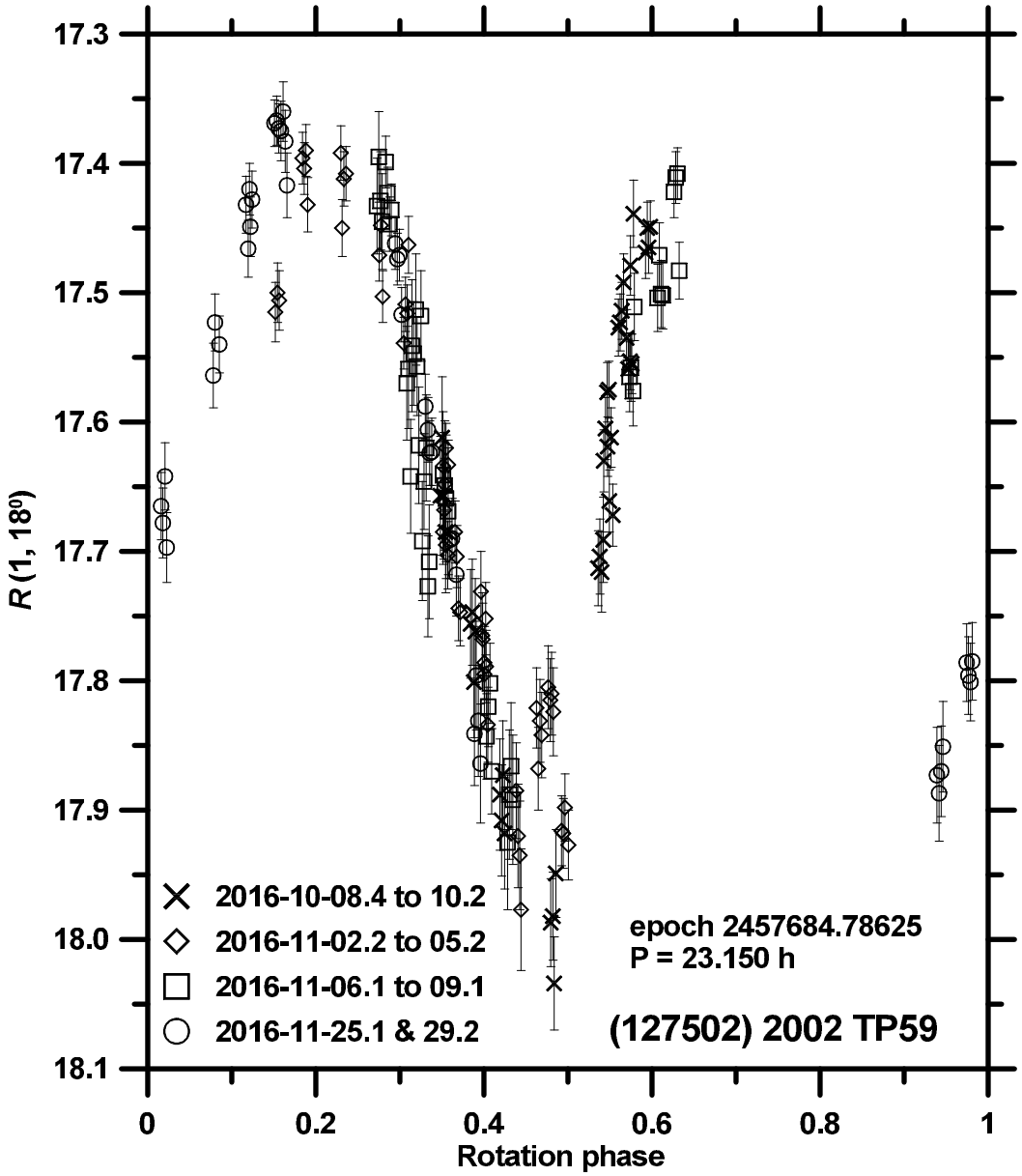

Suppl. Fig. 146. Composite lightcurve of (127502) 2002 TP59 from 2016.

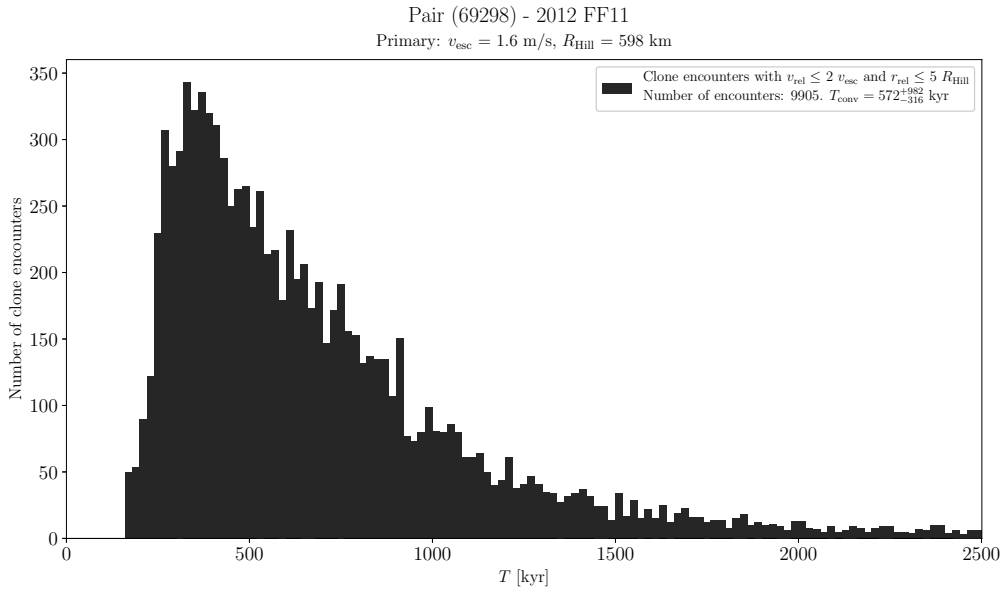

Suppl. Fig. 147. Distribution of past times of close and slow primary–secondary clone encounters for the asteroid pair 69298–2012FF11.

(69298) 1992 DR9 and 2012 FF11

The estimated age of this asteroid pair is about 600 kyr (Suppl. Fig. 147). We observed the primary (69298) from La Silla on 4 nights during 2014-02-04 to 2014-02-09 (Suppl. Fig. 148). We derived its mean absolute magnitude $H_1 = 16.33 \pm 0.05$, assuming $G = 0.15 \pm 0.10$, and refined the WISE effective diameter and geometric albedo (Masiero et al. 2011): $D_1 = 4.0 \pm 0.4$ km and $p_{V,1} = 0.032 \pm 0.007$.

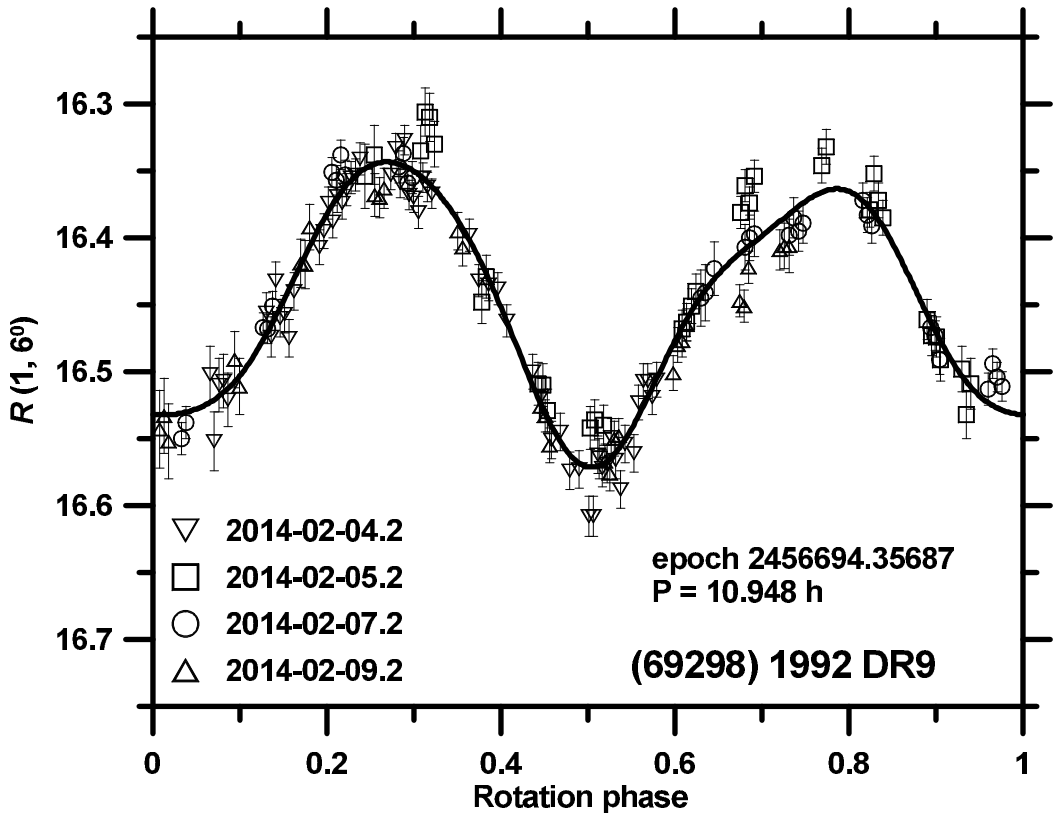

Suppl. Fig. 148. Composite lightcurve of (69298) 1992 DR9 from 2014.

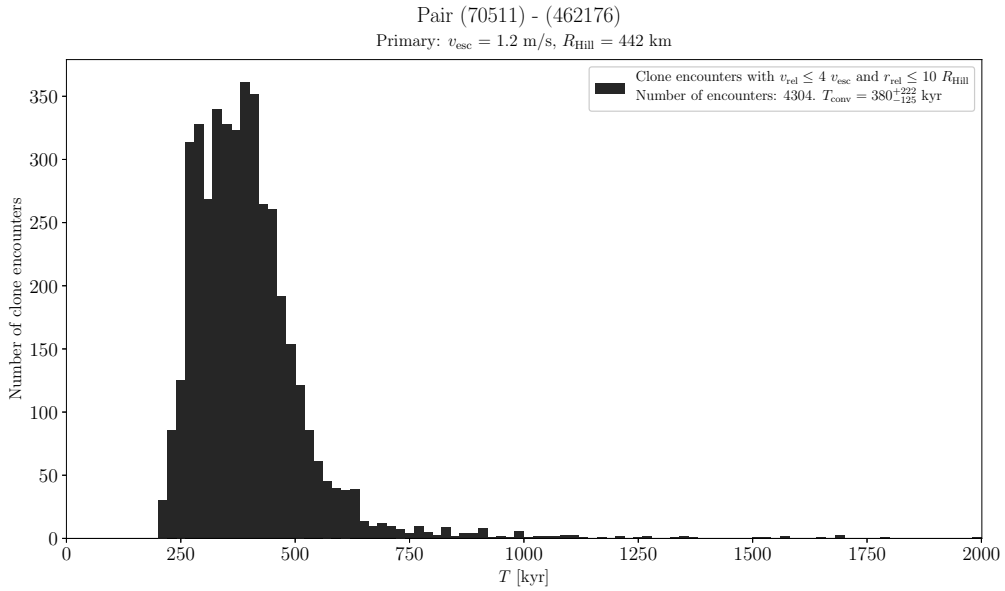

Suppl. Fig. 149. Distribution of past times of close and slow primary–secondary clone encounters for the asteroid pair 70511–462176.

(70511) 1999 TL103 and (462176) 2007 TC334

The estimated age of this asteroid pair is about 400 kyr (Suppl. Fig. 149). We observed the primary (70511) from Maidanak on 2 nights 2010-08-20 and 21, and from La Silla on 4 nights during 2016-03-14 to 2016-04-01 (Suppl. Figs. 150 and 151). We derived the mean absolute magnitude $H_1 = 15.61 \pm 0.06$ and the phase relation slope parameter $G = 0.36 \pm 0.05$.

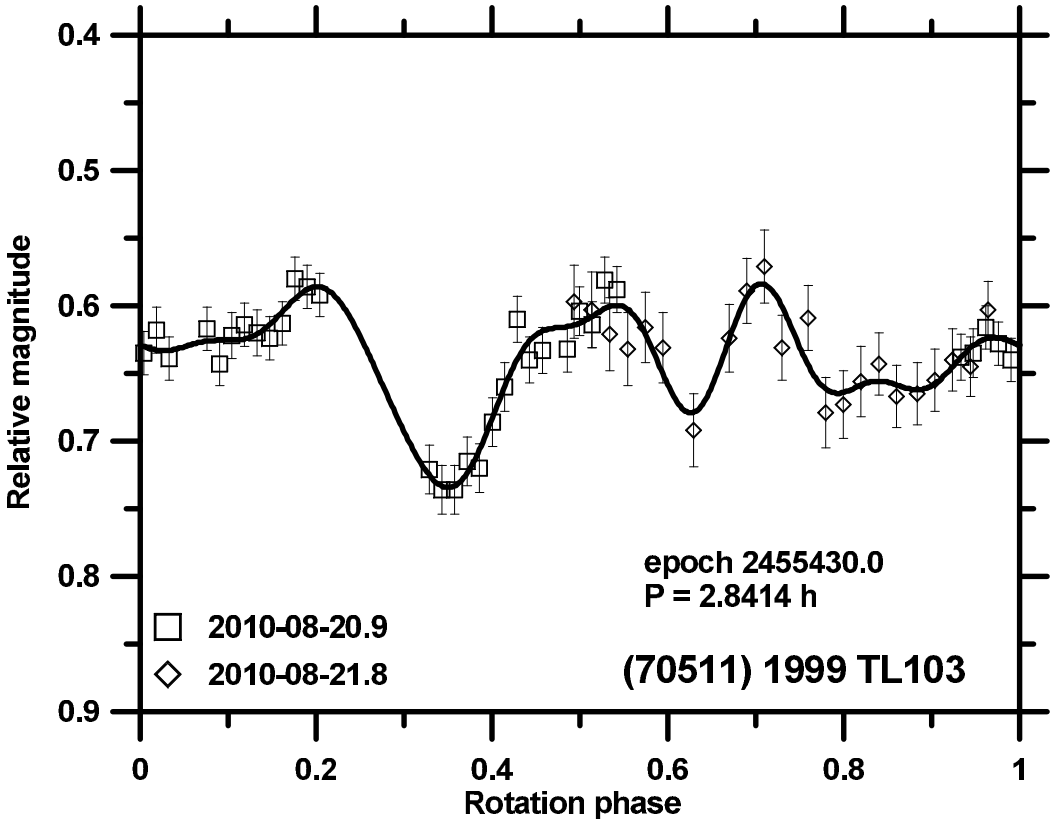

Suppl. Fig. 150. Composite lightcurve of (70511) 1999 TL103 from 2010.

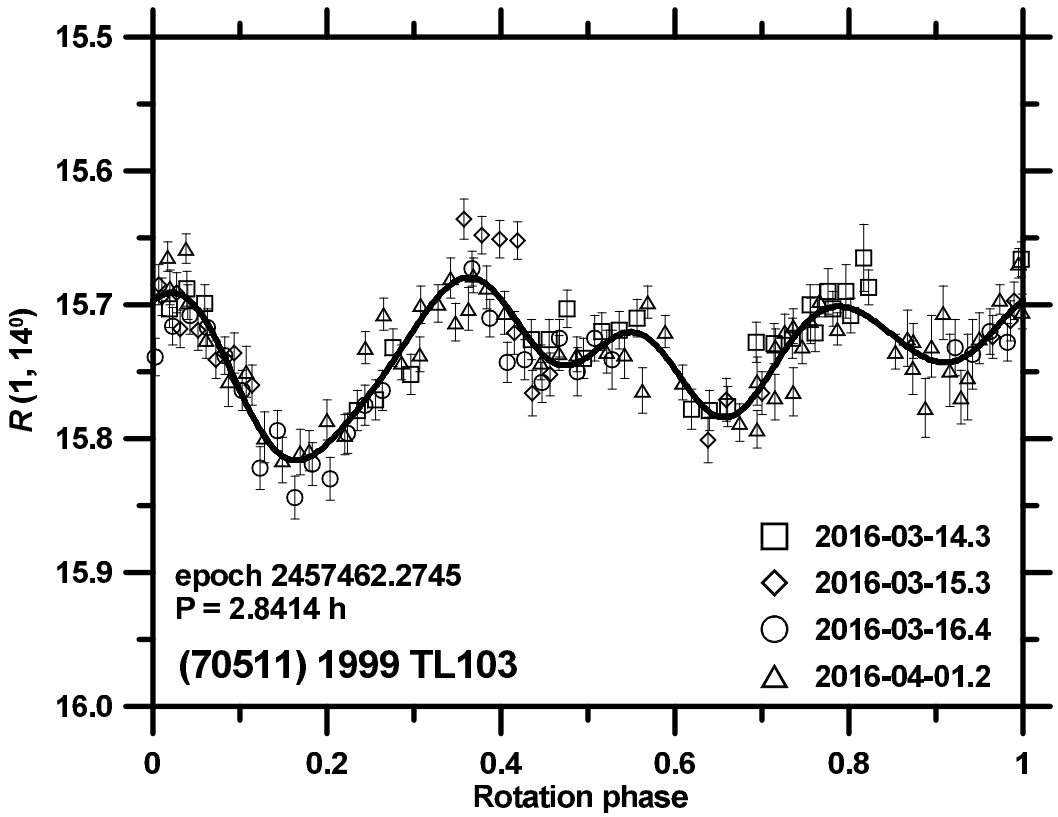

Suppl. Fig. 151. Composite lightcurve of (70511) 1999 TL103 from 2016.

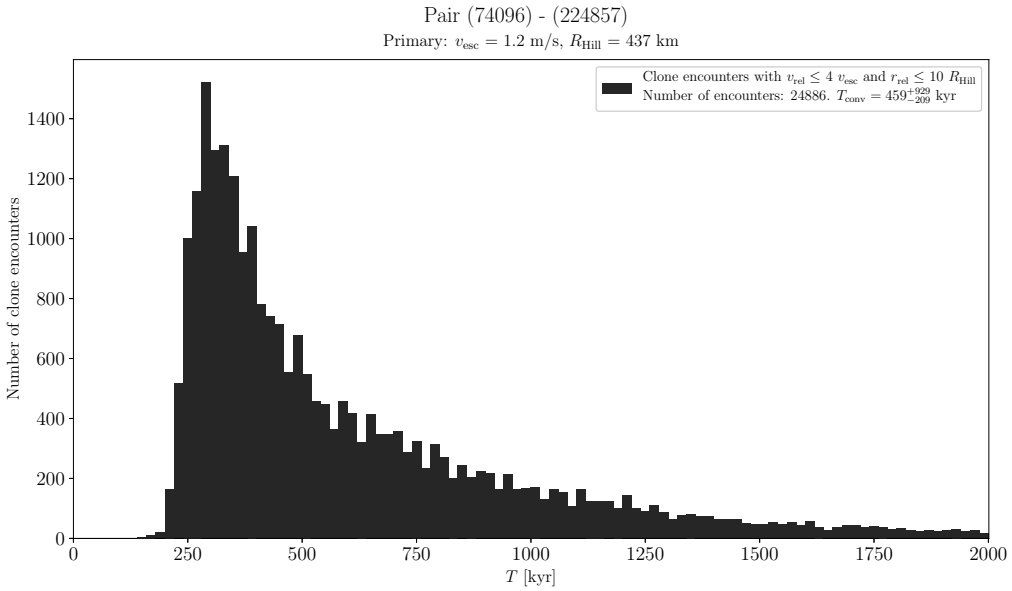

Suppl. Fig. 152. Distribution of past times of close and slow primary–secondary clone encounters for the asteroid pair 74096–224857.

(74096) 1998 QD15 and (224857) 2006 YE45

The estimated age of this asteroid pair is about 400 kyr (Suppl. Fig. 152).

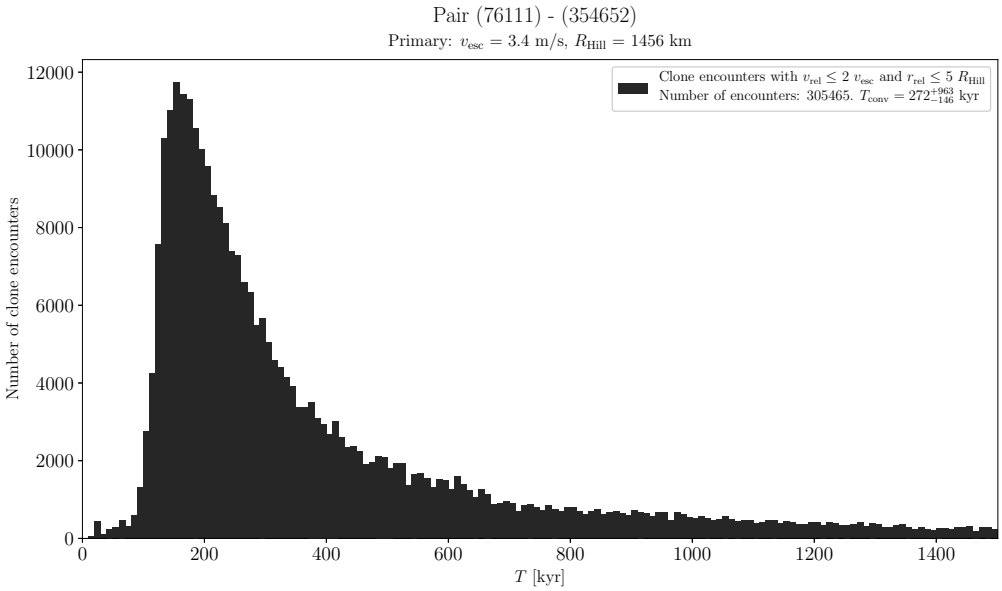

Suppl. Fig. 153. Distribution of past times of close and slow primary–secondary clone encounters for the asteroid pair 76111–354652.

(76111) 2000 DK106 and (354652) 2005 JY103

The estimated age of this asteroid pair is about 270 kyr (Suppl. Fig. 153). We observed the primary (76111) from La Silla on 6 nights during 2018-02-17 to 2018-03-11 (Suppl. Fig. 154). We derived the mean absolute magnitude $H_1 = 15.11 \pm 0.03$ and the phase relation slope parameter $G = 0.28 \pm 0.05$.

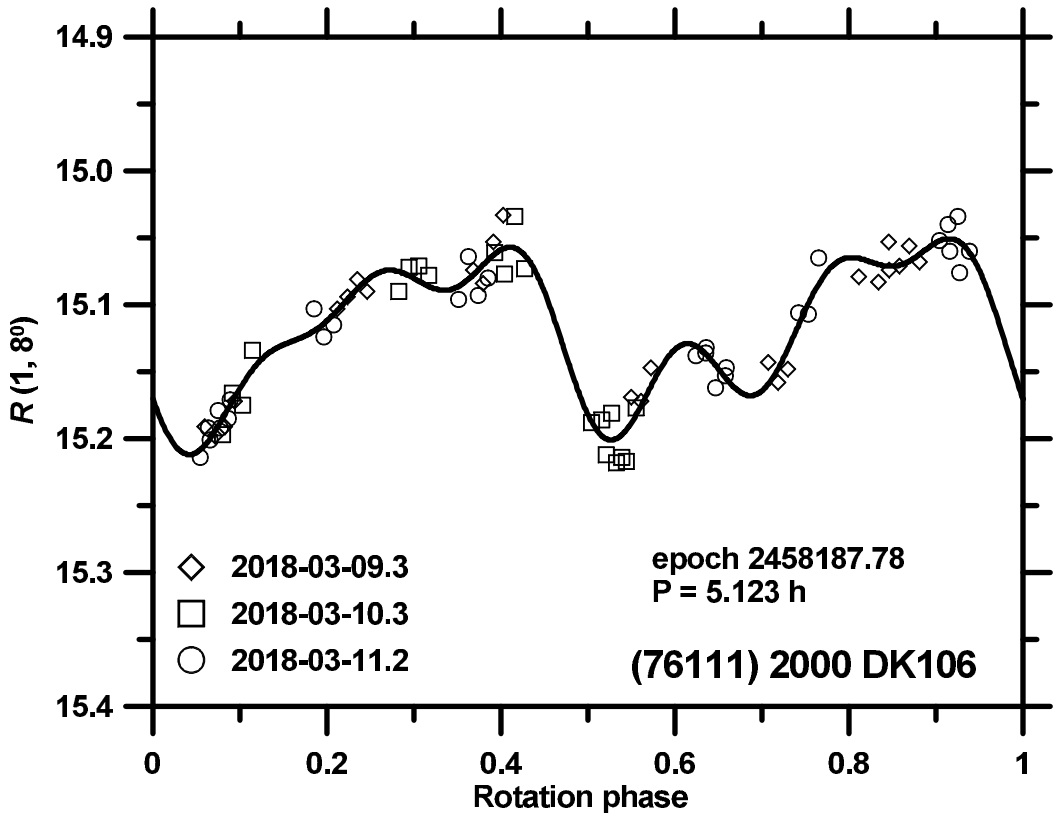

Suppl. Fig. 154. Composite lightcurve of (76111) 2000 DK106 from 2018.

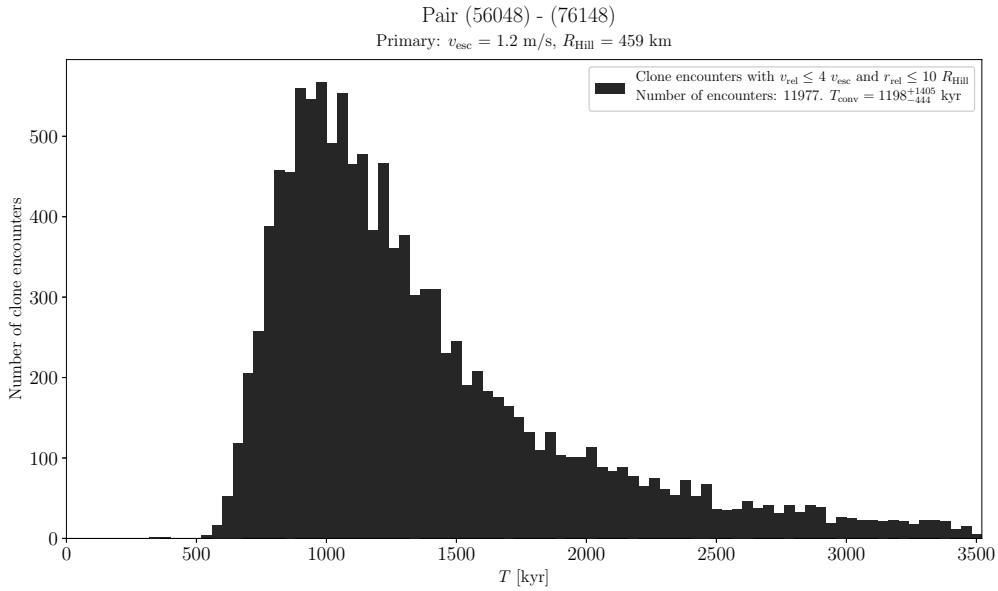

Suppl. Fig. 155. Distribution of past times of close and slow primary–secondary clone encounters for the asteroid pair 76148–56048.

(76148) 2000 EP17 and (56048) 1998 XV39

Backward orbital clone integrations suggest that these two asteroids separated about 1.2 Myr ago (Suppl. Fig. 155). We observed (76148) from La Silla on 12 nights during 2013-10-28 to 2013-12-07 and on 7 nights of 2016-09-04 to 10. The observations revealed a slow rotation with a formal best fit to the 2013 data for a period of $P_1 = 65.33 \pm 0.09$ h (Suppl. Fig. 156), but it is not an unique solution and other (long) periods are also possible. We derived its mean absolute magnitudes $H_1 = 15.52 \pm 0.04$ and 15.51 ± 0.04 in the two apparitions, assuming the (56048)'s mean phase relation slope parameter $G = 0.22 \pm 0.04$ (see below). We observed (56048) from La Silla on 5 nights during 2014-02-07 to 2014-03-03, on 3 nights during 2016-10-06 to 2016-10-10, and on 4 nights during 2018-02-19 to 2018-03-24. We derived its mean absolute magnitudes $H_2 = 15.40 \pm 0.04, 15.61 \pm 0.03$ and 15.78 ± 0.03 in the three apparitions, with the slope parameters $G = 0.21 \pm 0.04$ and 0.24 ± 0.04. The different absolute magnitudes correspond to its different aspects in the three apparitions. Using the mean $H_2 = 15.60 \pm 0.20$, we refined the WISE effective diameter and geometric albedo (Masiero et al. 2011): $D_2 = 2.4 \pm 0.5$ km and $p_{V,2} = 0.18 \pm 0.08$.

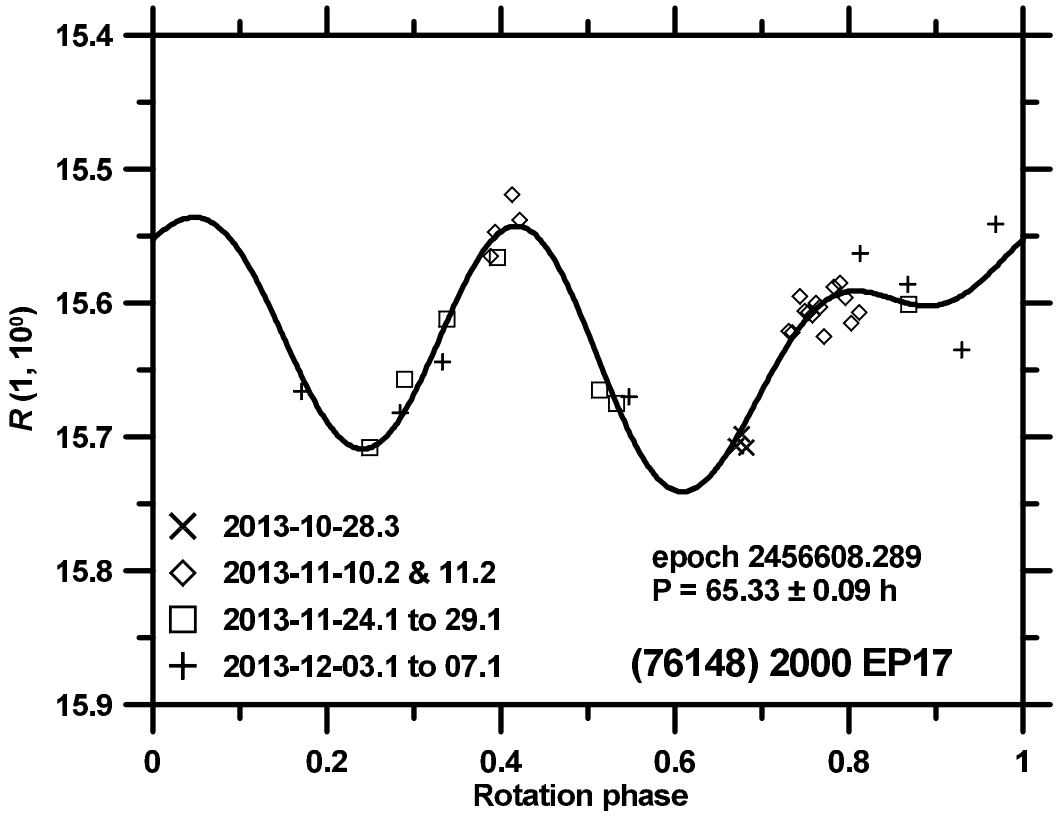

Suppl. Fig. 156. Composite lightcurve of (76148) 2000 EP17 from 2013.

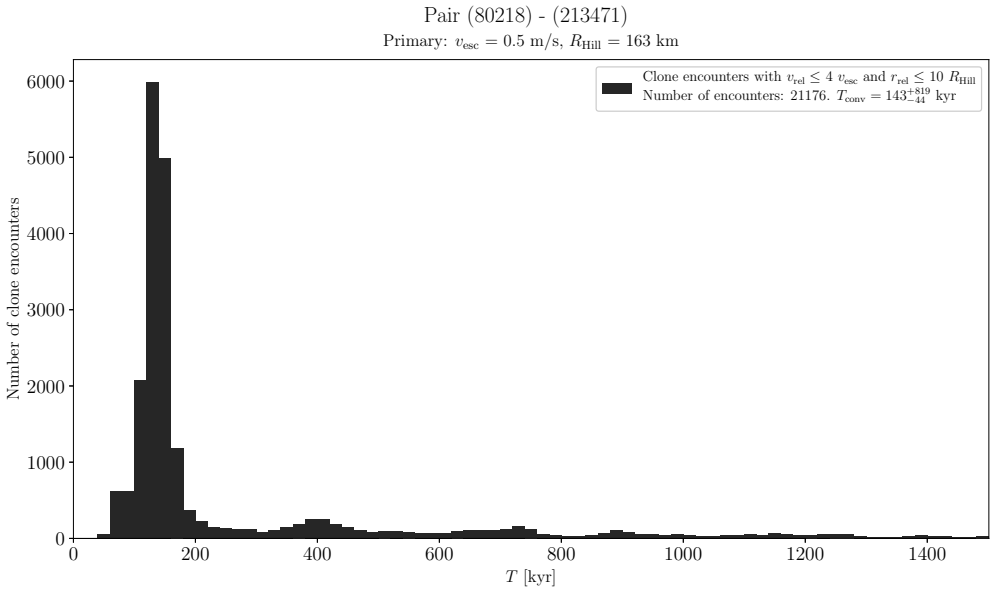

Suppl. Fig. 157. Distribution of past times of close and slow primary–secondary clone encounters for the asteroid pair 80218–213471.

(80218) 1999 VO123 and (213471) 2002 ES90

Backward orbital clone integrations suggest that these two asteroids separated about 140 kyr ago (Suppl. Fig. 157). The observations of (80218) were published in Pravec et al. (2016). We derived the mean absolute magnitudes of the whole binary system (outside mutual events between the primary and its satellite) $H_1 = 17.11 \pm 0.05$ and 17.08 ± 0.05 in 2012 and 2014, with the slope parameters $G = 0.68 \pm 0.15$ and 0.57 ± 0.15, respectively. We observed (213471) from La Silla on 5 nights during 2015-02-12 to 2015-02-19. We derived the mean absolute magnitude $H_2 = 17.37 \pm 0.03$, assuming the primary's mean slope parameter $G = 0.62 \pm 0.15$.

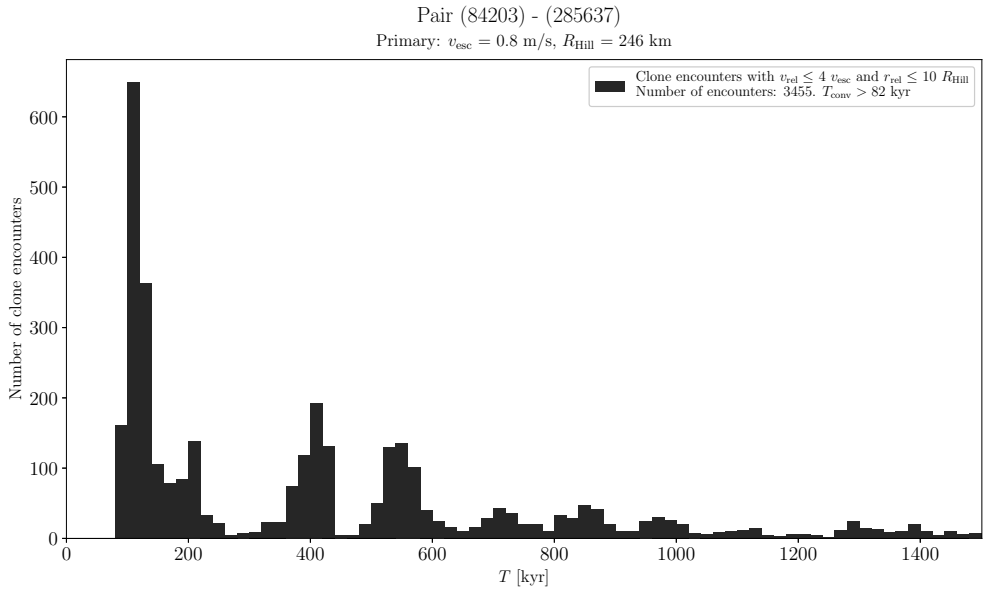

Suppl. Fig. 158. Distribution of past times of close and slow primary–secondary clone encounters for the asteroid pair 84203–285637.

(84203) 2002 RD133 and (285637) 2000 SS4

For this asteroid pair, we estimate a lower limit on its age of about 80 kyr (Suppl. Fig. 158).

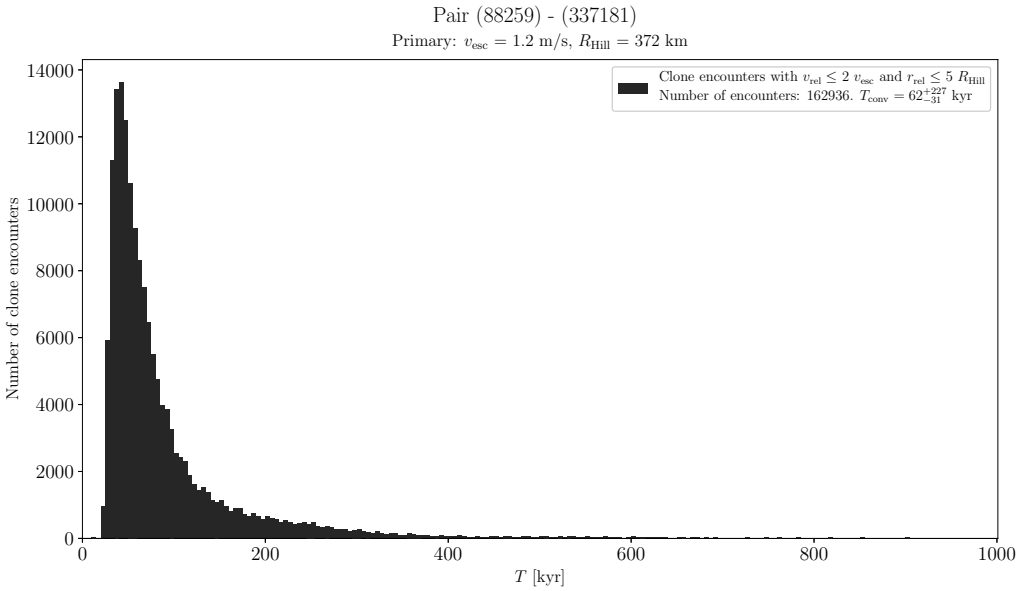

Suppl. Fig. 159. Distribution of past times of close and slow primary–secondary clone encounters for the asteroid pair 88259–337181.

(88259) 2001 HJ7 and (337181) 1999 VA117

The estimated age of this asteroid pair is about 60 kyr (Suppl. Fig. 159). We have obtained lightcurve data for the primary (88259) from 4 apparitions. The observations taken in 2009 were published in Pravec et al. (2010). The observations taken from Palmer Divide Observatory in 2012 were published in Warner (2012). We observed it from Maidanak on 2 nights 2010-08-25 and -26 and from La Silla on 9 nights during 2013-11-27 to 2014-01-02 (Suppl. Figs. 161 and 161). From the La Silla data that were taken in the Johnson-Cousins VR photometric system, we derived the mean absolute magnitude $H_1 = 15.56 \pm 0.04$ and the slope parameter $G = 0.29 \pm 0.04$.

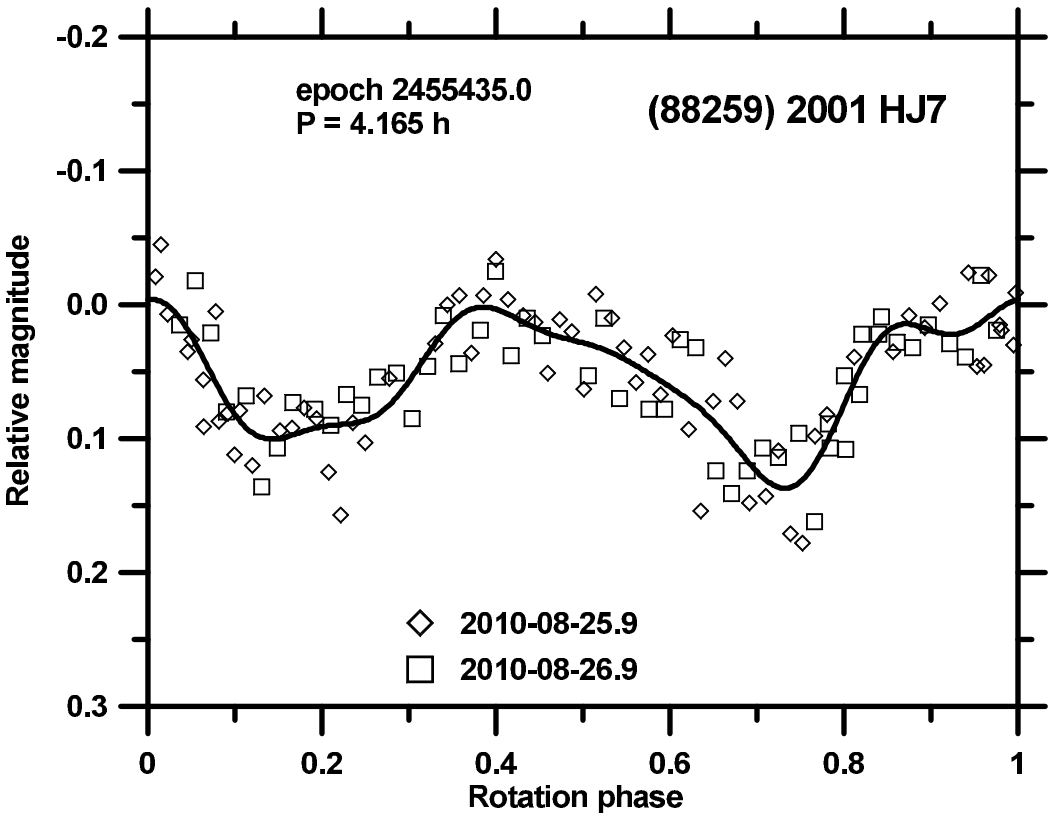

Suppl. Fig. 160. Composite lightcurve of (88259) 2001 HJ7 from 2010.

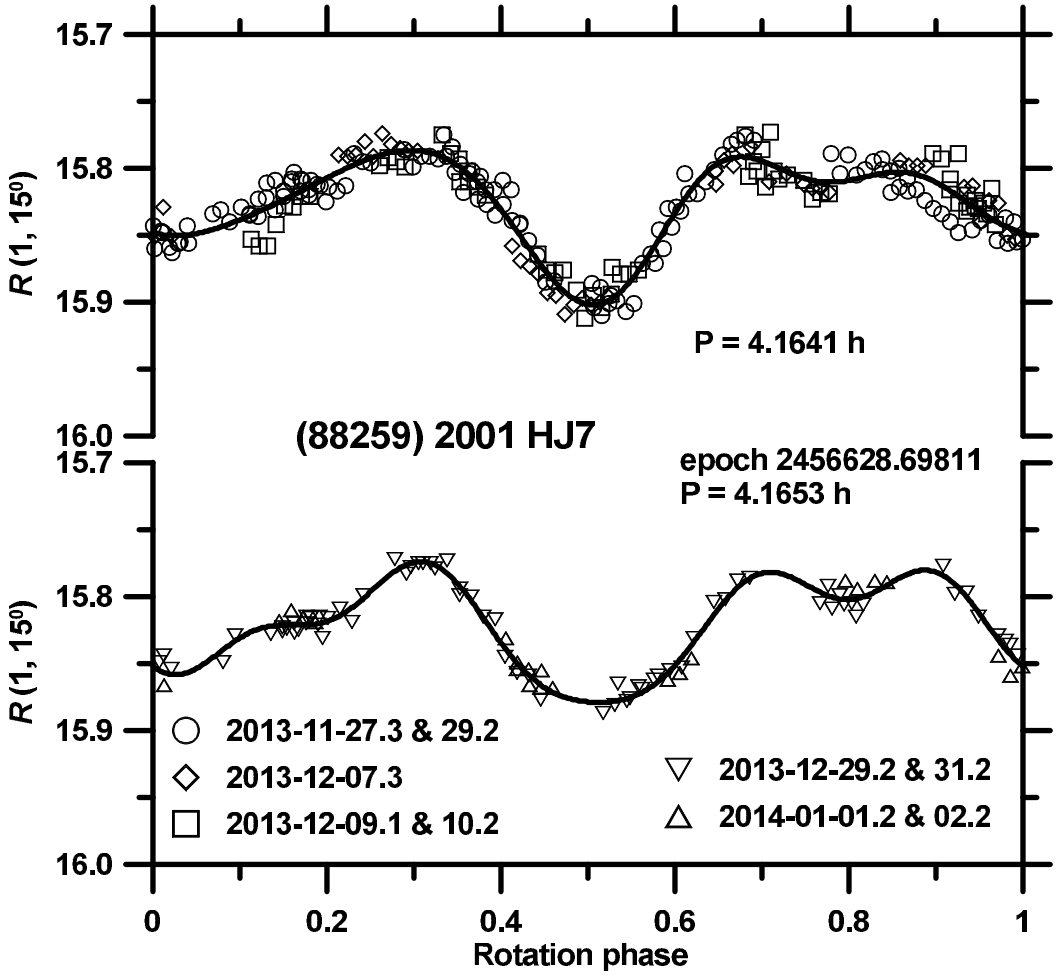

Suppl. Fig. 161. Composite lightcurves of (88259) 2001 HJ7 from 2013–2014.

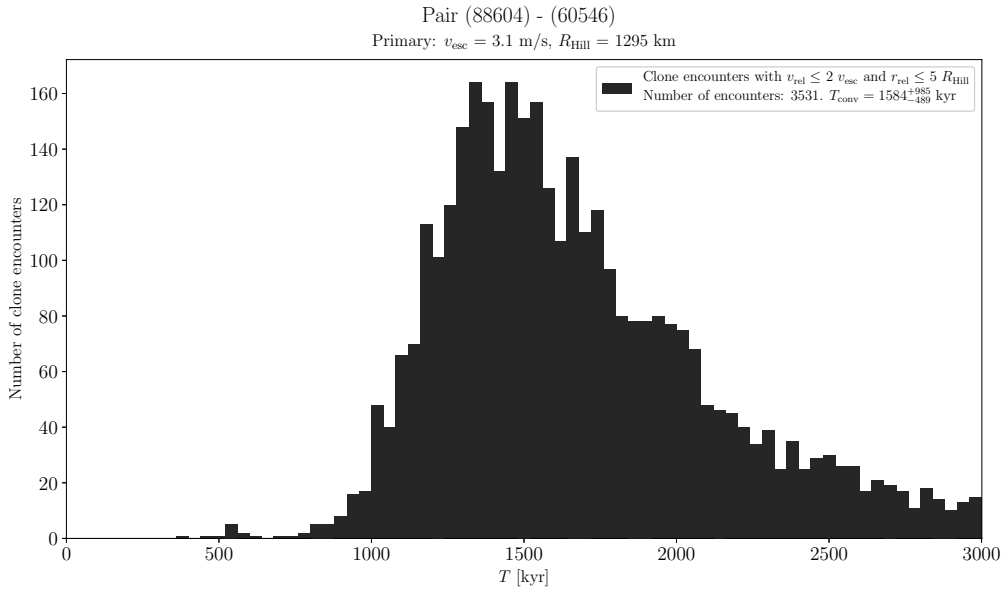

Suppl. Fig. 162. Distribution of past times of close and slow primary–secondary clone encounters for the asteroid pair 88604–60546.

(88604) 2001 QH293 and (60546) 2000 EE85

The estimated age of this asteroid pair is about 1.5 Myr (Suppl. Fig. 162). The observations of the primary (88604) taken in 2009 were published in Pravec et al. (2010). We observed it from Modra and Skalnaté Pleso on 6 nights during 2010-10-01 to 2010-10-14 (Suppl. Fig. 163). Masiero et al. (2011) measured $D_1 = 5.8$ km. We observed the secondary (60546) from La Silla on 2 nights 2018-04-22 and 23 (Suppl. Fig. 164) and derived its mean absolute magnitude $H_2 = 14.94 \pm 0.07$, assuming the phase relation slope parameter $G = 0.24 \pm 0.11$.

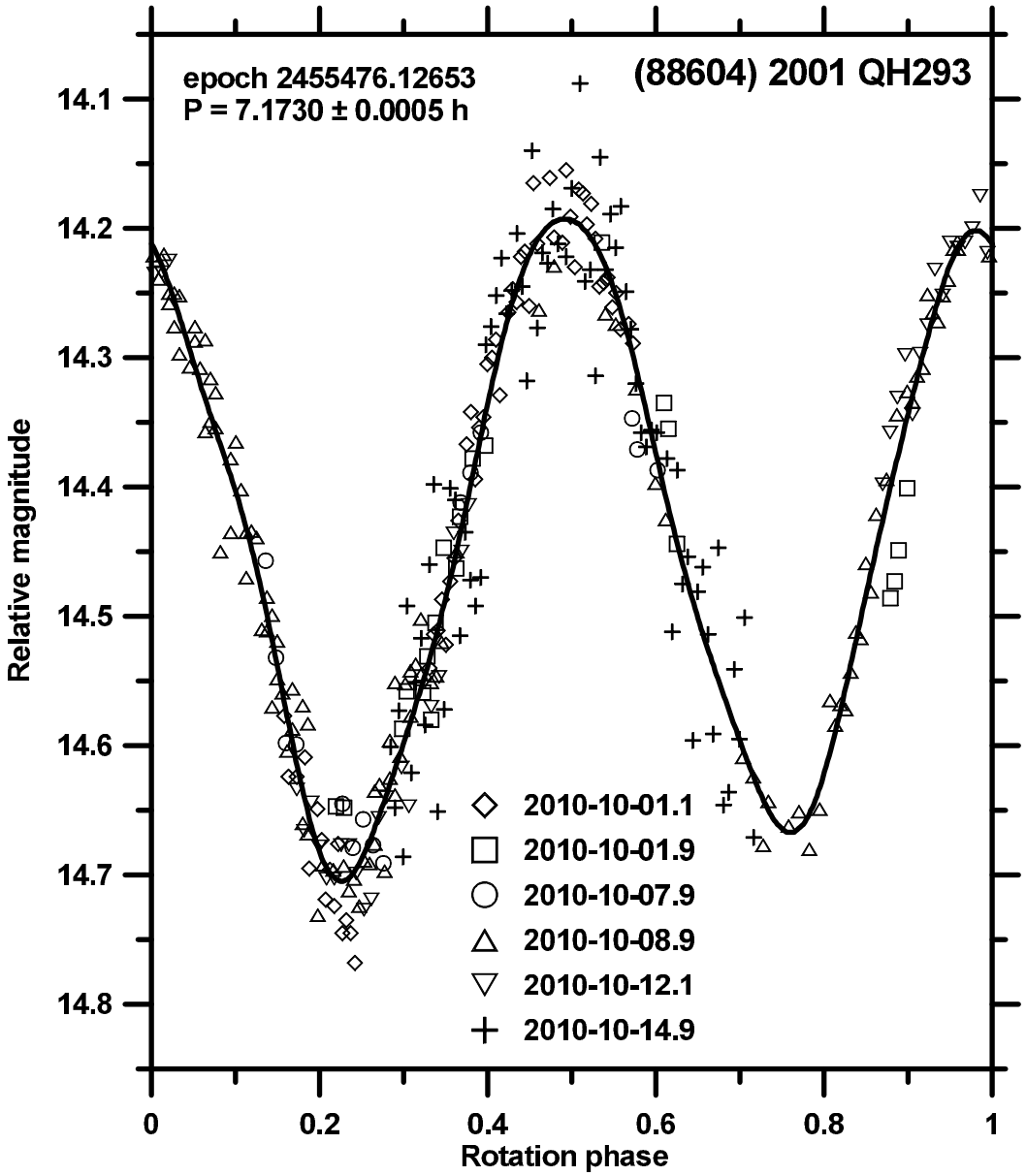

Suppl. Fig. 163. Composite lightcurve of (88604) 2001 QH293 from 2010.

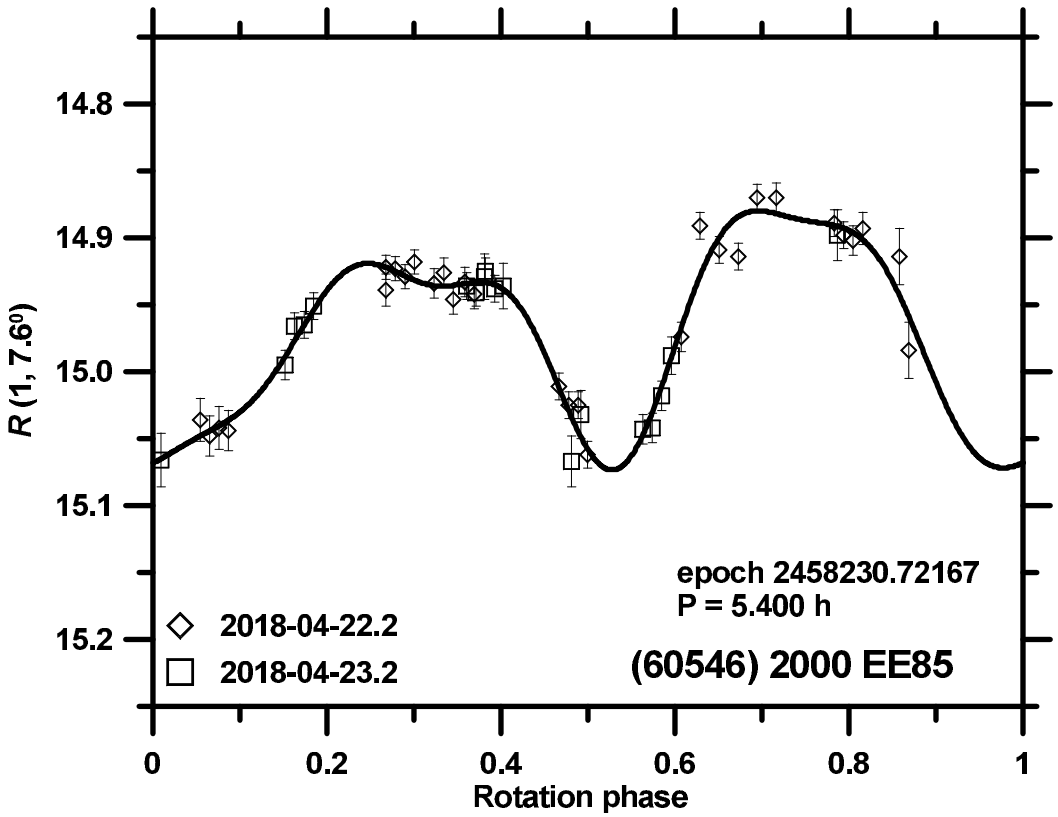

Suppl. Fig. 164. Composite lightcurve of (60546) 2000 EE85 from 2018.

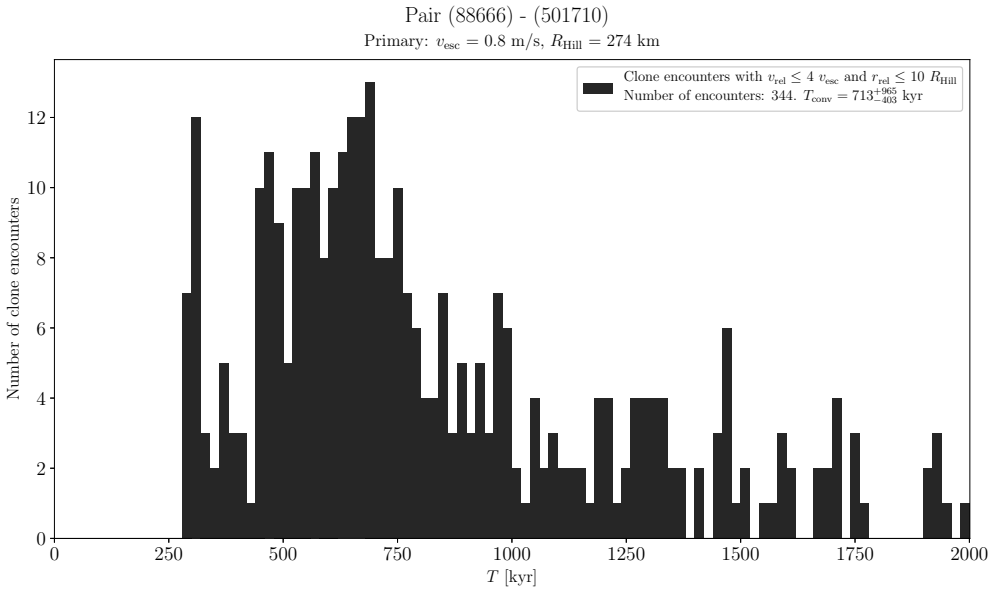

Suppl. Fig. 165. Distribution of past times of close and slow primary–secondary clone encounters for the asteroid pair 88666–501710.

(88666) 2001 RP79 and (501710) 2014 UY23

The estimated age of this asteroid pair is about 700 kyr (Suppl. Fig. 165). We observed the primary (88666) from La Silla on 4 nights during 2016-03-03 to 2016-03-09 (Suppl. Fig. 166) and derived its mean absolute magnitude $H_1 = 16.46 \pm 0.07$, assuming the phase relation slope parameter $G = 0.33 \pm 0.10$.

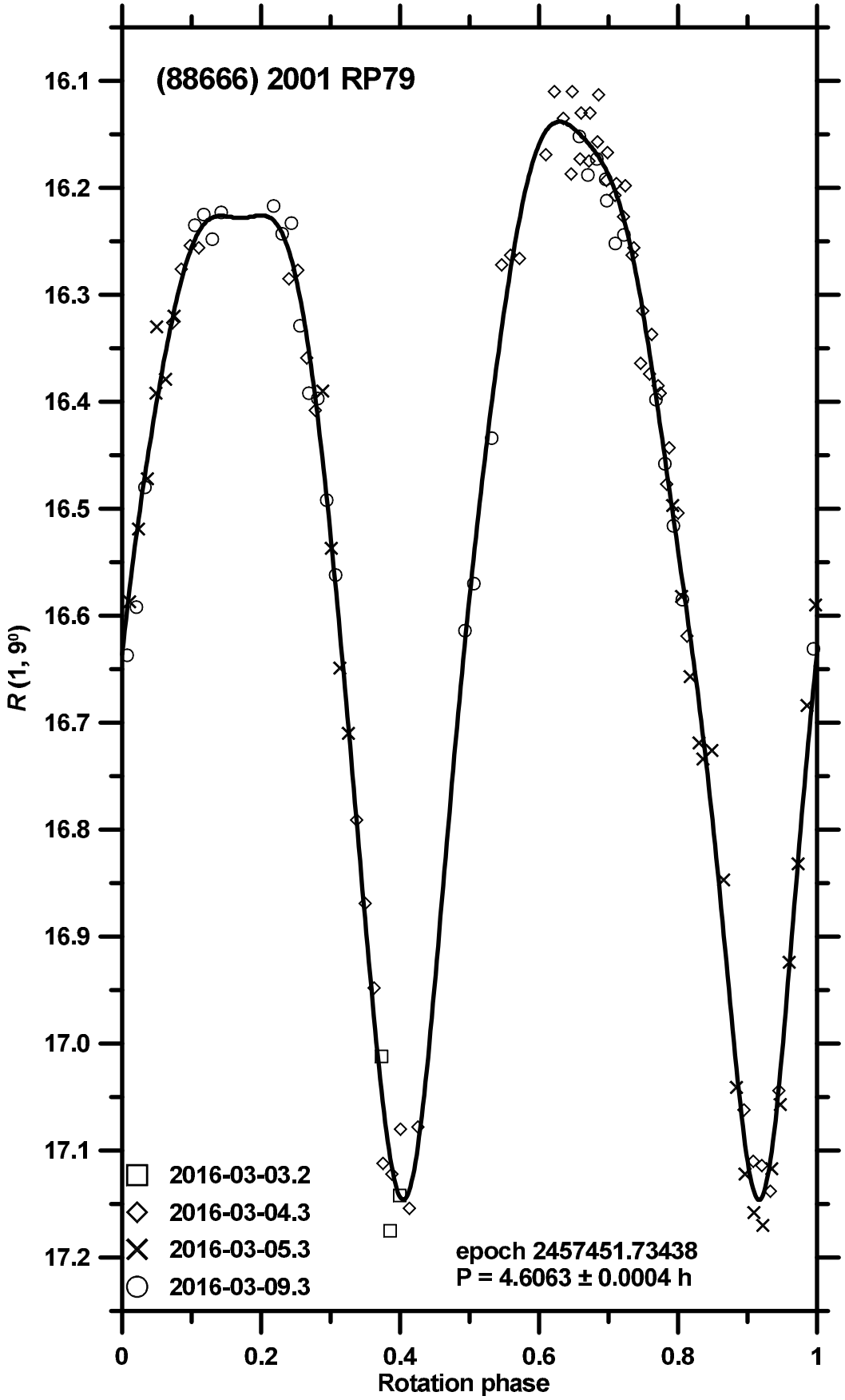

Suppl. Fig. 166. Composite lightcurve of (88666) 2001 RP79 from 2016.

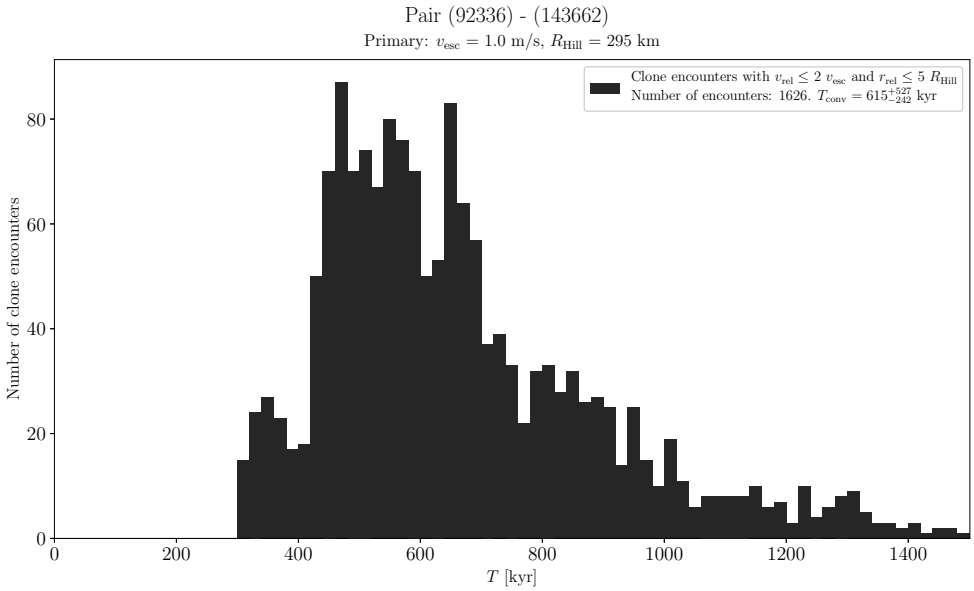

Suppl. Fig. 167. Distribution of past times of close and slow primary–secondary clone encounters for the asteroid pair 92336–143662.

(92336) 2000 GY81 and (143662) 2003 SP84

The estimated age of this asteroid pair is about 600 kyr (Suppl. Fig. 167). The observations of the primary were published in Pravec et al. (2010). We observed the secondary (143662) from La Silla on 4 nights during 2018-02-08 to 2018-02-12 (Suppl. Fig. 168) and derived its mean absolute magnitude $H_2 = 17.22 \pm 0.09$, assuming the phase relation slope parameter $G = 0.43 \pm 0.08$ that is the mean value for E-type asteroids (Warner et al. 2009), which is a likely classification for this Hungaria asteroid with our measured $(V - R)_2 = 0.408 \pm 0.018$.

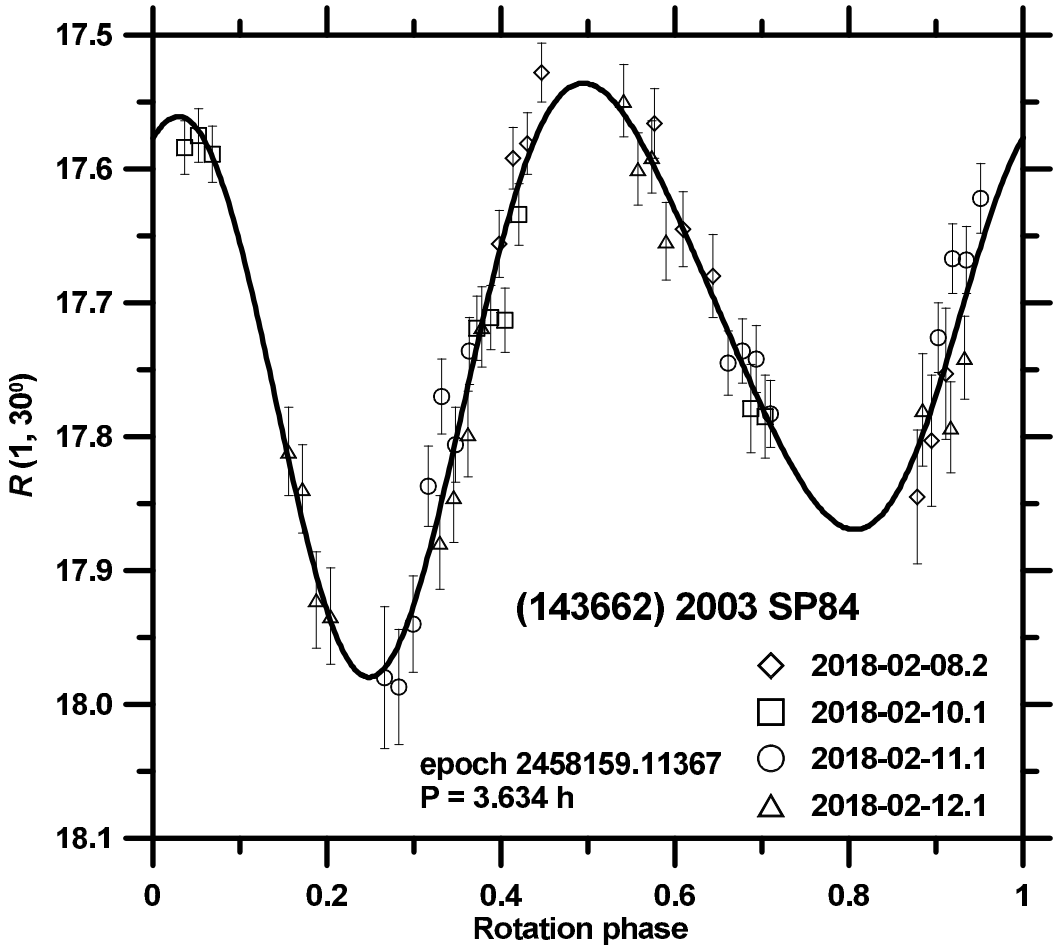

Suppl. Fig. 168. Composite lightcurve of (143662) 2003 SP84 from 2018.

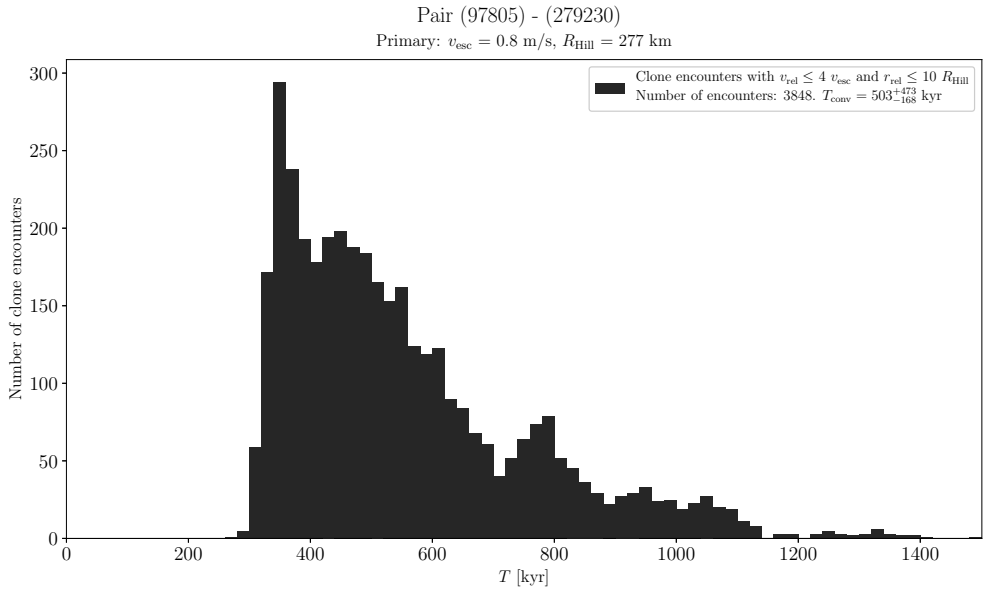

Suppl. Fig. 169. Distribution of past times of close and slow primary–secondary clone encounters for the asteroid pair 97805–279230.

(97805) 2000 OJ15 and (279230) 2009 UX122

The estimated age of this asteroid pair is about 500 kyr (Suppl. Fig. 169). We observed the primary (97805) from La Silla on 7 nights during 2014-11-15 to 2014-11-28 (Suppl. Fig. 170) and derived its mean absolute magnitude $H_1 = 16.05 \pm 0.04$ and the slope parameter $G = 0.32 \pm 0.07$.

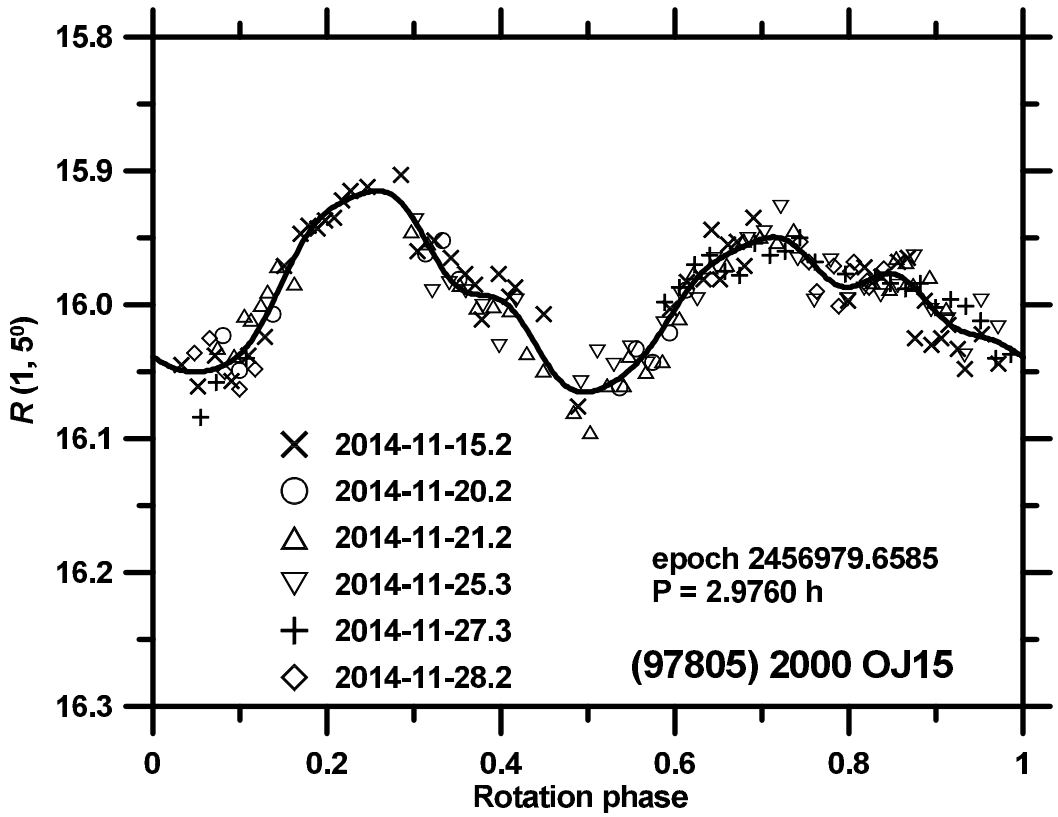

Suppl. Fig. 170. Composite lightcurve of (97805) 2000 OJ15 from 2014.

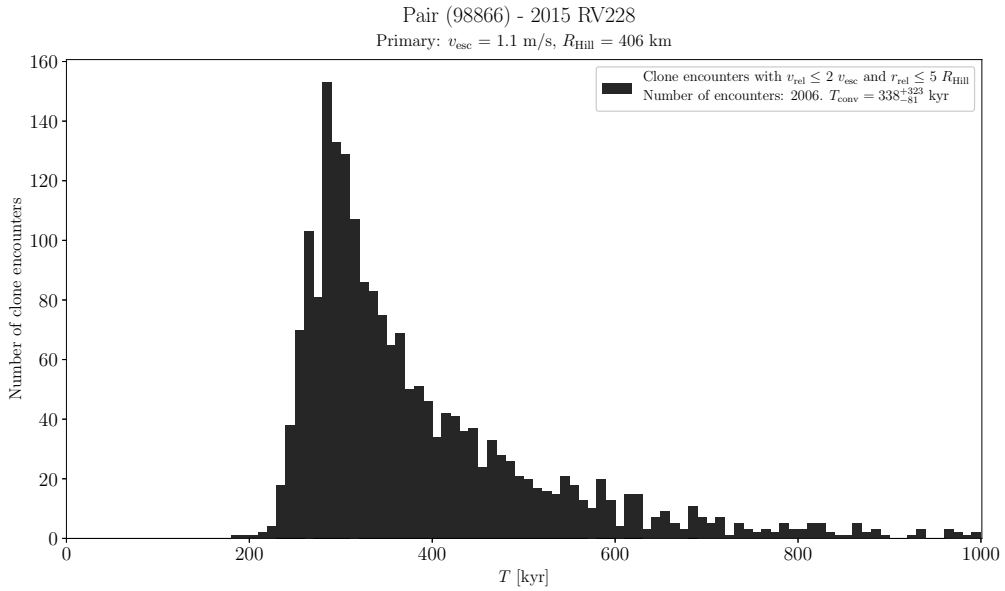

Suppl. Fig. 171. Distribution of past times of close and slow primary–secondary clone encounters for the asteroid pair 98866–2015RV228.

(98866) Giannabussolari and 2015 RV228

The estimated age of this asteroid pair is about 300 kyr (Suppl. Fig. 171). We observed the primary (98866) from La Silla on 5 nights during 2016-01-08 to 2016-01-14 (Suppl. Fig. 172). We derived the mean absolute magnitude $H_1 = 15.85 \pm 0.05$, assuming $G = 0.24 \pm 0.11$.

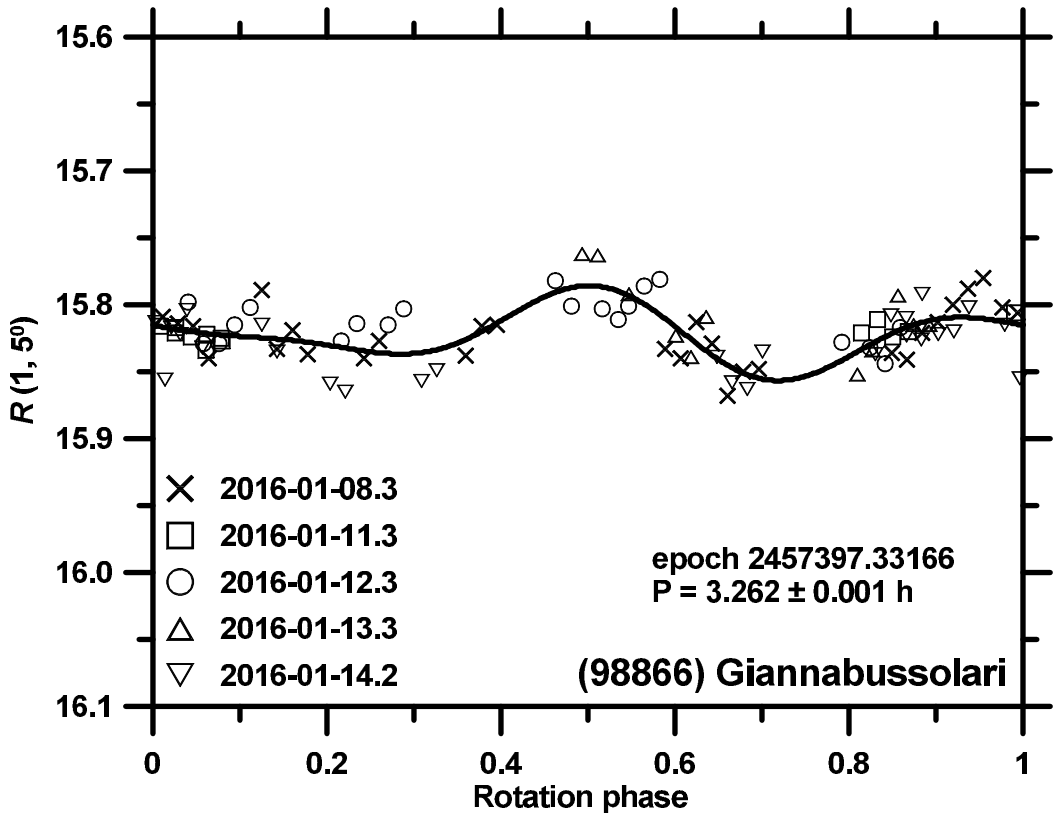

Suppl. Fig. 172. Composite lightcurve of (98866) Giannabussolari from 2016.

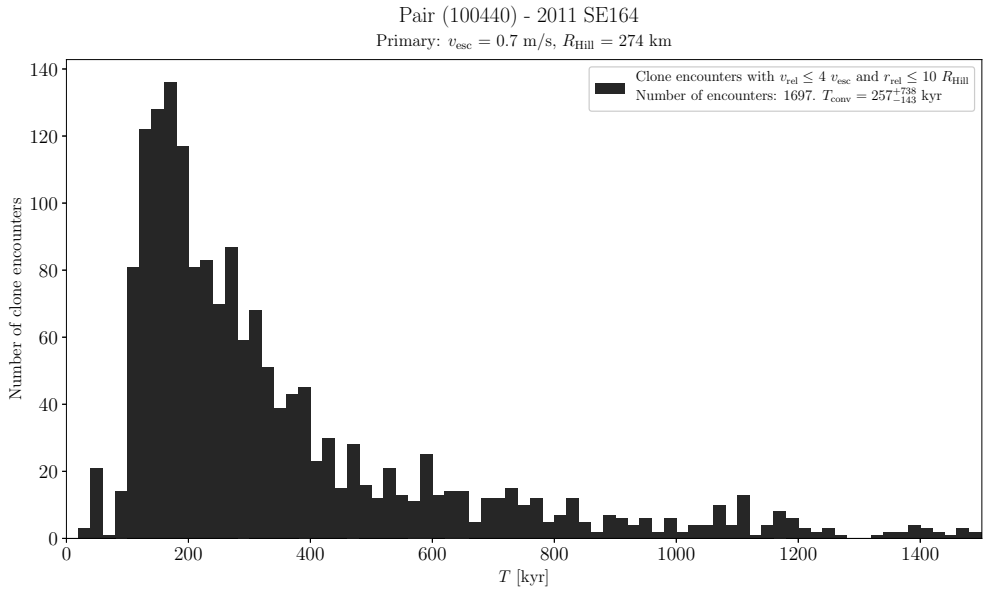

Suppl. Fig. 173. Distribution of past times of close and slow primary–secondary clone encounters for the asteroid pair 100440–2011SE164.

(100440) 1996 PJ6 and 2011 SE164

The estimated age of this asteroid pair is about 250 kyr (Suppl. Fig. 173). We observed the primary (100440) from La Silla on 3 nights during 2014-10-19 to 2014-10-25 (Suppl. Fig. 174). We derived the mean absolute magnitude $H_1 = 16.61 \pm 0.10$, assuming $G = 0.24 \pm 0.11$.

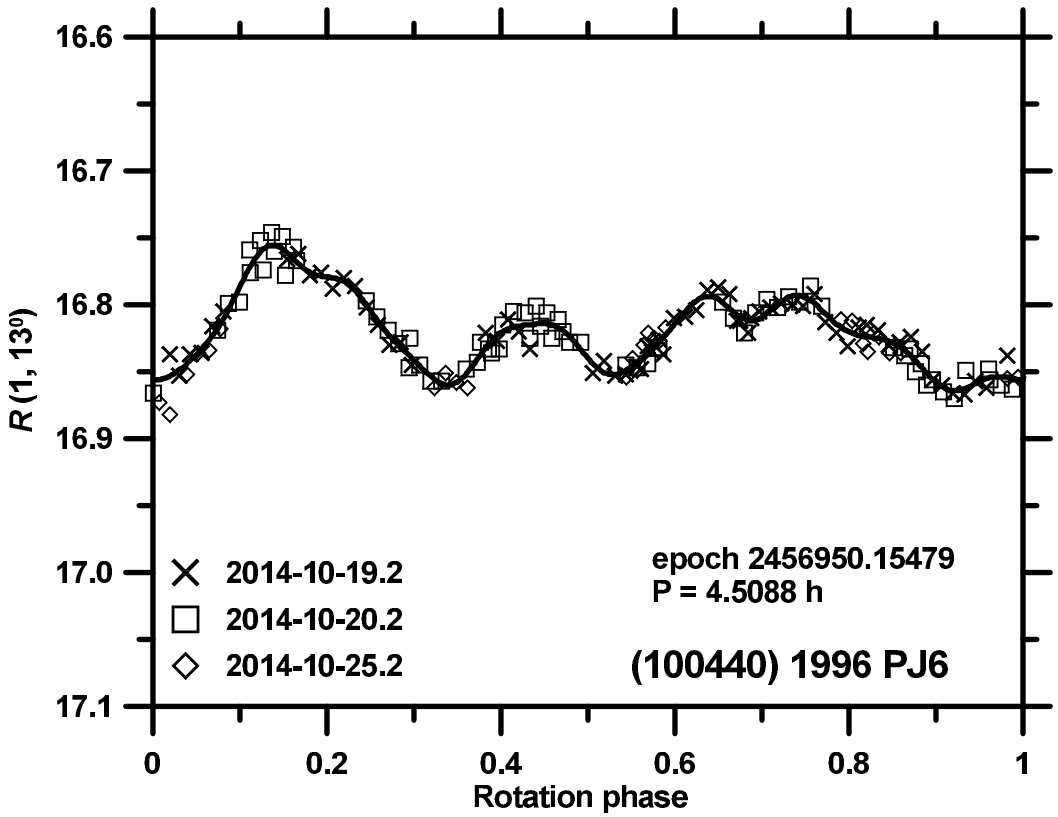

Suppl. Fig. 174. Composite lightcurve of (100440) 1996 PJ6 from 2014.

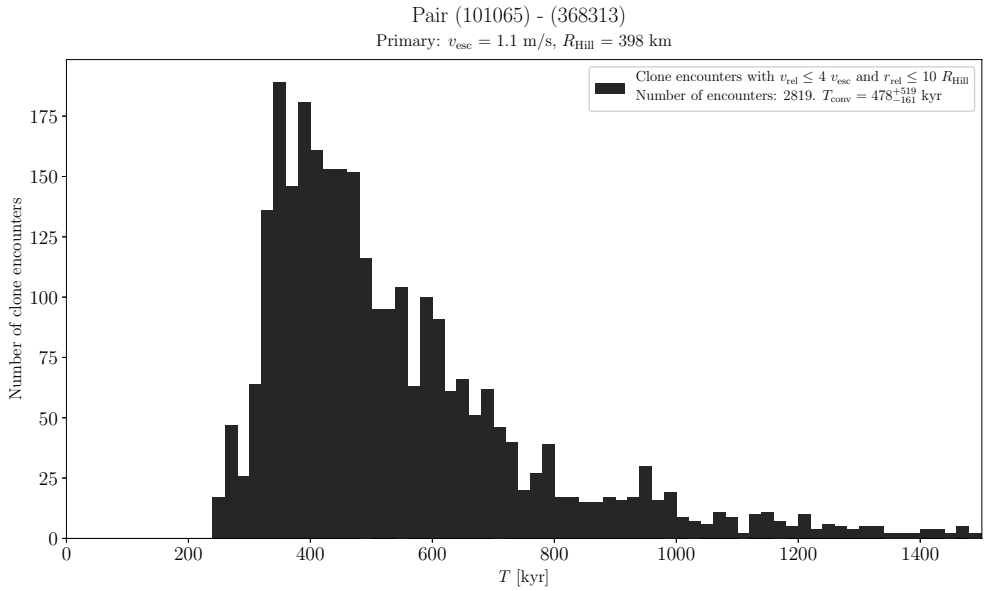

Suppl. Fig. 175. Distribution of past times of close and slow primary–secondary clone encounters for the asteroid pair 101065–368313.

(101065) 1998 RV11 and (368313) 2002 PY103

The estimated age of this asteroid pair is about 500 kyr (Suppl. Fig. 175).

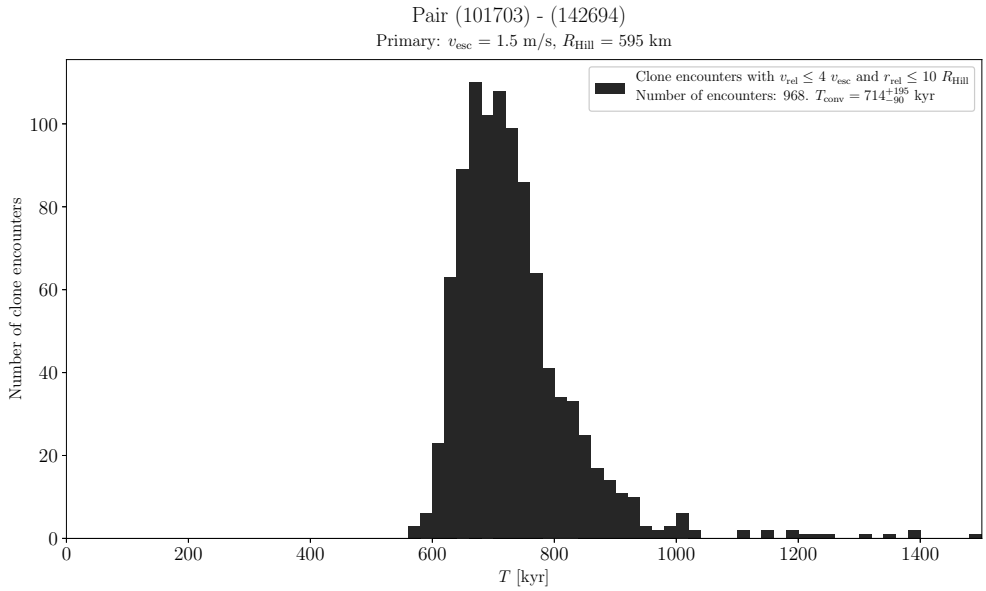

Suppl. Fig. 176. Distribution of past times of close and slow primary–secondary clone encounters for the asteroid pair 101703–142964.

(101703) 1999 CA150 and (142694) 2002 TW243

Backward orbital clone integrations suggest that these two asteroid separated 714^{+195}_{-90} kyr (Suppl. Fig. 176). We obtained data for the primary (101703) from 2 apparitions. The observations from 2009 were published in Pravec et al. (2010). We observed it from La Silla on 6 nights during 2013-10-12 to 2013-10-28. We derived the mean absolute magnitude $H_1 = 15.58 \pm 0.09$ and the phase relation slope parameter $G = 0.32 \pm 0.10$.

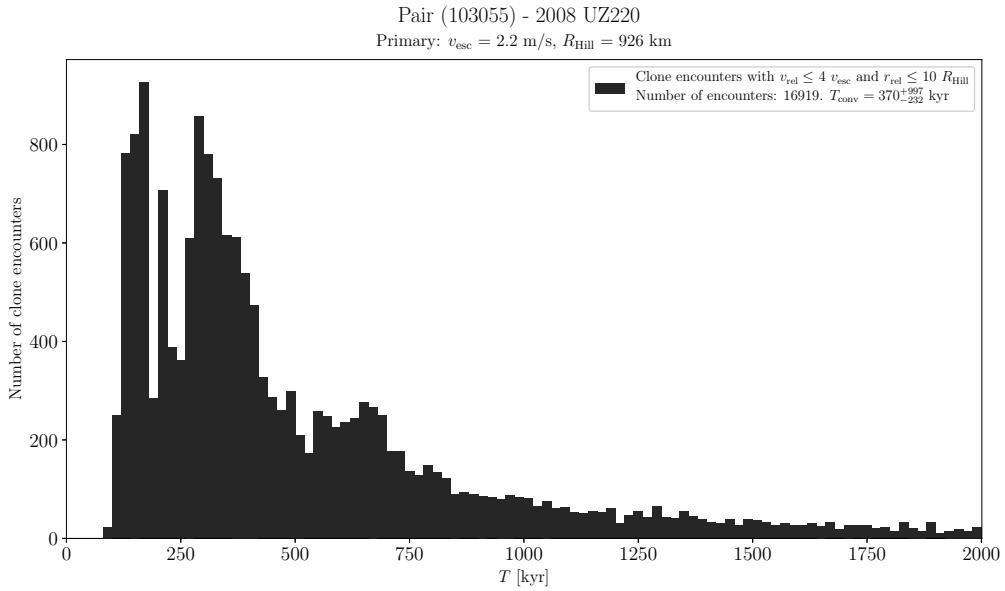

Suppl. Fig. 177. Distribution of past times of close and slow primary–secondary clone encounters for the asteroid pair 103055–2008UZ220.

(103055) 1999 XR134 and 2008 UZ220

The estimated age of this asteroid pair is about 400 kyr (Suppl. Fig. 177). We observed the primary (103055) from La Silla on 2 nights 2016-11-29 and -30 (Suppl. Fig. 178). We derived the mean absolute magnitude $H_1 = 15.00 \pm 0.06$, assuming $G = 0.15 \pm 0.20$.

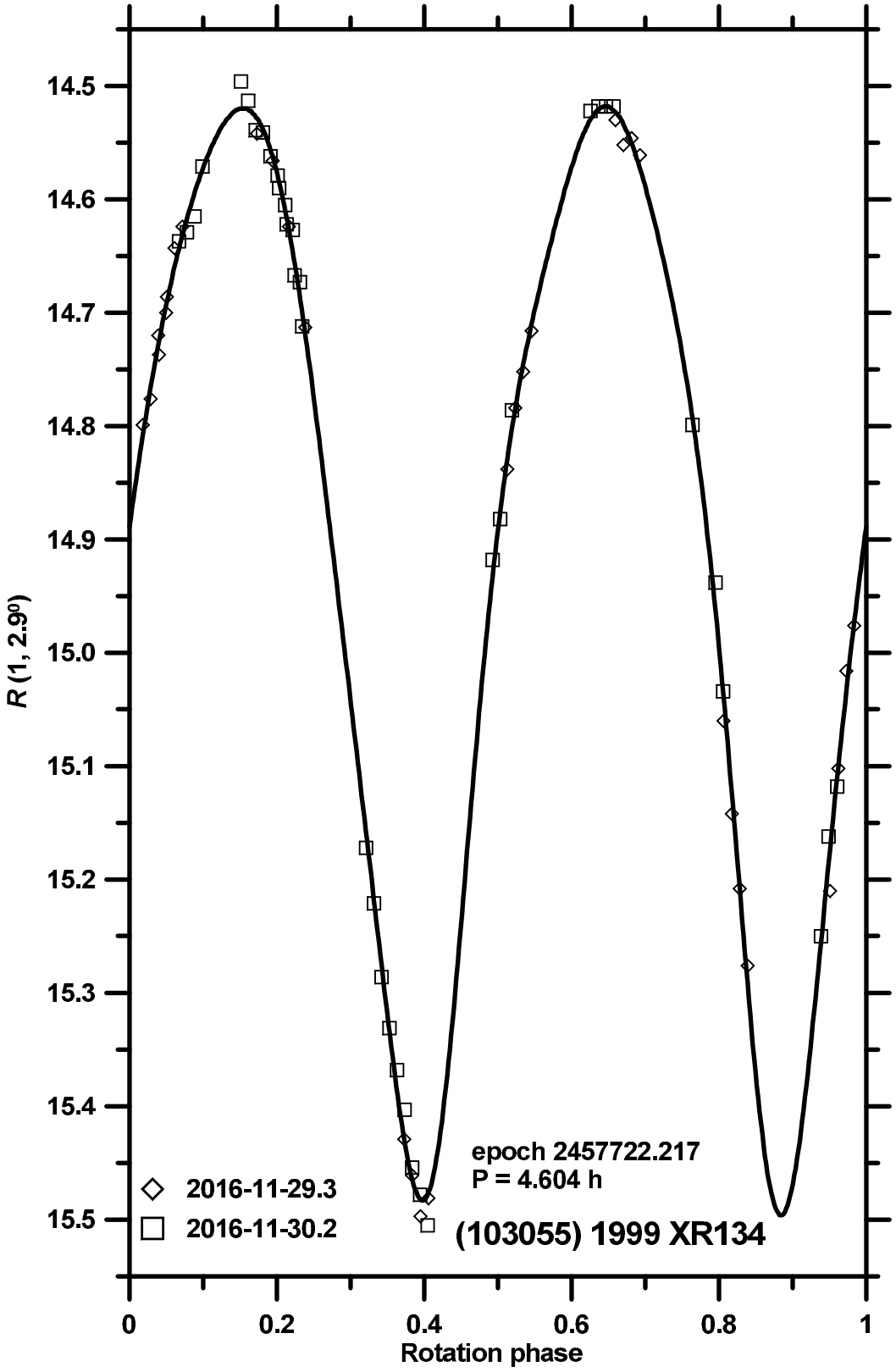

Suppl. Fig. 178. Composite lightcurve of (103055) 1999 XR134 from 2016.

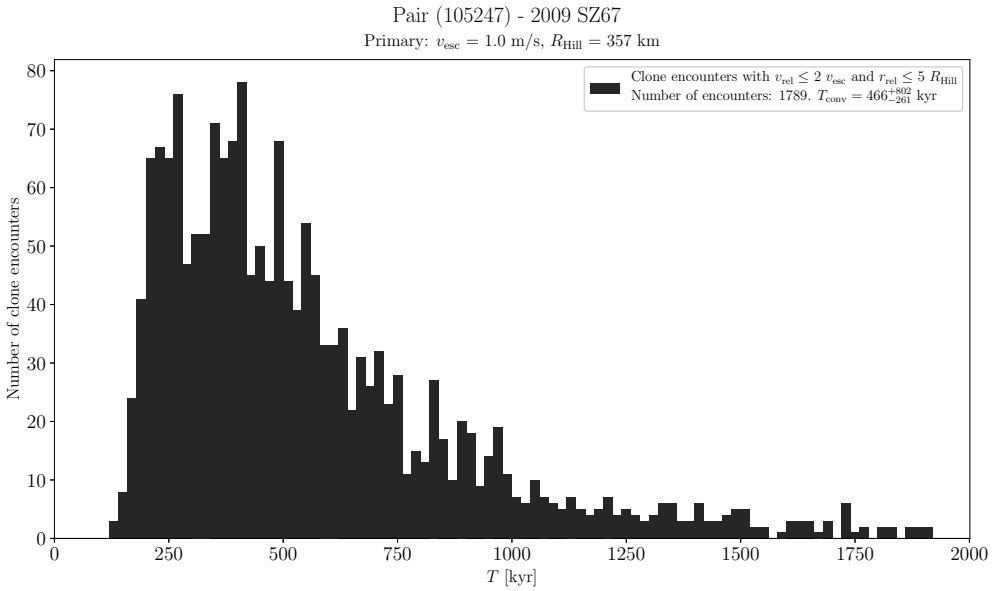

Suppl. Fig. 179. Distribution of past times of close and slow primary–secondary clone encounters for the asteroid pair 105247–2009SZ67.

(105247) 2000 QH3 and 2009 SZ67

The estimated age of this asteroid pair is about 500 kyr (Suppl. Fig. 179). We observed the primary (105247) from Maidanak on 7 nights 2010-08-07 to 2010-08-31 (Suppl. Fig. 180).

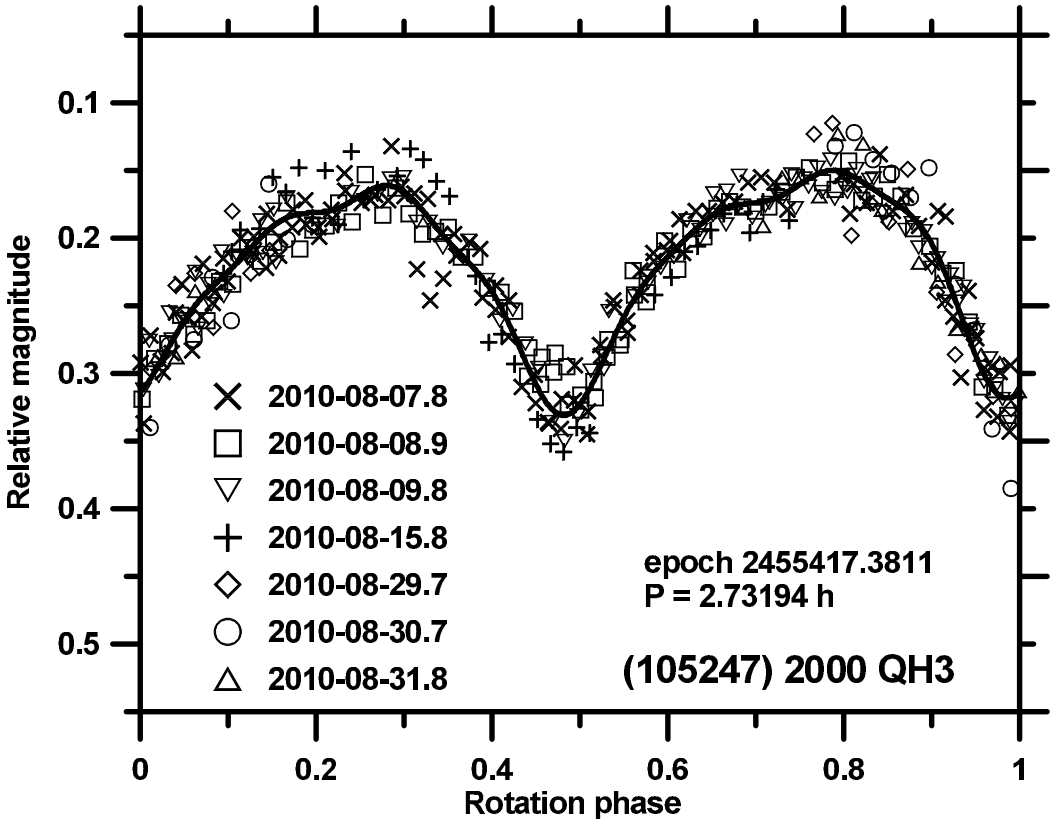

Suppl. Fig. 180. Composite lightcurve of (105247) 2000 QH3 from 2010.

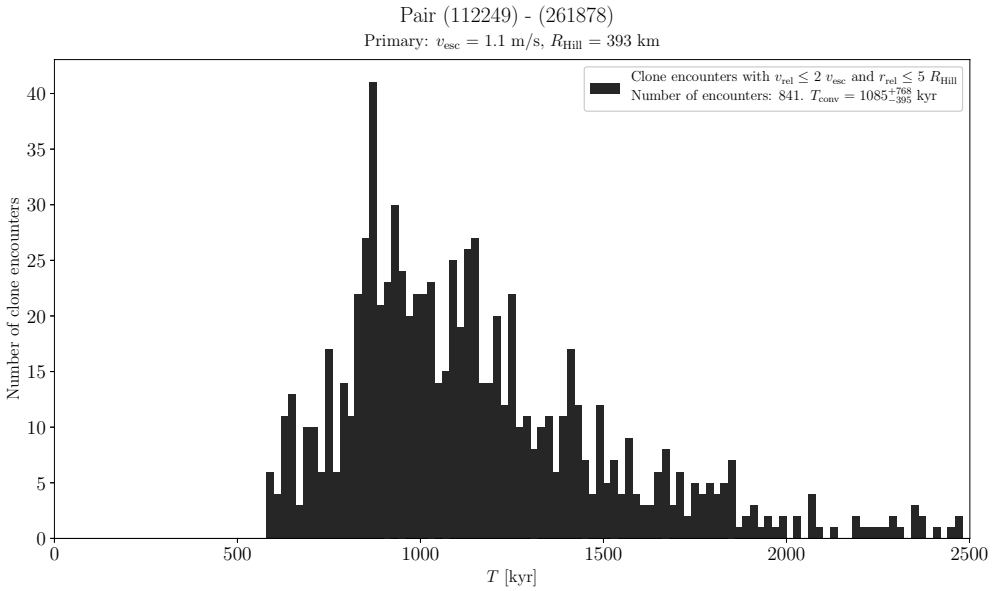

Suppl. Fig. 181. Distribution of past times of close and slow primary–secondary clone encounters for the asteroid pair 112249–261878.

(112249) 2002 LM9 and (261878) 2006 GR49

The estimated age of this asteroid pair is about 1000 kyr (Suppl. Fig. 181). We observed the primary (112249) from La Silla on 2 nights 2015-03-15 2015-03-29 and on 4 nights during 2016-09-03 to 2016-09-09 (Suppl. Fig. 182). We derived the mean absolute magnitude $H_1 = 16.51 \pm 0.08$, assuming $G = 0.15 \pm 0.20$.

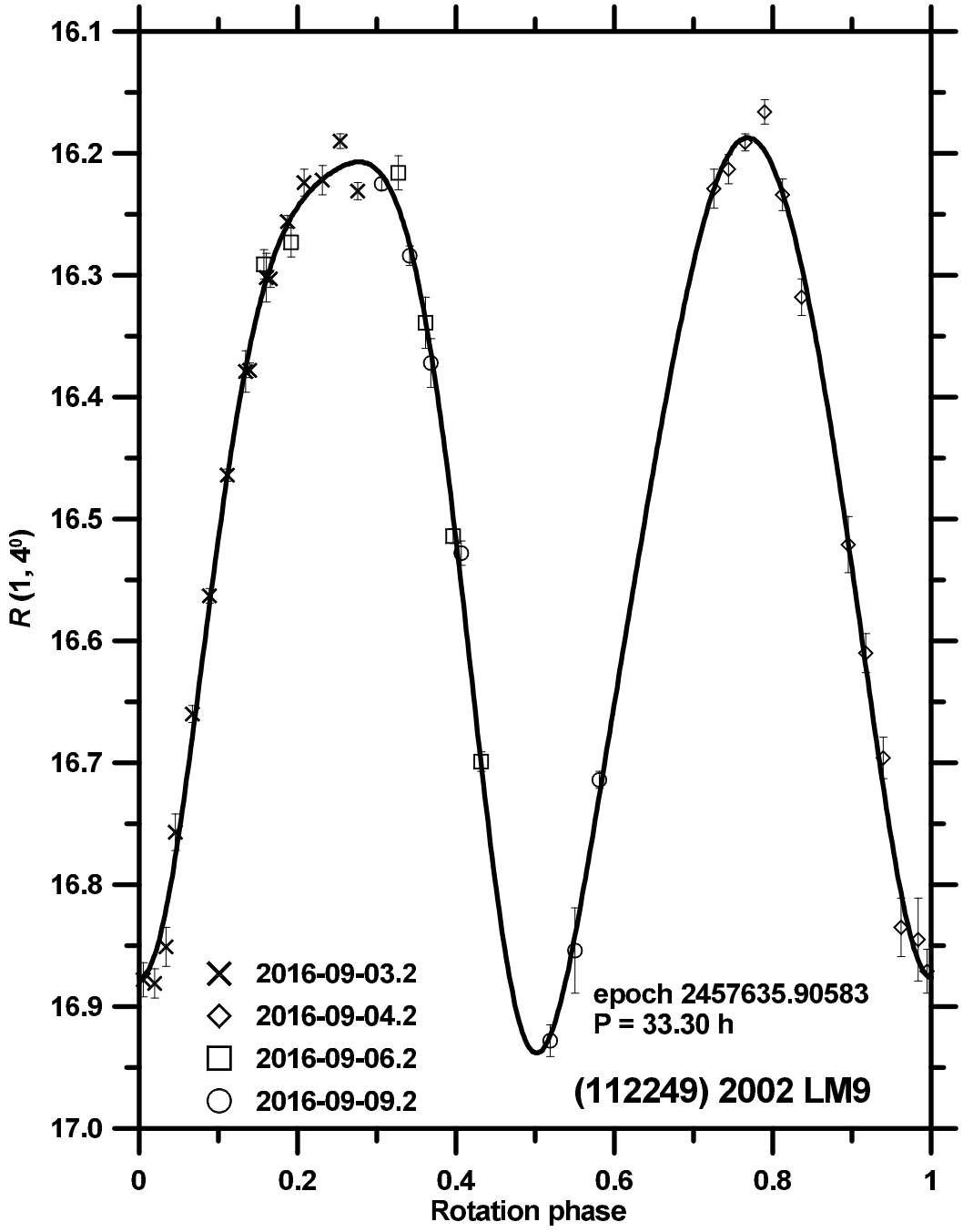

Suppl. Fig. 182. Composite lightcurve of (112249) 2002 LM9 from 2016.

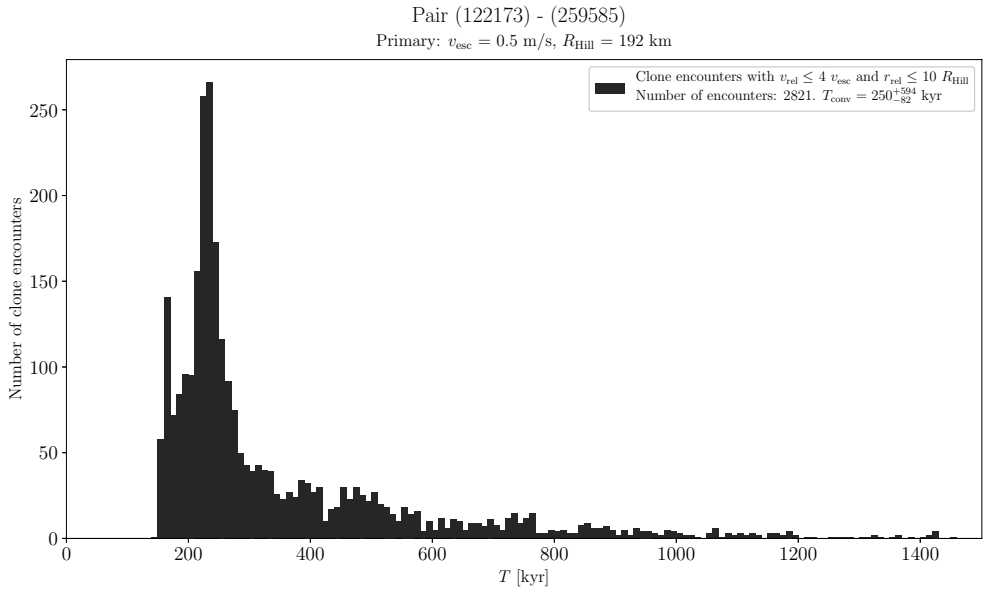

Suppl. Fig. 183. Distribution of past times of close and slow primary–secondary clone encounters for the asteroid pair 122173–259585.

(122173) 2000 KC28 and (259585) 2003 UG220

Backward integrations of their heliocentric orbits suggest that these two asteroids separated 250^{+594}_{-82} kyr ago (Suppl. Fig. 183). We observed (122173) from La Silla on 5 nights during 2015-10-11 to 2015-11-15 and on 4 nights during 2017-03-21 to 2017-03-25. We derived its mean absolute magnitudes $H_1 = 16.68 \pm 0.03$ and 16.71 ± 0.03 in the two apparitions, assuming the secondary's G (below). We observed (259585) from La Silla on 6 nights during 2015-01-14 to 2015-02-17 and derived its mean absolute magnitude $H_2 = 17.05 \pm 0.03$ and the phase relation slope parameter $G = 0.43 \pm 0.03$.

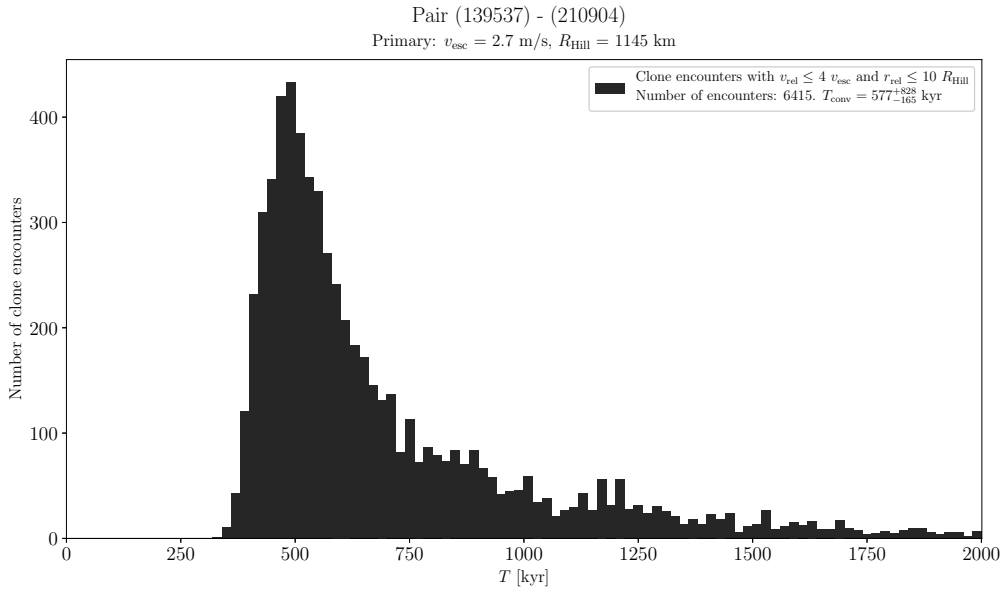

Suppl. Fig. 184. Distribution of past times of close and slow primary–secondary clone encounters for the asteroid pair 139537–210904.

(139537) 2001 QE25 and (210904) 2001 SR218

The estimated age of this asteroid pair is about 600 kyr (Suppl. Fig. 184). We observed the primary (139537) from La Silla on 11 nights during 2018-02-12 to 2018-03-18 (Suppl. Fig. 185). We derived its mean absolute magnitude $H_1 = 15.30 \pm 0.12$, assuming the phase relation slope parameter $G = 0.12 \pm 0.08$, and we refined the WISE effective diameter and geometric albedo (Masiero et al. 2011): $D_1 = 5.1 \pm 0.5$ km and $p_{V,1} = 0.052 \pm 0.012$.

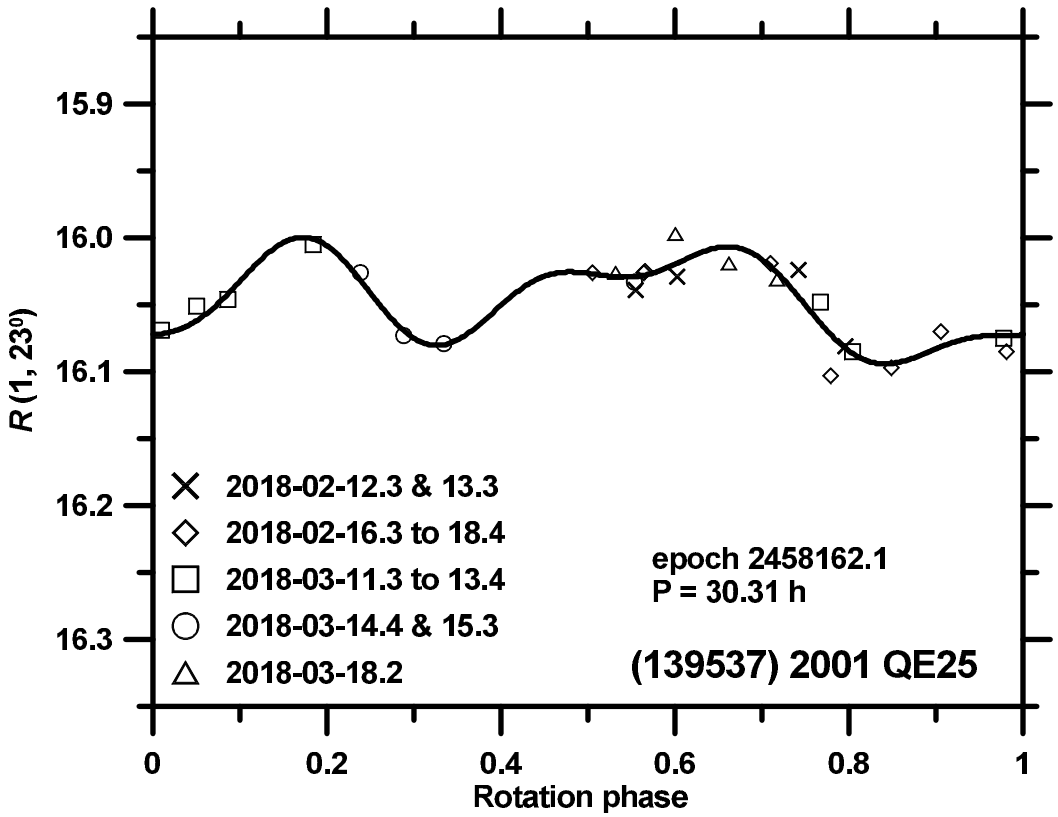

Suppl. Fig. 185. Composite lightcurve of (139537) 2001 QE25 from 2018.

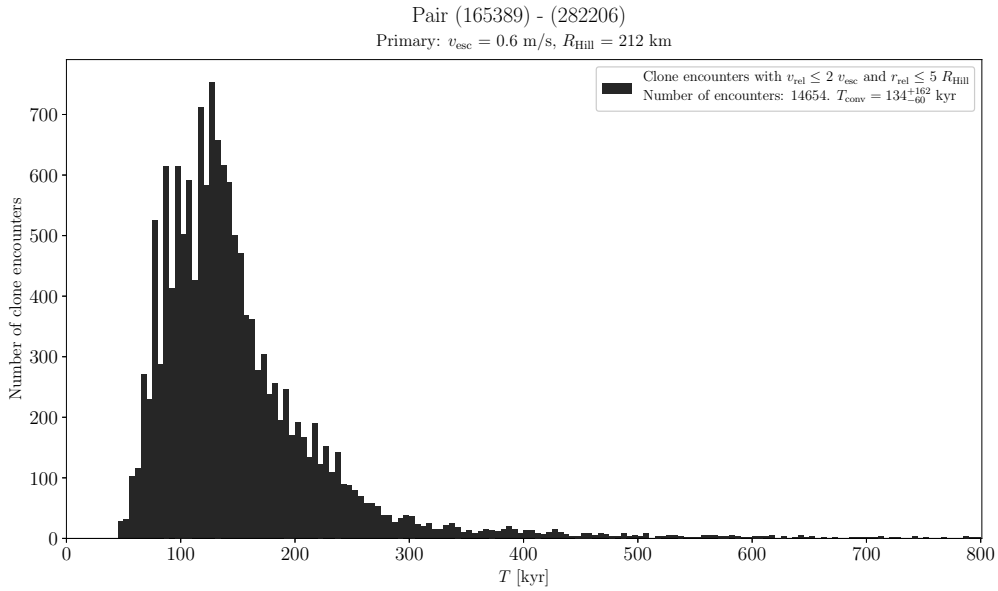

Suppl. Fig. 186. Distribution of past times of close and slow primary–secondary clone encounters for the asteroid pair 165389–282206.

(165389) 2000 WC188 and (282206) 2001 VN61

The estimated age of this asteroid pair is about 130 kyr (Suppl. Fig. 186). We observed the primary (165389) from La Silla on 16 nights during 2014-10-18 to 2014-11-28 (Suppl. Fig. 187). We derived the mean absolute magnitude $H_1 = 17.07 \pm 0.04$ and the slope parameter $G = 0.31 \pm 0.04$. We observed the secondary (282206) from La Silla on 6 nights during 2015-11-06 to 2015-11-19. It showed a low lightcurve amplitude and we could not estimate its period, but we derived the mean absolute magnitude $H_2 = 17.63 \pm 0.04$, assuming the primary's slope parameter $G = 0.31 \pm 0.04$.

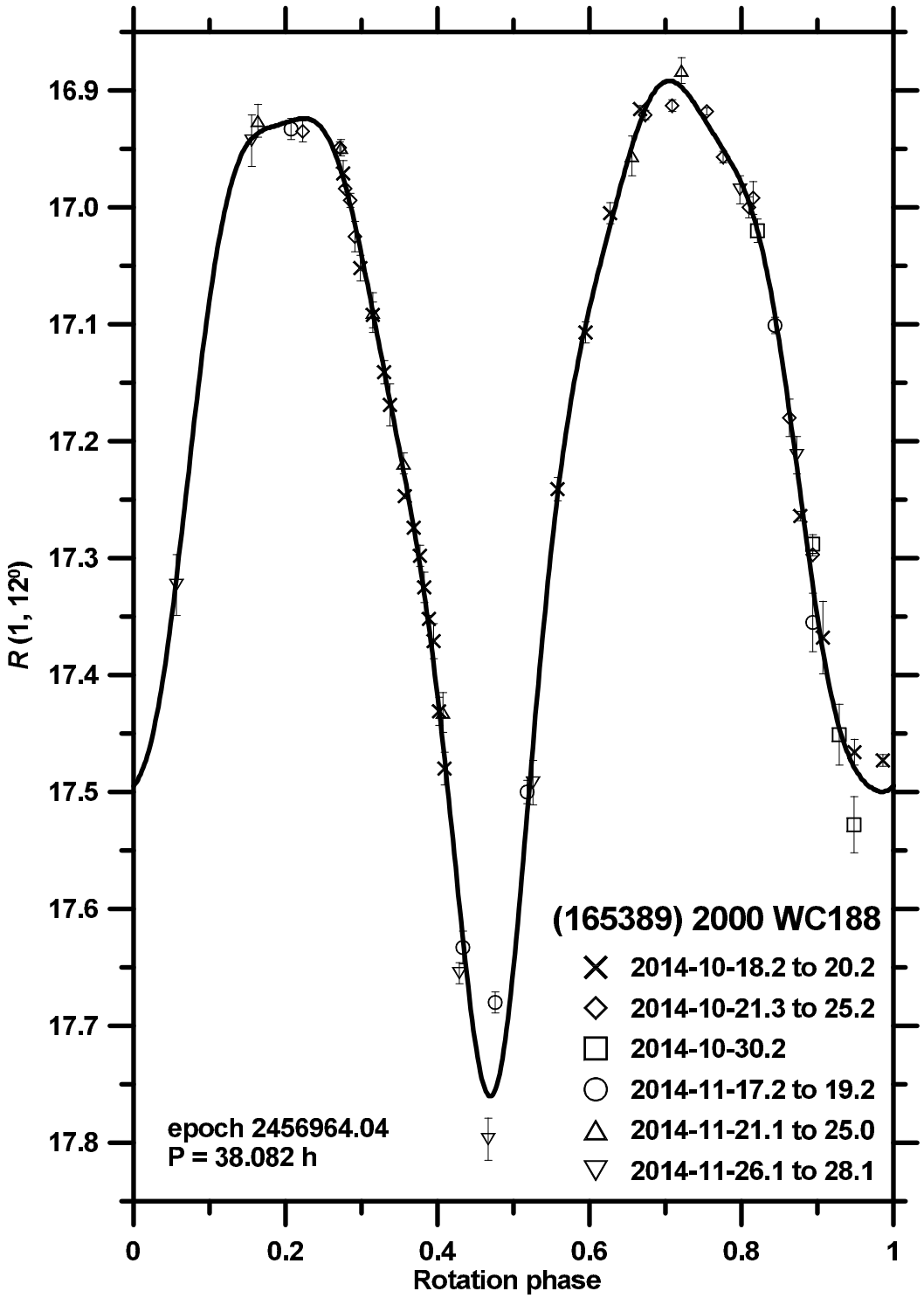

Suppl. Fig. 187. Composite lightcurve of (165389) 2000 WC188 from 2014.

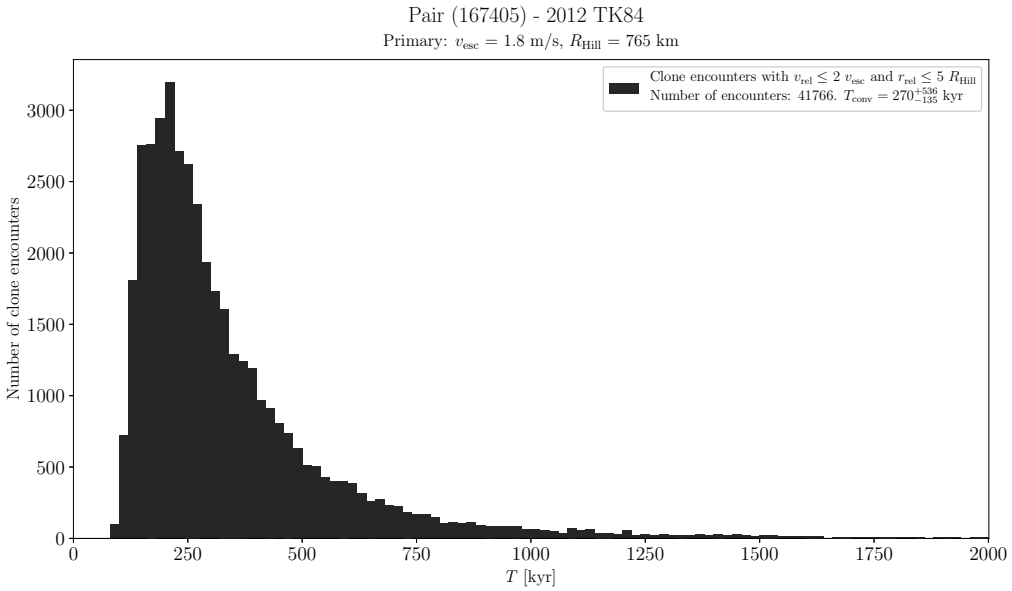

Suppl. Fig. 188. Distribution of past times of close and slow primary–secondary clone encounters for the asteroid pair 167405–2012TK84.

(167405) 2003 WP118 and 2012 TK84

The estimated age of this asteroid pair is about 270 kyr (Suppl. Fig. 188). We observed the primary (167405) from La Silla on 4 nights 2016-11-06 to -09 (Suppl. Fig. 189). We derived the mean absolute magnitude $H_1 = 16.10 \pm 0.04$, assuming $G = 0.12 \pm 0.08$ that is the mean slope parameter for C-type asteroids.

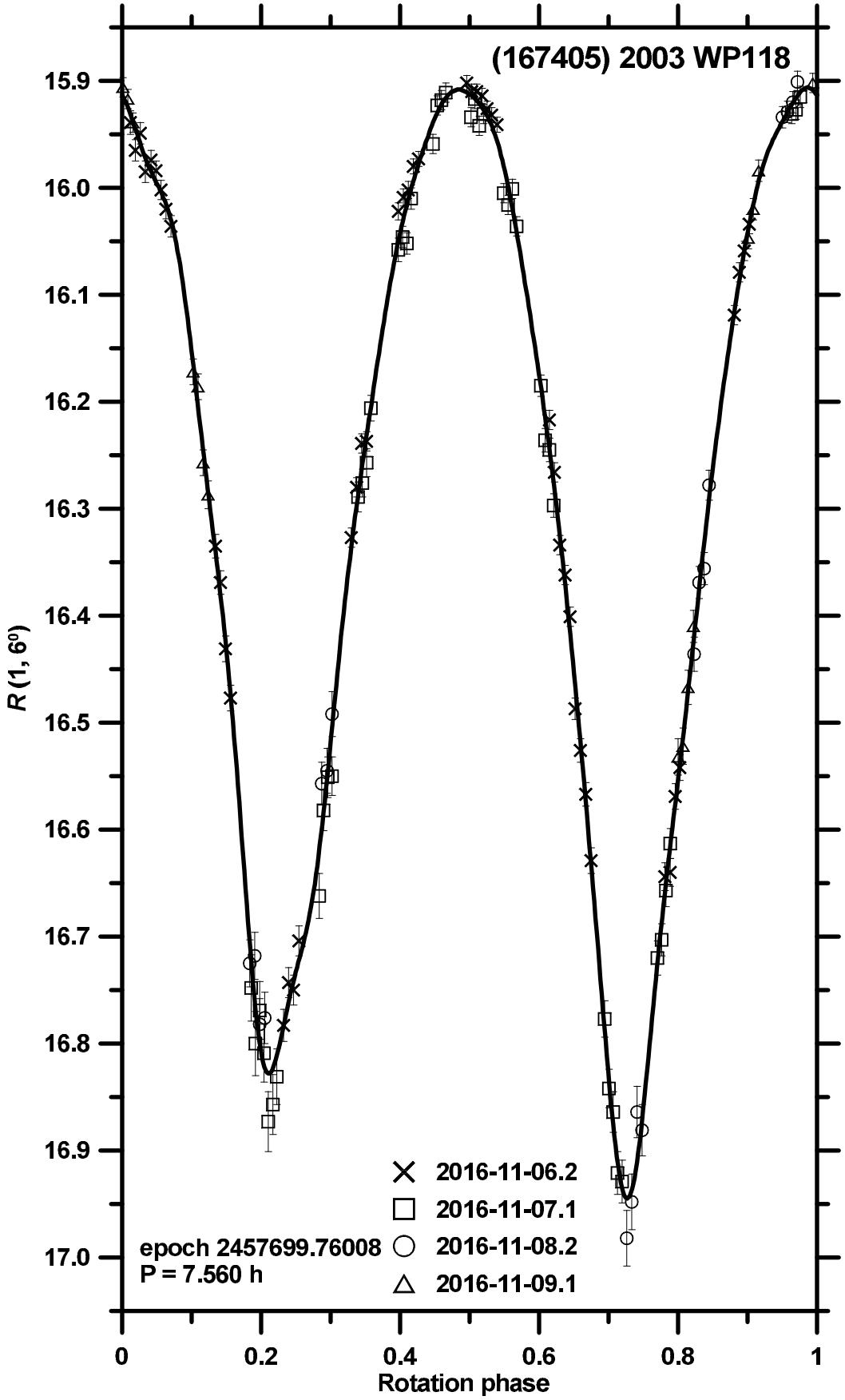

Suppl. Fig. 189. Composite lightcurve of (167405) 2003 WP118 from 2016.

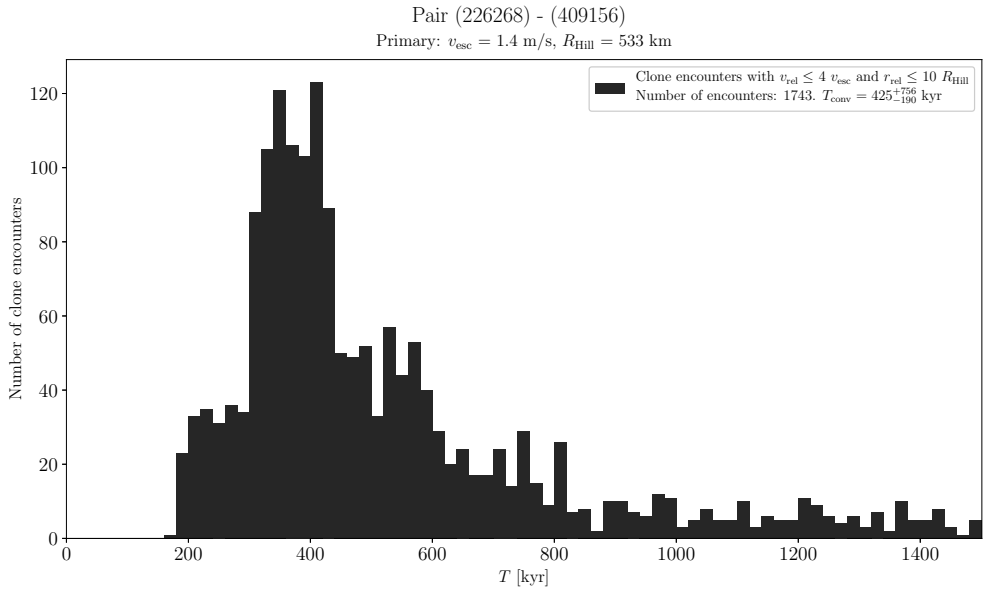

Suppl. Fig. 190. Distribution of past times of close and slow primary–secondary clone encounters for the asteroid pair 226268–409156.

(226268) 2003 AN55 and (409156) 2003 UW156

The estimated age of this asteroid pair is about 400 kyr (Suppl. Fig. 190). Masiero et al. (2011) derived the effective diameter of the primary (226268) $D_1 = 2.7 \pm 0.2$ km.

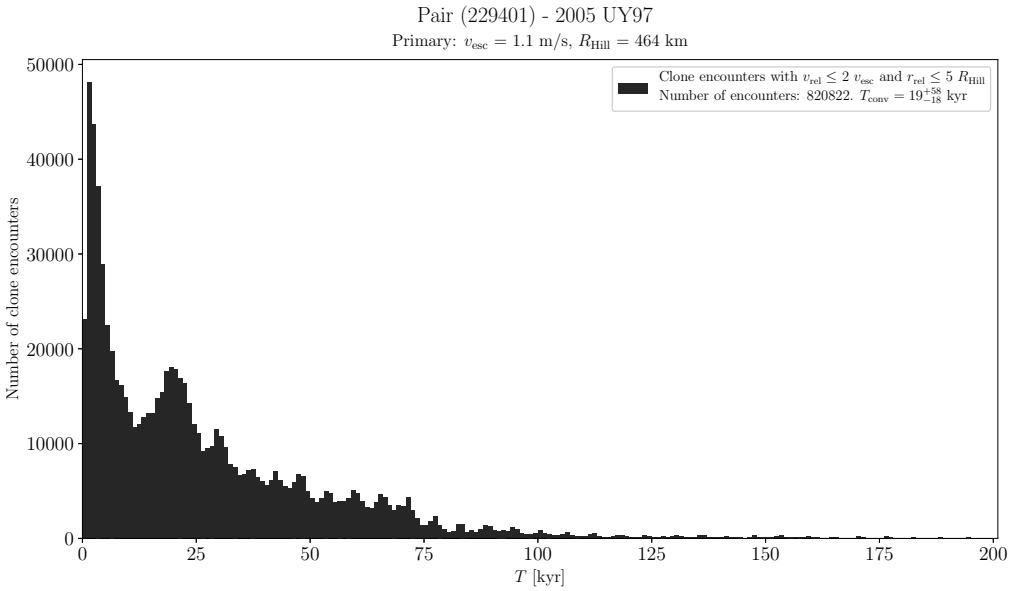

Suppl. Fig. 191. Distribution of past times of close and slow primary–secondary clone encounters for the asteroid pair 229401–2005UY97.

(229401) 2005 SU152 and 2005 UY97

For this asteroid pair, ages in a wide range from 1 to about 100 kyr are possible (Suppl. Fig. 191).

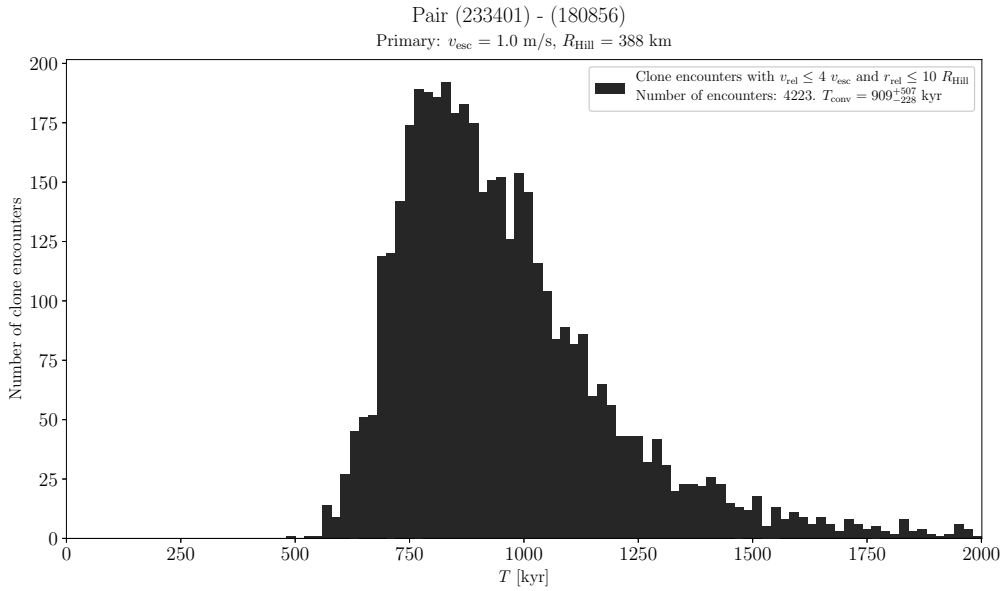

Suppl. Fig. 192. Distribution of past times of close and slow primary–secondary clone encounters for the asteroid pair 233401–180856.

(233401) 2006 FF39 and (180856) 2005 HX5

The estimated age of this asteroid pair is about 900 kyr (Suppl. Fig. 192). We observed the primary (233401) from La Silla on 4 nights during 2016-09-03 to 2016-09-10 (Suppl. Fig. 193) and derived its mean absolute magnitude $H_1 = 16.32 \pm 0.10$, assuming the slope parameter $G = 0.24 \pm 0.11$.

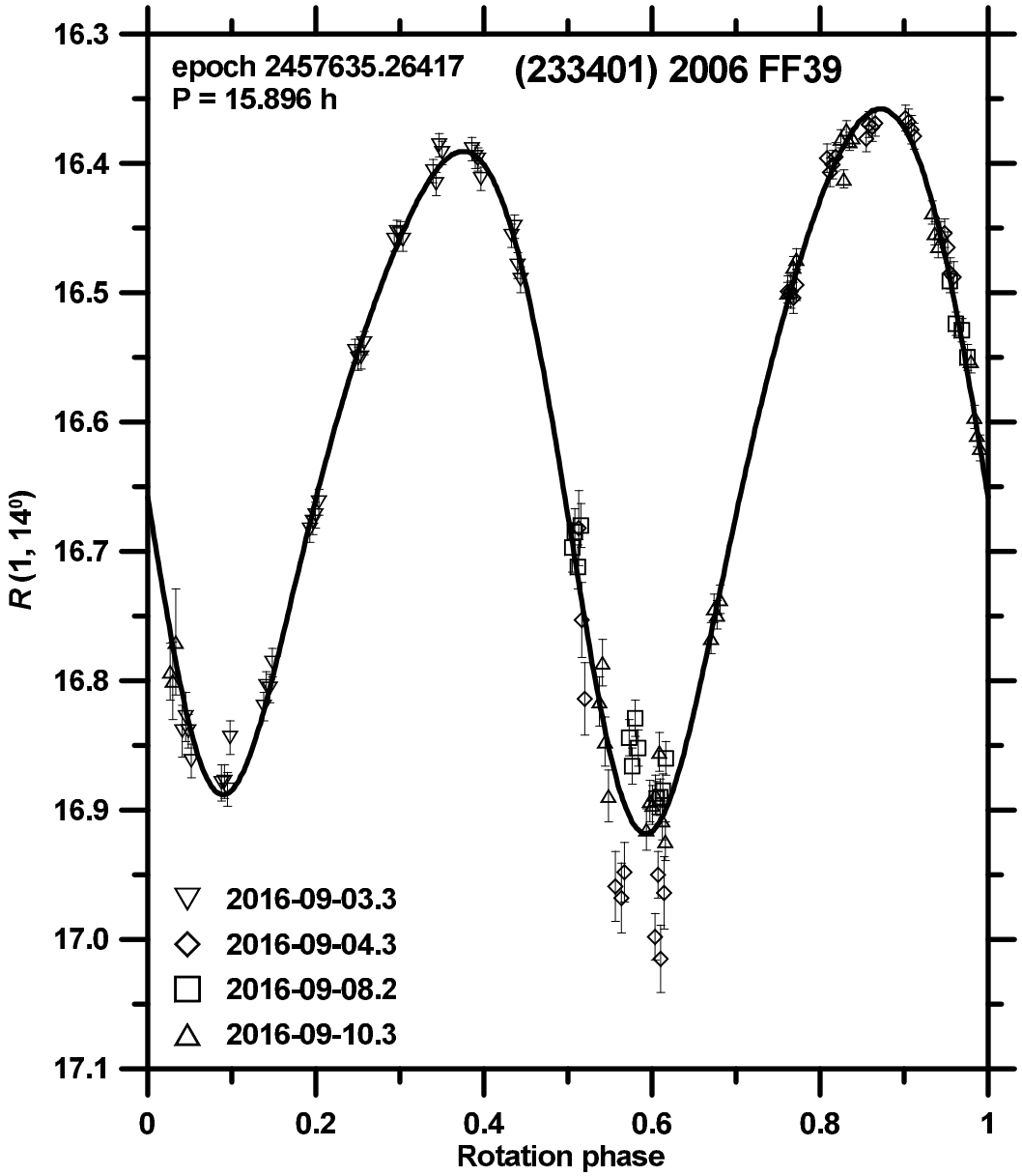

Suppl. Fig. 193. Composite lightcurve of (233401) 2006 FF39 from 2016.

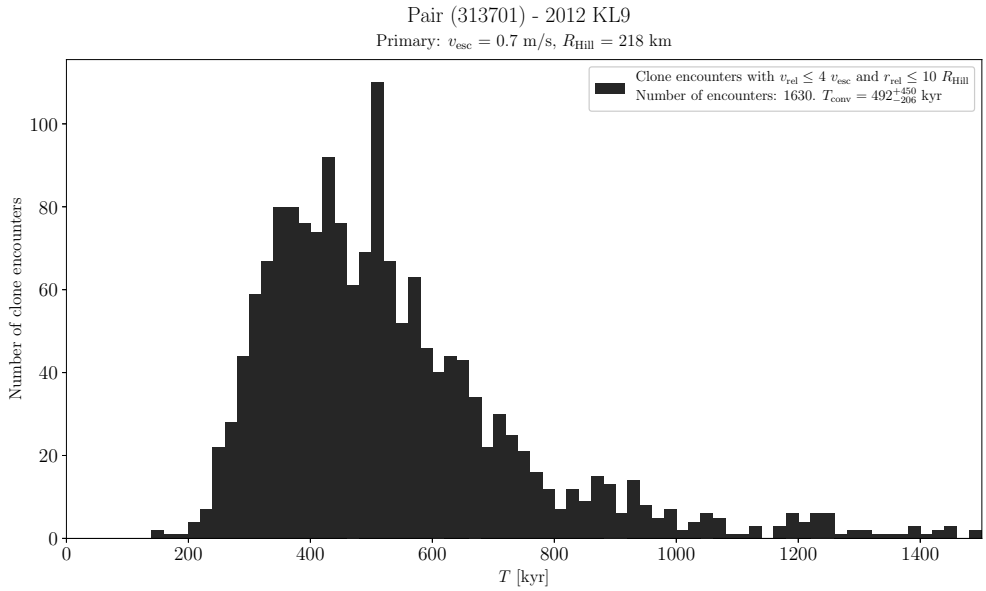

Suppl. Fig. 194. Distribution of past times of close and slow primary–secondary clone encounters for the asteroid pair 313701–2012KL9.

(313701) 2003 UN3 and 2012 KL9

The estimated age of this asteroid pair is about 500 kyr (Suppl. Fig. 194). We observed the primary (313701) from La Silla on 2 nights 2016-12-22 and -23 (Suppl. Fig. 195). We derived the mean absolute magnitude $H_1 = 16.98 \pm 0.20$, assuming $G = 0.15 \pm 0.20$.

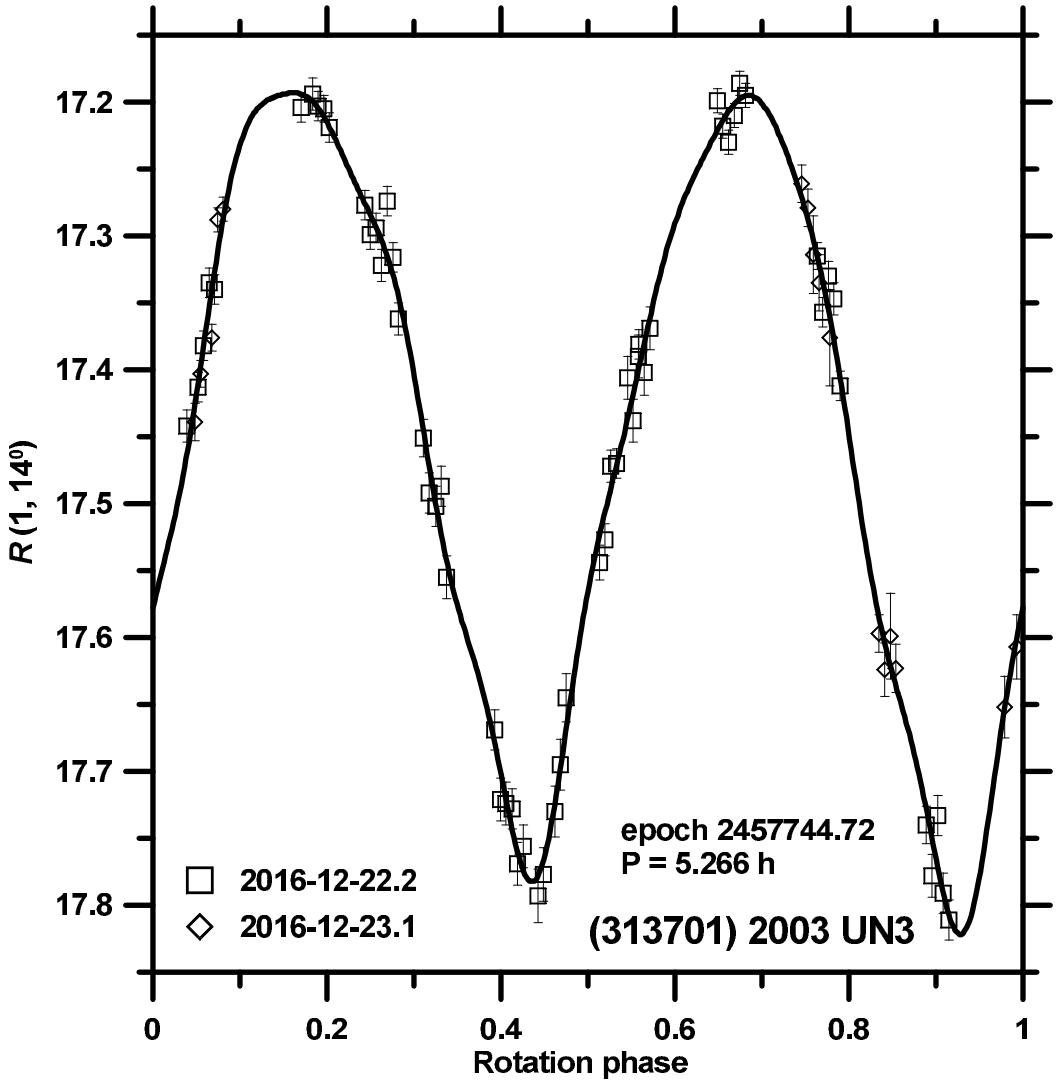

Suppl. Fig. 195. Composite lightcurve of (313701) 2003 UN3 from 2016.

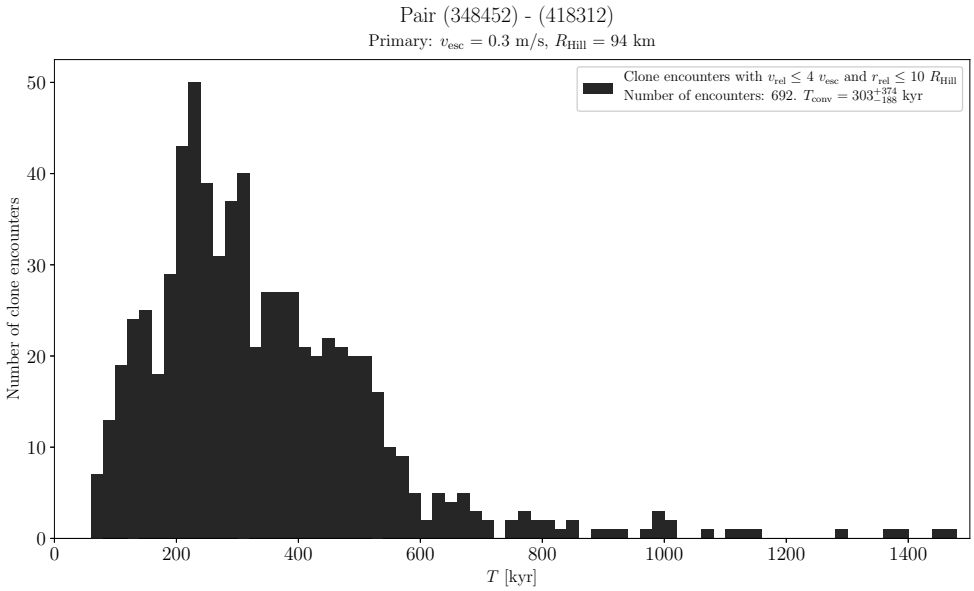

Suppl. Fig. 196. Distribution of past times of close and slow primary–secondary clone encounters for the asteroid pair 348452–418312.

(348452) 2005 RU20 and (418312) 2008 FF88

The estimated age of this asteroid pair is about 300 kyr (Suppl. Fig. 196). We observed the primary (348452) and the secondary (418312) from La Silla on 9 nights 2014-01-02 to -10 and on 3 nights 2014-10-27 to -29, respectively. The primary's composite lightcurve is shown in Suppl. Fig. 197. The secondary showed a low lightcurve amplitude and we could not estimate its period, but we derived its absolute magnitude. The mean absolute magnitudes in the Cousins R system are $H_{R,1} = 17.61 \pm 0.11$ and $H_{R,2} = 18.37 \pm 0.08$, assuming $G = 0.33 \pm 0.10$ that is the mean value for Hungarias. These values give $\Delta H = 0.76 \pm 0.14$. For conversion to $H_1 \equiv H_{V,1}$, we assumed $(V - R) = 0.45 \pm 0.10$.

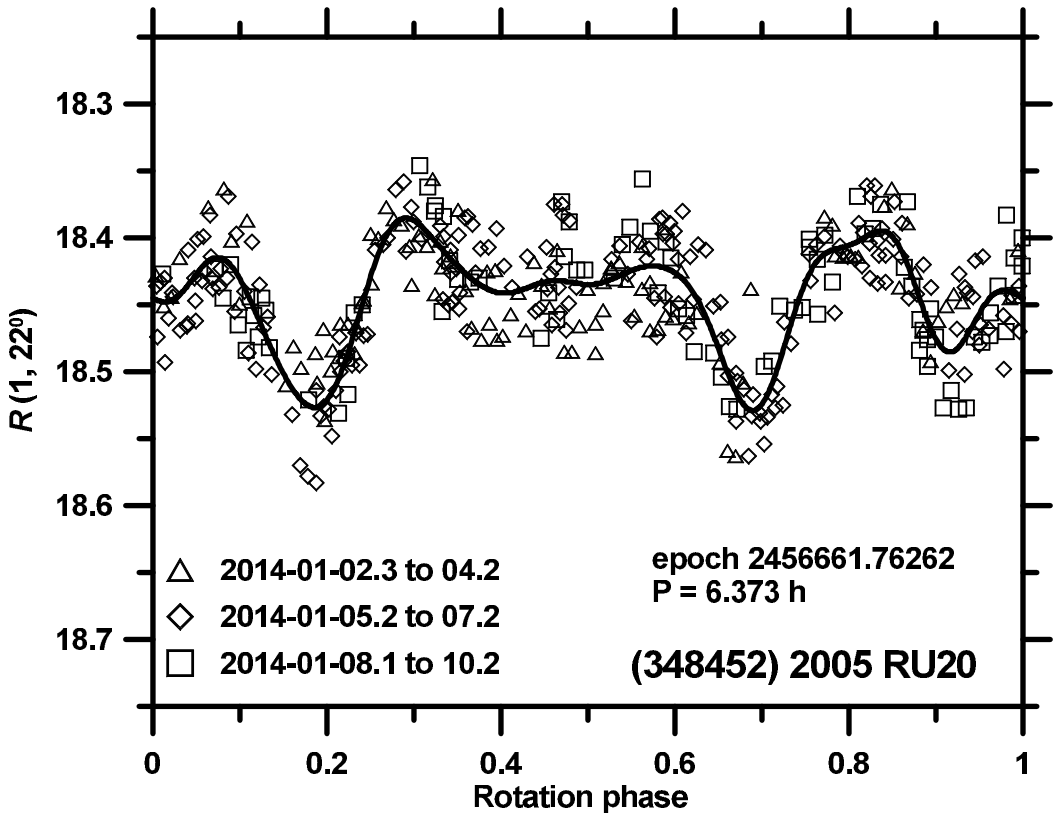

Suppl. Fig. 197. Composite lightcurve of (348452) 2005 RU20 from 2014.

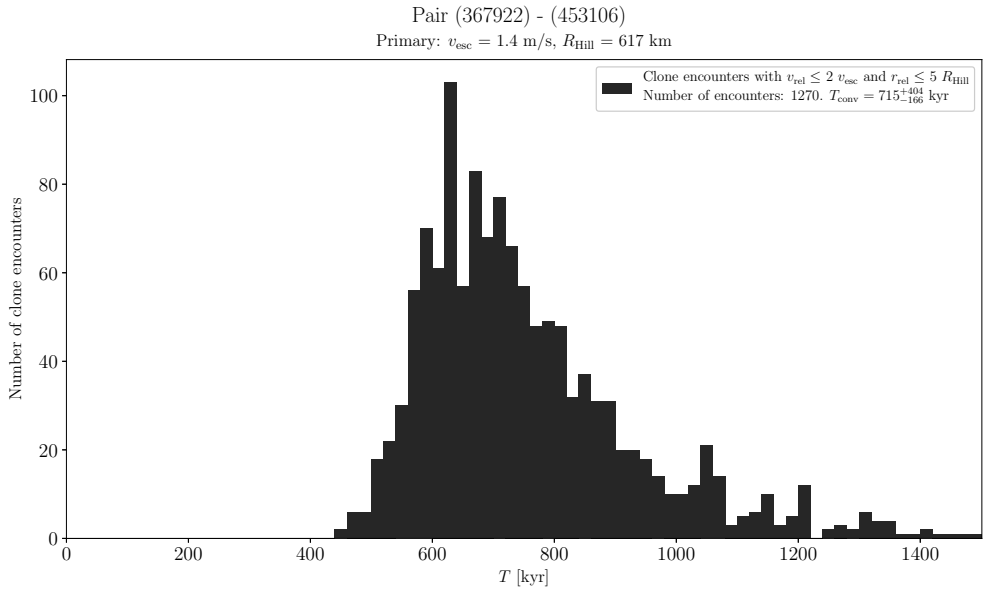

Suppl. Fig. 198. Distribution of past times of close and slow primary–secondary clone encounters for the asteroid pair 367922–453106.

(367922) 2012 BG133 and (453106) 2007 WR62

The estimated age of this asteroid pair is about 700 kyr (Suppl. Fig. 198). We observed the primary (367922) and the secondary (453106) from La Silla on 7 nights during 2017-03-22 to 2017-04-03 and on 3 nights 2017-02-19 to -21, respectively (Suppl. Figs. 199 and 200). We derived their mean absolute magnitudes $H_1 = 15.95 \pm 0.18$ and $H_2 = 16.46 \pm 0.10$, assuming $G = 0.15 \pm 0.20$.

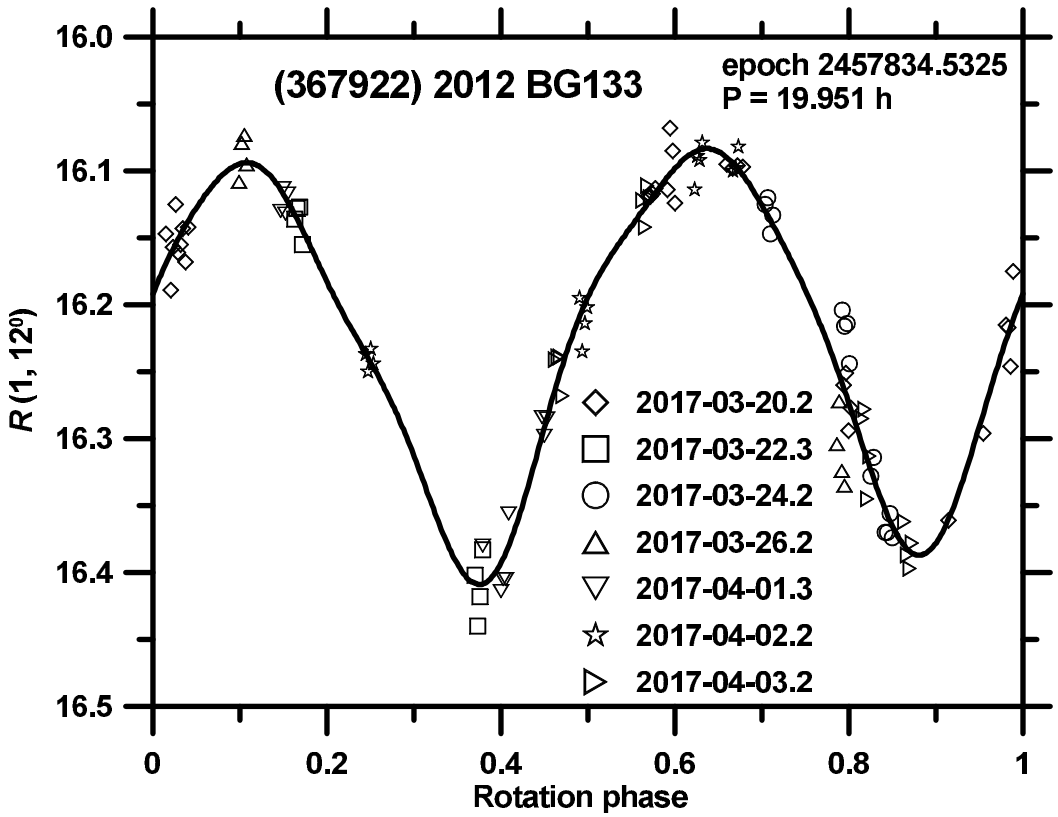

Suppl. Fig. 199. Composite lightcurve of (367922) 2012 BG133 from 2017.

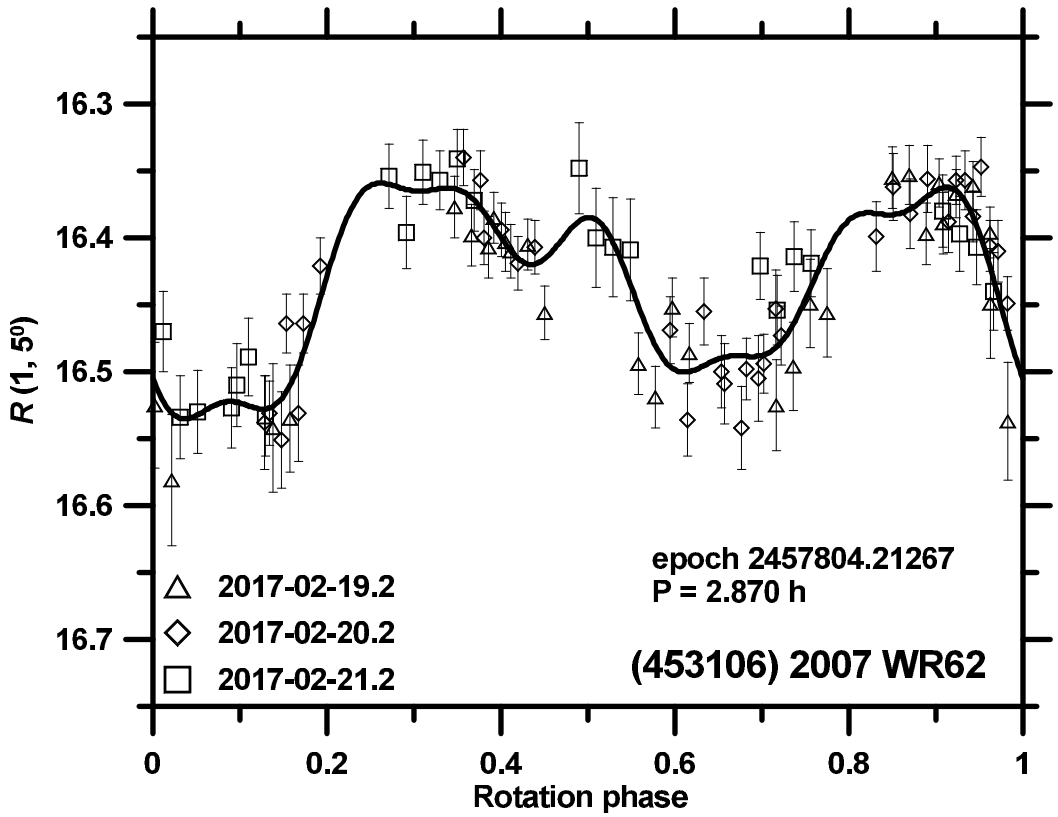

Suppl. Fig. 200. Composite lightcurve of (453106) 2007 WR62 from 2017.

References

Bertin, Arnouts, 1996. Astron. Astrophys. Suppl. 317, 393.

Brosch, N., et al., 2008. The Centurion 18 telescope of the Wise Observatory. Astrophys. Space Sci. 314, 163-176.

Ehgamberdiev, Sh. A., 2018. Modern astronomy at the Maidanak observatory in Uzbekistan. Nature Astronomy 2, 349-351.

Erikson, A., Mottola, S., Lagerros, J.S.V., et al., 2000. The Near-Earth Objects Follow-up Program III. 32 Lightcurves for 12 Objects from 1992 and 1995. Icarus 147, 487–497.

Fernández-Valenzuela, E., et al., 2016. 2008 OG19: a highly elongated Trans-Neptunian object. Mon. Not. Roy. Astron. Soc. 456, 2354–2360.

Flewelling, et al., 2016. eprint arXiv:1612.05243

Galád, A., Pravec, P., Gajdoš, Š., et al., 2007. Seven asteroids studied from Modra observatory in the course of binary asteroid photometric campaign. Earth Moon Planets 101, 17–25.

Harris, A.W., et al., 1989. Photoelectric observations of asteroids 3, 24, 60, 261, and 863. Icarus 77, 171–186.

Husárik, M., Kušnirák, P., 2008. Relative photometry of asteroids (1314), (2257), (3541), (4080), (4155), (12081) and (15415). Contributions of the Astronomical Observatory Skalnaté Pleso 38, 47–60.

Kim, M.-J., 2014. PhD thesis. Yonsei University, Korea

Krugly, Yu. N., Belskaya, I. N., Shevchenko, V. G., et al., 2002. The Near-Earth Objects Follow-up Program. IV. CCD Photometry in 1996-1999. Icarus 158, 294–304.

Krugly, Yu. N., 2004. Problems of CCD Photometry of Fast-Moving Asteroids. Sol. Syst. Res. 38(3), 241–248.

Lang, D., Hogg, D.W., Mierle, K., et al., 2010. Astrometry.net: Blind astrometric calibration of arbitrary astronomical images. Astron. J. 137, 1782-1800.

Marchis, F., et al., 2013. Characteristics and large bulk density of the C-type main-belt triple asteroid (93) Minerva. Icarus 224, 178–191.

Masiero, J. R. et al., 2011. Main belt asteroids with WISE/NEOWISE. I. Preliminary albedos and diameters. Astrophys. J. 741, 68–89.

Mommert, M., 2017. Astronomy and Computing 18, 47–53.

Mottola, S., De Angelis, G., Di Martino, M., et al., 1995. The near-Earth objects follow-up program: first results. Icarus 117, 62–70.

Oey, J., 2011. Minor Planet Bull. 38, 221–223.

Oey, J., 2014. Minor Planet Bull. 41, 276–281.

Oey, J., 2016. Minor Planet Bull. 43, 45–51.

Oey, J., et al. 2017. Minor Planet Bull. 44, 193–199.

Polishook, D., 2014a. Minor Planet Bull. 41, 49–53.

Polishook, D., 2014b. Spin axes and shape models of asteroid pairs: Fingerprints of YORP and a path to the density of rubble piles. Icarus 241, 79–96.

Polishook, D., Brosch, N., 2008. Photometry of Aten asteroidsMore than a handful of binaries. Icarus 194, 111-124.

Polishook, D., Brosch, N., 2009. Photometry and spin rate distribution of small main belt asteroids. Icarus 199, 319-332.

Polishook, D., Brosch, N., Prialnik, D., 2011. Icarus 212, 167–174.

Polishook, D., Aharonson, O., 2019. Surface slopes of asteroid pairs as indicators of mechanical properties and cohesion. https://arxiv.org/abs/1904.09627

Pravec, P., Scheirich, P., Kušnirák, P., et al., 2006. Photometric survey of binary near-Earth asteroids. Icarus 181, 63–93.

Pravec, P., Vokrouhlický, D., Polishook, D., et al., 2010. Formation of asteroid pairs by rotational fission. Nature 466, 1085–1088.

Pravec, P., et al., 2012b. Absolute magnitudes of asteroids and a revision of asteroid albedo estimates from WISE thermal observations. Icarus 221, 365–387.

Pravec, P., Scheirich, P., Ďurech, J., et al. 2014. The tumbling spin state of (99942) Apophis. Icarus 233, 48–60.

Pravec, P., et al., 2016. Binary asteroid population. 3. Secondary rotations and elongations. Icarus 267, 267–295.

Santos-Sanz, P., et al., 2015. Short-term variability of comet C/2012 S1 (ISON) at 4.8 AU from the Sun. Astron. Astrophys. 575, A52 (6pp).

Slivan, S.M., et al., 2008. Rotation rates in the Koronis family, complete to $H \approx 11.2$. Icarus 195, 226–276.

Stephens, R.D., Warner, B.D., 2015. Minor Planet Bull. 42, 96–100.

Warner, B.D., 2007. Minor Planet Bull. 34, 72–77.

Warner, B.D., 2008. Minor Planet Bull. 35, 67–71.

Warner, B.D., 2009. Minor Planet Bull. 36, 7–13.

Warner, B.D., 2010. Minor Planet Bull. 37, 112–118.

Warner, B.D., 2012. Minor Planet Bull. 39, 245–252.

Warner, B.D., 2014. Minor Planet Bull. 41, 102–112.

Warner, B.D., 2014b. Minor Planet Bull. 41, 144–155.

Warner, B.D., 2015. Minor Planet Bull. 42, 108–114.

Warner, B.D., Pray, D.P., 2009. Analysis of the Lightcurve of (6179) Brett. Minor Planet Bull. 36, 166–168.

Warner, B.D., Stephens, R.D., 2013. Minor Planet Bull. 40, 221–223.

Warner, B.D., Husárik, M., Pravec, P., 2008. Minor Planet Bull. 35, 75–76.

Warner, B.D., et al., 2012. Minor Planet Bull. 39, 152–153.